



**Predicting in-lake responses to short and long-term changes  
using lake physical models**

A thesis presented to the School of Health and Science, Dundalk Institute of  
Technology

in fulfilment of the requirements of the degree of

Doctor of Philosophy

Tadhg Nolan Moore

April 2020

Academic Supervisors: Professor Eleanor Jennings<sup>1</sup>

Dr Elvira de Eyto<sup>2</sup>

<sup>1</sup>Dundalk Institute of Technology, Dundalk, Co. Louth, Ireland

<sup>2</sup>Marine Institute, Furnace, Newport, Co. Mayo, Ireland

## DECLARATION

I hereby certify that this material, which I now submit for assessment on the programme of study leading to the award of doctor of philosophy (PhD) is entirely my own work, and that I have exercised reasonable care to ensure that the work is original, and does not to the best of my knowledge breach any law of copyright, and has not been taken from the work of others save and to the extent that such work has been cited and acknowledged within the text of my work.

Signed: 

Student ID N°: D00190184

Date: 2020-04-20

Supervisor Name: Eleanor Jennings

Supervisor Signature: 

Date: 2020-04-20

## **FUNDING**

The work described in this thesis was carried out as part of the PROGNOS and WATExR projects. PROGNOS was financed under the ERA-NET WaterWorks2014 Co-funded Call, Water JPI: (IE) EPA (Grant number: 2016-W-MS- 22); (SE) FORMAS; (DK) IFD; (Israel) MoE-IL; (RO) RCN, with co-funding from the EU Commission. The WATExR project is part of ERA4CS, an ERA-NET initiated by JPI Climate, and funded by MINECO (ES), FORMAS (SE), BMBF (DE), EPA (IE), RCN (NO), and IFD (DK), with co-funding by the European Union (Grant number: 690462).

*Dedicated to the life and memory of Evan McArdle*

## ACKNOWLEDGEMENTS

I would like to express my sincere gratitude to my supervisors, Dr Eleanor Jennings (DkIT) and Dr Elvira de Eyto (Marine Institute) for all their guidance and support throughout my time in Dundalk and Furnace. They have both been instrumental in guiding me through the last four years, pointing me in the right direction when lost and being a constant support throughout.

Many thanks to post-doc Dr Sean Kelly (from county Dublin which recently won the 5-in-a-row All-Ireland Gaelic Football Championship, just in case you didn't know), *alumni* of Trinity College Dublin, for his helpful critiques and suggestions throughout the writing of this thesis. Dr R. Iestyn Woolway provided crucial feedback for two of my chapters for which I would like to thank him for. Dr Andrew French for his help with R, general silly statistics questions and for introducing me “to what extent does  $x$  influence  $y...$ ”, a very useful tool.

I would like to also like to thank Dr Robert Ladwig for his collaboration on the ISIMIP work with GLM, it goes to prove that even one day Sisyphus will finally leave the boulder atop the mountain and move on to different things. I would also like to thank Johannes Feldbauer and Jorrit Mesman for their collaboration and comradery within the AEMON-J group and for the ongoing development of open-source hydrodynamic modelling tools.

I would also like to sincerely thank our project partners within the PROGNOS and WaterX projects Don Pierson, Gideon Gal, Dennis Trolle, Anders Nielsen, Erik Jeppesen, Jorn Bruggeman, Karsten Bolding, Rafael Marce, Karsten Rinke, Muhammad Shikhani, Daniel Mercado Bettin, Gosia Golub, Jose-Luis Guerrero, Francois Clayer, Maria Dolores Frias, Sixto Herrera, Maialen Iturbide and Raoul-Marie Couture. This work could not have been done without the work carried out by the staff at the Marine Institute, Newport particularly Mary Dillane for the work in data collection and management.

The work in this thesis could not have been supported without the work of Alexandra Elbakyan in her pursuit of ensuring scientific research is open and freely available and thus reducing inequality in access to knowledge through the website Sci-Hub.

Many thanks to my colleagues in the Centre for Freshwater and Environmental Studies especially Victor C. Perelló, Laura Holland, Patricia Antunes, Ewan Geoffroy, Maria Caldero Pascual, Harriet Wilson, Alexa Hoke, Stephen Kneel, Clodagh King, Hammond Sarpong, Emma Drohan and Sofia La Fuente Pillco for all their help and expertise provided and our laboratory technician Allison Murdock.

Cheers to all my housemates in Kinvara who have supported me and been great friends throughout my time in Dundalk: Karen, Mark, Niamh, Aoife. I would especially like to thank Smiley for being a brilliant friend throughout my time here in Dundalk and has helped me with countless things throughout the years. You are all very much appreciated.

A huge thanks to my colleagues at the Marine Institute, Newport for their support throughout the final few months.





## Table of Contents

Declaration .....	i
Funding.....	ii
Acknowledgements .....	iv
List of Figures.....	ix
List of Tables.....	xviii
Abstract.....	1
CHAPTER 1. Introduction .....	3
CHAPTER 2. Literature review .....	8
CHAPTER 3. Lake study sites .....	35
CHAPTER 4. Evaluation of global meteorological reanalyses as potential forcing datasets for one-dimensional hydrodynamic modelling.....	41
CHAPTER 5. Impact of monitoring frequency on error reduction when using data assimilation for short-term hydrodynamic forecasts .....	82
CHAPTER 6. Ensemble modelling of future climate impacts on lake thermal dynamics.....	116
CHAPTER 7. Synthesis.....	201
References .....	212
Appendix .....	280

## List of Figures

Figure 1.1 Overview of thesis. ....	7
Figure 2.1 Major heat exchange processes operating in an enclosed water body (Adapted from Saur and Anderson, 1956). ....	9
Figure 2.2 Example of the flexible Lagrangian layer structure within the General Lake Model for Langtjern, Norway, with example temperature profiles from April, June and September. Note that the layer thickness decreases around the thermocline when it develops in summertime. ....	22
Figure 3.1 Site map of Lake Erken, Sweden and its location in Sweden (inset). ....	36
Figure 3.2 Site map of Lough Feeagh, Ireland and its location in Ireland (inset). ....	37
Figure 3.3 Site map of Lake Kinneret, Israel and showing its location in Israel (inset). ....	38
Figure 3.4 Site map of Langtjern, Norway and showing its location in Norway (inset). ....	39
Figure 4.1 Difference between modelled and observed temperatures for Erken for the four meteorological datasets; ERA-Interim, ERA5, EWEMBI and Local and for the four lake models; FLake, GLM, GOTM and Simstrat. Grey areas indicate periods of missing data for either observed or modelled. ....	55
Figure 4.2 Difference between modelled and observed temperatures for Feeagh for the four meteorological datasets; ERAI, ERA5, EWEMBI and Local and for the four lake models; FLake, GLM, GOTM and Simstrat. Grey areas indicate periods of missing data for either observed or modelled. ....	56
Figure 4.3 Difference between modelled and observed temperatures for Langtjern for the four meteorological datasets; ERA-Interim, ERA5, EWEMBI and Local and for the four lake models; FLake, GLM, GOTM and Simstrat. Grey areas indicate periods of missing data for either observed or modelled. ....	57
Figure 4.4 Distribution of residuals for four meteorological datasets; ECMWF ERA-Interim (ERAI), ERA5, EWEMBI and Local, for Erken, Feeagh and Langtjern for the full profile (A) (Erken: n=84240; Feeagh: n=83076; Langtjern: n=30457), surface (B) (Erken: n=3120; Feeagh: n=7224; Langtjern: n=4296), and bottom (C) (Erken: n=3120; Feeagh: n=7224; Langtjern: n=4296). The residuals from the four lake models: FLake, GLM, GOTM and Simstrat were grouped within this plot. ....	59

Figure 4.5 Density distributions of annual root mean squared error (RMSE) values for the total water column temperature profile for Feeagh (n=20), Erken (n=20) and Langtjern (n=14) for each meteorological dataset: ERAI, ERA5, EWEMBI and Local, and for each lake model FLake, GLM, GOTM and Simstrat.....	61
Figure 4.6 Density distributions of annual bias values for Feeagh (n=20), Erken (n=20) and Langtjern (n=14) for each meteorological dataset: ERAI, ERA5, EWEMBI and Local and for each lake model: FLake, GLM, GOTM and Simstrat.....	63
Figure 4.7 Scatterplot of residuals in predicting surface maximum temperature ( $T_{S_{max}}$ ) and the day of surface maximum temperature for each of the three lakes with the four lake models: FLake, GLM, GOTM and Simstrat forced with the four meteorological datasets: ERA-Interim (ERAI), ERA5, EWEMBI and Local. Points from the same year are connected by the coloured polygons. ....	65
Figure 4.8 Scatterplot of residuals in predicting the day when stratification starts ( $St_{start}$ ) and ends ( $St_{end}$ ) for each of the three lakes with the four lake models: FLake, GLM, GOTM and Simstrat being forced with the four meteorological datasets: ERA-Interim (ERAI), ERA5, EWEMBI and Local. Points from the same year are connected by the coloured polygons. ....	67
Figure 4.9 Scatterplot of residuals in predicting the day of ice onset ( $Ice_{on}$ ) and offset ( $Ice_{off}$ ) for each of the three lakes with the four lake models: FLake, GLM, GOTM and Simstrat being forced with the four meteorological datasets: ERA-Interim (ERAI), ERA5, EWEMBI and Local. Points from the same year are connected by the coloured polygons. ....	68
Figure 4.10 Improvements in model fitness (RMSE) for each model and meteorological dataset after calibration against observed temperature profiles for Erken (n=84240); Feeagh (n=83076) and Langtjern (n=30457). A RMSE of 2 °C is used as a reference point for a ‘good’ calibration (Bruce <i>et al.</i> , 2018; Read <i>et al.</i> , 2019). ....	69
Figure 4.11 Range of calibrated scaling factors for wind and incoming shortwave radiation (swr) applied to each of the four meteorological datasets; ERAI, ERA5, EWEMBI and Local and for each of the four lake models: FLake, GLM, GOTM and Simstrat for each of the three lakes: Erken, Feeagh and Langtjern. ....	71

Figure 4.12 Monthly bias of daily mean for air temperature (A), wind speed (B) and incoming solar radiation (C) for Erken, Feeagh and Langtjern for ERA5, ERAI and EWEMBI compared to the measured local data. ....	73
Figure 5.1 Conceptual scheme of the hot-start functionality showing the continuous forcing and boundary conditions from t0 to t1. The free model run with no data assimilation (NDA) is forced continuously with the initial conditions at t0. The forecast with assimilated data has a model spin-up from t0 and finishes at t1. At t1 a “hotstart” file is produced for GOTM which contains the process and variable states for the model. An observed temperature profile is inserted into this file, updating the model states for water temperature and then the model is reinitialised with the updated restart file.....	90
Figure 5.2 Schematic describing different simulated forecasts that were used. The dates chosen are for example purposes to demonstrate how Figure 5.1 corresponds to an actual forecast. The date 2012-01-01 is t0, t1 is the corresponding date for each forecast and 2013-04-14 represents t2.....	92
Figure 5.3 An example forecast of surface water temperature for Feeagh on 2007-03-13 for 14 days showing the model ensemble (100 simulations; red) and the observed water temperature (black dots) for each forecast where data was assimilated at the time of the forecast (T000), one day previous (T024), one week previous (T168), two weeks previous (T336), one month previous (T672) and the free model run with no data assimilation (NDA). ....	93
Figure 5.4 Observed water temperature at different depths for the three study lakes: A) Feeagh B) Langtjern and C) Kinneret. Green background indicates periods when the lake was isothermal, red for when the lake was stratified and blue for when the lake was inversely stratified (only Langtjern). White spaces indicate time periods where observation data were missing.....	97
Figure 5.5 Impact of the length of time between data assimilation and start of the forecast on the mean absolute error (MAE) for forecast water temperature for the three lakes: A) Feeagh, B) Langtjern and C) Kinneret during stratified and isothermal conditions. Each dot represents the mean absolute error of the 14-day ensemble forecast on that day for the entire water column. The numbered arrows highlight peaks where notable events occurred.....	101
Figure 5.6 MAE averaged across the 14-day forecasts of water temperature in three lakes: Langtjern, Kinneret and Feeagh. The colours of the lines	

represent the length of time between data assimilation and start of the forecast. Forecasts during isothermal (left panel) and epilimnion and hypolimnion water during stratified periods (middle and right panels) are presented separately. Each line represents the MAE of all the forecasts generated during each thermal period (Feeagh-Isothermal: n=86; Feeagh-Stratified: n=53; Kinneret-Isothermal: n=28; Kinneret-Stratified: n=104; Langtjern-Isothermal: n=62; Langtjern-Stratified: n=66). .....102

Figure 5.7 Mean bias of water temperature profiles in three lakes Feeagh, Langtjern and Kinneret for forecasts averaged across the isothermal (Feeagh: n=73; Langtjern: n=64; Kinneret: n=31) and stratified periods (Feeagh: n=69; Langtjern: n=64; Kinneret: n=104). The colours of the lines represent the length of time between data assimilation and start of the forecast. Forecasts during stratified and isothermal conditions are presented separately in each panel. Each line represents the bias of all the 14-day forecasts generated during that thermal period. Dashed horizontal lines indicate the mean top and bottom of the metalimnion during the stratification period. ....104

Figure 5.8 Density plots of the distribution of the mean absolute error for all 14-day forecasts for the three lakes: Feeagh (Isothermal: n=114; Stratified: n=71); Langtjern (Isothermal: n=62; Stratified: n=66), and Kinneret (Isothermal: n=28; Stratified: n=104) with panels for the different thermal periods. Colours represent the length of time between data assimilation and start of the forecast. ....107

Figure 6.1 Distribution of lakes that are included in the global (A) and local (B) ISIMIP lake study. The data for the global lakes comes from the Global Lake Data Base (Kourzeneva *et al.*, 2010). ....124

Figure 6.2 Schematic of the ISIMIP workflow, detailing how the GCMs are bias corrected with EWEMBI, the lake models are calibrated with EWEMBI and then are both used to simulate future lake thermal states under different greenhouse gas (GHG) emission scenarios which are the RCPs. ....127

Figure 6.3 Development of RCPs. Scenarios are generated and used by three broad types of models and analytic frameworks in climate change research: integrated assessment models, climate models and other approaches used to help assess impacts, adaptation and vulnerability. (Adapted from Moss *et al.*, 2010). ....133

Figure 6.4 Examples of discretization depths of layers within GOTM for three example study lakes A) Bourget, FR (145 m; 100 layers), B) Green Lake, US (73 m; 100 layers) and C) Langtjern, NO (9 m; 24 layers).....	139
Figure 6.5 Daily averaged hourly GLM output versus output at 08:00 every day for the time period 2005-2014.....	145
Figure 6.6 Global distribution of calibrated lakes that are included in the local study with associated shorthand labels. Regions are outlined as described in Seneviratne <i>et al.</i> (2012): CEU = Central Europe, CNA = Central North America, ENA = East North America, MED = Mediterranean, NAU = North Australia, SAU = South Australia and New Zealand, WNA = Western North America. See Table 6.6 for site reference names. ....	148
Figure 6.7 Mean observed surface (surftemp) and bottom temperature (bottemp) for 46 calibrated lakes. Sites are ordered according to regions with labels on the right side, separated by a bold line. White blocks indicate no recorded data from that period. See Table 6.6 for site reference names. ....	155
Figure 6.8 Monthly mean observed density difference between surface and bottom for 46 calibrated lakes. Sites are ordered according to regions with labels on the right side, separated by a bold line. White blocks indicate no recorded data from that period. See Table 6.6 for site reference names. ....	156
Figure 6.9 Root mean square error (RMSE) results from calibration of the General Ocean Turbulence Model (GOTM) and the General Lake Model (GLM) (A). Nash-Sutcliffe Efficiency (NSE) results from calibration of the General Ocean Turbulence Model (GOTM) and the General Lake Model (GLM) (B). Lakes with a RMSE greater than 2 and NSE less than 0.5 are coloured grey and referred to as uncalibrated (Uncalib). See Table 6.6 for values corresponding to each site.....	157
Figure 6.10 Calibrated values for wind scaling factor (A) and light attenuation (Kw) (B), the two common parameters which were calibrated for the two lake models: GLM and GOTM. Kw values have been log transformed. Dashed line is the 1:1. See Table 6.6 for actual values.....	158
Figure 6.11 Mean and standard deviation (SD) of the annual anomaly for air temperature for 46 lakes across four GCMs for RCP 6.0 for the time period 2006 – 2099 (n =1460). Sites are ordered according to regions with labels on the right side, separated by a bold line. See Table 6.6 for site reference names. ....	159

Figure 6.12 Mean and standard deviation (SD) of the annual anomaly for wind speed for 46 lakes across four GCMs for RCP 6.0 for the time period 2006 – 2099 (n =1460). Sites are ordered according to regions with labels on the right side, separated by a bold line. See Table 6.6 for site reference names.....	161
Figure 6.13 Mean and standard deviation (SD) of the annual anomaly for short-wave radiation for 46 lakes across four GCMs for RCP 6.0 for the time period 2006 – 2099 (n =1460). Sites are ordered according to regions with labels on the right side, separated by a bold line. See Table 6.6 for site reference names. ....	162
Figure 6.14. Mean and standard deviation (SD) of the monthly anomaly for air temperature, for 46 lakes across four GCMs for RCP 6.0 for the time period 2069-2099 (n=3600). Sites are ordered according to regions with labels on the right side, separated by a bold line. See Table 6.6 for site reference names. ....	164
Figure 6.15 Mean and standard deviation (SD) of the monthly anomaly for wind speed for 46 lakes across four GCMs for RCP 6.0 for the time period 2069-2099 (n=3600). Sites are ordered according to regions with labels on the right side, separated by a bold line. See Table 6.6 for site reference names. ....	165
Figure 6.16 Mean and standard deviation (SD) of the monthly anomaly for short-wave radiation for 46 lakes across four GCMs for RCP 6.0 for the time period 2069-2099 (n=3600). Sites are ordered according to regions with labels on the right side, separated by a bold line. See Table 6.6 for site reference names. ....	166
Figure 6.17 Mean surface (surftemp), bottom (bottemp) and volumetrically averaged lake temperature (wholelaketemp) anomaly across 46 lakes, four GCMs and two lake models (n=134320), under the historical, RCP 2.6, RCP 6.0 and RCP 8.5 scenarios from 1970-2100. Shaded areas represent one standard deviation from the mean. ....	168
Figure 6.18 Mean anomaly of the duration, start and end of stratification each year across 46 lakes, four GCMs and two lake models (n=368) under the historical, RCP 2.6, RCP 6.0 and RCP 8.5 scenarios from 1970 to 2100. Shaded errors represent one standard deviation from the mean.....	169
Figure 6.19 Mean and standard deviation (SD) of the annual surface temperature anomaly for 46 lakes across four GCMs and two lake models (n=2920) for	

RCP 6.0. Sites are ordered according to regions with labels on the right side, separated by a bold line. See Table 6.6 for site reference names.....	170
Figure 6.20 Mean and standard deviation (SD) of the annual bottom temperature anomaly for 46 lakes across four GCMs and two lake models (n=2920) for RCP 6.0 for the time period 2006-2099. Sites are ordered according to regions with labels on the right side, separated by a bold line. See Table 6.6 for site reference names.....	172
Figure 6.21 Mean and standard deviation (SD) of the annual volumetrically averaged whole lake temperature anomaly for 46 lakes across four GCMs and two lake models (n=2920) for RCP 6.0 for the time period 2006-2099. Sites are ordered according to regions with labels on the right side, separated by a bold line. See Table 6.6 for site reference names.....	173
Figure 6.22 Mean and standard deviation (SD) of the monthly surface temperature anomaly for 46 lakes across four GCMs and two lake models (n=7200) for RCP 6.0 for the time period 2069-2099. Sites are ordered according to regions with labels on the right side, separated by a bold line. See Table 6.6 for site reference names.....	175
Figure 6.23 Mean and standard deviation (SD) of the monthly bottom temperature anomaly for 46 lakes across four GCMs and two lake models (n=7200) for RCP 6.0 for the time period 2069-2099. Sites are ordered according to regions with labels on the right side, separated by a bold line. See Table 6.6 for site reference names.....	176
Figure 6.24 Mean and standard deviation (SD) of the monthly volumetrically averaged whole lake temperature anomaly for 46 lakes across four GCMs and two lake models (n=7200) for RCP 6.0 for the time period 2069-2099. Sites are ordered according to regions with labels on the right side, separated by a bold line. See Table 6.6 for site reference names.....	177
Figure 6.25 Mean and standard deviation (SD) of the anomaly for duration of stratification across the four GCMs and two lake models for 35 lakes (n=8) for RCP 6.0. Only dimictic and monomictic lakes are shown. Sites are ordered according to regions with labels on the right side, separated by a bold line. See Table 6.6 for site reference names.....	179
Figure 6.26 Mean and standard deviation (SD) of the anomaly for the start of stratification across the four GCMs and two lake models for 35 lakes (n=8)	

for RCP 6.0 for the time period 2006-2099. Only dimictic and monomictic lakes are shown. See Table 6.6 for site reference names. ....	180
Figure 6.27 Mean and standard deviation (SD) of the anomaly for the end of stratification across the four GCMs and two lake models for 35 lakes (n=8) for RCP 6.0 for the time period 2006-2099. Only dimictic and monomictic lakes are shown. Sites are ordered according to regions with labels on the right side, separated by a bold line. See Table 6.6 for site reference names.....	181
Figure 6.28 Mean and standard deviation (SD) of the annual anomaly for density difference of stratification averaged across the four GCMs and two lake models (n=2920) for 46 lakes for RCP 6.0 for the time period 2006-2099. Sites are ordered according to regions with labels on the right side, separated by a bold line. See Table 6.6 for site reference names. ....	183
Figure 6.29 Mean and standard deviation (SD) of the monthly anomaly for density difference of stratification averaged across the four GCMs and two lake models (n=7200) for 46 lakes for RCP 6.0 for the time period 2069-2099. Sites are ordered according to regions with labels on the right side, separated by a bold line. See Table 6.6 for site reference names.....	184
Figure 6.30 30-year rolling mean of the annual summer anomaly for thermocline depth for 46 lakes simulated using GLM, averaged across four GCMs (n=14400) for RCP 6.0 for the time period 2036-2099. Sites are ordered according to regions with labels on the right side, separated by a bold line. See Table 6.6 for site reference names. Positive values indicate that the thermocline is getting deeper while negative indicates it is getting shallower. ....	186
Figure 6.31 30-year rolling mean of the annual anomaly for thermocline depth for 46 lakes simulated using GOTM averaged across four GCMs (n=14400) for RCP 6.0 for the time period 2036-2099. Sites are ordered according to regions with labels on the right side, separated by a bold line. See Table 6.6 for site reference names. Positive values indicate that the thermocline is getting deeper while negative indicates it is getting shallower. ....	187
Figure 6.32 Distribution of anomalies for 4 GCM for GOTM (n=122640) for six lakes from the local and global simulations for RCP 6.0 for the time period 2015-2099 for surface and bottom temperature. See Table 6.6 for site reference names. ....	188

Figure 6.33 Paired scatter plot. distributions and correlations of the 30-year rolling mean anomaly for air temperature (A) the four GCMs across all 46 lakes from 2036-2099.....	192
Figure 6.34 Paired scatter plot, distributions and correlations of the 30-year rolling mean anomaly for wind speed for the four GCMs across all 46 lakes from 2036-2099.....	193
Figure 6.35 Paired scatter plot, distributions and correlations of the 30-year rolling mean anomaly for downwelling shortwave radiation for the four GCMs across all 46 lakes from 2036-2099.....	194
Figure 6.36 Hexagon density scatterplot of annual GOTM anomaly versus GLM anomaly for the four GCMs and for the four scenarios for volumetrically averaged temperature for 46 lakes.....	195
Figure 6.37 Hexagon density scatterplot of annual GOTM anomaly versus GLM anomaly for the four GCMs and for the four scenarios for density difference between the surface and bottom for 46 lakes. ....	196
Figure 6.38 Hexagon density scatterplot of annual GOTM anomaly versus GLM anomaly for the four GCMs and for the four scenarios for thermocline depth for 46 lakes. ....	197

## List of Tables

Table 2.1 Characteristics of the five lake models, the General Lake Model (GLM), the General Ocean Turbulence Model (GOTM), the Freshwater Lake model (FLake), Simstrat and Dynamic Reservoir Model (DYRESM). .....	24
Table 3.1 The location, characteristics and climates of each of the four lakes, Erken, Feeagh, Kinneret and Langtjern (mono = monomictic, di = dimictic, oligo = oligotrophic, meso = mesotrophic, eutro = eutrophic). .....	40
Table 4.1 Description of the meteorological reanalysis datasets. ....	49
Table 4.2 Summary of meteorological variables available and associated references for calculations for those which were not present. A: Rothfusz, 1990 B: Crawford and Duchon, 1999, C: Lowe, 1976. ....	50
Table 4.3 Uncalibrated model fitness statistics calculated for the entire simulation period and full water column for each lake, Erken, (n=84240), Feeagh (n=83076) and Langtjern (n=30457), with each climate dataset ERA-Interim (ERA-Interim), ERA5, EWEMBI and Local for each of the four lake models FLake, GLM, GOTM and Simstrat. Statistics calculated were root mean square error (RMSE), Nash-Sutcliffe Efficiency (NSE) and Bias. ....	62
Table 4.4 Calibrated model performance statistics calculated for the entire simulation period for each lake: Erken (n=84240); Feeagh (n=83076) and Langtjern (n=30457), with four meteorological datasets: ERA-Interim (ERA-Interim), ERA5, EWEMBI and Local for each of the four lake models: FLake, GLM, GOTM and Simstrat. Statistics calculated were root mean square error (RMSE), Nash-Sutcliffe Efficiency (NSE) and Bias. ....	70
Table 5.1 Model performance over the entire study period for each lake comparing modelled temperatures to observed temperatures at corresponding depths.....	99
Table 5.2 Data assimilation performance for the different temporal frequencies showing the percentage improvement in forecast compared to the model run without data assimilation.....	109
Table 5.3 Run time (in seconds) for GOTM for the spin-up period and for each of the forecast periods and the free model run (NDA).....	114
Table 6.1 Summary of General Circulation Models used for the Inter-Sectorial Inter-Model Intercomparison Project (ISIMIP). ....	130

Table 6.2 Climate variables provided by each General Circulation Model (GCM). .....	131
Table 6.3 The four Regional Concentration Pathways (RCPs) (adapted from Moss <i>et al.</i> , 2010).....	134
Table 6.4 Parameters used in the GLM calibration with their default values and ranges. ....	141
Table 6.5 Parameters used in the GOTM calibration with their default values and ranges. ....	143
Table 6.6 Description of the location, characteristics and climates of each of the 60 sites. Lakes which did not meet the criteria for being included in this study are denoted by being in <b>bold</b> with an asterisk (*) next to the name. The criteria were that the RMSE had to be less than 2 °C and the NSE was greater than 0.5 for both models. Regions are outlined as described in Seneviratne <i>et al.</i> (2012): CEU = Central Europe, CNA = Central North America, ENA = East North America, EAF = East Africa, MED = Mediterranean, NAU = North Australia, SAU = South Australia and New Zealand, WNA = Western North America.....	149

## List of Abbreviations

<b>Abbreviation</b>	<b>Full description</b>
ACPy	Auto calibration utility for GOTM written in Python
AED	Aquatic Ecosystems Dynamics library
AEMON-J	Aquatic Ecosystem Modelling Network - Junior
ALA	Alaska
ALBM	Advanced Lake Biogeochemical Model
AU	Australia
CA	Canada
CAEDYM	Computational Aquatic Ecosystem Dynamics Model
CDS	Climate Data Store
CEU	Central Europe
CH	Switzerland
CLM4-LISS	Community Land Model version4 – Lake, Ice, Snow and Sediment simulator
CMA-ES	Covariance Matrix Adaptive Evolutionary Strategy
CMIP	Coupled Model Intercomparison Project
CNA	Central North America
COP	Conference of Parties
CORDEX	Coordinated Regional Downscaling Experiment
CZ	Czech Republic
DE	Germany
DkIT	Dundalk Institute of Technology
DLM	Dynamic Lake Model
DOC	Dissolved Organic Carbon

DOM	Dissolved Organic Matter
DOMCAST	Dissolved Organic Matter forecast model
DP	Don Pierson
DYRESM	Dynamic Reservoir Simulation Model
EAWAG	Swiss Federal Institute of Aquatic Science and Technology
EC	European Council
ECMWF	European Centre for Medium-range Weather Forecasts
EE	Estonia
EJ	Eleanor Jennings
ENA	Eastern North America
EnKF	Ensemble Kalman Filter
EPA	Environmental Protection Agency
ERA	ECMWF Re-Analysis
ERA-I	ERA-Interim
ES	Spain
ESM	Earth System Model
EU	European Union
EWEMBI	Earth2Observe WATCH forcing data methodology applied to ERA-Interim reanalysis data and ERA-Interim data Merged and Bias-corrected for ISIMIP
FABM	Framework for Aquatic Biogeochemical Models
FCR	Falling Creek Reservoir
FI	Finland
FME	A Flexible Modelling Environment for Inverse Modelling, Sensitivity, Identifiability and Monte Carlo Analysis
FR	France
GCM	General Circulation Model

GDP	Gross Domestic Product
GEWEX	Global Energy and Water Exchanges
GFDL-ESM2M	Geophysical Fluid Dynamics Laboratory Earth System Model with Modular Ocean Model version 4 (MOM4) component
GHG	Greenhouse Gases
GLEON	Global Lake Ecological Observation Network
GLM	General Lake Model
GOTM	General Ocean Turbulence Model
HAB	Harmful Algal Blooms
HADGEM	Met Office Hadley Centre Earth System Model
HFM	High Frequency Monitoring
IE	Ireland
IL	Israel
IPCC	Intergovernmental Panel on Climate Change
IPSL-CM5A-LR	Institut Pierre-Simon Laplace Climate Model 5A - Low Resolution
ISIMIP	Inter-Sectoral Impact Model Intercomparison Project
JPI	Joint Programme Initiative
KF	Kalman Filter
LLZ	Lower Lake Zurich
MAE	Mean Absolute Error
MED	Mediterranean
MIP	Model Intercomparison Project
MIROC5	Model for Interdisciplinary Research on Climate
MM	Madeline Magee
MOM	Modular Ocean Model
NASA	National Aeronautics and Space Administration

NAU	Northern Australia
NDA	No Data Assimilation
NEMO	Nucleus for European Modelling of the Ocean
NEU	Northern Europe
NIVA	Norwegian Institute for Water Research
NLDAS	North American Land Data Assimilation System
NO	Norway
NOAA	National Oceanic and Atmospheric Administration
NS	Noam Shachar
NSE	Nash-Sutcliffe Efficiency
NZ	New Zealand
OPW	Office of Public Works
ORCHIDEE	Organising Carbon and Hydrology In Dynamic Ecosystems
ParSAC	Parallel Sensitivity Analysis and Calibration
PAR	Photosynthetically Active Radiation
PROGNOS	Predicting in lake responses to change using near real time models
PRT	Platinum Resistant Thermistors
RCM	Regional Climate Model
RCP	Representative Concentration Pathways
RIW	Richard Iestyn Woolway
RL	Robert Ladwig
RM	Rafael Marcé
RMSE	Root Mean Square Error
RU	Russia
RW	Rwanda

SAU	South Australia
SD	Standard Deviation
SE	Sweden
SEK	Swedish Krone
SELMA	Simple Ecological Model for the Aquatic environment
SK	Sean Kelly
SRB	Surface Radiation Budget
SWR	Incoming Short-Wave Radiation
TKE	Turbulent Kinetic Energy
TM	Tadhg Moore
UK	United Kingdom
UNFCCC	United Nations Framework Convention on Climate Change
US	United States of America
UWA	University of Western Australia
WATCH	Water and Global Change
WFDEI	Earth2Observe WATCH forcing data methodology
WI	Wisconsin
WNA	Western North America
WT	Wim Thiery

## ABSTRACT

Lakes and reservoirs are under increasing pressure from urbanisation, agricultural intensification, and directional climate change, including an increasing occurrence of extreme climatic events. These pressures can reduce water quality by promoting the occurrence of nuisance algal blooms and higher levels of dissolved organic carbon (DOC), two issues that can cause substantial problems for water treatment, aquatic ecology and recreational users. Thus, there is a need to develop a modelling framework that is flexible, adaptable and provides information that can be utilised to mitigate potential risks to lakes and reservoirs. This thesis describes three specific pieces of work which in combination, further the use of hydrodynamic models for adaptive management. Firstly, the suitability of different meteorological datasets for forcing one-dimensional hydrodynamic models and accurately simulating water temperatures was examined. The European Centre for Medium-Range Weather Forecasts produces freely available gridded meteorological datasets: ERA-Interim, ERA5 and EWEMBI. Lake temperature simulations produced using these three datasets were compared to those based on local meteorological data. Simulations with ERA5 and ERA-Interim simulated water temperatures to a similar degree of accuracy as those forced with local measured data. This highlighted how gridded meteorological datasets can be used to simulate lake thermodynamics in areas where there is no locally measured meteorological data. Secondly, the improvement in short-term model performance when assimilating observed water temperature profile data into model simulations was assessed. Single profiles were inserted into simulations for three lakes that reflected potential monitoring programmes of different temporal frequencies. These monitoring data were compiled by subsetting high frequency data from the sites. Assimilating measured temperature profiles of up to one month prior to the forecast, greatly reduced forecast error. This will allow for short-term forecasting frameworks to be developed for low-frequency monitoring programmes. In the last results section, the effects of different future climate change scenarios on water temperature for a global set of lakes were characterised, using an ensemble of lake models forced with an ensemble of General Circulation Models. The responses in lake temperature and in functional characteristics such as the strength and length of stratification were shown to be highly variable across 46 lakes of varying morphometries. Comprehensively, there was an unequivocal warming of lake water temperature throughout the water column and an extension of the duration of

stratification. Such increases in water temperature, heighten the risk of anoxia and the occurrence of algal blooms which are water quality issues which can be actively managed. Overall, this study has found that lake forecasting frameworks (short and long term) can be setup using open access software and data, for sites with low-frequency monitoring data, forced with freely available meteorological data and produce high quality forecasts. These finding will be of increasing importance as we seek to simulate our freshwater ecosystems in a rapidly changing climate to aid in their management.

# CHAPTER 1. INTRODUCTION

## *1.1. Background*

Lakes and other inland water bodies are critically important to sustain food production (Foley *et al.*, 2011), provide drinking water (Delpla *et al.*, 2009), and a range of other ecosystem services (Schallenberg *et al.*, 2013). The structure, functioning and stability of lake ecosystems are, however, under increasing pressure from climate change and other human-related pressures including the intensification of agriculture and increased urbanisation (Blois *et al.*, 2013; Isaac and Williams, 2013; Bunting *et al.*, 2016; Hundey *et al.*, 2016). There is a clear need to monitor and project the impacts of climate change, which are already having large effects on lakes globally (Reilly *et al.*, 2003). A significant decrease in the duration of lake ice cover (Benson *et al.*, 2012), and changes in the duration and nature of thermal stratification in lakes have already been reported (Woolway *et al.*, 2016). These changes have subsequent effects on lake chemistry and biology, impacting the ecosystem services provided by lakes, including water aesthetics, recreational use, fisheries, water treatment processes and drinking water quality (Delpla *et al.*, 2009; Whitehead *et al.*, 2009). All of these water quality issues occur throughout Europe (Sanseverino *et al.*, 2016) and in Ireland (Irvine *et al.*, 2011), and can affect water quality status as defined by the EU Water Framework Directive (WFD) (European Council, 2000).

The overarching goal of environmental monitoring is the development of a causal and mechanistic understanding of processes (Stow *et al.*, 1998). Many ecological processes occur at varying temporal and spatial scales and without monitoring for long-time periods, the ability to actively manage ecosystems is reduced (Magnuson, 1990). In the context of lakes, collecting *in-situ* data allows the state of the lake to be assessed and, when carried out over long periods of time, it can be used to monitor changes in the lake's state. However, such monitoring is resource intensive, and only a very small proportion of global lakes are actively monitored (Toming *et al.*, 2016). Remote sensing can now be used to fill some of the spatial and temporal gaps in lake monitoring programs by providing snapshots of water quality at global and regional spatial scales that were previously impossible (Mantzouki *et al.*, 2018). In addition, there has been an increase in the number of lake sites worldwide which are being monitored using high frequency

monitoring equipment on moored buoys within lakes (Hanson *et al.*, 2016). This has led to improvements in our understanding of the hydrodynamics and aquatic ecology of lakes at very fine temporal scales, and has also contributed to the development of aquatic ecosystem models (Hipsey *et al.*, 2019). Monitoring provides data for calibrating and validating model behaviour which is fundamental to any modelling development (Hamilton *et al.*, 2015). Numerical lake models combined with monitoring data have been shown to have the potential to be used for the optimisation of water quality management through scenario testing and forecasting (Imberger *et al.*, 2017; Tranmer *et al.*, 2020).

Modelling of lake ecosystems involves using numerical models to represent dynamic in-lake processes. The development of such models serves two main purposes. First, models can be used to test a hypothesis or theory related to an ecosystem process or functioning. Several iterations of this process have led to the advancement of our knowledge within physical limnology (Fischer *et al.*, 1979; Imberger and Patterson, 1989; Wüest *et al.*, 2000; Goudsmit *et al.*, 2002; Mironov, 2008; Dutra *et al.*, 2010; Hu *et al.*, 2016). Secondly, they are used to provide information on the future state of the lake ecosystem (Peng *et al.*, 2019). This can provide short-term prediction, on the scale of one day to one year, referred to as forecasts, or long-term future states on decadal to centennial time scales, referred to as projections. Significant advances in computing power and data collection has greatly accelerated the use of process-based modelling in ecology (Hallgren *et al.*, 2016; Farley *et al.*, 2018). A wide range of numerical models have been developed that simulate differing aspects of lake systems with varying degrees of complexity (Stepanenko *et al.*, 2010). These include many widely used models of lake hydrodynamics, which are fundamental to any simulations of ecosystems responses in lakes. Coupling these lake hydrodynamic models with biogeochemical models can provide crucial information to lake managers as they seek to mitigate the effects of climate on these crucial ecosystems (Bruggeman and Bolding, 2014).

Active management is required to deal with the many pressures lake face, whether it is water security (Tzabiras *et al.*, 2016), nutrient limitation (Maberly *et al.*, 2020a) or hydropower (Jahandideh-Tehrani *et al.*, 2014). Decision making in these circumstance needs to be informed with sound scientific evidence. Tools for analysis and aiding decision making are constantly being developed for environmental purposes (Dorner *et al.*, 2007; McIntosh *et al.*, 2011). Environmental models can sometimes carry large risks if the uncertainty is not quantified and communicated effectively (Uusitalo *et*

*al.*, 2015). Hydrodynamic models have been applied for management scenarios focused on reducing the occurrence of cyanobacteria blooms (Ladwig *et al.*, 2018) and controlling the lake mixing regime (Mi *et al.*, 2019). A real-time adaptive management system which would utilise available monitoring data with numerical modelling would provide up-to-date pro-active management steps which could be carried out as needed to aid in lake management (Imberger *et al.*, 2017).

## *1.2. Research objective*

The primary aim of the research undertaken for this dissertation was to examine the application of hydrodynamic models to provide accurate information on lake thermal structure, over both short term (forecasts) and long term (future projections) timescales.

The overall objectives of this PhD thesis are to:

1. Investigate the ability of gridded climate reanalysis datasets to accurately force lake models when compared to locally measured meteorological data.
2. Assess the potential for assimilating measured lake temperature profiles into model runs to produce short-term water temperature forecasts using data from three lakes with differing local climates and morphologies.
3. Design a modelling framework for assessing projected climate change impacts on lake thermal dynamics and quantify these impacts for three different future emission scenarios, across 46 different lakes using an ensemble of climate and lake models.

Together, the work described in this thesis addresses some of the key issues associated with implementing automated lake modelling workflows, including efficiency, coverage, uncertainty and accuracy. By adapting lake models for forecasting for existing monitoring systems (objective 2), expanding their use to sites that do not have measured met data (objective 1) and developing a modelling framework to understand the threats posed to these systems by future changes in the climate (objective 3), this work significantly contributes to the use of lake models as a tool for managing lake ecosystems.

### *1.3. Synergies*

The work described here was linked to both the PROGNOS project (Predicting in lake responses to change using near real time models) (PROGNOS, 2020) and the WateXr project (WateXr, 2020). PROGNOS was a Water JPI funded project which focused on developing a modelling framework that could predict changes in the water quality of lakes and reservoirs in the short-term i.e. 5-7 days. The modelling frameworks adopted within PROGNOS included coupling a lake physical model with a lake biogeochemical model and using local meteorological forecast data to drive the coupled lake model. Chapters 4 and 5 describes some of the work that went into developing that framework. WateXr is focused on co-developing tools for water resource managers which integrate seasonal weather forecasts and future climate projections with impact models for lake and reservoirs. The PROGNOS modelling framework is currently being utilised and developed further within WateXr. It is envisaged that the WateXr modelling frameworks will be used to inform water resource management and support the decisions making process to safeguard the ecosystem services the lake provides such as drinking water or recreational uses. Within WateXr, project members also contributed to the development of a new sector of impact models (Lake Sector) within the Inter-Sectoral Impact Model Intercomparison Project (ISIMIP) (ISIMIP, 2020). One of the aims of ISIMIP is to quantify the impacts of an increase of 1.5 °C in global air temperature, following the agreement of the Conference of the Parties (COP) in Paris, France in December 2015 (UNFCCC, 2015; Frieler *et al.*, 2017). Knowledge acquired during both the PROGNOS and WateXr projects allowed the timely development of the lake modelling framework for ISIMIP.

### *1.4. Thesis outline*

This thesis is arranged into seven chapters (Figure 1.1). This introduction is followed by a comprehensive review of the literature with a focus on the areas relevant to lake physics, monitoring, modelling and the impacts of climate change on thermal dynamics in lakes and reservoirs (chapter 2). The lake study sites used in chapters 4 and 5 are

described in chapter 3. Chapters 4-6 are three draft articles related to each of the three objectives outlined above. Chapters 4 and 5 have an introduction, materials and methods, results, discussion and conclusions. Chapter 6 has an introduction, a description of data sources and simulation protocol for the ISIMIP Lake sector, results, discussion and conclusion. There is a synthesis of the overall findings, outlining of future areas for research and describing the potential application of the described framework in an Irish context in chapter 7.

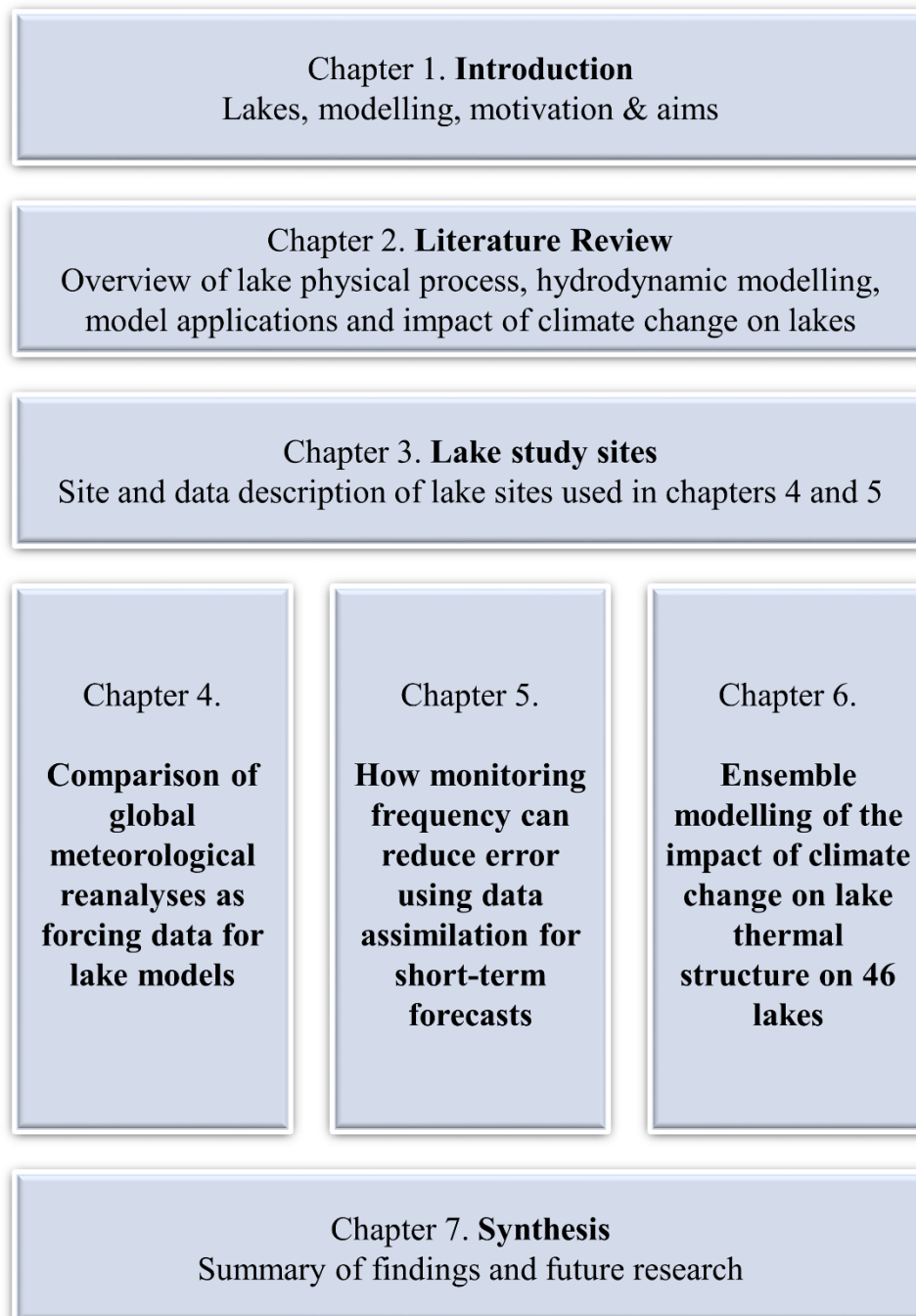


Figure 1.1 Overview of thesis.

## CHAPTER 2. LITERATURE REVIEW

### 2.1. Lake physics

#### 2.1.1. Thermal structure of lakes

The thermal structure of lakes controls many aspects of chemical and biological lake functioning (Wetzel, 2001; Reilly *et al.*, 2003; Cantin *et al.*, 2011). Most aquatic organisms are ectotherms, relying on the temperature of the local environment to control their biological activity (Bullock, 1955; Goldman, 1974). Water temperature also influences water chemistry. At higher temperatures reactions occur more quickly and this is a major controlling factor for chemical and biological activity, including in lakes (Butterwick *et al.*, 2005). Dissolved oxygen is one of the main chemical elements in water that is affected by temperature as at higher temperatures the water holds less oxygen so while the water could be saturated with oxygen at very high temperatures, it still may not have enough to support aquatic life (Downing and Truesdale, 1955).

Within lakes, the main source of heat is from incoming solar radiation (Henderson-Sellers, 1986). Water has a high specific heat capacity and when the light enters the water, it dissipates in the form of heat energy (Mikulski, 1973; Wetzel, 2001). Heat can also be transferred by conduction with the air (McCombie, 1959) and by the addition of heat from the sediment (Tsay *et al.*, 1992). Heat is lost from the lake by thermal radiation (Saur and Anderson, 1956), conduction (Williams, 1963), evaporation (Dake, 1972) and through the outflows (Saur and Anderson, 1956) (Figure 2.1) . Wind is the main force which controls the vertical distribution of heat within a lake (Peeters *et al.*, 2002). Wind stress on the surface of the lake generates turbulence which causes mixing of heat energy from the upper layers to the lower layers (Imberger, 1985; Boehrer and Schultze, 2008; Branco and Torgersen, 2009). When the lake is isothermal there is a similar temperature throughout the lake water column. In this isothermal state, mixing occurs even with a small amount of wind energy (Smith, 1979).

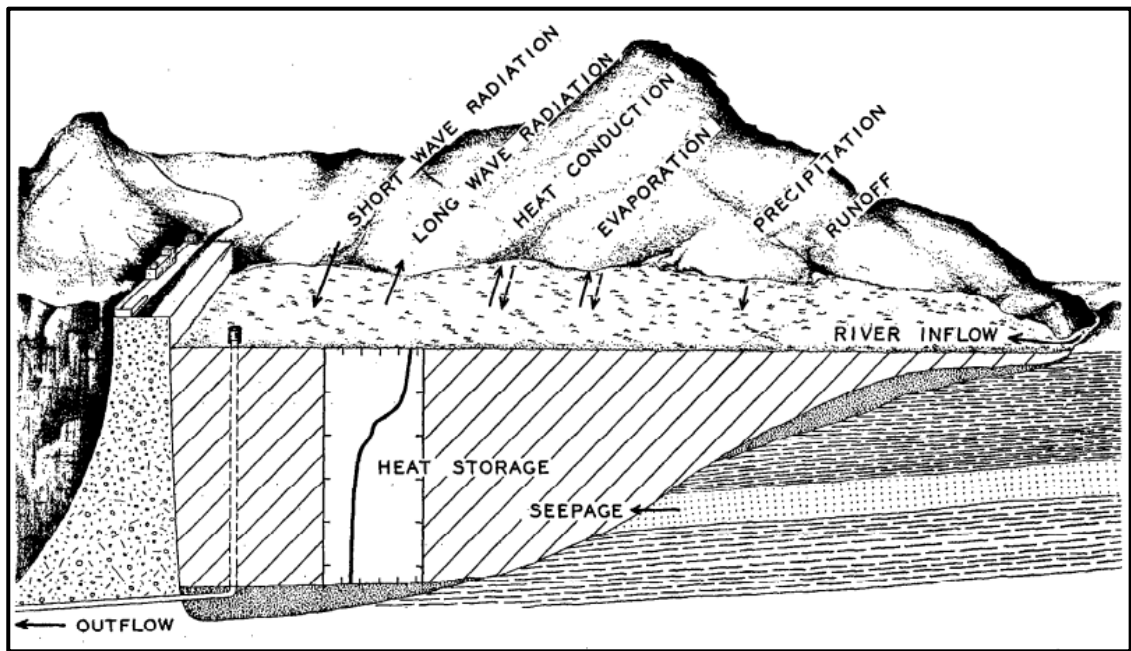


Figure 2.1 Major heat exchange processes operating in an enclosed water body (Adapted from Saur and Anderson, 1956).

During the spring, when solar radiation begins to increase, there is generally an increase in the water temperature at the surface of a lake (Imberger, 1985; Kirk, 1988). This warmer water becomes less dense, and a density difference forms between the surface and bottom which prevents the whole water column from mixing and the lake is stratified (Boehrer and Schultze, 2008). A lake is referred to as thermally stratified when there is a temperature gradient greater than  $1\text{ }^{\circ}\text{C m}^{-1}$  (Stefan *et al.*, 1996; Wetzel, 2001; Foley *et al.*, 2012). The occurrence of stratification in lakes does not happen suddenly, generally it occurs over a period of time (Stainsby *et al.*, 2011). There is no universal definition of stratification with variations such as a temperature difference of  $1\text{ }^{\circ}\text{C}$  between top and bottom (Stefan *et al.*, 1996; Read *et al.*, 2014; Woolway *et al.*, 2014), a density difference between top and bottom of  $0.025 - 0.07\text{ kg m}^{-3}$  (Staehr *et al.*, 2012; Woolway *et al.*, 2017b) or a consistent stability threshold related to Schmidt stability (e.g.  $>30\text{ J m}^{-2}$  Read *et al.*, 2011). As the summer progresses, temperatures generally increase in the upper layers of the water column, leading to the creation of three layers in the water column which are referred to as the epilimnion, the metalimnion and the hypolimnion. The epilimnion is the upper layer which generally has a uniform warm temperature and in which the water is circulating (Hutchinson and Loffler, 1956). The metalimnion is the water layer with a steep thermal gradient. The thermocline occurs within the metalimnion and it is the plane of the maximum rate of decrease in temperature with respect to depth, usually  $>1\text{ }^{\circ}\text{C m}^{-1}$  (Balon and Coche, 1974). The hypolimnion is

the region below the metalimnion which is distinctly colder than the epilimnion and usually has a relatively uniform water temperature (Wetzel, 2001).

Heat is transferred to lower depths in a lake by incoming light radiation, convection currents, diffusion and turbulence (Dake and Harleman, 1969). The depth to which light can penetrate into the water column is controlled by light attenuation (Wetzel, 2001). Light attenuation is the exponential decrease of light intensity with depth according to Beer-Lambert Law (Swinehart, 1962). Factors which affect light attenuation include concentration of chlorophyll-a (Sánchez *et al.*, 2017), dissolved organic matter (DOM) (Watras *et al.*, 2015) and suspended solids. (James *et al.*, 2004). In high concentrations, these can increase the turbidity of the water and reduce the depth to which light can penetrate. Thermocline depth has been shown to be positively correlated with water transparency in Arctic lakes (Fortino *et al.*, 2014).

Turbulence within the epilimnion can carry heat energy into the metalimnion and further into the hypolimnion (Imberger and Patterson, 1989). In temperate climates, throughout the summer season, as the lake gets more heat energy, the epilimnion and metalimnion deepen down into the hypolimnion as the lake stores more heat energy (Wetzel, 2001). During the period of stratification, the lake is referred to as stable. This stability is defined mathematically as the amount of energy required to mix the entire volume of the lake without the addition or subtraction of heat energy (Schmidt, 1928; Hutchinson, 1957; Idso, 1973). It is a way of quantifying the resistance of the lake to mixing forced by the wind due to the potential energy inherent within the water column.

Towards the end of the summer season the amount of heat energy coming into the lake is generally reduced and the lake begins to cool. Autumn turnover is the period when the summer stratification breaks down and the lake mixes (Boehrer and Schultze, 2008). This breakdown can occur over a couple of weeks (Lake Mendota, WI, US) or in a few hours (Lake Wingra, WI, US) (Jenkin, 1942; Coulter, 1963; Reynolds, 1980; Magee and Wu, 2017). The main drivers of this breakdown are usually higher wind speeds coupled with heat losses. Monomictic lakes then return to an isothermal state until the onset of stratification in the following spring or early summer (Boehrer and Schultze, 2008). River inflows and outflows can also influence lake stratification as depending on the density they will entrain at different depths (Cortés *et al.*, 2014). Inflows affect the depth of the thermocline, surface temperature in summer, hypolimnion temperature, surface temperature in winter and the rate of heating and cooling within the water column

(Fenocchi *et al.*, 2017). Nutrients within the inflows enter at the intrusion depth of the inflow and only become mixed when a mixing event occurs within the lake (Marti *et al.*, 2011).

Lakes can be classified according to their mixing regime with the three most common types of lakes being monomictic, dimictic and polymictic (Lewis, 1983). Monomictic lakes are lakes which undergo mixing once a year, usually in the autumn period. Dimictic lakes have two mixing periods per year, one following summer stratification and another following ice cover and inverse stratification in winter. Polymictic lakes are lakes which stratify and mix multiple times a year.

Stratification can control the distribution of dissolved and suspended materials (Etemad-Shahidi and Imberger, 2001) and allow them to concentrate above and below the thermocline (Elçi, 2008). The materials tend to concentrate near the thermocline and in a layer just above the sediment water interface (Harrsch and Rea, 1982). The thermocline plays a role in regulating the vertical distribution of bacterial community composition, but this is due to its control of water quality parameters such as dissolved oxygen, conductivity, and nutrients (Yu *et al.*, 2014; Zhang *et al.*, 2015). The thermocline can also act as a barrier to dissolved oxygen and increase the probability of anoxia occurring in the hypolimnion (Elçi, 2008). It also plays an important role in zooplankton and phytoplankton biomass and composition. Deepening of the thermocline as a result of increased mixing has been shown to increase zooplankton biomass (Sastri *et al.*, 2014) and dominance by smaller fish-evasive species (Gauthier *et al.*, 2014). Phytoplankton has exhibited greater production in the epilimnion in response to deepening thermocline (Cantin *et al.*, 2011).

#### 2.1.1.1. Heat Fluxes

Lakes have a dynamic interaction with the atmosphere with regards energy, mass and momentum fluxes (Samuelsson *et al.*, 2010). They integrate climate signals and respond quickly to local changes in meteorology (Adrian *et al.*, 2009; Jennings *et al.*, 2012). This interaction at the air-water interface has been well researched in the context of oceanography for gas exchange (Hasse and Liss, 1980), biogeochemistry interactions (Haese, 2006) and heat and mass exchanges (Kondo, 1975; Liu *et al.*, 1979; Fairall *et al.*,

1996) where the same principles can be applied for lakes. Heat fluxes can affect lake stratification and ice cover duration (Anderson *et al.*, 1996). Lake surface heat fluxes, are influenced by the surface area and the latitudinal position, where larger lakes and those at low latitudes have a higher rates of heat loss (Woolway *et al.*, 2018).

### 2.1.2. Turbulence

Within lakes there are two main types of flow: laminar flow and turbulent flow (Wetzel, 2001). Laminar flow occurs at slow speeds where water moves in straight lines with no interaction (Smith, 1979; Saggio and Imberger, 2001). Turbulent flow occurs when the water reaches a critical velocity or when there is opposing horizontal movement between layers of water of different densities (Wetzel, 2001). Turbulent flow is the main flow that is found within lakes. Wind is the main driver of turbulence, particularly at the surface boundary layer (Kocsis *et al.*, 1999; Wüest *et al.*, 2000). Turbulent flow allows for the exchange of heat energy within a lake. Turbulent kinetic energy (TKE) is the mean kinetic energy per unit mass associated with eddies in turbulent flow (Pope, 2000). The transfer of heat energy across a thermal gradient can be used to approximate how much turbulent transport is present. The coefficient of eddy diffusivity ( $K_z$ ) is a measure of the rate of exchange of mixing across the plume. This also allows the estimation of turbulence from changes in temperature. Hondzo and Haider (2004) found that within small stratified lakes, a turbulent boundary layer develops. The thickness of this layer is dependent on 1) the dissipation of TKE, 2) the strength of stratification, 3) the length of the sloping boundary and 4) the angle of inclination of the sloping boundary. When a lake has gently sloping boundaries, it reduces the energy from internal waves. In shallow lakes, the occurrence of submerged macrophytes also increases the dissipation of TKE and attenuates wind-induced vertical mixing (Herb and Stefan, 2004).

The irregular, diffusive, dissipative flow of water with no velocity direction causes changes in water column turbulence (Tennekes and Lumley, 1972). Diapycnal mixing, that is mixing across surfaces of equal density, is a hugely important physical process within lakes. It plays a role in the vertical distribution of chemical and biological constituents (Goudsmit *et al.*, 1997). Diapycnal fluxes are mainly determined by mixing which occurs in the bottom boundary layer (Goudsmit *et al.*, 1997).

Eddy diffusion coefficients of turbulence depend on the degree of stratification in lakes (Hondzo and Stefan, 1993). Vertical eddy diffusivity is the main process which determines heat transfer at lower depths within lakes (McCormick and Scavia, 1981). Vertical eddy diffusivity within the water column is ten times less than that at the lake-atmosphere boundary layer (Etemad-Shahidi and Imberger, 2001). Boundary mixing that occurs at the thermocline plays an important role in propagating internal waves throughout the lake. This transfers energy between different zones within the lake (Lorke, 2007). High frequency internal waves have a large contribution to temperature and current velocity in the littoral zone. They can cause large fluctuations and the period of these fluctuations is directly related to the buoyancy frequency (Lorke *et al.*, 2006).

Turbulent kinetic energy is supplied by wind shear. This can be calculated using data on the lake surface area and shear velocity (Hondzo and Stefan, 1993). The vertical transfer of thermal energy is primarily driven by turbulent mechanisms, even below the epilimnion (Jassby and Powell, 1975). Horizontal turbulence is generated by shear at the surface, while towards the bottom of the lake it is generated by inertial subrange diffusion. Shear is of critical importance because it is highly correlated with wind forcing and diffusion coefficients during events where there is high wind speeds (Lemmin, 1989).

Lake thermodynamics are driven by exchanges of energy between the lake water and the atmosphere. When air temperature increases, surface water temperatures increase concurrently (Rempfer *et al.*, 2010). Studies to date indicate that surface waters and lake stability will increase across lakes because of warmer air temperatures in response to increased greenhouse gas emissions (O'Reilly *et al.*, 2015; Sahoo *et al.*, 2016; Woolway and Merchant, 2019). Lake surface temperatures are projected to increase by 70 – 85 % of air temperature increases in the coming decades (Schmid *et al.*, 2014), leading to longer stratification periods (Palmer *et al.*, 2008; Adrian *et al.*, 2009; Vincent, 2009; Sahoo *et al.*, 2016). The response of bottom temperatures in lakes to higher temperatures is more complex and variable because of its dependence on mixing and other energy inputs (Kraemer *et al.*, 2015). Under projections of increased air temperature, deep lakes are likely to be more resistant to thermal changes, while in northern lakes it is predicted that there will be a reduction in the length of ice cover during winter (Butcher *et al.*, 2015). This effect of climate warming could possibly be reduced and maybe even reversed by the associated changes in river discharge regimes as a result of climate change (Zhang *et al.*, 2014; Fenocchi *et al.*, 2017). Råman Vinnå *et al.* (2017) found that the river water

temperature had to be lower than that of the lake to have a cooling effect to counteract warming by climate change. They also concluded that the tributaries can have an influence on the whole lake system in lakes with a residence time of less than 1000 days.

Within lakes there are different types of mixing: buoyant convection (Carmack and Weiss, 1991), wind-driven eddy diffusivity (Jassby and Powell, 1975) and molecular diffusivity (Imboden and Wüest, 1995). One-dimensional lake models capture these processes by parameterizing the mechanical energy balance or with turbulence and diffusion equations (McCormick and Scavia, 1981). They parameterise the boundary effects of lake bathymetry and lake surface exchanges with the atmosphere.

### *2.1.3. Mass Transport*

There are two main types of mass transport in lakes: diffusive mass transport and advective mass transport. Diffusive mass transport occurs *via* two processes: molecular diffusion, which is slow, and turbulence diffusion, which is much faster (Auer *et al.*, 2013). The onset of stratification is a product of this type of mass transport. In large lakes, water can heat up close to the shore and lead to the creation of a horizontal density gradient between shallow waters and deeper waters. Water moves towards the density gradient from both sides and sinks at the gradient creating convective cells (Rao *et al.*, 2004). This region of a density gradient is called a thermal bar and it can trap suspended sediment near the shorelines of the lake. It disappears as water temperature begins to increase and the bar moves outwards into deeper regions of the lake (Schertzer *et al.*, 1987; Holland and Kay, 2003).

Advective mass transport is when the transport is unidirectional and the identity of the substance being transported remains the same (Auer *et al.*, 2013). Exchanges occur between the pelagic and littoral zones and these occur when there are horizontal differences in density (MacIntyre and Melack, 1995). This includes current and temperature gradients, Coriolis force in large lakes, seiche movements and river plumes. Currents are driven by temperature and wind interacting with the bathymetry of the lake (Bennington, *et al.*, 2010). The Coriolis force is noticeable in deep large lakes such as the Great Lakes (Tsvetova, 1998) or long deep lakes in Italy (Pilotti *et al.*, 2018; Piccolroaz *et al.*, 2019). Seiche movement in a lake is when a strong wind force pushes the lake

water mass towards one shore. When the wind force then drops, the water returns in the form of a wave (Trebitz, 2006). Seiches can occur at regular intervals with a lake, with periods of 2-14 hours, and this creates internal waves. This is particularly evident when the lake is stratified, and it can lead to oscillation of the thermocline and drive mixing, thus deepening the surface mixed layer (Antenucci *et al.*, 2000; Saggio and Imberger, 2001). It influences the spatial heterogeneity and horizontal differences in production of phytoplankton (Hingsamer *et al.*, 2014). It usually occurs along the long-axes of the lake and lake morphometry and bathymetry also play an important role in how this wave propagates through the basin (Auer *et al.*, 2013). Valerio *et al.* (2012) used the presence of an island in Lake Iseo to analyse the effect of lake bathymetry by comparing models of the internal wave in the lake with and without the island. The island disrupted the symmetry of the wave and amplified the vertical displacement in the area around the island.

Rivers and withdrawals can transport heat, nutrients and suspended sediment into and out of lakes. The transport of these within the lake is mainly controlled by density differences (Fischer *et al.*, 1979). River and stream inflows are key to heating parts of the lake which are not reached by sunlight such as areas across the thermocline and also within the hypolimnion by aiding convective mixing (Fenocchi *et al.*, 2017). The rate and size of the inflows are one of the controlling factors in the distribution of water masses within the lake. The circulation driven by rivers depends on the rate of the inflow and also the temperature of the lake relative to the temperature of the inflow (Carmack *et al.*, 1986). Carmack (1979) showed that, for Kamloops Lake in Canada, the riverine flow-controlled lake-wide circulation patterns particularly prior to spring overturn. Depending on the residence time of the lake, the overall contribution of inflows to the lake's thermal budget is dependent on the inflow mass but in comparison to the contribution of atmospheric fluxes, it is generally quite low (Peeters *et al.*, 2002).

## 2.2. *Limnological monitoring*

Monitoring of lakes allows for further understanding of the complexities of processes occurring within the lake. In addition to the rate at which these processes occur, there are strong physical, chemical and biological interactions occurring between differing processes. Lakes have been referred to as sentinels of climate change because they are

known to integrate long-term climatic signals (Adrian *et al.*, 2009) and can respond quickly to local meteorological perturbations (Maberly, 1996; MacIntyre *et al.*, 1999; Woolway *et al.*, 2015). Long-term studies of lake surface temperature have been used as indicators of the varying effects of climate change globally during summer (Peeters *et al.*, 2002; Livingstone, 2003; Coats *et al.*, 2006; O'Reilly *et al.*, 2015; Sahoo *et al.*, 2016). The temporal resolution of traditional monitoring would be weekly to monthly time scales using handheld sensors, but these do not capture sub-daily changes in lake function. To capture short-term changes within lakes, moored buoys with suites of high frequency sensors have been deployed in lakes which measure water temperature throughout the depth profile, meteorological conditions above the lake, and an array of chemical parameters using a selection of sondes (Daly *et al.*, 2004; Porter *et al.*, 2009; Marcé *et al.*, 2016). Lake water temperature profiles are generally one of the commonly measured parameters (Jennings *et al.*, 2017).

Monitoring of lakes is often supplemented with numerical modelling. Models are crucial tools used to test hypotheses and to gain further understanding of how systems behave. Furthermore, long-term monitoring data provided the basis for calibrating such models (Gal *et al.*, 2009; Arhonditsis *et al.*, 2017; Luo *et al.*, 2018; Ayala *et al.*, 2019; Moras *et al.*, 2019).

### 2.3. Lake and reservoir modelling

#### 2.3.1. Hydrodynamic models

Changes in lake thermodynamic structure profoundly influence lake functioning, including biological activity. These physical changes include the timing of autumn overturn, the onset and offset of winter ice-cover, the earlier occurrence of stratification in spring, the development of a stronger gradient in the thermocline and a general warming of the entire water column (Perroud *et al.*, 2009). There are two main types of lake models: empirical models where the structure is based on the observational relationship among experimental data, and mechanistic models which represent physical, chemical and biological processes within a lake. A mechanistic model is a model that uses differential equations and changes with reference to time and represents behaviour

(Dowd, 2006). Models of lake physical structure help to summarise and integrate current knowledge of lake dynamics and the various factors which influence water quality (Stepanenko *et al.*, 2010). They also help to increase understanding of how a lake responds under specific environmental conditions. Lake models are a tool that allows water resource managers to evaluate different in-lake scenarios at a moderate cost to more expensive monitoring practices (Hamilton and Schladow, 1997; Omlin *et al.*, 2001). There have been recent developments of a hybrid model, “air2water”, which simulates surface temperature based on both a mechanistic model and an empirical model (Piccolroaz, 2016; Piccolroaz *et al.*, 2018).

Lake hydrodynamics can be modelled in two different ways: finite difference models and bulk-lake models (Stepanenko *et al.*, 2010). Finite-difference models use a down-gradient approximation for heat transfer equations to parameterize turbulent fluxes of heat using finite difference methods (Cheng *et al.*, 1976). The k-epsilon (k- $\epsilon$ ) turbulence model is the most common model used in computational fluid dynamics to simulate mean flow characteristics for turbulent flow conditions (Versteeg and Malalasekera, 1995). It is a two-equation model which gives a general description of turbulence by means of two transport equations. The two equations allow it to account for historical effects from convection and diffusion (Bardina *et al.*, 1997). K-epsilon parameterisation is a more sophisticated way of calculating turbulence fluxes.

Bulk lake models are generally applied in atmospheric or numerical weather prediction models to calculate the lower boundary condition of surface temperature and moisture needed to compute turbulent fluxes at the lake–atmosphere interface (Hodges *et al.*, 2000a; Mironov, 2008; Wang *et al.*, 2015). They are mostly used to model surface lake temperature (Stepanenko *et al.*, 2010). There is no single lake model that can be used to model lakes across a wide variety of climate scenarios and different physical types of lakes (Mooij *et al.*, 2010; Stepanenko *et al.*, 2010). Turbulence models, however, are usually computationally expensive, and they generally require extensive lake-specific data which is one of the reasons they have not yet been used in any climate models (Subin *et al.*, 2012).

### 2.3.2. Modelling in different dimensions

Lake models can differ in their spatial dimension and the choice of dimension to use is dependent on the application of the model. One dimensional (1D) modelling requires that variables change predominantly in one defined direction and within lakes the vertical gradient is where the most change is. When modelling lake physics, and where there is no focus on horizontal variability, then 1D modelling is the best option (Hipsey *et al.*, 2014).

Two-dimensional (2D) models have been used to model basin currents in large lakes (Boegman *et al.*, 2001), lake level fluctuations (Schwab *et al.*, 1981; Paul *et al.*, 2019) and eutrophication dynamics (Li-kun *et al.*, 2017). These work well when predicting horizontal variability in lakes but they tend to poorly replicate the vertical variability with a high enough level of accuracy to simulate the thermal structures and fluxes correctly (Swayne *et al.*, 2005).

Three dimensional (3D) modelling of lakes is more advantageous than 1D or 2D modelling because it allows for modelling of internal waves, mixing, spatial gradients and higher resolution (Hodges *et al.*, 2000b). The main drawbacks of 3-D modelling are that it requires high computational power and memory, higher data requirements and higher level of expertise (Castelletti *et al.*, 2009; Acosta *et al.*, 2015).

Generally 3D models are used mainly for large lakes and are often coupled with climate models for global and regional climate studies (Swayne *et al.*, 2005) and incorporated into atmospheric forecast models (Huang *et al.*, 2010). One dimensional models are more frequently used for characterisation of lake physics within a target lake (Kirillin, 2003; Kara *et al.*, 2012; Read and Rose, 2013; Rose *et al.*, 2016a) or on a regional scale (Read *et al.*, 2014; Le Moigne *et al.*, 2016; Woolway *et al.*, 2019). They have also been coupled with biogeochemical models to assess, for example, nutrient cycling within a lake (Mukherjee *et al.*, 2008), phytoplankton abundance (Zwart *et al.*, 2015) or the impact of macrophytes on water quality (Hilt *et al.*, 2010). A study on two reservoirs in Australia which combined 1D and 3D hydrodynamic models with one biogeochemical model found that this approach provided much more insight into simulating biogeochemical fluxes and a more accurate representation of ecological processes (Romero *et al.*, 2004).

### 2.3.3. Finite-difference models

Eddy diffusion models are finite-difference models where the diffusion of energy within a lake is mixed by eddy motion. Turbulence-based models calculate the amount of turbulent kinetic energy that is available, parameterise the vertical transport by eddies, and include functions for the dissipation of energy (Imberger *et al.*, 1978; Burchard and Baumert, 1995).

The structure of 1D models varies but the two most common structures are Lagrangian and Eulerian. Lagrangian models divide the lake into horizontal layers with uniform properties but wherein the layers can get larger, smaller, and even merge with other layers in accordance with how the mixing equations have been parameterised (Imberger and Patterson, 1981; Hipsey *et al.*, 2019). The General Lake Model (GLM) and the Dynamics Reservoir Simulation Model (DYRESM) are examples of Lagrangian models. Eulerian models are oriented on a fixed grid structure with fluxes occurring between the different grids. The General Ocean Turbulence model, Simstrat and the multi-year lake simulation model (MyLake) are examples of models that use a Eulerian grid (Goudsmit *et al.*, 2002; Burchard *et al.*, 2006; Saloranta and Andersen, 2007).

### 2.3.4. Coupling a physical model with a biogeochemical model

Numerous biogeochemical models have been developed of varying degrees of complexity with process-specific modules. The Framework for Aquatic Biogeochemical Models (FABM) is a very powerful tool as it allows the user to dynamically couple biogeochemical models to physical models and to select different modules from different biogeochemical models. At runtime modules from different models can be combined to create custom-tailored models to adapt the model to the needs of different lakes (Bruggeman and Bolding, 2014). While such coupling is not part of the current study, the modelling work described here forms the basis for coupled physical-biogeochemical modelling using FABM in the wider PROGNOS project.

### 2.3.5. Widely used lake models

There are many 1D hydrodynamic models in the literature that have been developed for different applications and purposes. Here, we briefly introduce and describe the similarities, differences of each of the models. The most popularly used models are presented.

The Freshwater Lake model (FLake) is a bulk fresh-water lake model (Mironov, 2008) (Table 2.1). It is based on a two-layer parametric representation of the evolving temperature profile and on the integral budget of energy for the layers in question. The two layers are a mixed layer and a layer below this which is separated from the mixed layer by the mathematically calculated mixed layer depth. It calculates the mixed layer depth based on temperature. The depth of the thermocline is a function of non-dimensional depth. This model has been embedded in a number of land surface models and climate models (Mironov *et al.*, 2010; Stepanenko *et al.*, 2014; Le Moigne *et al.*, 2016). It has been used for regional and global studies due to its computational speed and relative accuracy in simulating surface temperatures (Woolway *et al.*, 2017b; Shatwell *et al.*, 2019; Woolway and Merchant, 2019) and integrated in numerical weather prediction to improve weather forecasts (Mironov *et al.*, 2010, 2012) and regional climate models to account for flux exchange between the atmosphere and lakes (Bogomolov *et al.*, 2016).

The Freshwater Lake model (FLake) was developed by Mironov (2008) and uses the concept of a self-similarity curve to simulate lake-atmosphere exchanges, mixed layer depth and surface and bottom temperatures. FLake does not require detailed lake bathymetry information, beyond lake mean depth. This is known to be a parameter within FLake where small changes can noticeably alter the simulated mixed layer depth (Samuelsson *et al.*, 2010). This model has been integrated into numerical weather prediction models to improve weather forecasts by accounting for the influence of surface fluxes from lakes (Mironov *et al.*, 2010). It has also been used in large regional scale modelling studies due to its computational efficiency (Shatwell *et al.*, 2019; Woolway *et al.*, 2019) and for analysis of lake surface energy fluxes and stratification (Stepanenko *et al.*, 2014).

Simstrat is a one-dimensional model that is capable of modelling thermal stratification and mixing of deep lakes (Goudsmit *et al.*, 2002) (Table 2.1). It has the

potential to be coupled with biogeochemical models such as the Aquatic Ecosystems Dynamics library (AED) (Hipsey *et al.*, 2013) through the Framework of Aquatic Biogeochemical Models (FABM) (Bruggeman and Bolding, 2014). It is a k- $\epsilon$  model which accounts for turbulent mixing and has been developed to account for mixing by calculating internal seiches. This model has the flexibility for inflows to be added in at different depths or with intrusions based on their density (Goudsmit *et al.*, 2002). It has been used in several case studies quantifying the impact of inflows (Råman Vinnå *et al.*, 2017) and solar brightening (Schmid and Koster, 2016) on lake thermal dynamic, parametrising seiches and deep mixing (Gaudard *et al.*, 2017) and interfaced with an atmospheric model (Goyette and Perroud, 2012).

The General Lake Model (GLM) is a one-dimensional hydrodynamic model which combines energy and mass fluxes to simulate water column temperatures (Hipsey *et al.*, 2012, 2014, 2019) (Table 2.1). It uses a Lagrangian layer structure which changes over time in correspondence to the changes in density. The thickness of the layers can increase or decrease over time. When there are density instabilities or when the turbulent kinetic energy between layers exceeds the potential energy threshold, the layers merge accounting for the mixing process. This process allows for thinner layers when calculating mixing in areas where there are strong density gradients and thicker layers where there are weak density gradients (Figure 2.2). This is a computational advantage and increases the model's flexibility to resolve mixing and more accurately replicate the structure of fine-scale mixing processes around the metalimnion, where large density jumps might occur over abrupt depth intervals. It uses heat transfer and mixing algorithms summarised by Hamilton and Schladow (1997) to calculate the transfer of heat in the water column. It can be coupled with either the Aquatic Ecodynamics (AED) library or the FABM framework (Bruggeman and Bolding, 2014) to simulate biogeochemistry within the lake. Some of the key mixing algorithms for GLM were inherited and inspired by both the Dynamic Reservoir and Lake Model (DYRESM) (Imberger and Patterson, 1981; Hamilton and Schladow, 1997) and the Dynamic Lake Model (DLM) (Chung *et al.*, 2008) but have been further developed. It has been rigorously tested across lakes of differing morphometries within different climatic zones and has demonstrated a remarkable ability to simulate water profile temperatures (Bruce *et al.*, 2018; Bueche *et al.*, 2017; Bueche and Vetter, 2014; Fenocchi *et al.*, 2018; Fenocchi *et al.*, 2017).

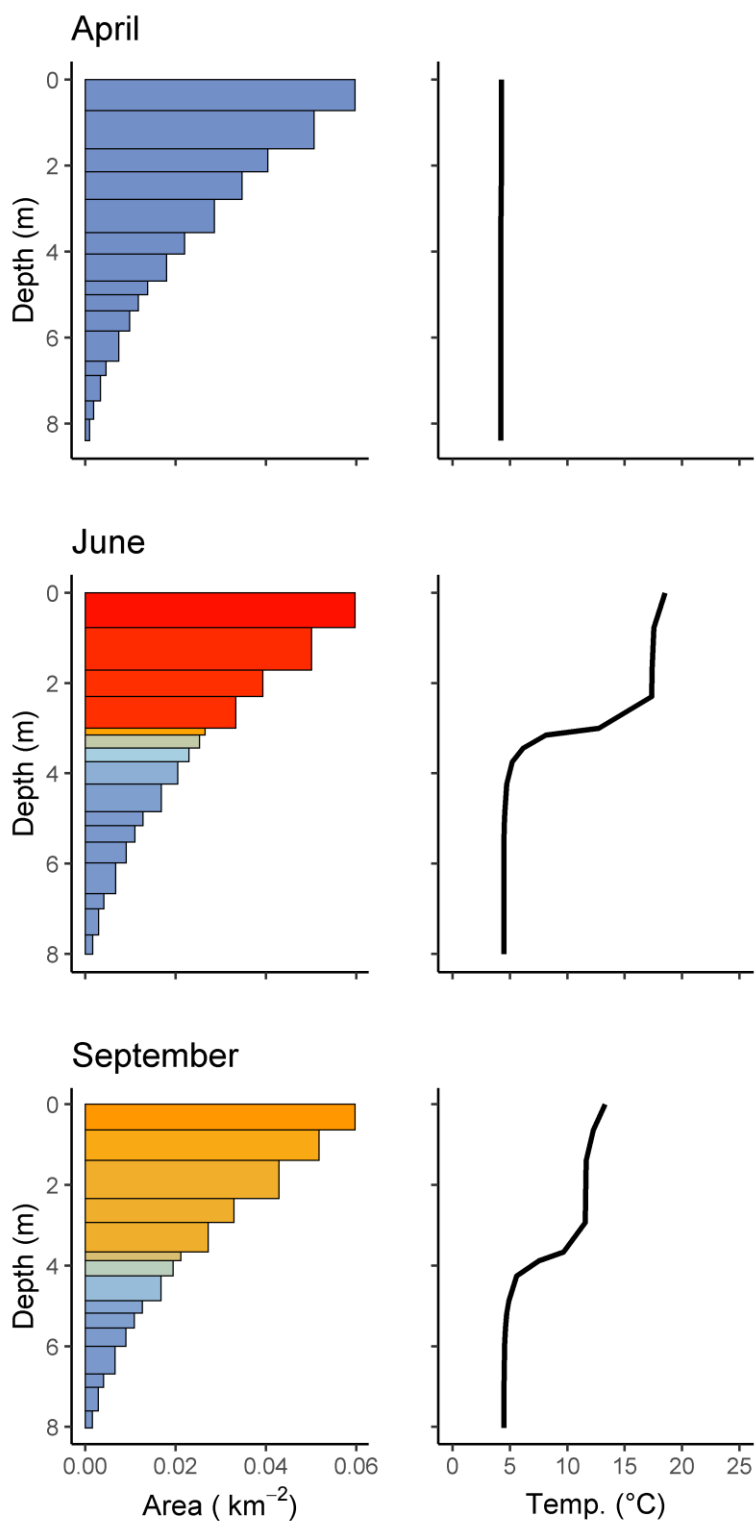


Figure 2.2 Example of the flexible Lagrangian layer structure within the General Lake Model for Langtjern, Norway, with example temperature profiles from April, June and September. Note that the layer thickness decreases around the thermocline when it develops in summertime.

The General Ocean Turbulence Model (GOTM) is a one-dimensional water column model that parameterises key hydrodynamical processes related to vertical mixing in water (Burchard *et al.* 1999; Umlauf *et al.* 2005) (Table 2.1). It was initially developed for modelling turbulence in the oceans, but it has been recently adapted for use in hydrodynamic modelling in lakes (Enstad *et al.*, 2008; Sachse *et al.*, 2014). It provides the option of using different turbulence closure parameterisations to model the interaction between mixing and stratification (Burchard *et al.*, 2006). GOTM is usually used for investigating physical processes in natural waters but it can also be dynamically coupled to a biogeochemical model using the Framework for Aquatic Biogeochemical Models (FABM) (Bruggeman and Bolding, 2014). GOTM has been used to model the dissolution of CO<sub>2</sub> in lakes (Enstad *et al.*, 2008), extreme events in a eutrophic marine system (Ciglenc̆ki *et al.*, 2014), impact of macrophytes on water quality (Sachse *et al.*, 2014) and hindcasting and future climate change projections (Ayala *et al.*, 2019; Moras *et al.*, 2019).

The Dynamic Reservoir Model (DYRESM) was designed to predict the vertical distribution of salinity, temperature and density within lakes and reservoirs (Imberger and Patterson, 1981) (Table 2.1). It is a process-based model that uses a Lagrangian layer scheme which then allows layers to mix when the turbulent kinetic energy in the top layer exceeds the potential energy threshold between that layer and the lower layer. It can be run on its own to investigate hydrodynamics of the water body or it can be easily coupled to an aquatic ecological model, the Computational Aquatic Ecosystem Dynamics Model (CAEDYM) (Hipsey and Hamilton, 2008). It has been used to model the effects of climate change on case study lakes (Tanentzap *et al.*, 2007; Weinberger and Vetter, 2012; Hetherington *et al.*, 2015; Takkouk and Casamitjana, 2015), effects of using an air-bubbler in a reservoir (Helfer *et al.*, 2011) and changes in ice cover and thermal stratification (Magee and Wu, 2017a, 2017b).

Table 2.1 Characteristics of the five lake models, the General Lake Model (GLM), the General Ocean Turbulence Model (GOTM), the Freshwater Lake model (FLake), Simstrat and Dynamic Reservoir Model (DYRESM).

<b>Model</b>	<b>GLM</b>	<b>GOTM</b>	<b>FLake</b>	<b>Simstrat</b>	<b>DYRESM</b>
<b>Met forcing data</b>	Downwelling short-wave, downwelling long-wave, cloud cover, air temperature, relative humidity, wind speed, rainfall, snowfall	Downwelling short-wave, air pressure, cloud cover, air temperature, relative humidity, wind speed, precipitation	Downwelling short-wave, air temperature, humidity, wind speed, cloud cover, downwelling long-wave	Wind speed, air temperature, downwelling shortwave, vapour pressure, downwelling long-wave	Downwelling short-wave, downwelling long-wave, cloud cover, air temperature, relative humidity, wind speed, rainfall, snowfall
<b>Sub daily integration</b>	✓	✓	✓	✓	✓
<b>Type</b>	Energy balance	k-ε turbulence	Bulk	k-ε turbulence	Energy balance
<b>Hypsograph used</b>	✓	✓	X	✓	✓
<b>Model version</b>	3.0.0 beta 12	5.1.0 (lake – branch)	-	2.2	-

<b>Website</b>	<a href="http://aed.see.uwa.edu.au/research/models/GLM/">http://aed.see.uwa.edu.au/research/models/GLM/</a>	<a href="https://gotm.net/">https://gotm.net/</a>	<a href="http://www.flake.igb-berlin.de/">http://www.flake.igb-berlin.de/</a>	<a href="https://www.eawag.ch/en/department/surf/projects/simstrat/">https://www.eawag.ch/en/department/surf/projects/simstrat/</a>	-
<b>Code Availability</b>	<a href="https://github.com/AquaticEcoDynamics/GLM">https://github.com/AquaticEcoDynamics/GLM</a>	<a href="https://github.com/gotm-model/code">https://github.com/gotm-model/code</a>	<a href="http://www.flake.igb-berlin.de/site/download">http://www.flake.igb-berlin.de/site/download</a>	<a href="https://github.com/Eawag-AppliedSystemAnalysis/Simstrat/">https://github.com/Eawag-AppliedSystemAnalysis/Simstrat/</a>	NA
<b>Reference</b>	Hipsey <i>et al.</i> , 2019	Burchard <i>et al.</i> , 2006; Burchard <i>et al.</i> , 1999	Mironov, 2008	Goudsmit, 2002	Imberger and Patterson, 1981

---

## 2.4. Model parameterisation

Although these models have been rigorously tested during development with regards parameterisation of the different model equations for momentum, heat, turbulent kinetic energy and turbulent dissipation. However, due to the reductions in dimensionality (i.e. 1D models), these equations do not universally apply to each lake. Initially the DYRESM model claimed to be “calibration free”, that the hydrodynamics were well parameterised and tested on many lakes and reservoirs (Imberger *et al.*, 1978; Hamilton and Schladow, 1997). Following further investigation and wider usage across lakes of different morphometry, in different climatic zones further parameter adjustment and calibration was needed to improve simulation accuracy (Weinberger and Vetter, 2012; Hetherington *et al.*, 2015; Magee and Wu, 2017a). Parameter optimisation is a methodology used to improve the accuracy of the model. However, model parameterisation is generally required on a site-by-site basis as often to account for biases and uncertainty in the meteorological data, as it is measured directly on the lake (Bueche and Vetter, 2014; Thiery, Martynov, *et al.*, 2014). Consequently, uncertainty in measured values, for example, the light extinction coefficient (Perroud *et al.*, 2009; Bruce *et al.*, 2018) leads to an underestimation of mixing parameters (Subin *et al.*, 2012; Deng *et al.*, 2013; Dong *et al.*, 2020).

These examples illustrate that across different models and different types of lakes, there can be wide variations in the model results. If different lake models are applied to the same lake with the same meteorological data, the results will be different. This is due to the different models being based on different physical concepts (Perroud *et al.*, 2009).

### 2.4.1. Sensitivity analysis

Sensitivity analysis is used in modelling to identify which parameters and forcing data variables a model is most sensitive to (Pianosi *et al.*, 2016). This procedure is beneficial because it helps in the understanding of how the model works and aids in the interpretation of results (Pannell, 1997). Prior to the use of any environmental model, it has been stated that it is highly important that a parameter sensitivity analysis, calibration and validation are carried out (Jørgensen, 1995; Refsgaard *et al.*, 2007). For example,

Bueche and Vetter (2014) carried out a sensitivity analysis on the meteorological input data on DYRESM. From this they were able to identify errors in the modelled water temperature and hypothesise why the errors occurred based on the sensitivity analysis. Understanding the sensitivity of model outputs to changes in model parameters can inform the selection of a range of parameters for use in calibration to improve the model performance. A sensitivity analysis has been used to assess whether a model is generalizable and can be applied to other ecosystems through identification of parameters which are site specific (Mieleitner and Reichert, 2006). Shatwell *et al.* (2019) found that changes in lake water temperature were moderately sensitive to changes in water transparency by running simulations with different light extinction coefficients.

Patterns seen within the sensitivity analysis were used to show which types of lakes exhibited similar behaviours, for example lakes with high transparency had deeper thermocline depths (Bruce *et al.*, 2018). Analysing model sensitivity to changes in meteorological forcing data allows the identification of in-lake variations as a result of meteorological changes and also it gives an insight to the possible source of error within the model as a result of inaccurate measurements of the meteorological parameters (Bueche and Vetter, 2014). When calibrating DYRESM, for example, for a high alpine lake, a sensitivity analysis determined that the two model parameters which were most sensitive were maximum layer thickness in the model and the mixing coefficient (Valerio *et al.*, 2015). The model was tested by comparing different scenarios such as with and without inflows, and with increases and decreases in wind speed of 25 %. A sensitivity analysis was carried out for GLM by Bruce *et al.* (2018) across many different lakes with a focus on analysing the different stresses within the different lakes. The surface boundary layer of the lakes was found to play a dominant role in balancing the thermal budget of the lakes in this study (Arritt, 1987; Wüest and Lorke, 2003; Verburg and Antenucci, 2010).

Sensitivity analysis of the model parameters helps to understand the changes that will result from changes in model parameters during calibration. It helps to inform parameter selection for calibration and can be used to characterise uncertainty within model results. It is used consistently in modelling both physical and biogeochemical lake models (Arhonditsis and Brett, 2005; Luo *et al.*, 2018; Bhagowati and Ahamad, 2019). The process of determining which parameters are most sensitive to change allows the calibration effort to be focused on these parameters and for ranges to be determined for each parameter. The sensitivity of the model to a parameter is usually measured by

measuring responses in one of the main variables, for example, water temperature profiles relative to changes in the parameter (Fasham *et al.*, 1990; Schladow and Hamilton, 1997; Bueche and Vetter, 2014; Bruce *et al.*, 2018).

#### 2.4.2. Uncertainty, calibration and validation

Uncertainty is an area that has been extensively studied in recent years as global emphasis has shifted to quantification of future conditions using impact models across many sectors such as hydrology (Bastola *et al.*, 2011; Broderick *et al.*, 2016), fisheries (Cheung *et al.*, 2016), forestry (Herr *et al.*, 2016; Daniel *et al.*, 2017) and aquatic ecosystem modelling (Jia *et al.*, 2018; Robson *et al.*, 2018). There have been studies examining how uncertainty can be incorporated and the information utilised within the decision making framework (Refsgaard *et al.*, 2007; Ascough II *et al.*, 2008; Durbach and Stewart, 2012). General areas within models which have been the focus of this thesis include uncertainty in model input data, model parameters and model structure (Maier *et al.*, 2016).

If a model is to be expected to replicate real world conditions then parameterisation of the model is necessary. Some model parameters are included within a model to allow for differences between measured meteorological data and actual meteorological conditions on the lake. For example, wind speed is sometimes not measured directly on the lake, and the data might come from a nearby meteorological station. In such circumstances a scaling parameter is used within many models to allow for differences between the windspeed at differing locations. However, unless some data are available at both sites, these scaling factors cannot be validated. Other parameters used within the model structure will be constants that are not directly measured but can be assumed based on previous studies or approximated through automated calibration such as minimum TKE (Ayala *et al.*, 2019), diffusivity (Deng *et al.*, 2013) and minimum buoyancy frequency (Saloranta and Andersen, 2007). Traditionally this was achieved by a process of trial and error which was a slow process that required model expertise and prone to subjective results (Fabio *et al.*, 2010; Afshar *et al.*, 2011). Many tools and programs have been developed to facilitate automatic calibration for lake models (Gaudard *et al.*, 2017; Luo *et al.*, 2018). Automated calibration algorithms tend to use one cost function and minimise the errors between modelled and observed. This has been shown to have limitations due to the possibility of there being more than one

“optimum” parameter set (Beven, 2006). This is known as equifinality and tends to occur in open systems. Reducing the number of calibrated parameters or including strong prior assumptions for the parameters are potential ways to tackle this problem (Beven, 2012).

Split sample testing has been an approach to model calibration and validation that has been adopted in hydrology since the 1980s and has been widely adapted in environmental modelling (Klemeš, 1986). This philosophy is based on the premise that the model should be tested to show that it can simulate the conditions it was designed to. This is carried out by splitting the available observational data into a calibration and validation period. This has also been a rigorous philosophy applied within limnological modelling (Jørgensen, 1995; Refsgaard *et al.*, 2007; Bueche and Vetter, 2014; Ladwig *et al.*, 2018; Feldbauer *et al.*, 2020). The reasoning behind this is to prevent model bias towards the data available for the calibration period. The effects of using sparse data and warm or cold years for calibration of a lake model were rigorously tested and the model simulated lake temperature accurately (median RMSE of 1.65 °C across 68 lakes (Read *et al.*, 2019).

On the other hand, Oreskes *et al.* (1994) highlighted the inherent knowledge (epistemic) error that is present within environmental models renders the validation of numerical models impossible. They noted that environmental models are only heuristic, and that the terms used such as ‘verify’ or ‘validate’ are affirmative terms while model confirmation is always a matter of degree. When a model has a better performance in the validation period compared to the observed dataset it makes it difficult to justify this behaviour so using the entire dataset for calibration is sometimes preferred (Ledesma and Futter, 2017). The robustness in parameter estimation was shown to increase with the longer the time period used for calibration (Larssen *et al.*, 2007). The reasoning behind this is that it allows the calibration to be more balanced across a wider range of environmental conditions.

## 2.5. Lake Model Applications

Models can inform management programmes by allowing water managers to take proactive measures to preserve water quality in their water body (Langsdale *et al.*, 2013). For example, Tanentzap. *et al.* (2008) investigated decreasing lake water temperature in Canada despite a general trend in increasing air temperatures. They attributed the 28-year decrease in water temperature to a 35 % reduction in wind speeds as a result of tree felling around and near the lake. The 1D lake model, DYRESM, was used to calculate this. Models have also been used to simulate the effects of reducing nutrient loads (Lindim *et al.*, 2015), altered management and land use (Hanh *et al.*, 2017). These techniques can be very informative as Lindim *et al.*, (2015) found that the internal loads of phosphorus in the Lower Havel were the main drivers of chlorophyll-a as when they modelled reduced external loads of N it had no impacts on the ecosystem. Three-dimensional lake models have been used to understand how current speed and direction within a lake affects nutrient concentrations in different parts of the lake (Zhang *et al.*, 2013). A cyanobacterial bloom forecast system was developed for western Lake Erie which issued bulletins to subscribers informing the of the bloom status in the lake on a weekly basis (Wynne *et al.*, 2013). Some species of cyanobacteria, such as *Anabaena circinalis*, are known to be toxic to humans, damaging the liver and gastrointestinal tract (Falconer, 1996). A forecasting framework was developed for Lake Chaohu in China, which gives real-time forecasts and it is used to forecast exceedance in water quality variable such as dissolved oxygen, total nitrogen and total phosphorus (Peng *et al.*, 2019). Empirical models have been developed to predict changes in ice cover for a range of lakes in Canada (Shuter *et al.*, 2013).

## 2.6. Forecasting

Ecological forecasting is a growing field of science due to improvements in systems understanding, ecological model development and statistical methodologies, faster computers and high frequency data monitoring (Luo *et al.*, 2011). This allows a framework to be setup where historical data can be used to build a model based on a hypothesised relationship between observed variables. This model can then be driven by forecasts of driving data to predict model states into the future. With observations in near

real time, this model can then be validated or invalidated on shorter time scales allowing for the hypothesis and experimental design to be continuously improved to gain a better systems understanding (Dietze, 2017). There is a growing requirement for ecological forecasting as we adapt to a wide range of societal pressures that include climate change (Otto *et al.*, 2017), challenges to public health such as infectious diseases (Bloom and Cadarette, 2019) and reduction in local environment quality for air and water quality (Balvanera, 2019; Han *et al.*, 2019; Stone *et al.*, 2019). Forecasting allows proactive management of such challenges and can be used to reduce the financial and environmental costs (Bakker *et al.*, 2013; Ho *et al.*, 2019). This is particularly true with regards to responding to rapid and sudden extreme events. In Ireland, for example, there has been a number of large storms in recent years which have caused coastal damage and large areas of flooding (Guisado-Pintado and Jackson, 2018, 2019; Andersen *et al.*, 2020) with an increased probability of such events due to anthropogenic-induced climate change (Matthews *et al.*, 2018). Building a comprehensive forecasting system requires not just the ability to predict atmospheric changes but also how these changes will affect freshwater systems, including the hydrology, lake thermodynamics, nutrient fluxes and biological responses on a catchment-scale. Water quality forecast can improve how safe a drinking water supply is (Peng *et al.*, 2019). For reservoirs used for power generation, short-term forecasts allow management to respond by optimising water levels in anticipation of large flood events (Raso *et al.*, 2014). Forecasting key lake phenology events, such as autumn overturn, allows resource managers of reservoirs to actively control releases to improve water quality (Nandalal *et al.*, 2010).

Statistical models have historically been used for water quality forecasting due to their relative simplicity (Cohn *et al.*, 1992). Common examples of such models would include regression models and artificial neural networks (Liu *et al.*, 2010; Avila *et al.*, 2018). The problem with these models is that they require long-extensive datasets and do not accurately represent the actual processes potentially limiting their ability to capture out of range events (Saber *et al.*, 2019).

## 2.7. Data Assimilation

Data assimilation is a method used to bridge the gap between model simulations and observations in an optimal manner (Reich, 2019). It is an invaluable tool when modelling

and particularly forecasting as it allows model states to be updated with observed values. It is used in numerical weather prediction (Rontu *et al.*, 2012; Hatfield *et al.*, 2018) and within global meteorological reanalysis datasets (Dee *et al.*, 2011; Laloyaux *et al.*, 2016). This has greatly enhanced the effectiveness of these products by constraining the error (Slivinski *et al.*, 2019). There are many different methods to implement the assimilation of measured data but the most widely used one is the Ensemble Kalman Filter (EnKF) (Luo *et al.*, 2011; Bauer *et al.*, 2015; Zwart *et al.*, 2019). It has been used in ocean, hydrological and meteorological modelling and is known to work well within a non-linear framework in comparison to other methods of assimilation (Vrugt and Robinson, 2007). This subject is described in further detail within the introduction of chapter 5.

## 2.8. Climate change

Lakes integrate long-term climatic signals due to the interaction they have with the atmosphere and are known to respond to sudden changes and capture long-term changes within a catchment. For this reason they are regarded as sentinels of climate change (Adrian *et al.*, 2009). Lake summer surface temperatures have increased globally but the rate at which this is occurring is highly variable and has a weak regional coherency (O'Reilly *et al.*, 2015). Focusing on seasonal patterns and changes can potentially overlook changes occurring on smaller time scales such as monthly changes as they can influence key lake phenology events such as stratification in summer and ice-cover in winter which are strong controllers of lake physical responses (Winslow *et al.*, 2017a). Changes in lake stratification are not strongly linked to changes in water temperature, they are more influenced by lake morphometric characteristics such as mean depth (Kraemer *et al.*, 2015), light attenuation (McCullough *et al.*, 2019) and inflows (Fenocchi *et al.*, 2017). Under various climate change projections, lake mixing regimes have been projected to change (e.g. warm monomictic to meromictic, dimictic to warm monomictic) by 2080-2100 (Woolway and Merchant, 2019). Further impacts of climate change on lake ecosystems is discussed in further detail in the introduction for chapter 5.

Lakes and reservoirs are under continuous pressure from urbanization and agricultural intensification, and from changes in climate. Directional climate change can result in a wide range of pressures on aquatic ecosystems, such as oxygen depletion at lower levels within lakes as a result of a decrease in the solubility of oxygen (Foley *et*

*al.*, 2012; Missaghi *et al.*, 2017; North *et al.*, 2014), water scarcity (Haddeland *et al.*, 2014; AghaKouchak *et al.*, 2015) and drinking water production (Bates *et al.*, 2008; Delpla *et al.*, 2009).

Cultural eutrophication is a key phenomenon which is directly affecting and fundamentally changing the ecological status of water bodies all round the world (Carpenter *et al.*, 1998, 2011). It is defined by the acceleration of eutrophication in aquatic ecosystems as a result of those human activities which have increased limiting nutrients, particularly nitrogen and phosphorus. It is a recognised cause of harmful algal blooms, fish kills and ecosystem degradation (Schindler, 1974, 2012). As a result of intensification of agriculture in the US, there has been a measured increase in carbon burial rates in lakes (Heathcote and Downing, 2012). Policies that have been adopted within Europe have focused on decreasing the amount of diffuse pollution from agriculture to waterways which have been shown to have an impact on lakes which are sensitive to nutrient enrichment (O'Dwyer *et al.*, 2013). Increasing water temperatures as a result of climate change has been shown to exacerbate the effects of eutrophication. It has been shown to negatively affect hypolimnetic dissolved oxygen in temperate lakes (Foley *et al.*, 2012). The percentage of phytoplankton biovolume attributed to cyanobacteria has experienced a sharp gain with increases in water temperatures on a global scale (Kosten *et al.*, 2012).

The projected shifts in stratification duration as a result of climate change have been known to influence the timing of autumn blooms in Lake Washington (Winder and Schindler, 2004). Availability of thermal habitat is at risk, especially for cold water fish species (Warren *et al.*, 2017). This impact has been known about for decades (Magnuson *et al.*, 1990). It is not just the impact of increasing temperature for cold-water sensitive fish, but also the increase in range for predatory fish, for example Arctic Char *Salvelinus alpinus* are projected to disappear from greater than 70 % of lakes in Sweden as a result of increasing temperatures coupled with expansion of range for pike *Esox Lucius*, a natural predator of Arctic char (Hein *et al.*, 2012). Changes in migratory behaviour has also been documented as a response to changes in temperatures as a result of climate change prevalence of some species of fish has been projected to decline as a result of shifts in air temperature and precipitation patterns (Finstad and Hein, 2012).

There are areas in the world where lakes are a fundamental underpinning of a region's economic output, such as the peri-alpine lakes in Europe where it is estimated

the four largest lakes provide up to 40 % of Italy's GDP (Iammarino *et al.*, 2019) or the lakes in the Yunnan plateau in China which are used for freshwater aquaculture, irrigation and drinking water for the surrounding area (Li *et al.*, 2007; Liu *et al.*, 2012).

### *2.9. Summation of literature*

The literature described herein describes the complex and diverse field in how lake models are designed, formulated and applied throughout limnology. They have been a crucial tool in furthering understanding of lake physics and lake ecosystem interactions. There is a description in chapter 3 of the four lake study sites used in chapter 4 and 5. Chapter 4 will focus on how a variety of meteorological reanalysis datasets can be used with a number of lake models to accurately simulate lake thermal dynamics. The introduction will further review the literature around limnological monitoring and lake thermal properties. Chapter 5 will detail the application of a lake model in a short-term forecasting system where the introduction targets ecological forecasting and data assimilation techniques. Finally, chapter 6 will detail the impacts of climate change across 46 lakes using an ensemble modelling approach. Analysis of the literature here is focused on describing the impacts of climate change on lake ecosystems and highlighting previous studies in this area.

## CHAPTER 3. LAKE STUDY SITES

In chapters 4-5 there are four lake sites that are used in the modelling studies: Lake Erken in Sweden, Lough Feeagh in Ireland, Lake Kinneret in Israel and Langtjern in Norway. These are all long-term ecological research sites and are described in detail here.

### *3.1. Erken*

Lake Erken is in east central Sweden (Table 3.1; Figure 3.1). Average annual air temperature is 6.2 °C with a max of 27.6°C and a min of -20°C. Average annual precipitation for the catchment is 578 mm year<sup>-1</sup>. The shoreline of the lake is predominantly coniferous woodland giving way to agricultural land behind. Lake Erken is ice covered each year, usually from January to late April. Summer stratification usually begins in May and lasts until September, but mixing occurs during colder summer months. Ice cover is defined as the period when most of the lake is seen to be covered in ice from the field station.

Water temperature data were measured using a thermocouple chain on a buoy moored in the eastern end of the main basin, at a depth of 15 m. Sensors were positioned every 0.5 m from the surface to a depth of 15 m. The buoy is removed from the lake each year at the end of summer before the onset of ice and deployed in springtime following the offset of ice. Temperatures were measured every minute and then averaged for each 30-minute interval. Wind speed, air temperature and relative humidity were measured at the Malma weather station located on an island in the lake (N 59.84, E 18.63). Mean sea level pressure was measured at Svanberga meteorological station which is 400 m from the lake shore (N 59.83, E 18.63). Cloud cover was recorded at Svenska Hogarna station located 59 km from the lake (N 59.45, E 19.51).

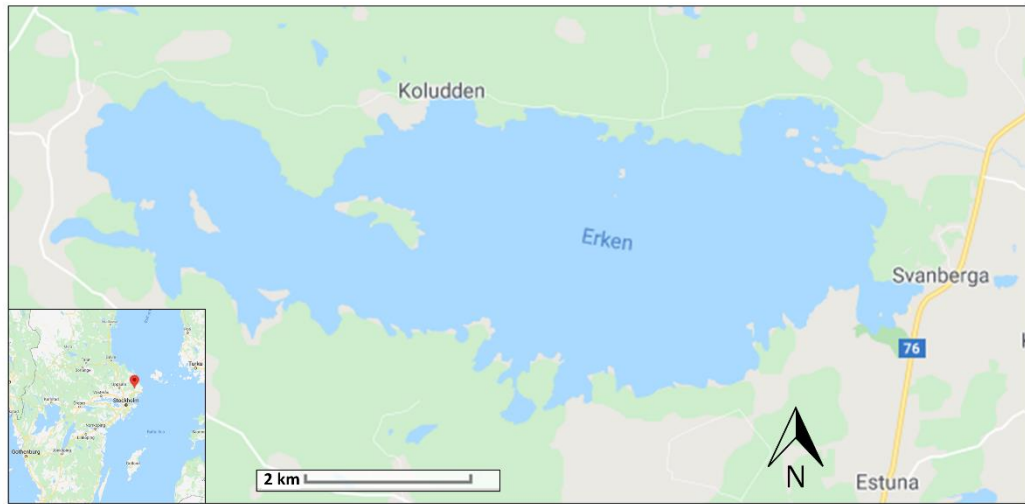


Figure 3.1 Site map of Lake Erken, Sweden and its location in Sweden (inset).

### 3.2. Feeagh

Lough Feeagh is located within the Burrishoole catchment, in the northwest of Ireland (Table 3.1; Figure 3.2). The landcover in the catchment is mainly upland peat bog and the main land uses are upland sheep grazing and coniferous forest plantation (Dalton *et al.*, 2014). The catchment is very close to the Atlantic Ocean and as a result it experiences a temperate oceanic climate with mild wet winters and cool wet summers. The long-term average annual air temperature is 10 °C with a maximum of 28.8 °C and a minimum of -8 °C while average annual precipitation is relatively high at 1570 mm year<sup>-1</sup> (Dalton *et al.*, 2014). Lough Feeagh drains into Lough Furnace, a coastal lagoon, via two short channels, both approximately 200m in length. Partial ice cover occurs only on rare occasions. Feeagh is usually stratified from May to October.

Water temperature data were measured using a thermistor chain on an automatic water quality monitoring station located at the deepest point in the lake. The water temperature was measured at depths of 0.9 m, 2.5 m, 5 m, 8 m, 11 m, 14 m, 16 m, 18 m, 20 m, 22 m, 27 m, 32 m and 42 m at 2-minute intervals. An hourly mean was then taken from this data which was used as the observed dataset. Meteorological data were measured onshore at the nearby Newport Automatic Weather Station, and included air temperature, relative humidity, mean sea level pressure, wind speed and direction,

precipitation and short-wave radiation. Cloud cover was measured at Knock airport (~50 km from the site). These data were aggregated to an hourly time step.



Figure 3.2 Site map of Lough Feeagh, Ireland and its location in Ireland (inset).

### 3.3. Kinneret

Lake Kinneret (or, alternatively, the Sea of Galilee or Lake Tiberias) ( $32^{\circ} 78' N$ ,  $35^{\circ} 59' W$ ) is the largest freshwater body in the Middle East and is a monomictic subtropical lake located at -210 m altitude, i.e., below sea level. It has a maximum depth of 46 m and an average depth of 25 m. The surface area of the lake is  $167 \text{ km}^2$  with a catchment of  $2730 \text{ km}^2$  (Table 3.1; Figure 3.3). The main inflow is from the Jordan River, which contributes on average 70 % of the total inflow (Gal *et al.*, 2003), while the main outflow, until 2014, was pumped to Israel's National Water Carrier. Kinneret is usually stratified from April to December and isothermal between January and March. Residence time of the lake is on the order of 8 years though has varied greatly in recent years due to large fluctuations in rainfall.

Meteorological data were measured at a weather station mounted on a sampling platform located at the deepest point in the lake. The station was located 7.5 m above the water level and measured air temperature, relative humidity, wind speed and direction, and precipitation at 10-minute intervals. Water temperature was monitored with a chain of 40 thermistors measuring at 10-minute intervals every 1 m throughout the water column (Sukenik *et al.*, 2014).

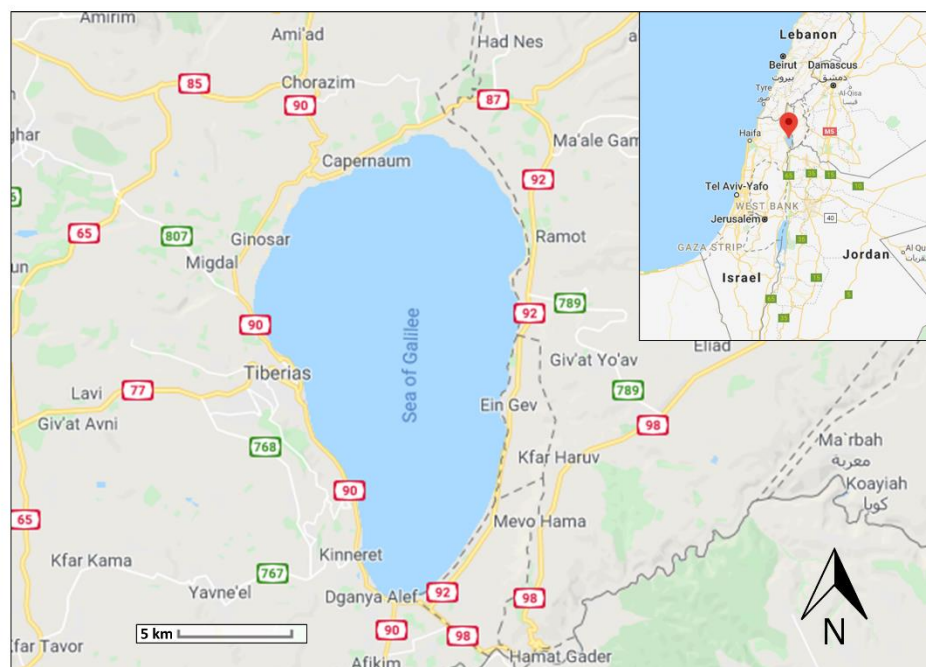


Figure 3.3 Site map of Lake Kinneret, Israel and showing its location in Israel (inset).

### 3.4. Langtjern

Langtjern is a small dimictic humic lake in central Norway (Table 3.1; Figure 3.4). The catchment is largely forested on podzolic soils with granite bedrock. The mean air temperature is 4.4 °C with an annual maximum of 28.2 °C and minimum of -25.6 °C. Mean annual precipitation is 979 mm year<sup>-1</sup>. Langtjern experiences ice cover usually from December to April and during the summer it usually stratifies from May until September. There is a webcam that takes a photograph each day and from these photographs, ice cover is defined as when all the lake in the photograph is covered in ice (NIVA, 2020).

The lake temperature profile was measured using a thermocouple at 8 different depths; 0.5 m, 1 m, 1.5 m, 2 m, 3 m, 4 m, 6 m and 8 m. This is at the deepest point in the

lake. A weather station located on the lake shore measures air temperature, relative humidity, wind speed and direction and precipitation at 1-hour intervals. Cloud cover was not measured at this site, so cloud cover from the nearest meteorological station (Gulsvik-II located 6.8 km from Langtjern) as reported in Couture *et al.* (2015) was used.



Figure 3.4 Site map of Langtjern, Norway and showing its location in Norway (inset).

Table 3.1 The location, characteristics and climates of each of the four lakes, Erken, Feeagh, Kinneret and Langtjern (mono = monomictic, di = dimictic, oligo = oligotrophic, meso = mesotrophic, eutro = eutrophic).

Site	Lat	Long	Area (km <sup>2</sup> )	Max depth (m)	Mean depth (m)	Residence time (years)	Mixing regime	Trophic status	Colour	Mean annual air temperature (°C)	Max annual air temperature (°C)	Min Air Temperature (°C)	Precipitation (mm yr <sup>-1</sup> )
Erken, Sweden	59°51' N	18° 15' E	23.7	21	9	7	Di	Eutro	Coloured	7	>30	<-20	560
Feeagh, Ireland	53° 56' N	09° 34' W	3.9	45	16	0.45	Mono	Oligo	Coloured	10	>25	<-5	1570
Langtjern, Norway	60°8' N	10°23' E	0.23	12	2	0.2	Di	Oligo	Coloured	4.4	>25	<-25	979
Kinneret	32.78' N	35.59' E	166	46	25	7-9	Mono	Meso-eutro	Clear	21	>35	<5	380

## **CHAPTER 4. EVALUATION OF GLOBAL METEOROLOGICAL REANALYSES AS POTENTIAL FORCING DATASETS FOR ONE-DIMENSIONAL HYDRODYNAMIC MODELLING**

### *4.1. Abstract*

Lake thermal dynamics are closely coupled to climatic conditions. Consequently, hydrodynamic lake model simulations in conjunction with timeseries of meteorological input data provide a powerful tool for evaluating climate-induced changes in lake ecosystems. Global meteorological reanalyses datasets are used for climate research at high spatial and temporal resolution. In this study, we investigated the suitability of using these meteorological datasets for forcing one-dimensional lake hydrodynamic models and accurately simulating water temperatures in three different lakes. Four established lake models were used to simulate lake temperature profiles for three well-studied European lakes of varying morphometry. Multi-annual model simulations forced by locally measured meteorological data were compared with simulations forced by three freely available meteorological reanalysis datasets from the European Centre for Medium-range Weather Forecasts (ECMWF). Uncalibrated model simulations forced by the meteorological reanalyses datasets replicated water temperature profiles with a similar degree of accuracy (median bias:  $-0.27$  °C) to models forced by local observed meteorological data (median bias:  $-0.25$  °C), particularly when using meteorological datasets with sub-daily temporal resolution. This was also true for the prediction of the start and end of thermal stratification in the lakes. We then calibrated each of the lake model/meteorological dataset combinations and found that calibrating the models, even with just two scaling parameters, reduced the error between simulated and observed lake temperature profiles. We conclude that meteorological reanalyses can be used in place of observed measurements to accurately replicate the overall seasonal dynamics in lake thermal structure.

## 4.2. Introduction

### 4.2.1. Lake thermal properties and climate

The thermal properties of lakes are directly regulated by climatic conditions. Changes in lake thermal structure can have profound implications for physical properties including the timing of autumn overturn (Arvola *et al.*, 2010; Moras *et al.*, 2019), the earlier start of lake stratification in spring (King *et al.*, 1997; Peeters *et al.*, 2007), the development of a stronger thermocline (Posch *et al.*, 2012; Valerio *et al.*, 2015), and a general warming of the entire water column (Sahoo *et al.*, 2016; Schmid and Köster, 2016; Woolway, *et al.*, 2017b). These changes in thermal characteristics, and the subsequent effects on lake biogeochemistry, will also be a function of lake-specific characteristics such as lake morphometry, latitude and elevation. Lake characteristics, for example, have been found to mediate the effects of the historical warming on lake surface temperatures in summer (O'Reilly *et al.*, 2015). Kraemer *et al.* (2017) showed how the effects of historical warming on estimates of lake metabolism were stronger in lakes at low latitudes and low elevations, effects that can potentially shift food web dynamics, species interactions and carbon cycling. Changes in lake ice cover can impact dissolved oxygen in spring (Couture *et al.*, 2015), diatom species assemblages (Griffiths *et al.*, 2017), habitat availability (Guzzo and Blanchfield, 2017) and strengthening of stratification (Niedrist *et al.*, 2018). The importance of lake temperature for all these processes means that any study of the sensitivity of lake ecosystems to a changing climate requires analysis of changes in lake physical and thermal properties as a fundamental step. Where the effects of short-term or long-term climate change are the focus, simulations of lake thermal structure using hydrodynamic models will be essential.

### 4.2.2. Monitoring lake temperatures

Assessment of historical and future changes in lake temperature profiles require observed data. Traditional monitoring of lakes involves the deployment of field staff to directly measure lake characteristics including water temperature profiles. Among the main factors that govern the collection of such datasets are the cost and time required to collect

data. For this reason, long term datasets of lake temperature profiles are relatively scarce. There are a small number of lakes which have long-term historic lake temperature data such as Lake Zurich for which data are available for 52 years (Livingstone, 2003). Recent advancements in monitoring technology has led to the deployment of sensors that monitor variables at high frequency but can also relay this information in near-real time using telemetry. These include sensors to measure lake water temperature profiles. Scientific community networks have developed around such data collection, leading to a large increase in data availability and fuelling an advancement of knowledge of in-lake processes (Rose *et al.*, 2016b). There is no single monitoring strategy that can answer all research questions but carefully designed and executed programs with a focus on the required scales can capture insightful information on lake dynamics (Mantzouki *et al.*, 2018). Satellite monitoring of lakes has exponentially increased the number of lakes that can be monitored but comes with many limitations compared to automated monitoring. These include the temporal frequency and measurable variables (e.g. only lake surface temperature and transparency) (MacCallum and Merchant, 2012) and region specific coverage issues (e.g. reduced data due to clouds) (Stadelmann *et al.*, 2001). High frequency monitoring data, when available, can be used to validate models of lake thermal structure, which can help to expand our knowledge about key in-lake physical and biological processes (Hamilton *et al.*, 2015).

#### 4.2.3. Lake Models

Numerical models have been widely used to examine the long-term impacts of climate change on lake physical structure (Ayala *et al.*, 2019; Butcher *et al.*, 2015; Shatwell *et al.*, 2019; Woolway *et al.*, 2019) and lake biogeochemistry (Trolle *et al.*, 2014; Darko *et al.*, 2019). These studies span a wide variety of scales, from localized single site studies to those describing regional and global responses to climate change. Lake models have also been coupled with atmospheric models (Perroud and Goyette, 2012) and can play an important role in numerical weather prediction (Mironov, 2008; Mironov *et al.*, 2010). A range of lake models have been developed that facilitate the simulation of in-lake biogeochemical processes (Jöhnk and Umlauf, 2001; Elliott *et al.*, 2007, 2016; Saloranta and Andersen, 2007; Jöhnk *et al.*, 2008; Hu *et al.*, 2016; Page *et al.*, 2017). These have been used to model oxygen dynamics (Jöhnk and Umlauf, 2001), changes in

phytoplankton communities (Elliott *et al.*, 2007; Page *et al.*, 2018; Page *et al.*, 2017) and nutrient cycling and food-web dynamics (Bruggeman and Bolding, 2014; Hu *et al.*, 2016; Arhonditsis *et al.*, 2017). Each of these biogeochemical models is, however, underpinned by the simulation of the lake physical structure. They require modelling of lake thermal dynamics to simulate temperature profiles, and which in turn govern the availability of nutrients, mixing dynamics and settling rates in the water column.

There are a wide range of existing 1D hydrodynamic models with different model structure and varying degrees of complexity. These include the Freshwater Lake model (FLake), General Lake Model (GLM), the General Ocean Turbulence Model (GOTM) adapted for lakes and Simstrat (as described in section 2.3.5). In limnological modelling, ensemble modelling has not been a widely used approach to date. It has been used in two studies for projecting the climate change response of phytoplankton (Nielsen *et al.*, 2014; Trolle *et al.*, 2014). There have also been studies carried out focused on inter-model comparisons, but only for single sites (Stepanenko *et al.*, 2013; Thiery *et al.*, 2014a), as part of the Lake Model Intercomparison Project (LakeMIP; Stepanenko *et al.*, 2010).

There are notable advantages when using more than one model which has been developed separately. It allows for different sources of uncertainty to be quantified through comparison of the differences when forced with the same data. Applying a combination of lake models to a site, however, allows the user to overcome potential limitations of using one single model, such as the inherent biases of each model, and has the potential to improve the generalization of errors.

#### 4.2.4. Meteorological Reanalysis Datasets

Any multi-site study of lake thermal structure requires a full set of consistent forcing data from all study locations. Such observed data may not, however, always be available. Meteorological reanalysis data come from a combination of observations, a global forecast model and data assimilation. These data sources are used to generate best estimates of atmosphere states from the surface to the upper atmosphere (Parker, 2016). There are a large number of different reanalysis products available which cover varying timescales and temporal and spatial resolutions (Lindsay *et al.*, 2014). They are generated on a regional or global scale on a gridded axis and are sometimes referred to as gridded

datasets. They are used within the atmospheric science field to further understanding about atmospheric processes, to validate atmosphere-chemistry models and to investigate the effects of climate change on a global scale (Fujiwara *et al.*, 2017). There have been a number of known issues related to the use of reanalysis data with regards preserving trends and accuracy (Thorne and Vose, 2010), capturing precipitation (Bosilovich *et al.*, 2008) and warm biases in the Southern Hemisphere (Fréville *et al.*, 2014). Overall, however, their development has enabled studies at large spatial scales (e.g. regional or global) across many different fields such as hydrology (Ledesma and Futter, 2017; Tarek *et al.*, 2019), forestry (Abatzoglou and Williams, 2016), regional climate modelling (Solman *et al.*, 2013; Warrach-Sagi *et al.*, 2013) and ice-ocean models (Smith *et al.*, 2014). The benefits of gridded reanalysis meteorological datasets over locally observed meteorological data are that they are based on observed data, incorporate laws of atmospheric motion, are physically and dynamically coherent, include a full set of meteorological variables and are consistent in time and space (Parker, 2016).

The output of general circulation models (GCMs) are gridded climate data that have been often used as forcing data for ecosystem models that such as simulating future projections based on differing global emission scenarios (Frieler *et al.*, 2017). Dibike *et al.* (2011), for example, used gridded data from the European Centre for Medium-Range Weather Forecasts (ECMWF) Reanalysis (ERA)-40 dataset to simulate the effects of projected climate change on the formation and break-up of ice cover on mid to high latitudinal lakes. Read *et al.* (2014) used the North American Land Data Assimilation System (NLDAS) gridded climate product to simulate water temperature across 2,368 lakes across the world and found a strong coherence among lakes in surface temperatures. Frassl *et al.* (2018) explored the benefits and limitations of using ERA-Interim (ERA-Interim) as forcing data on Lake Chaohu, China, using a three-dimensional hydrodynamic model and found that ERA-Interim data reproduced seasonal patterns and captured lake phenology patterns of stratification but did not accurately capture sub-daily variations in temperature. Historical lake warming trends across Europe were captured using a calibrated 1D lake hydrodynamic model forced with ERA-20C climate reanalysis data (Woolway *et al.*, 2017b). Global lake surface water temperatures were simulated to a high degree of accuracy for the period 1900-2010 using ERA-20C (Piccolroaz *et al.*, 2020).

#### 4.2.5. Comparisons of reanalyses and local observations

An important consideration in the use of climate reanalysis datasets is how well they compare to locally measured meteorological data. In some instances, use of these gridded datasets may be preferred. For example, locally measured meteorological data can be subject to many different sources of error such as sampling frequency where the sampling frequency is lower than known variation in the climate e.g. daily wind speeds (Hupet and Vanclooster, 2001). In addition, not all the meteorological variables necessary to force a lake model may be measured on-site, or for the full time period. For example, the availability of gap-free long-term local datasets is quite rare. However, there are also issues with the use of reanalysis datasets. The degree of error in gridded climate reanalysis datasets is strongly influenced by the number of stations used in the analysis (Haylock *et al.*, 2008). There are many uncertainties within reanalysis climate data due to the combination of errors from observations, models and methodology (Thorne and Vose, 2010). It was also noted that in some regions, there can be non-climatic artefacts, such as warming trends seen above 62°N (Thorne, 2008). Gridded climate reanalysis datasets have also been found to poorly replicate observations of air temperature in areas of heterogeneous terrain (DeGaetano and Belcher, 2007). Similar patterns have been seen for variables such as wind speed (Ramon *et al.*, 2019) and precipitation (Yang and Villarini, 2019). Nevertheless, gridded reanalysis data have often been used as forcing in hydrological modelling and have been shown to work just as well as locally measured data (Hurkmans *et al.*, 2008; Ledesma and Futter, 2017; Vu *et al.*, 2012).

#### 4.2.6. Study aim

The aim of this study was to evaluate the suitability of three widely used gridded reanalysis datasets as meteorological forcing data for simulating lake temperature profiles using uncalibrated 1D lake models. The selected lake models were set-up for three European lakes of varying morphometry and local climatic conditions. We compared the performance of the models in terms of capturing seasonal patterns throughout the water column and the phenology of seasonal patterns of stratification when driven by both the gridded meteorological datasets (hereafter referred to as ‘gridded datasets’) and local observed data over a multi-year period for each site. Initially

we assess the use of the gridded datasets to simulate lake temperatures without any model calibration. We then calibrated each model against observed lake temperature data by scaling wind speed and incoming short-wave radiation, in order to demonstrate any improvements in model accuracy gained by calibration. Our results highlight the capabilities and limitations of using these gridded datasets for future modelling studies.

### *4.3. Materials and Methods*

#### *4.3.1. Study sites and data availability*

The three lake study sites, Erken, Feeagh and Langtjern, were selected based on their geographic spread, difference in lake surface area and depth, and the availability of high frequency water temperature profile data. These catchments are all long-term ecological research sites, which have been well studied. Each of the sites are described in chapter 3.

#### *4.3.2. Gridded datasets*

Local observed meteorological data (referred to as Local) were collected at each site as described in chapter 3. In addition to these local data, three different gridded reanalysis datasets (referred to as gridded datasets) were used as forcing data: ECMWF's ERA Interim reanalysis (ERA-Interim, Dee, *et al.*, 2011), ECMWF's Re-Analysis 5 (ERA5, ECMWF, 2020) and Earth2Observe WATCH forcing data methodology applied to ERA-Interim reanalysis data and ERA-Interim data Merged and Bias-corrected for ISIMIP (EWEMBI) (Dee *et al.*, 2011; Weedon *et al.*, 2014; Calton *et al.*, 2016; Lange, 2019).

The ERA-Interim dataset was available at a spatial resolution of  $0.75^\circ \times 0.75^\circ$  and a timestep of 6-hour (Dee *et al.*, 2011). Before simulating lake temperature profiles, the ERA-Interim dataset was linearly interpolated to hourly values across each climate variable. The ERA5 dataset was available at a spatial resolution of  $0.28^\circ \times 0.28^\circ$  at a time step of 1-hour. The EWEMBI dataset covered the time period of 1979-2016 at a spatial resolution of  $0.5^\circ \times 0.5^\circ$ . Each of these datasets had a global distribution which made them applicable for any lake in the world. The reason EWEMBI was included in this analysis was because

this was the data that was used to bias correct the General Circulation Model (GCM) data for the impact assessments carried out in phase 2b of the Inter-Sectoral Impact Model Inter-comparison Project (Frieler *et al.*, 2017). For the lake sector, this dataset was used to calibrate the models prior to simulating hydrothermal dynamics under the different climate change scenarios (Table 4.1).

When the meteorological drivers long-wave radiation, relative humidity, vapour pressure or cloud cover were not present in the meteorological datasets, they were estimated using established empirical relationships (Table 4.2).

Table 4.1 Description of the meteorological reanalysis datasets.

<b>Dataset</b>	<b>ERA-Interim</b>	<b>ERA5</b>	<b>EWEMBI</b>
Description	The system includes a 4-dimensional variational analysis (4D-Var) with a 12-hour analysis window on 60 levels in the vertical from the surface up to 0.1 hPa.	Hourly estimates of many atmospheric, land and oceanic climate variables. Resolves the atmosphere using 137 levels from the surface up to a height of 80km. ERA5 includes information about uncertainties for all variables at reduced spatial and temporal resolutions.	Data sources of EWEMBI are ERA-Interim reanalysis data WATCH forcing data methodology applied to ERA-Interim reanalysis data, earth2Observe forcing data, and NASA/GEWEX Surface Radiation Budget data.
Spatial resolution	0.75°x0.75°	0.28°x0.28°	0.5°x0.5°
Temporal resolution	6h	1h	24h
Availability	1979-2019	1979-present*	1979-2016
Reference	Dee <i>et al.</i> (2011)	ECMWF (2020)	Lange (2019)
Website	<a href="https://www.ecmwf.int/en/forecasts/datasets/reanalysis-datasets/era-interim">https://www.ecmwf.int/en/forecasts/datasets/reanalysis-datasets/era-interim</a>	<a href="https://www.ecmwf.int/en/forecasts/datasets/reanalysis-datasets/era5">https://www.ecmwf.int/en/forecasts/datasets/reanalysis-datasets/era5</a>	<a href="https://dataservices.gfz-potsdam.de/pik/showshort.php?id=escidoc:3928916">https://dataservices.gfz-potsdam.de/pik/showshort.php?id=escidoc:3928916</a>

\*within 5 days of real time

Table 4.2 Summary of meteorological variables available and associated references for calculations for those which were not present. A: Rothfus, 1990  
 B: Crawford and Duchon, 1999, C: Lowe, 1976.

	Air Temperature	Air Pressure	Precipitation	Wind Speed	Wind Direction	Incoming Short-wave Radiation	Relative Humidity	Cloud Cover	Dewpoint Temperature	Longwave Radiation Downwelling	Vapour Pressure
Local-Erken	✓	✓	✓	✓		✓	✓	✓	A	B	C
Local-Feeagh	✓	✓	✓	✓	✓	✓	✓	✓	A	B	C
Local-Langtjern	✓	✓	✓	✓	✓	✓	✓	✓	A	B	C
ERA5	✓	✓	✓	✓	✓	✓	A	✓	✓	✓	C
ERA1	✓	✓	✓	✓	✓	✓	A	✓	✓	✓	C
EWEMBI	✓	✓	✓	✓	✓	✓	A	✓	✓	✓	C

### *4.3.3. Model descriptions*

For model descriptions, please refer to section 2.3.5.

### *4.3.4. Model setup*

For each lake, the models were set up using a standardised format for meteorological forcing data which are the boundary conditions for the lake models. Measured lake bathymetry and light extinction data were included in the model configuration although for FLake, the mean depth value is used instead of bathymetry. Each model set up included the same default parameters to ensure a common configuration between lakes and between gridded datasets. Non-dimensional scaling for wind speed and incoming shortwave radiation were set to a value of 1. Default mixing and turbulence parameters from each associated model publication were used. Each lake simulation was set up with no inflows or outflows to mimic a situation where such data were unavailable. In addition, FLake also does not calculate a water balance within the model excluding the influence of inflows and outflows resulted in simulations that were comparable across all lake models.

Each model was run for the same time period for each lake to ensure that there was a fair comparison between the selected forcing datasets. For Feeagh this time period was 2009-01-01 to 2014-12-30 (including a 364 day spin up). For Erken this was from 2010-05-15 to 2015-12-30 (including a 364 day spin up). For Langtjern, the time period was from 2013-05-23 to 2016-12-30 (including a 222 day spin up). The models were initialized when the lake was isothermal, which was defined as when there was a temperature difference  $< 1$  °C between surface and bottom temperatures. The spin-up period was discarded when assessing model performance. The reason Langtjern had a shorter spin-up time was to ensure that at least three full-years were included in the analysis period. Each model was run on an hourly timestep but only the temperature values at 18:00 on each day were saved. An exception was FLake when using the EWEMBI forcing dataset, where a daily time step was used because the integration timestep must equal the timestep of the forcing data.

#### 4.3.5. Model calibration

For model calibration, we adopted a ‘light touch’ approach where we opted to adjust as few parameters as possible. This was to reduce dimensionality in the parameters and avoid the issue of equifinality based on recommendations from Beven (2006). Scaling factors for incoming short-wave radiation (SWR) and wind speed were chosen as the two parameters to calibrate because they are the forcing variables to which the lake models are most sensitive (Imberger and Hamblin, 1982; Lewis, 2011; Bruce *et al.*, 2018) and because they were common input parameters across all models and measured directly at each site. Latin hypercube sampling was used to sample 100 parameters for both scaling factors within a range of 0.5-1.5 for SWR and 0.5-1.5 for wind, except for Langtjern where 0.1-1.5 was used because of the strong bias seen in wind speed when comparing observed to reanalysis datasets (McKay *et al.*, 2000). Latin hypercube sampling has been used in other lake modelling applications (Gal *et al.*, 2014) and is efficient when parameter sets are limited. The parameter sets were generated using the ‘LatinHyper’ function from the ‘FME’ package in R (Soetaert and Petzoldt, 2010). The ‘best’ parameter set was chosen by selecting the parameter set with the lowest RMSE. Latin hypercube sampling assumes a uniform parameter distribution. The entire period of observed data was used for the calibration period, as recommended by Oreskes *et al.* (1994) with regards calibration of environmental models. It is increasingly common to calibrate a model on a training set and validate the calibrated model on its ability to capture out of sample predictions. It is straightforward to interpret the situation when the calibrated dataset has a model performance that is equal to or lower than that observed in the calibration dataset. However, it is more difficult to explain the situation when the model performs better during the validation period. We choose to include the entire available dataset for calibration to estimate model parameters, similarly to Moras *et al.* (2019), as this represents the widest possible range of climatic conditions experienced during the simulation period. Larssen *et al.* (2007) found that more robust parameter sets for future simulations were found when using longer time series because they are balanced to a wider range of environmental conditions.

#### 4.3.6. Data analysis

Data analysis was carried out using the R program (R Core Team, 2020). Residuals were calculated by subtracting modelled data from observed data extracted at the corresponding depths. Surface temperatures were defined as the temperatures measured closest to the surface (Erken: 0.5 m; Feeagh: 0.9 m; Langtjern 0.5 m) while bottom temperatures were classified as the temperature measured at the lowest sensor in the lake (Erken: 15 m; Feeagh: 42 m; Langtjern 8 m). Density distributions of the residuals were compared between gridded datasets for each lake using measurements from the total profile, surface temperature and bottom temperature. The value for the maximum surface temperature and the day of year when it occurred was compared to the corresponding observed values. The timing of the start and end of stratification (Erken, Feeagh and Langtjern) and ice cover (Erken and Langtjern) for each year and each lake were calculated for each model and compared to the observed timings.

For metrics of model fitness, we calculated bias, root mean square error (RMSE) and Nash-Sutcliffe Efficiency (NSE).

$$Bias = \frac{1}{n} \left( \sum_{i=1}^n (y_i - \hat{y}_i) \right) \quad (4.1)$$

$$RMSE = \sqrt{\frac{1}{n} \sum_{i=1}^n (y_i - \hat{y}_i)^2} \quad (4.2)$$

$$NSE = 1 - \frac{\sum_{i=1}^n (y_i - \hat{y}_i)^2}{\sum_{i=1}^n (y_i - \bar{y})^2} \quad (4.3)$$

Where  $y_i$  was the observed; and  $\hat{y}_i$  was the simulated water temperatures at time  $i$ ; and  $\bar{y}$  was the mean observed water temperature; and  $n$  was the number of samples. These metrics were compared for both the uncalibrated and calibrated model setups.

#### 4.4. Results

Overall, using Local at Erken with any of the four lake models (GOTM, GLM, Flake or Simstrat) produced the best simulation of the seasonal pattern in temperature profiles and captured the mixing dynamics throughout the water column (Figure 4.1). Local produced the smallest range in model error, with only small overestimates of water temperature at the lower depths. The ERAI dataset simulated warmer temperatures in the bottom for simulations with GLM, GOTM and Simstrat. Irrespective of the meteorological dataset used, (ERAI, ERA5, EWEMBI or Local), FLake consistently simulated lower bottom temperatures for Erken. Simulations using EWEMBI data consistently underestimated water temperature with errors  $< -5$  °C with FLake. In contrast ERA5 simulated a small warm bias across all models, particularly towards the surface.

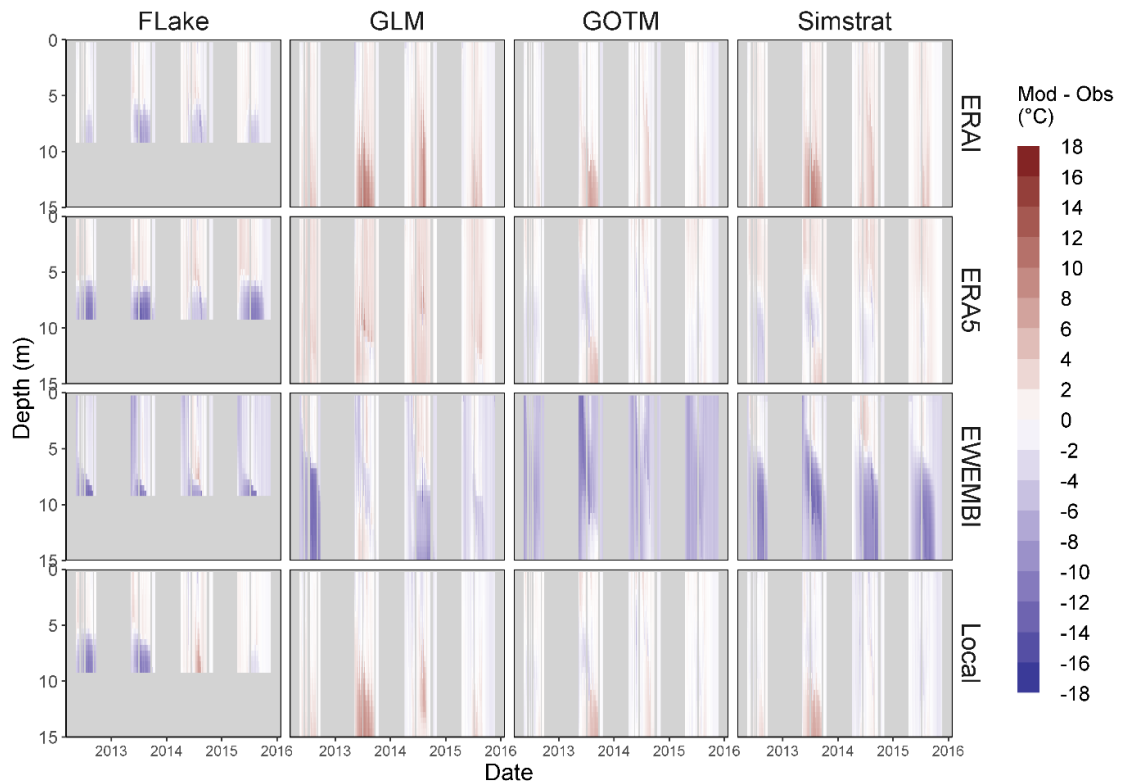


Figure 4.1 Difference between modelled and observed temperatures for Erken for the four meteorological datasets; ERA-Interim, ERA5, EWEMBI and Local and for the four lake models; FLake, GLM, GOTM and Simstrat. Grey areas indicate periods of missing data for either observed or modelled.

For Feeagh, the most accurate simulations throughout the whole period and for the entire water column were those forced with ERAI (Figure 4.2). Forcing the model with Local underestimated temperatures in 2010-2011 but produced smaller errors throughout 2012-2014. EWEMBI consistently underestimated the water temperatures, particularly in the lower depths, with errors ranging between -5 and -9 °C in the hypolimnion during the summer of 2010. ERA5 overestimated temperatures in the epilimnion while underestimating temperatures in the hypolimnion during summer. Across all forcing datasets, FLake underestimated bottom temperatures in Feeagh during the summer period, even for the shallower depths over which FLake operates. FLake, GLM and Simstrat all had a warm bias in the surface for ERAI and ERA5 (Figure 4.2). The use of EWEMBI data consistently underestimated hypolimnetic temperatures across all models.

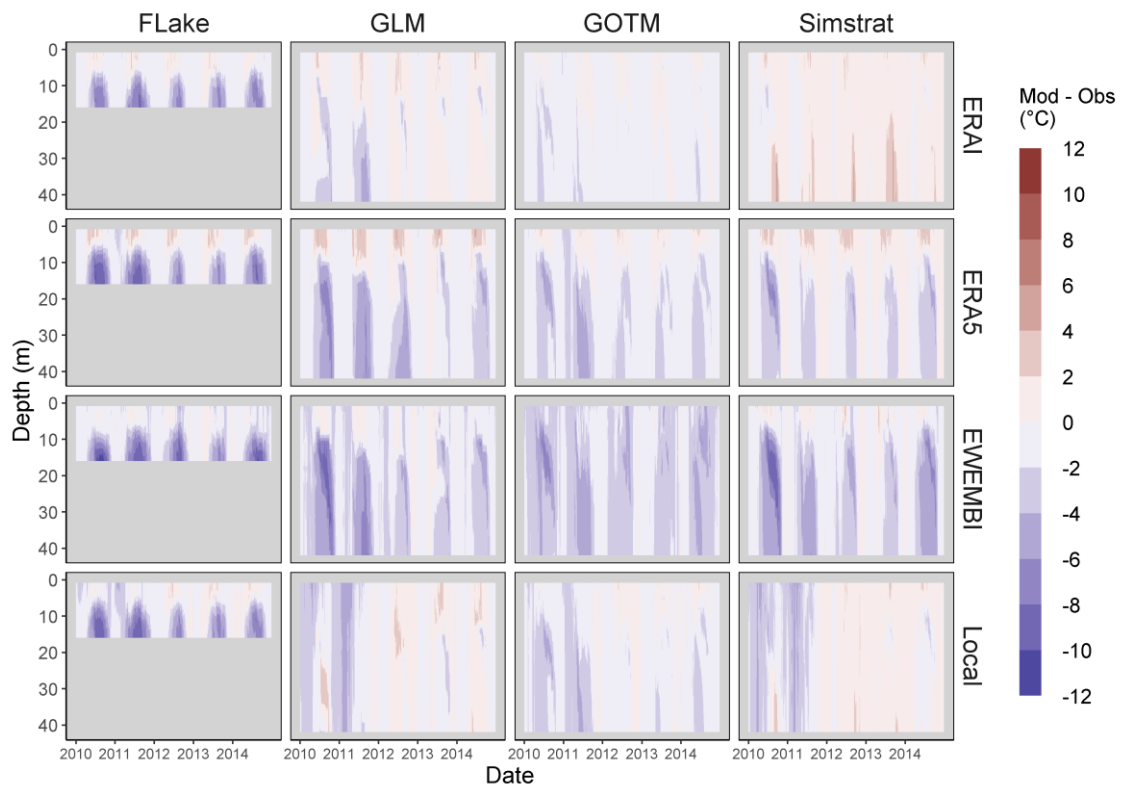


Figure 4.2 Difference between modelled and observed temperatures for Feeagh for the four meteorological datasets; ERAI, ERA5, EWEMBI and Local and for the four lake models; FLake, GLM, GOTM and Simstrat. Grey areas indicate periods of missing data for either observed or modelled.

In general, all models and all forcing datasets overestimated the water temperature of Langtjern (Figure 4.3). However, the difference across gridded datasets was quite small although the use of EWEMBI and Local data produced slightly lower error. There was a distinct difference between the results for FLake and GLM versus those for GOTM and Simstrat, with the latter two models being unable to reproduce the stratification dynamics within Langtjern. This resulted in large overestimations of temperature during summer at the lower depths ( $>10$  °C). During winter, both models consistently exhibited a cold bias throughout the water column across all gridded datasets. The only period where GOTM and Simstrat had small errors was during the period of onset and offset of stratification. Simulations using EWEMBI and Local data had the smallest errors throughout the water column for FLake and GLM, particularly at lower depths during the summer period. ERAI and ERA5 both had a warm bias at the surface during the summer period for both FLake and GLM. During the summer period of 2016, FLake and GLM showed a consistent warm bias across ERAI, ERA5 and EWEMBI while for Local this was much smaller (Figure 4.3).

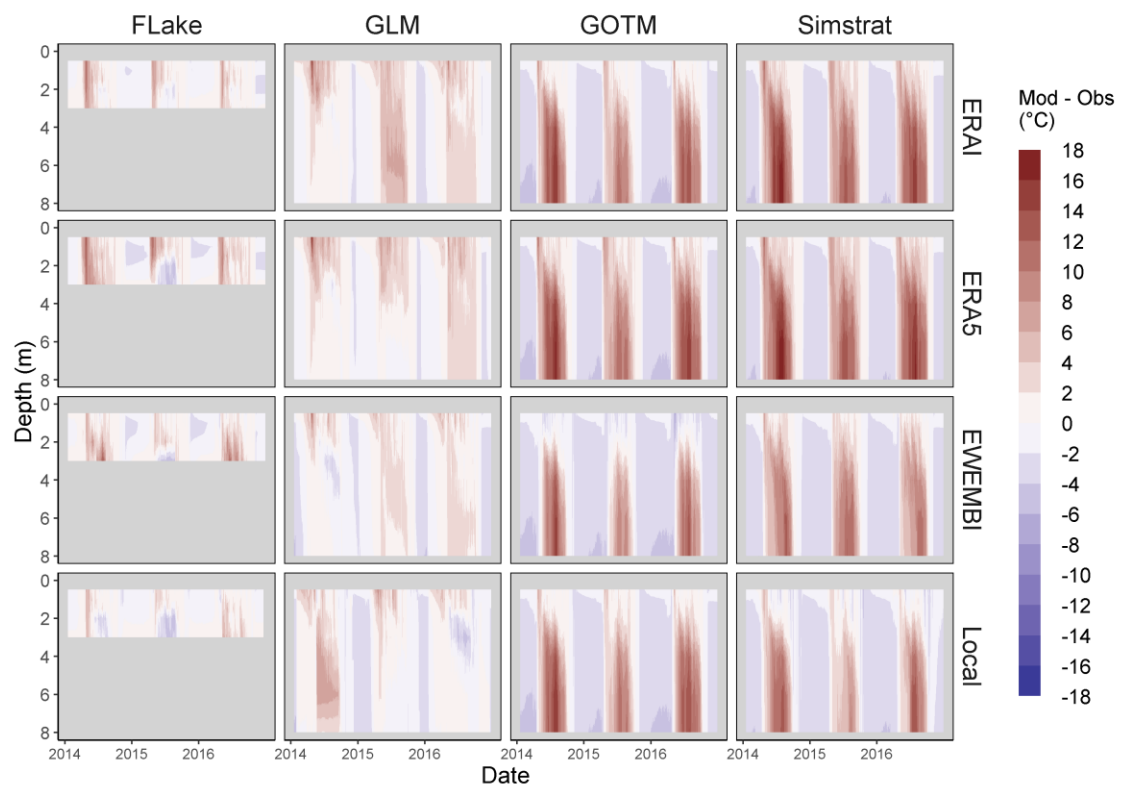


Figure 4.3 Difference between modelled and observed temperatures for Langtjern for the four meteorological datasets; ERA-Interim, ERA5, EWEMBI and Local and for the four lake models; FLake, GLM, GOTM and Simstrat. Grey areas indicate periods of missing data for either observed or modelled.

Local meteorological data produced the best simulations for Lake Erken, with the smallest distribution of residuals around 0 for the full water temperature profile (Figure 4.4 A), surface temperature (Figure 4.4 B) and bottom temperature (Figure 4.4 C). Simulations using ERAI and ERA5 had slightly wider distributions but were similar in shape for the full profile, surface and the bottom. The residuals of the models driven by EWEMBI data were skewed to the left, indicating a tendency to underestimate temperatures for the full profile, surface and the bottom. EWEMBI simulations also exhibited a slight bimodality which was due to the residuals from GOTM and Simstrat being strongly negatively biased.

ERAI had the smallest distribution of residuals around 0 for Feeagh for the full profile (Figure 4.4 A), the surface (Figure 4.4 B) and the bottom temperatures (Figure 4.4 C). The Local and ERA5 simulations followed similar distributions for the full profile, surface and the bottom temperatures. EWEMBI had a negative bias for the surface temperature which was reflected in the density distribution for the full profile and surface temperatures. There was a slight bimodality in the bottom residuals across each of the datasets and this pattern was consistent across all lake models.

For the full profile in Langtjern there was a similar distribution for all the datasets with a bimodal distribution with a peak at  $-3\text{ }^{\circ}\text{C}$  and one around  $0\text{ }^{\circ}\text{C}$ . Bottom temperatures followed a similar pattern across all datasets (Figure 4.4 A). The bimodality was a result of both the GOTM and Simstrat models persistently underestimating bottom temperatures in winter and a large overestimation of bottom temperatures in summer (Figure 4.4 C). At the surface, the Local data had the smallest spread of residuals around 0 followed by EWEMBI while ERA5 was slightly positively skewed (Figure 4.4 A).

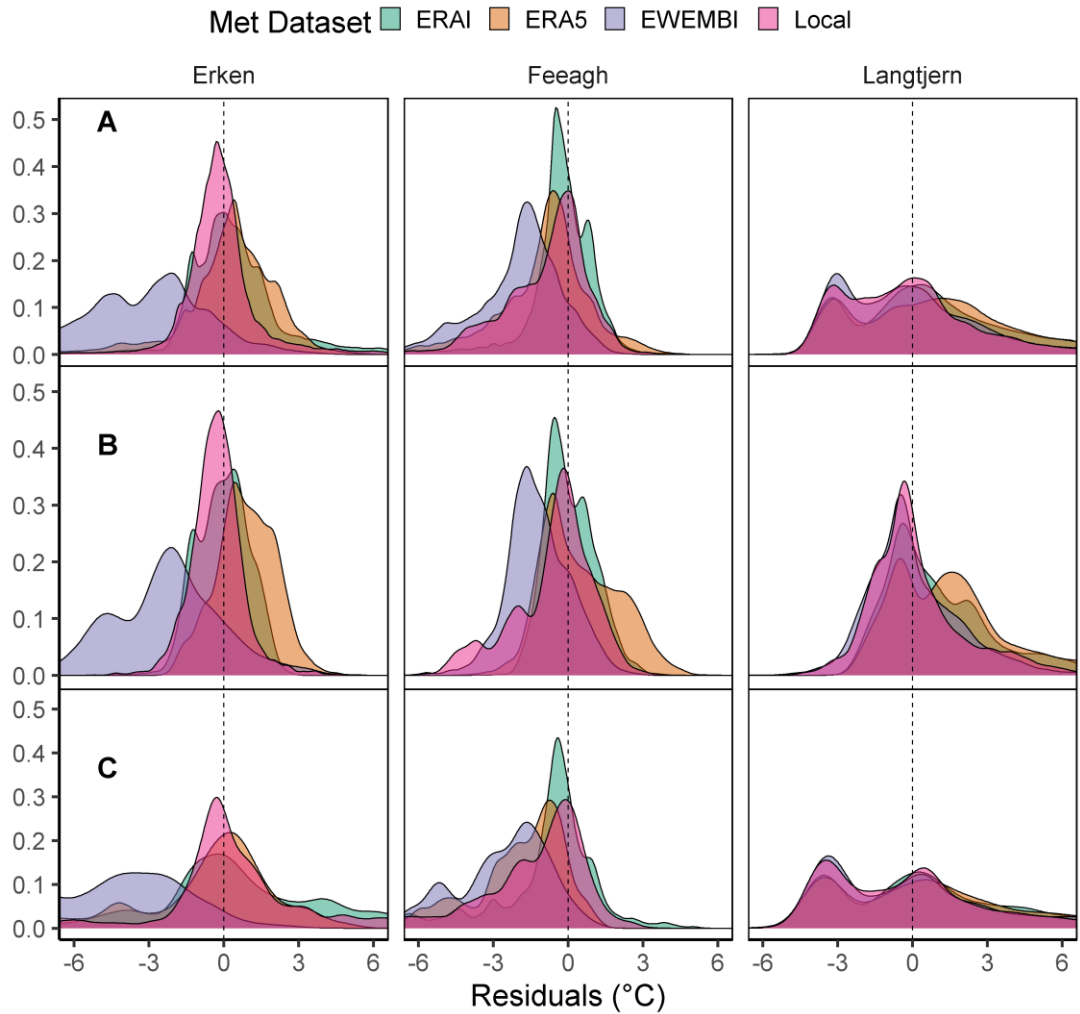


Figure 4.4 Distribution of residuals for four meteorological datasets; ECMWF ERA-Interim (ERA-I), ERA5, EWEMBI and Local, for Erken, Feeagh and Langtjern for the full profile (A) (Erken:  $n=84240$ ; Feeagh:  $n=83076$ ; Langtjern:  $n=30457$ ), surface (B) (Erken:  $n=3120$ ; Feeagh:  $n=7224$ ; Langtjern:  $n=4296$ ), and bottom (C) (Erken:  $n=3120$ ; Feeagh:  $n=7224$ ; Langtjern:  $n=4296$ ). The residuals from the four lake models: FLake, GLM, GOTM and Simstrat were grouped within this plot.

Root mean square error (RMSE) and mean absolute error (MAE) were both calculated between observed temperature profiles and simulated temperature profiles, but they showed very similar patterns, so the results are focused on RMSE. The RMSE values indicated that the ERA-I dataset produced simulations with a lower RMSE for Feeagh (Figure 4.5). Simulations using Local data had the narrowest RMSE distribution for Erken while those using ERA-I and ERA5 had similar ranges of model fit for Erken and Langtjern. The EWEMBI forcing data was the second best in terms of model fit for Langtjern after the Local data, but it is important to note that there was a strong bimodality across all datasets, driven mainly by the diverging performance of GOTM

and Simstrat, which both had large error in the bottom, compared to Flake and GLM. For Erken, the EWEMBI simulations had a high RMSE which was driven by GOTM and Simstrat. GOTM and Simstrat had distinctly higher RMSE values for Langtjern when forced with ERAI and ERA5 data. The simulations using ERAI, ERA5 and Local data all had mean RMSE values less than 2.5 for Erken (2.13, 2.19, 1.79) and Feeagh (1.44, 2.22, 2.00), while those for EWEMBI were larger (4.84; 2.86).(Table 4.3).

The density distributions of RMSE for Feeagh and Erken were similar in pattern for the models GLM, GOTM and Simstrat, with Flake being an obvious outlier in terms of model error (Figure 4.5). For Langtjern, the distribution of the RMSE values for FLake and GLM indicated a much better model fit than those for GOTM and Simstrat. For Erken, GLM and GOTM simulations had mean RMSE values less than 2.5 °C (2.47 °C, 2.43 °C) while those for Simstrat and FLake were less than 3 °C (2.75 °C, 2.97 °C) (Table 4.3). For Feeagh, GLM, GOTM and Simstrat all had mean RMSE values less than 2 (1.87 °C, 1.68 °C, 1.75 °C). The value for the FLake simulations was much larger (3.14 °C) (Table 4.3). For Langtjern, mean RMSE values for FLake and GLM were noticeably lower (2.45 °C, 2.48 °C) than those for GOTM and Simstrat (4.41 °C and 4.59 °C) but still relatively high to be considered a “good” calibration (i.e. less than 2 °C; Bruce *et al.*, 2018; Read *et al.*, 2019) (Table 4.3).

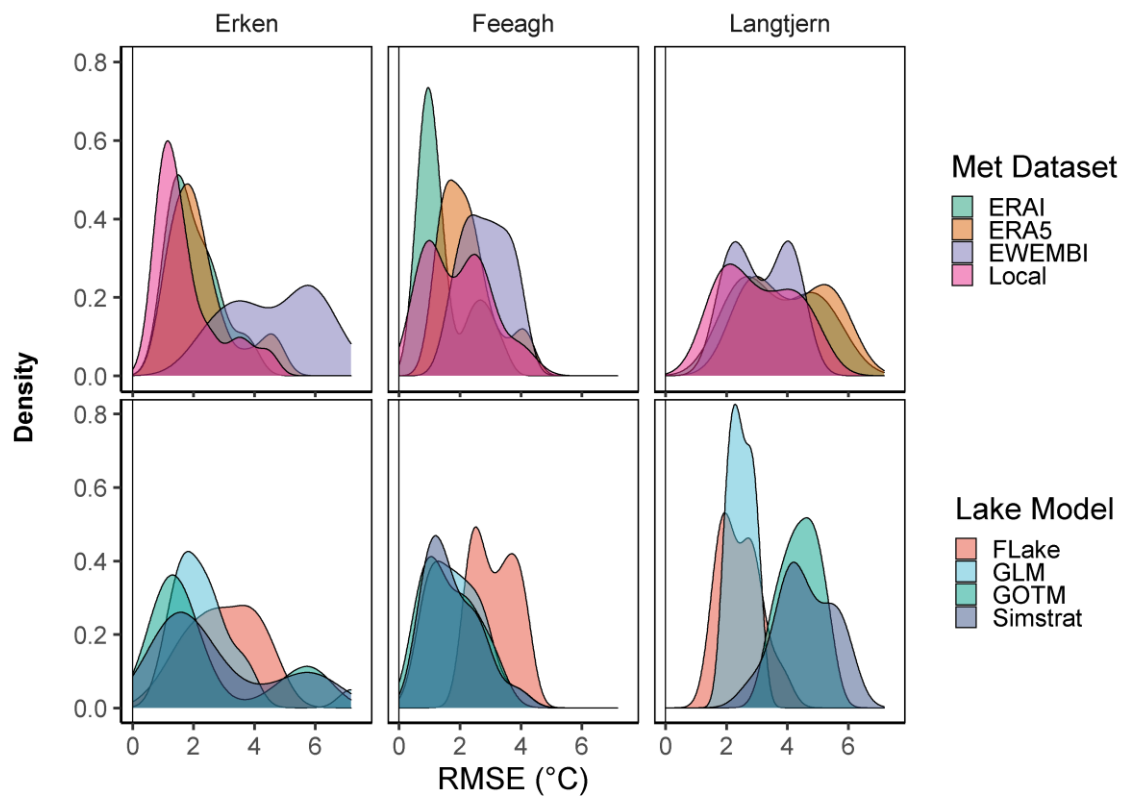


Figure 4.5 Density distributions of annual root mean squared error (RMSE) values for the total water column temperature profile for Feeagh ( $n=20$ ), Erken ( $n=20$ ) and Langtjern ( $n=14$ ) for each meteorological dataset: ERAI, ERA5, EWEMBI and Local, and for each lake model FLake, GLM, GOTM and Simstrat.

Table 4.3 Uncalibrated model fitness statistics calculated for the entire simulation period and full water column for each lake, Erken, (n=84240), Feegh (n=83076) and Langtjern (n=30457), with each climate dataset ERA-Interim (ERA-I), ERA5, EWEMBI and Local for each of the four lake models FLake, GLM, GOTM and Simstrat. Statistics calculated were root mean square error (RMSE), Nash-Sutcliffe Efficiency (NSE) and Bias.

<b>Model</b>	<b>Erken</b>				<b>Feegh</b>				<b>Langtjern</b>			
RMSE (°C)	ERA-I	ERA5	EWEMBI	Local	ERA-I	ERA5	EWEMBI	Local	ERA-I	ERA5	EWEMBI	Local
FLake	2.12	3.62	3.48	2.68	2.77	3.36	3.42	3.22	2.34	3.29	2.49	1.74
GLM	2.58	1.96	3.72	1.92	1.16	2.26	2.66	1.80	2.80	2.66	2.11	2.39
GOTM	1.54	1.46	5.55	1.21	0.88	1.74	2.86	1.45	4.46	4.94	3.91	4.42
Simstrat	2.13	1.84	5.69	1.46	1.03	1.79	2.74	1.80	5.23	5.44	4.04	3.70
<b>NSE</b>												
FLake	0.77	0.33	0.38	0.63	0.52	0.30	0.27	0.35	0.85	0.70	0.83	0.92
GLM	0.63	0.79	0.23	0.79	0.90	0.61	0.46	0.75	0.68	0.71	0.82	0.77
GOTM	0.87	0.88	-0.72	0.92	0.94	0.77	0.38	0.84	0.20	0.01	0.38	0.21
Simstrat	0.75	0.81	-0.81	0.88	0.92	0.76	0.43	0.75	-0.11	-0.20	0.34	0.44
<b>Bias (°C)</b>												
FLake	-0.94	-1.25	-2.56	-0.60	-1.56	-1.79	-2.26	-1.94	0.73	1.23	0.65	0.17
GLM	1.14	1.40	-2.42	0.27	-0.20	-1.02	-1.95	-0.71	1.42	1.26	0.29	0.16
GOTM	-0.03	-0.35	-5.23	-0.09	-0.55	-1.12	-2.54	-0.94	0.67	1.38	-0.67	0.55
Simstrat	1.18	0.17	-4.32	-0.42	0.61	-0.50	-1.82	-0.56	1.88	2.15	0.73	0.03

The bias in the model simulations varied with lake and with the forcing dataset used. Simulations with models using the Local data had the smallest range in bias and were centred around 0 for both Erken and Langtjern, while for Feeagh, it was negatively skewed (Figure 4.6). ERA5 was centred around 0 for Erken but it had a larger range than Local data. The bias for EWEMBI was strongly negatively skewed for both Erken and Feeagh and negatively skewed relative to ERAI and ERA5 across all three lakes. ERA5 and ERAI were positively skewed for Langtjern. For Feeagh the distribution for the ERAI simulations was closest to 0 while the results using ERA5 had quite a small variance. The bias for EWEMBI was strongly negatively skewed for both Erken and Feeagh and negatively skewed relative to ERAI and ERA5 across all three lakes. ERA5 and ERAI were positively skewed for Langtjern. For Feeagh the distribution for the ERAI simulations was closest to 0 while the results using ERA5 had quite a small variance.

FLake had a negatively skewed bias for Erken and Feeagh. In contrast for Langtjern it had the closest bias to 0 with a low variance. GLM had a positively skewed bias for Erken and Langtjern and a slight negative skew for Feeagh. Simstrat had a slight negative bias for both Erken and Feeagh driven by the EWEMBI dataset (Figure 4.6).

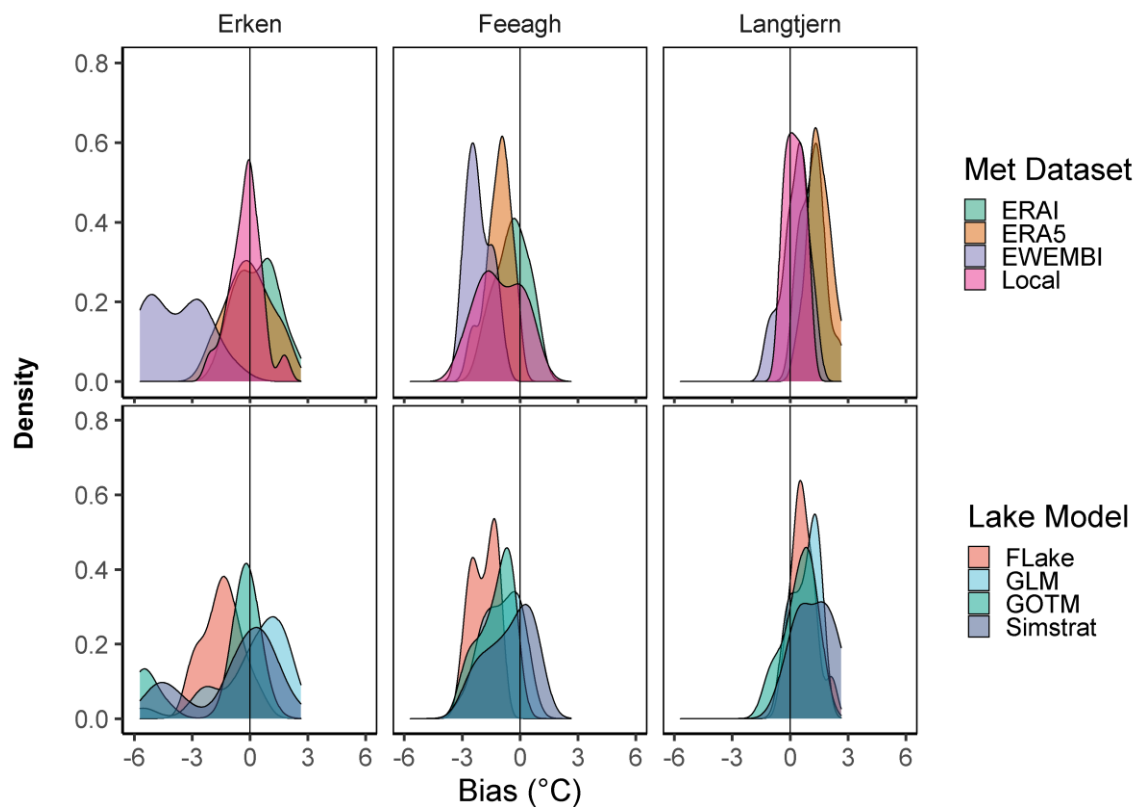


Figure 4.6 Density distributions of annual bias values for Feeagh (n=20), Erken (n=20) and Langtjern (n=14) for each meteorological dataset: ERAI, ERA5, EWEMBI and Local and for each lake model: FLake, GLM, GOTM and Simstrat.

Erken has the largest interannual variability across datasets and models in predicting maximum surface temperatures and the timing of when this temperature occurred. Annual biases were mainly model specific rather than associated with a specific forcing dataset (Figure 4.7). Maximum surface temperatures were most accurately simulated by the simulations using the ERAI forcing data for Erken, clustered around 0, while the results using ERA5 were positively skewed as it consistently overestimated maximum surface temperature (Figure 4.7). Simulations using Local and ERAI captured the timing well, with smaller errors. EWEMBI consistently underestimated the surface temperature and the timing, as indicated by most of the points being in the bottom left quadrant of the graph. The clustering around zero was mainly seen in simulations using Local and ERAI forcing data while simulations based on ERA5 had a warm bias and tended to overestimate temperatures.

For Feeagh, Local and ERAI simulations had the smallest distribution around zero for both the magnitude of maximum temperature and the timing of when this occurs. The simulations using EWEMBI had a negative bias while ERA5 had a positive bias. Interannual variation in error was quite large in 2010 and 2012 and for one point in 2014. The outliers were either with the EWEMBI forcing dataset or GLM or Simstrat. FLake captured the timing and magnitude of the maximum surface temperature most accurately, with a large clustering around zero (Figure 4.7).

There was a large clustering of values around zero for Langtjern for all gridded datasets (Figure 4.7). Overall, simulations using Local forcing data had the largest number of values close to zero indicating that it performed best at capturing the timing and magnitude of maximum surface temperature. Simulations using ERA5 has a slight warm bias while those using EWEMBI data has a slight negative bias. The model GLM consistently overestimated surface temperatures with the ERAI, ERA5 and EWEMBI forcing data.

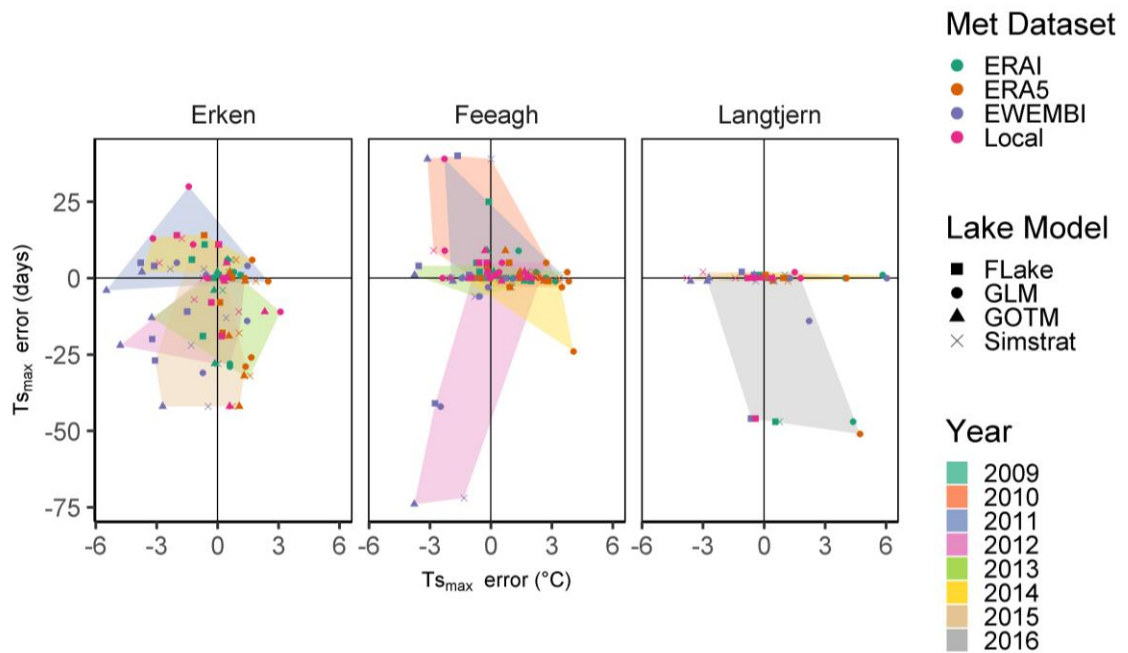


Figure 4.7 Scatterplot of residuals in predicting surface maximum temperature ( $T_{s_{max}}$ ) and the day of surface maximum temperature for each of the three lakes with the four lake models: FLake, GLM, GOTM and Simstrat forced with the four meteorological datasets: ERA-Interim (ERA-Interim), ERA5, EWEMBI and Local. Points from the same year are connected by the coloured polygons.

Simulation of the start and end of thermal stratification was quite varied between gridded datasets, lake models and lakes. There was large uncertainty around simulated Erken stratification dates because there were years when the monitoring buoy was deployed after the lake was already stratified. Feeagh and Langtjern had consistent biases in predictions which were a result of lake model biases (Figure 4.8).

For Erken, simulations using the Local data had the smallest error in predicting the start and end of stratification while those with the ERA5 dataset performed best over the five-year period with GLM. The simulations using the EWEMBI forcing data had small errors when used to drive the GLM and GOTM models for this lake, but in contrast had quite large errors with the FLake and Simstrat models. The simulations using the ERA-Interim forcing data predicted an earlier end of stratification when used with GLM, GOTM and Simstrat, while the simulations using FLake had a negative bias i.e., they predicted the end of stratification earlier than observed. FLake consistently predicted the end of stratification later than was observed while GLM, GOTM and Simstrat predicted the end too early. Values for FLake, GLM and Simstrat were omitted for 2012 and Simstrat for 2013 because these models simulated stratification for the entire period. It is important

to note that the Erken monitoring buoy is removed from the lake each winter and put back in the lake as soon as the ice melts but sometimes it has been seen that the lake is already stratified when the buoy is put back in or sometimes when it is taken out, so there is potential error associated with the observed dates.

Overall, there was a slight bias towards predicting the start of stratification too early for Feeagh (Figure 4.8). The simulations using the ERAI forcing data had the smallest error in predicting the start and end of stratification. Simulations using ERA5 data were biased towards predicting the end of stratification too late. Simstrat was biased towards predicting the end of stratification too early for Local and ERAI. There was small interannual variation with a clear bias for the FLake model which simulated stratification both starting too early and ending later than observed. FLake did not capture the stratification timing in Feeagh accurately, as it consistently simulated a start that was earlier than observed, and an end that was later than observed. This effect was irrespective of the forcing dataset, indicating that it was a model issue rather than a forcing data issue. Feeagh is a lake which does not stratify very strongly so the timing of the start and end of stratification is relatively sensitive to the criteria used for determination of stratification.

For Langtjern, there was a smaller range around the simulations of the start of stratification while there was a much larger variation in predicting the end, which was biased according to the different lake models used (Figure 4.8). ERA5 and ERAI have the smallest range in error for both FLake and GLM. GOTM and Simstrat were strongly biased and predicted the end of stratification too early no matter which dataset was used. The simulations using the FLake model had much more interannual and inter-dataset variation than those using GLM, resulting in GLM having the lowest errors in predicting stratification timings.

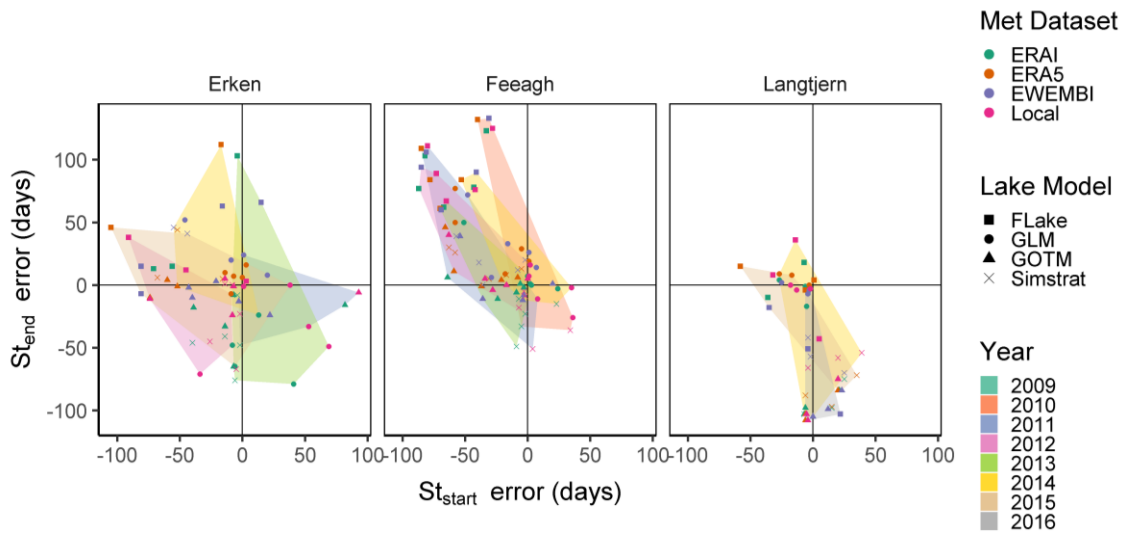


Figure 4.8 Scatterplot of residuals in predicting the day when stratification starts ( $St_{start}$ ) and ends ( $St_{end}$ ) for each of the three lakes with the four lake models: FLake, GLM, GOTM and Simstrat being forced with the four meteorological datasets: ERA-Interim (ERA-I), ERA5, EWEMBI and Local. Points from the same year are connected by the coloured polygons.

The magnitude of errors between measured and simulated ice phenology varied greatly between years. Ice did not form on Erken in the simulations using GLM with Local data for any of the years or in Langtjern for simulations with GLM in 2015 (Figure 4.9).

There was considerable interannual variation in the accuracy of the prediction of ice onset and offset at Erken across all models and gridded datasets (Figure 4.9). EWEMBI had a strong negative bias in simulating the onset of ice too early while ERA-I, ERA5 and Local had similar patterns for FLake, GOTM and Simstrat.

The interannual variability of model accuracy was also noticed for Langtjern, although to a lesser degree than Erken (Figure 4.9). There were no clear patterns within the data apart from the fact that GLM consistently predicted the onset of ice to be later than observed. In 2015 and 2016, all model and climate dataset combinations simulated ice off too early while in 2014 there was a bias in predicting the onset of ice too early.

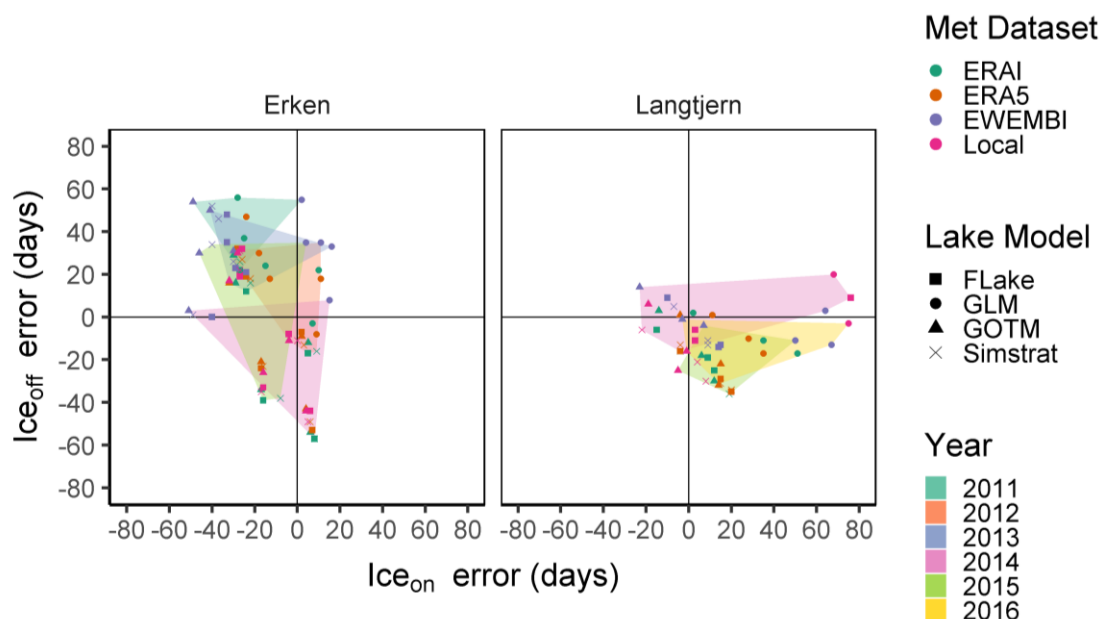


Figure 4.9 Scatterplot of residuals in predicting the day of ice onset ( $Ice_{on}$ ) and offset ( $Ice_{off}$ ) for each of the three lakes with the four lake models: FLake, GLM, GOTM and Simstrat being forced with the four meteorological datasets: ERA-Interim (ERA-I), ERA5, EWEMBI and Local. Points from the same year are connected by the coloured polygons.

Despite the relative success in reproducing water temperature profiles using uncalibrated models (described above), following model calibration and as might be expected, simulations using each of the climate forcing datasets showed an improvement, with a mean decrease in the RMSE value of  $1.07\text{ }^{\circ}\text{C}$  across all lakes, meteorological datasets and lake model combinations (Figure 4.10; Table 4.4). The improvement was most pronounced for the simulations using the EWEMBI and ERA5 forcing datasets. For the simulations of Erken, there was a large decrease in RMSE for EWEMBI ( $-2.12\text{ }^{\circ}\text{C}$ ), but the calibrated simulation still had a relatively high RMSE of  $2.24\text{ }^{\circ}\text{C}$ . Local and ERAI had similar measures of error across most models following calibration.

For Feeagh, values with an RMSE which were greater than  $2\text{ }^{\circ}\text{C}$  prior to calibration had the largest improvement (ERA-I-FLake:  $-1.6\text{ }^{\circ}\text{C}$ ; ERA5-FLake:  $-1.3\text{ }^{\circ}\text{C}$ ; EWEMBI-Simstrat:  $-1.6\text{ }^{\circ}\text{C}$ ) (Figure 4.10; Table 4.4). The Feeagh simulations for EWEMBI had the greatest reduction in RMSE following calibration with three of the models having values below  $2\text{ }^{\circ}\text{C}$ . The calibrated simulations using the ERA-I forcing data had a large reduction in RMSE for FLake ( $2.77$  to  $1.19\text{ }^{\circ}\text{C}$ ) with smaller reductions for the other models.

The simulations with each of the meteorological datasets for Langtjern were improved by calibration (Figure 4.10; Table 4.4). Despite slight improvements, the RMSE of all simulations using GOTM were relatively high (greater than 3 °C) (Table 4.4). There were relatively small differences in RMSE between each of the meteorological datasets for Langtjern following calibration.

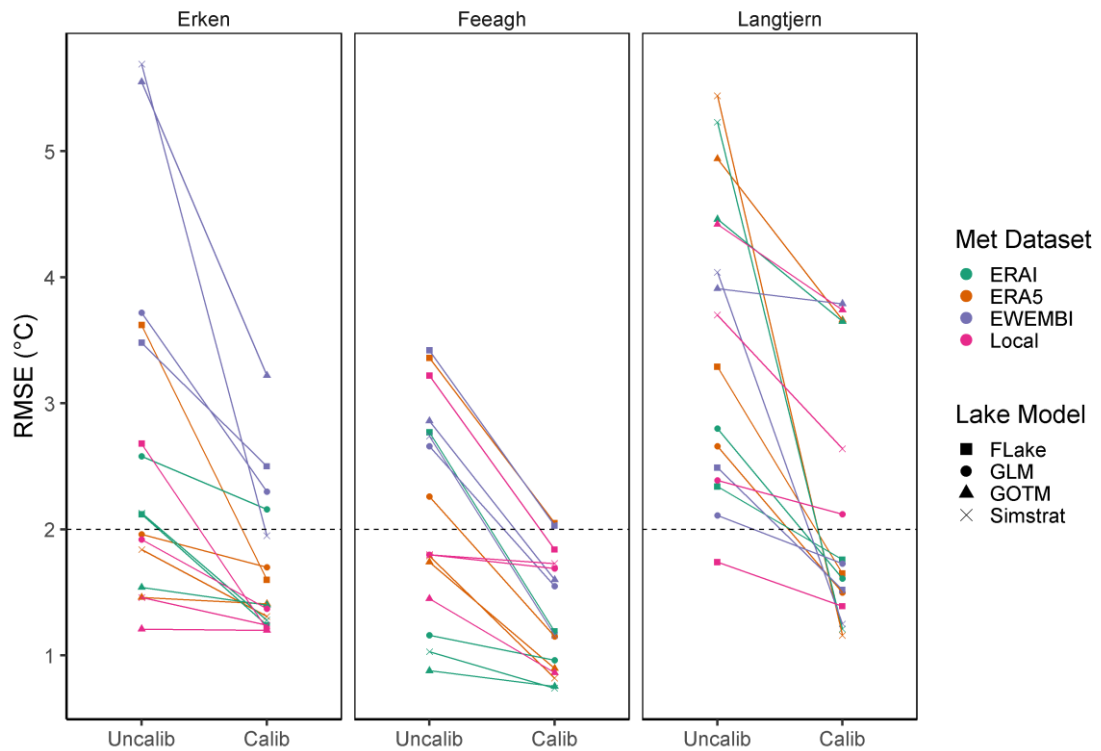


Figure 4.10 Improvements in model fitness (RMSE) for each model and meteorological dataset after calibration against observed temperature profiles for Erken (n=84240); Feeagh (n=83076) and Langtjern (n=30457). A RMSE of 2 °C is used as a reference point for a ‘good’ calibration (Bruce *et al.*, 2018; Read *et al.*, 2019).

Table 4.4 Calibrated model performance statistics calculated for the entire simulation period for each lake: Erken (n=84240); Feeagh (n=83076) and Langtjern (n=30457),. with four meteorological datasets: ERA-Interim (ERA-I), ERA5, EWEMBI and Local for each of the four lake models: FLake, GLM, GOTM and Simstrat. Statistics calculated were root mean square error (RMSE), Nash-Sutcliffe Efficiency (NSE) and Bias.

<b>Model</b>	<b>Erken</b>				<b>Feeagh</b>				<b>Langtjern</b>			
RMSE (°C)	ERA-I	ERA5	EWEMBI	Local	ERA-I	ERA5	EWEMBI	Local	ERA-I	ERA5	EWEMBI	Local
FLake	1.24	1.60	2.50	1.21	1.19	2.05	2.03	1.84	1.76	1.65	1.52	1.39
GLM	2.16	1.70	2.30	1.37	0.96	1.15	1.55	1.69	1.61	1.50	1.73	2.12
GOTM	1.40	1.41	3.22	1.26	0.75	0.90	1.60	0.86	3.65	3.66	3.79	3.74
Simstrat	1.28	1.31	1.95	1.24	0.74	0.82	1.16	1.73	1.21	1.16	1.25	2.64
<b>NSE</b>												
FLake	0.92	0.87	0.68	0.93	0.91	0.74	0.74	0.79	0.91	0.92	0.94	0.95
GLM	0.74	0.84	0.71	0.90	0.93	0.90	0.82	0.78	0.90	0.91	0.88	0.82
GOTM	0.89	0.89	0.42	0.91	0.96	0.94	0.81	0.94	0.46	0.46	0.42	0.43
Simstrat	0.91	0.90	0.79	0.91	0.96	0.95	0.90	0.77	0.94	0.95	0.94	0.72
<b>Bias (°C)</b>												
FLake	-0.04	-0.33	-0.62	0.10	-0.31	-0.58	-0.58	-0.69	-0.16	-0.57	-0.12	0.25
GLM	0.28	0.03	-0.38	-0.51	-0.06	-0.17	-1.15	-0.15	0.24	0.32	-0.43	-0.05
GOTM	-0.29	0.01	-2.54	0.09	-0.45	-0.41	-1.31	-0.27	-1.18	-0.94	-1.17	-0.95
Simstrat	0.18	-0.28	-0.36	-0.25	0.04	0.01	-0.60	-0.03	-0.35	-0.14	-0.26	-1.51

The calibrated scaling factors showed a high degree of variation across the three lake sites. There was large variability between lake models and meteorological datasets for Erken. For Feeagh, increases in the scaling of wind speed improved model simulations for each meteorological dataset (Table 4.4). Overall, Langtjern showed more improvement with reductions in short-wave radiation. This showed that even with just three lakes there was a wide range of sensitivity across all parameters (Figure 4.11).

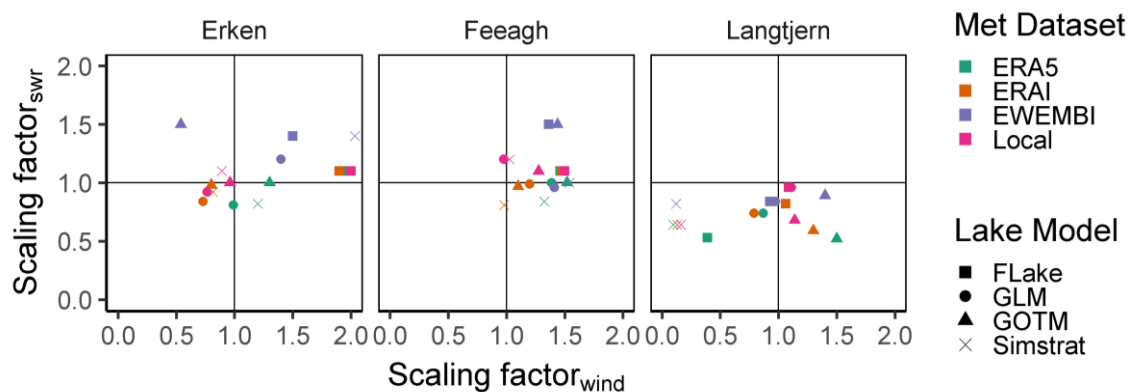


Figure 4.11 Range of calibrated scaling factors for wind and incoming shortwave radiation (swr) applied to each of the four meteorological datasets; ERAI, ERA5, EWEMBI and Local and for each of the four lake models: FLake, GLM, GOTM and Simstrat for each of the three lakes: Erken, Feeagh and Langtjern.

ERA5 was the gridded dataset that best replicated the local observed meteorological data, with much smaller biases across each of the main meteorological variables. It also captured maximum values accurately (Figure 4.12). Despite this, ERA5 did not simulate lake hydrodynamics as well as simulations using the ERAI datasets in some cases. For example, simulations using ERAI had large positive biases in windspeed for Feeagh and Erken, and this resulted in a better simulation of water temperature in Feeagh. (Figure 4.1). This may be because Feeagh is a windy site, and the local data were recorded at the southern shore of the lake. It is possible that the spatial scale at which ERAI data were calculated better replicates conditions across the whole lake surface than this local observed data. Hydrological models forced by reanalysis data have also previously been found to be more accurate than those forced by local meteorology data in several studies (Ledesma and Futter, 2017; Persaud *et al*, 2020; Tarek *et al.*, 2019). This was attributed to the fact that reanalysis data were internally coherent, while local

data can potentially be heterogeneous at spatial scales which do not reflect the processes across a whole catchment.

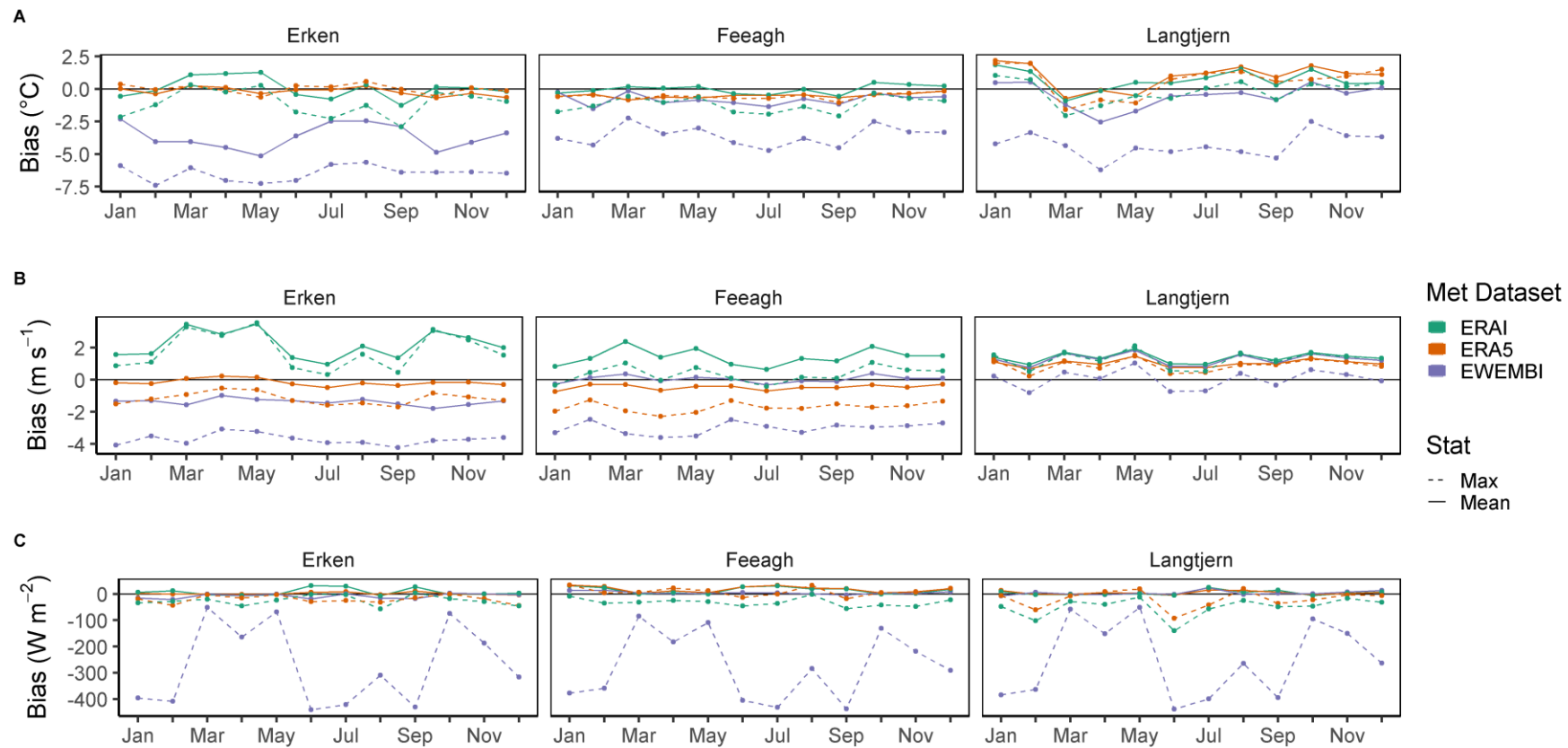


Figure 4.12 Monthly bias of daily mean for air temperature (A), wind speed (B) and incoming solar radiation (C) for Erken, Feeagh and Langtjern for ERA5, ERAI and EWEMBI compared to the measured local data.

#### 4.5. Discussion

Local and global-scale simulations of lake thermal dynamics and coupled biogeochemistry are now being more commonly used to inform short-term and longer-term lake conditions. Such simulations can greatly benefit from the use of gridded reanalysis datasets by increasing the number of lakes modelled to understand the response to meteorological changes on a regional level (Woolway *et al.*, 2020). This study evaluated, for the first time, the use of the gridded reanalysis datasets ERA5, ERAI and EWEMBI as potential meteorological forcing datasets for 1D lake hydrodynamic models by comparing them to simulations using Local data. These forcing datasets were comprehensively tested across three lakes with diverse characteristics using a set of lake models with varying structures. The lake models were initially run without any calibration to ensure a relatively fair comparison between lakes and to demonstrate the benefits and limitations of using uncalibrated models. We found that the lake models forced with the gridded meteorological data had a similar level of overall model accuracy as the simulations using locally measured data, but that this accuracy was influenced by lake morphometry and lake model applied. With regards to capturing in-lake events, such as the timing and magnitude of maximum surface temperature and start and end of stratification, simulations using both the ERAI and ERA5 forcing data had similar degrees of accuracy as simulations using the Local data. However, our study found that there were no ‘best’ combination of climate dataset and lake model but demonstrated the general levels of variability that can be expected to arise for many combinations of models and gridded datasets. We also showed that a simple and computationally efficient calibration procedure significantly improved model accuracy when observed temperature profile data were available.

#### 4.5.1. Differences in hydrothermal simulations using gridded datasets and Local data

Gridded datasets have previously been used to simulate lake temperatures on a global scale to understand the global lake response to directional climate change (ERAI - Woolway and Merchant, 2019; ERA 20C - Piccolroaz *et al.*, 2020). Other single lake studies have also used this approach, for example ERAI data were used to force a three-dimensional model for Lake Chaohu in China (Frassl *et al.*, 2018). Gridded datasets are widely used in hydrology (Persaud *et al.*, 2020; Tarek *et al.*, 2019) and could potentially be developed into an integrated catchment modelling system that incorporates lakes and stream networks on a regional scale in data-poor areas (Read *et al.*, 2014). However, to date there has been little focus on the performance of a workflow incorporating these datasets to successfully simulate temperature profiles in lakes of different morphometry. Such a workflow could either utilise an uncalibrated model setup, which can be required for studies on large spatial scales where observed data are absent, or to use measure temperature profile data to calibrate the model which could then be used in lakes with ongoing monitoring programs.

Simulations using the ERAI dataset produced either much more accurate (Feeagh) or slightly more accurate (Erken and Langtjern) simulations of lake temperature than ERA5 despite not reproducing local meteorological conditions as accurately as ERA5. This was surprising because the ERAI dataset was similar in structure to ERA5 but was of lower temporal and spatial resolution (Albergel *et al.*, 2018). For the Feeagh case study, when the ERA5 data were compared to Local meteorology, it was found to have a much lower bias than the ERAI dataset for mean wind speed. However, simulations using ERA5 considerably underestimated the maximum wind speed (Figure 4.12). It is possible that for Feeagh, maximum wind speeds are a crucial driver of in-lake processes. In this regard, it may be that ERAI, with its larger spatial resolution, captures more accurately the influence of the Atlantic Ocean which exerts a strong influence on the Burrishoole catchment (Andersen *et al.*, 2020; Jennings *et al.*, 2012).

The EWEMBI dataset captured the mean local air temperature, wind speed and solar radiation well but did not capture the maximum values. This was likely as a result of its daily timestep (Figure 4.12). Consequently, it did not accurately simulate the sudden occurrence of events such as the start and end of stratification and onset and offset of ice cover (Figure 4.8, Figure 4.9). Across both types of events, simulations using this forcing data tended to predict the offset of ice and stratification later than was observed and later than the simulations with other datasets. This issue could be addressed by applying a temporal downscaling technique similar to that presented in Shatwell *et al.* (2019) where they used downscaled daily data to a 6-hourly temporal resolution. Similarly, the shortcomings of using EWEMBI datasets could be overcome by using a simple calibration procedure which scales the most influential input variables (Figure 4.10). For example, Ayala *et al.* (2019) found that there were small differences in model simulations using synthetic hourly data and daily meteorological data when running GOTM for Erken, once the model had been calibrated.

#### 4.5.2. Differences between lake models

For the shallow lake Langtjern, there was a clear distinction between the use of the two turbulence models (GOTM and Simstrat) and both Flake, which is designed to capture lake profile temperature evolution and GLM, an energy balance model. In the uncalibrated GOTM and Simstrat simulations, hypolimnetic temperatures were overestimated because the models failed to simulate the development of thermal stratification throughout the year (Figure 4.4). One of the reasons for this may be because there was a clear positive bias for the uncalibrated wind data all year round for Langtjern for all data sets (Figure 4.12), resulting in an overestimate of turbulent kinetic energy within the models. A similar result has been reported from other studies where turbulence models over-estimated mixing within shallow lakes (Stepanenko *et al.*, 2010; Subin *et al.*, 2012). Potentially, the models used in this current study have

not been parameterized to capture the dissipation of turbulent kinetic energy in small lakes. Despite the errors associated with stratification dynamics, GOTM and Simstrat both captured the magnitude of maximum surface temperature and timing to a high degree of accuracy. For Feeagh and Erken, in contrast to Langtjern, there was generally common agreement in RMSE across all lake models except for FLake, which consistently underestimated hypolimnetic temperatures (Figure 4.4 B; Figure 4.4 C).

The selection of a lake model can greatly influence the accuracy of simulations for lakes with differing morphometry, as demonstrated by the high variation in performance which we saw across our three study sites. In particular, the accuracy of FLake in capturing key lake phenological events such as the start/end of stratification and ice onset/offset varied between sites. It should be noted however that FLake was designed to simulate the lake-surface heat fluxes, hence the large errors in the simulations for the hypolimnion (Subin *et al.*, 2012). This model-related bias would affect the outputs where that model is used for multiple sites. Woolway *et al.* (2019) for example used one lake model (FLake), with a fixed light attenuation coefficient, and with only surface temperature data to validate the model for 650 sites. Our results suggest that the results from such a modelling experiment would contain a high degree of uncertainty for a number of lake metrics, particularly bottom temperature, the simulation of which is a recognised difficulty when using 1D hydrodynamic models (Bueche and Vetter, 2014). In the Woolway *et al.* (2019) study, the model was forced with data from ERAI where wind speeds were compared to observations from nearby weather stations and homogenised. Thiery *et al.* (2014b) showed how sensitive the FLake model was to small changes in the wind speed, especially to a regime switch from permanent stratification to fully mixed conditions. Le Moigne *et al.* (2016) examined the use of FLake on a global scale and found that it had warm biases that were greater than 1 °C which they attributed to the fact that ERAI represented an atmospheric state that was dryer and warmer than local above lake conditions. They also found large errors when simulating the duration of ice cover ( $\pm 180$  days). Our results confirm the results of these studies and showed that even when using FLake with local observed meteorological data, there was a relatively large degree of error,

particularly towards the bottom lake depth, which influenced the accuracy in capturing stratification dynamics (Figure 4.8; Feeagh).

The present study has shown that uncalibrated models forced with gridded reanalysis data can capture surface temperatures with a high degree of accuracy. However, uncalibrated models were less successful at simulating water temperatures at depth and capturing aspects of the resulting phenology of stratification and ice cover. If gridded datasets are being used to simulate full water temperature profiles, our study showed that calibrating a model with observed temperature profile data improved accuracy. For Simstrat, this led to a reduction in RMSE in simulating the full temperature profile because it simulated the hypolimnetic temperature more accurately. This decrease in RMSE was a result of large reductions in SWR (0.64) and wind speed (0.13) which could be deemed extreme adjustments. However, such an adjustment would not be unusual for shallow lakes considering the positive bias present in the wind speed of the reanalysis data (Figure 4.12). Turbulent kinetic energy within the water column can be used to estimate vertical eddy diffusivity in the water column and is the premise for many 1D lake models (Henderson-Sellers, 1985; Wüest *et al.*, 2000). Eddy diffusivity is similar to molecular diffusivity but occurs on larger scales due to fluid motion (Lerman *et al.*, 1995). Deng *et al.* (2013) reduced diffusivity by 98 % to reproduce diurnal surface temperatures when modelling Lake Taihu in China, which is 2 m in depth, using the Community Land Model version4 – Lake, Ice, Snow and Sediment simulator (CLM4-LISS), which is a turbulence-based model. The reason why GOTM does not simulate stratification well for shallow lakes in an uncalibrated setup could be because it was originally developed for use in the ocean, where lateral boundary effects would be negligible while they would play a significant role in small shallow lakes (Yeates and Imberger, 2003). Hence, the simple calibration using just wind speed and incoming solar radiation was not enough to reduce RMSE for GOTM in this shallow lake (Figure 4.10).

After calibrating each lake model, we observed a divergent response between the calibrated scaling factors for wind and SWR. This is a result of the differing model structures and indicates how the sensitivity of each model to wind and SWR varies

with lake site. These results highlight the inherent model complexities that would make it difficult to extract exactly what the key drivers of change in lake thermal metrics are when comparing outputs across models and sites. A similar problem has also been reported in hydrology, where structural differences between hydrological models was the crucial source of uncertainty rather than the forcing data. (Quintana-Seguí *et al.*, 2019).

#### 4.5.3. Recommendations for applications

Even with the most accurate climate forcing data and site-specific calibration, there were still consistent biases in some of the model simulations (for example GOTM simulations for Langtjern). Downscaling and bias correct techniques are already used to correct inherent biases that are present in climate reanalysis datasets (Chen *et al.*, 2011). This approach is widely used in meteorology but has not yet been applied to lake models. We see this as a possible alternative to model calibration. A multi-variate bias correction could potentially remove some of the biases seen in our models (Cannon *et al.*, 2015). It is important to note that although these techniques can be used to reduced bias but they also bring another source of uncertainty into the models (Wootten *et al.*, 2017).

The ability of four different lake models to successfully capture the timing of ice was examined in the current study. Similar to Yao *et al.* (2014), there was large variability and uncertainty across all lake models indicating that there is still a need for further improvements in modelling ice dynamics. It has been shown that this has been constrained by the large uncertainties that exist in observations of lake ice (Le Moigne *et al.*, 2016).

Future work should focus on developing methodologies that take advantage of using an ensemble of lake models. Different lake models captured surface temperatures more accurately than others but different lake models captured

stratification timings better (Figure 4.8). Duan *et al.* (2007) highlighted how hydrological forecasts using a Bayesian model averaging approach generated more skilful and reliable predictions. Broderick *et al.* (2016) also recommended using a multi-model ensemble with a suitable averaging method in the context of climate assessment such as Bayesian model averaging and Grange-Ramanathan averaging. The key benefits of these approaches are that they work in the probabilistic space which allows uncertainty in the predictions to be quantified. Within lake modelling, Trolle *et al.* (2014) showed that when simulating phytoplankton biomass the simple arithmetic mean of three ecosystem models performed better than any one single model and that the uncertainty related to the different model structures could be compared. Ensemble modelling allows further partitioning of the drivers of uncertainty within the model predictions such as the forcing data, model parameterization, model process or initial conditions.

Modelling of water temperature profiles can be used to inform on past and future conditions in lakes and can therefore inform lake management and policy. However, the forcing data required for such simulations are not always available from nearby meteorological stations. Our results show that where local data are absent, gridded reanalysis datasets such as the ERAI or ERA5 can be used with confidence to simulate changes in lake temperature hydrodynamics, sometimes even performing better than using meteorological data measured on or near the lake. ERA5 currently has a temporal range of 1979-present but in the future, this will be extended back to 1950 (ECMWF, 2020). This will allow for further hindcast studies to infer historical events and trends with a high degree of confidence (Hadley *et al.*, 2014; Moras *et al.*, 2019; Piccolroaz *et al.*, 2020; Woolway *et al.*, 2017b).

#### 4.6. Conclusions

Global reanalysis datasets are a viable alternative to meteorological data measured on-site for sites for forcing 1D hydrodynamic models. There are significant limitations to

using daily meteorological forcing data for key lake indices e.g. stratification and ice cover duration, but that these can be overcome through calibration with observed lake data. A simple and efficient calibration of driving variables can significantly improve model performance. The use of just one lake model could potentially bias results owing to a model's structural inability to replicate observed lake conditions and produce spurious trends. Using an ensemble of lake models is desirable owing to different model characteristics leading to some models performing better than others. This study showed that there is no single meteorological dataset or lake model that will work universally across sites.

## **CHAPTER 5. IMPACT OF MONITORING FREQUENCY ON ERROR REDUCTION WHEN USING DATA ASSIMILATION FOR SHORT-TERM HYDRODYNAMIC FORECASTS**

### *5.1. Abstract*

Accurate short-term forecasts of processes in lakes and reservoirs can be used to inform water management decisions in the near future. Recent developments in ecological forecasting facilitate the assimilation of monitoring data into model simulations, thus producing forecasts that are informed by the most recent observed conditions. Data collection can be expensive, however, and it is currently unclear how frequently observational data, such as lake water temperature profiles, need to be collected for assimilation into models to reduce forecast error to acceptable levels. Here we used a one-dimensional hydrodynamic model to generate multiple 14-day water temperature profile forecasts for three different lakes. Using a model, that had first been calibrated against historical data, we ran a series of simulation experiments where we inserted a single measured profile to re-initialize the model on various dates prior to the start of the forecast. We obtained the re-initialization temperature profile data (at 0 hours, 24 hours, 168 hours, 336 hours, and 672 hours pre-forecast) by subsetting high frequency data from *in-situ* sensors. We assessed how the forecast error was affected by 1. the length of time between the re-initialization step and the start of the forecast, and 2. the thermal status of the lake at the time of the forecast. We found, as might be expected, that the error was largest when no observational data were assimilated. However, even when the observed assimilated data was measured at the longest time interval before the start of the forecast (one month), the forecast error was reduced relative to model runs without any data assimilation. For simulations with data assimilated, the magnitude of the model error diminished as the re-initialization time became shorter, which was particularly pronounced when the lake was stratified. The results of this study suggest that the design of high and low

frequency monitoring programmes can be tailored to the characteristics of individual lakes, to optimize the performance of near-term water temperature forecasts.

## 5.2. Introduction

Anthropogenic pressures, including directional climate change, nutrient enrichment, and land use change are affecting water quality on a global scale (Adrian *et al.*, 2009; Coats *et al.*, 2006; Rempfer *et al.*, 2010). The impacts of these pressures on lakes and reservoirs are especially important because of their use as drinking water sources, value to recreational and tourism industries and other ecosystem services (Delpla *et al.*, 2009; Smith *et al.*, 2015). Intensive monitoring of these systems can be warranted when there are potential health risks as a result of deterioration in quality, for example, from harmful algal blooms (Paerl *et al.*, 2011). To move towards more proactive water management, information on the potential near-future state of a water body is required. Such information can only be provided by short-term forecasts (days to weeks) of the possible changes in lake physics, chemistry and biology. These lake system forecasts rely on the use of modelling workflows which couple meteorological forecasts with hydrodynamic and water quality models in order to accurately predict future conditions within a number of days (Peng *et al.*, 2019).

It is becoming increasingly evident that such short-term forecasts have the potential to play a key role in advancing environmental decision-making and improving decision support systems (Dietze *et al.*, 2018). Studies have shown that lake and reservoir models can accurately predict events such as fluctuations in water level (Young *et al.*, 2015), carbon dynamics (Zwart *et al.*, 2019), phytoplankton communities (Page *et al.*, 2018) and algal blooms (Stumpf *et al.*, 2016; Wilkinson *et al.*, 2018; Wynne *et al.*, 2013). Different statistical and data-based models have been used to forecast water quality in lakes include Bayesian models (Obenour *et al.*, 2014), artificial neural networks (Najah *et al.*, 2013) and regression models (Nazeer and Nichol, 2016). The drawback of using such models, however, is that they tend to rely on static training datasets and are less likely to predict conditions outside of the range of the specific training data, which can be a problem for forecasting the effects of extreme events such as heat waves or storms (Saber *et al.*, 2019). In contrast, process-based models are frequently used for ecological forecasting (Luo *et al.*, 2011;

Cuddington *et al.*, 2013) and, in principle, should provide more accurate forecasts when forced with data outside of the range used for calibration, as long as the processes are adequately simulated by the model. In limnology, these process-based models link lake physics, which drive hydrodynamics, to non-linear biological processes that govern nutrient availability and ecological functioning (Hakanson and Boulion, 2002; Gal *et al.*, 2009; Toffolon *et al.*, 2014; Snorheim *et al.*, 2017; Bucak *et al.*, 2018). Process based models are more capable of dealing with shifts and changes within the system which are controlled by fundamental relationships that can be quantified by equations within the model, and are well suited for use within forecasting workflows. Data-driven approaches combined with mechanistic models have been shown to perform better than either approach used on its own based on a study of for 68 lakes (Read *et al.*, 2019). Process driven physical models are usually dynamically coupled to biogeochemical models for modelling in-lake responses.

The implementation of short-term forecasts will only be adopted routinely when it is demonstrated that workflows can accurately predict future conditions with an acceptable envelope of error. Process-based models require the input of initial conditions to start a model run, and the use of appropriate values for these initial conditions is crucial to minimize potential forecast error (Palmer *et al.*, 2005). Often, default initial conditions or “best guess” estimates are used along with the model parameter set that had the highest fitness. The model is then allowed to “spin-up” for some time period prior to the period of forecast which will lead to reasonable values of key model state variables, in what we defined hereafter as a “free model run”, defined similarly to Kourzeneva (2014) and Ren *et al.* (2016). For accurate short-term forecasts, especially those with human health and wellbeing implications, using such an approach may not be adequate. Assimilating observational data to re-initialize the model prior to the forecast, as opposed to using a free model run approach, may reduce forecast error in lake water quality predictions to a satisfactory level (Zwart *et al.*, 2019). How best to assimilate observational data has been a topic of much discussion as ecological forecasting has become more widely used (Luo *et al.*, 2011; Liu *et al.*, 2012; Dietze *et al.*, 2018). Sequential techniques for data assimilation include the

processing of observational data as they become available, via a two-step procedure. First a forecast is run simulating the future distribution and then secondly, the distribution of the forecast is updated based on the new observation (Hoteit *et al.*, 2012; Khaki *et al.*, 2017). Stroud *et al.* (2009) used two methods to assimilate observed data into a sediment transport model for Lake Michigan: direct insertion and a kriging approach. They found that by using direct insertion they decreased forecast error compared to using a modelled approach which was not updated with new observational data.

High frequency monitoring (HFM) of key aquatic variables using electronic sensors has been an area of rapid acceleration over the past 20 years and offers a viable source of observed data for inclusion in modelling workflows (Marcé *et al.*, 2016). Monitoring platforms with telemetry capabilities have been deployed for many lakes around the world and provide observational data in near-real-time (Hamilton *et al.*, 2015). There has been a large increase in the availability of HFM data (Porter *et al.*, 2012) and parallel developments in networked science has advanced the use of these data in limnology (Hanson *et al.*, 2016). High frequency data has improved understanding of under-ice dynamics (Bruesewitz *et al.*, 2015), inter-seasonal metabolism dynamics (Laas *et al.*, 2012), monitoring algal blooms (Pobel *et al.*, 2012) and general provision of ecosystem services (Marcé *et al.*, 2016). This has led to increased instrumentation of reservoirs and lakes of particularly high value (e.g. drinking water, recreation, fishing). HFM comes at a cost, however, as systems are expensive to acquire, deploy, and maintain (Horsburgh *et al.*, 2019). Nevertheless, HFM water quality data offer several advantages over traditional limnological data collection. They can be collected remotely, irrespective of weather conditions, and at a temporal resolution that can capture rapidly changing water conditions (i.e. sub-daily). It is also possible to automate the assimilation of these data into modelling workflows, as they can be streamed online and automatically quality controlled (Porter *et al.*, 2005).

Any forecast workflow which uses a mechanistic model for lake water quality is built on top of, and informed by, reliable simulations of lake thermal structure. This

study was the first, as far as we know, to investigate whether assimilating observational temperature profile data into a physical lake model, by direct insertion, reduced forecast error. If error was reduced, we also sought to identify the optimal length of the time at which the direct insertion should occur before any forecast, as this would inform the frequency at which observational data would need to be collected. These questions were explored using data from three well-studied lakes from which high frequency water temperature data were available: Lough Feeagh (Ireland), Kinneret (Israel) and Langtjern (Norway). The study evaluated model performance throughout one year of forecasting at a set of different re-initialization times prior to the forecast of between 0 and 14 days. It also assessed forecast performance throughout the lake depth profile.

### *5.3. Materials & Methods*

#### *5.3.1. Study sites*

The three lake study sites, Feeagh, Langtjern and Kinneret, were selected primarily because of the availability of high frequency water temperature profile data, but also based on their geographic spread and differences in lake surface area, depth and thermal structure. All sites have been the subject of long-term ecological research, meaning that the physical and ecological functioning of the lakes are well understood. Site descriptions are given in chapter 3. Stratified conditions were defined as a density difference between surface and bottom water greater than  $0.1 \text{ kg m}^{-3}$  and a surface temperature greater than  $4 \text{ }^{\circ}\text{C}$ .

#### *5.3.2. General Ocean Turbulence Model*

The model chosen for this study was GOTM because of its ability to accurately replicate lake hydrodynamics and the development of the “hot-start” facility within the model. See section 2.3.5 for the model description. The new “hot-start” facility which was recently developed for GOTM was utilised in this study to examine the effects of assimilating different temporal frequencies of observational lake temperature profile data on 14-day water temperature forecasts. In recent versions of Simstrat and GLM, there has been an incorporation of the “hot-start” facility into these models highlighting that this is a modelling tool which is useful for modelling lake hydrodynamics.

### 5.3.3. Modelling procedure

GOTM was calibrated using a differential evolution algorithm with 5000 iterations with the negative log likelihood as the cost function. The best parameter set was taken to be the one with the least error between modelled and observed data, determined by the maximum log likelihood score. This parameter set was then used to run the free model run, which has no observational data assimilated (NDA), for the study period with a one-year spin-up period. GOTM was first initialized during a time when each lake was isothermal ( $t_0$ ) and then re-initialized by insertion of a single measured temperature profile (also called a “hot start”) at a selected time prior to the forecast period ( $t_1$ ) (Figure 5.1). Bolding & Bruggeman ApS recently implemented this ‘hot-start’ functionality into GOTM. Conceptually, this feature allows a model run to be initialized from a restart file where given model state variables have been assigned values. The restart file is produced by GOTM and provides the model state variable values at the last time step of a given model run. The goal of the hot start functionality is to enable continuation of a model run which includes information on the process variables from a past period of simulation, without the need to run the entire historical period. Because of this functionality, one can also choose to manipulate one or several of the state variables in the restart file. In the present study, we replaced the temperature profiles in the restart file with observed profiles – i.e. using direct insertion as a means of data assimilation. Where the observed temperature depths did not exactly match the modelled depths, we linearly interpolated and extrapolated the data. This functionality allows the user to “hot-start” the lake model whenever new forcing data in the form of a weather forecast data becomes available. This allows a workflow to be developed where forecasts are continuously updated, i.e. the model state variables (water temperature profile), when measured values of these are available.

The timing of model initialisation varied for each site (Feeagh: 2006-01-01, Langtjern: 2013-05-15, Kinneret 2010-01-01). For Langtjern, this was at the beginning of May following the offset of ice. A minimum period of one year was used

to spin-up the model prior to the re-initialization, the time when the observed temperature profile was assimilated (Fenocchi *et al.*, 2019). A spin-up period helps to reduce the error that could be associated with the initial and boundary conditions and allows the model to reach statistical equilibrium (Hodges, 2014). The model was run with an hourly integration time step. Model output was averaged to a daily timestep and compared to daily averaged observed data.

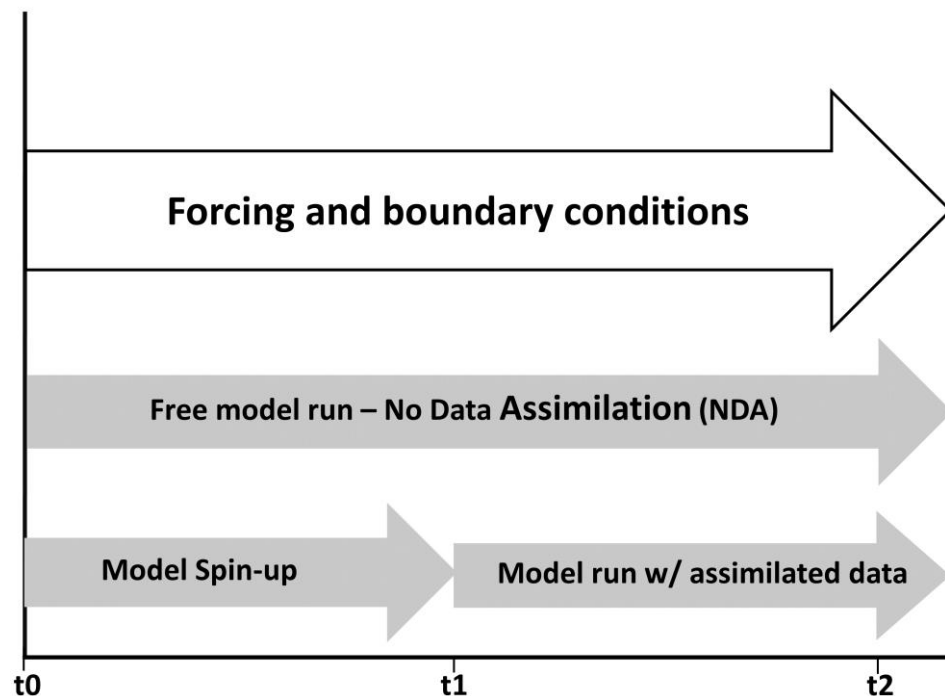


Figure 5.1 Conceptual scheme of the hot-start functionality showing the continuous forcing and boundary conditions from  $t_0$  to  $t_1$ . The free model run with no data assimilation (NDA) is forced continuously with the initial conditions at  $t_0$ . The forecast with assimilated data has a model spin-up from  $t_0$  and finishes at  $t_1$ . At  $t_1$  a “hotstart” file is produced for GOTM which contains the process and variable states for the model. An observed temperature profile is inserted into this file, updating the model states for water temperature and then the model is reinitialized with the updated restart file.

For each lake, a set of 14-day forecasts was produced that commenced approximately every three days throughout the study period. A similar number of forecasts was produced for each site (Feeagh: 142, Kinneret: 135, Langtjern: 128). Observed temperature profile data were then assimilated into the model by direct insertion before re-initializing the model to simulate a 14-day forecast. The observational data represented real time conditions at 0 hours (T000), 1 day (24 hours: T024), 1 week (168 hours: T168), 2 weeks (336 hours: T336) and 4 weeks (672 hours: T672) prior to the start of the targeted forecast period (Figure 5.2). These assimilation times were chosen to reflect different monitoring resolutions commonly used in lake monitoring programme, ranging from traditional low frequency operational monitoring (monthly: T672) to more frequent surveillance monitoring (weekly: T168) and up to near real time automatic monitoring (instantaneous: T000). At the data assimilation time, a single measured temperature profile was assimilated using direct insertion into the restart file that was generated following the spin-up period (Figure 5.2). The simulation was then run until the end of the target forecast period of 14 days. The data for the 14-day forecast period were then extracted for analysis.

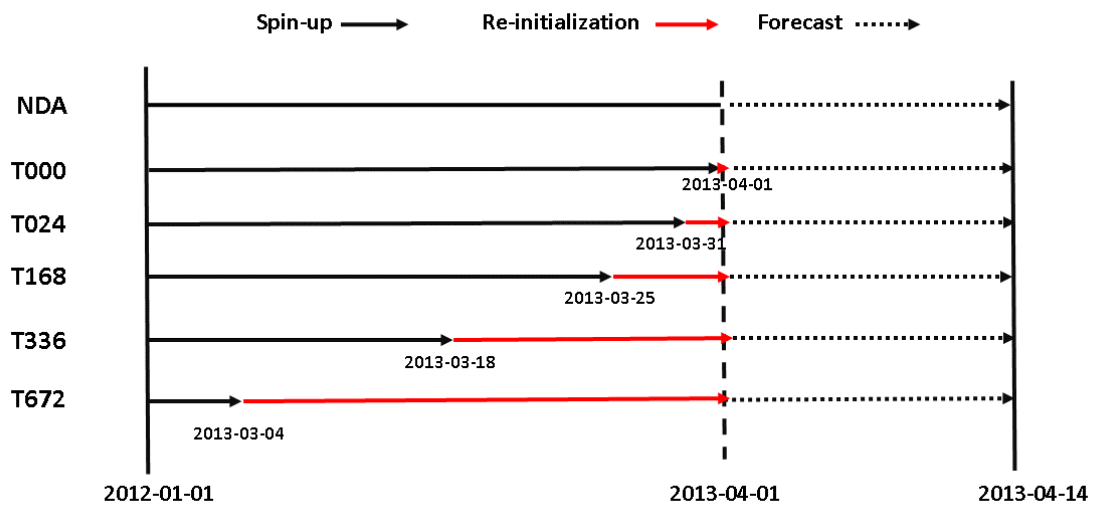


Figure 5.2 Schematic describing different simulated forecasts that were used. The dates chosen are for example purposes to demonstrate how Figure 5.1 corresponds to an actual forecast. The date 2012-01-01 is  $t_0$ ,  $t_1$  is the corresponding date for each forecast and 2013-04-14 represents  $t_2$ .

The forecasts produced by the models were classified according to the thermal status of the lake at that time (isothermal or stratified) to assess model performance under differing conditions. During the stratified conditions, results were also separated into results for the epilimnion and hypolimnion. The metalimnion was not included because for Feeagh this was not well defined. The presence and depths of the epilimnion, metalimnion and hypolimnion were calculated using the ‘rLakeAnalyzer’ package in R on the mean daily observed data (Read *et al.*, 2011).

The forecasts were generated using an ensemble parameter approach which has been used in lake modelling studies before (Gal *et al.*, 2014). We generated 100 parameter sets from a multivariate distribution of the upper 10<sup>th</sup> percentile of best performing parameters from the 5000 calibration iterations (Figure 5.3). The forecasts based on the five different data assimilation times were compared to simulations for that site with NDA (Figure 5.3).

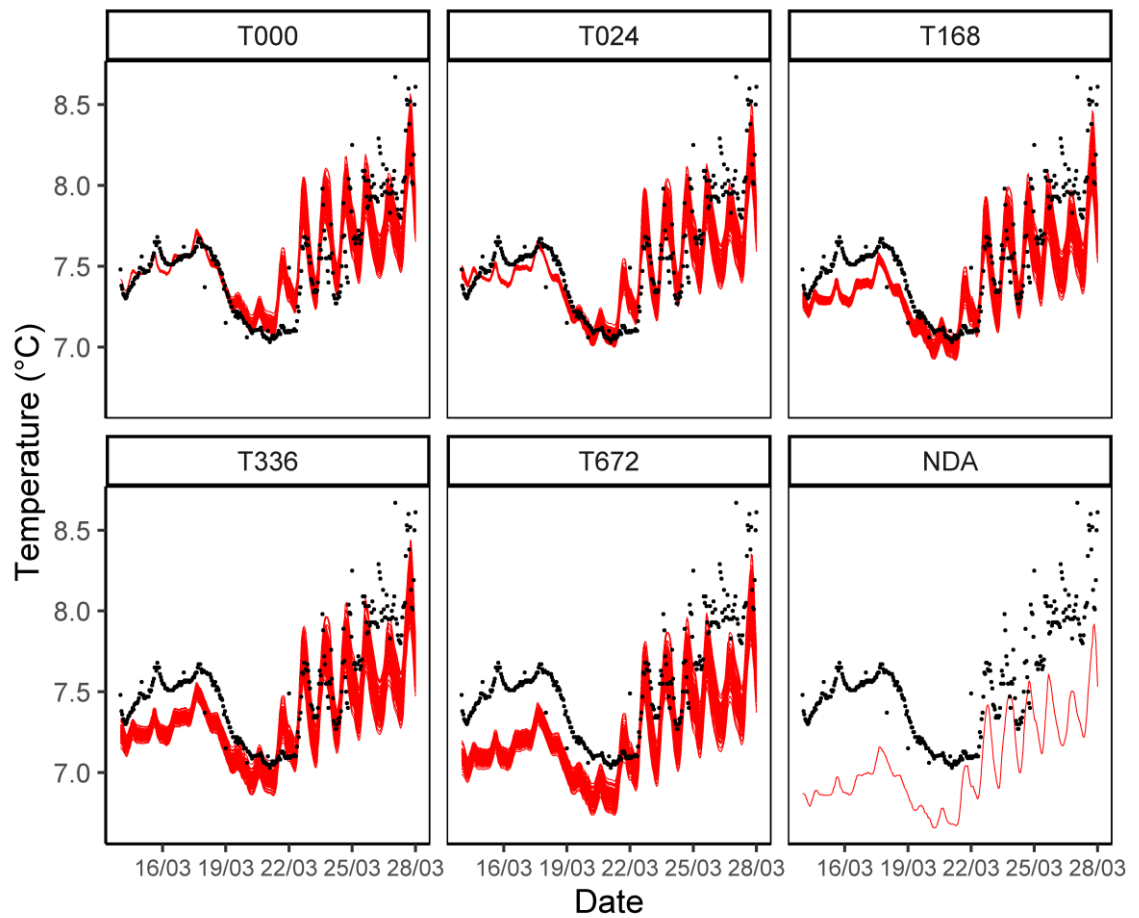


Figure 5.3 An example forecast of surface water temperature for Feagh on 2007-03-13 for 14 days showing the model ensemble (100 simulations; red) and the observed water temperature (black dots) for each forecast where data was assimilated at the time of the forecast (T000), one day previous (T024), one week previous (T168), two weeks previous (T336), one month previous (T672) and the free model run with no data assimilation (NDA).

#### 5.3.4. Data Analysis

The model forecast performance was assessed using the metrics bias, mean absolute error (MAE), Root mean square error (RMSE), and Nash-Sutcliffe efficiency (NSE) were used with bias and MAE to evaluate model performance following calibration.

$$Bias = \frac{1}{n} \left( \sum_{i=1}^n (y_i - \hat{y}_i) \right) \quad (5.1)$$

$$MAE = \frac{1}{n} \sum_{i=1}^n |y_i - \hat{y}_i| \quad (5.2)$$

$$RMSE = \sqrt{\frac{1}{n} \sum_{i=1}^n (y_i - \hat{y}_i)^2} \quad (5.3)$$

$$NSE = 1 - \frac{\sum_{i=1}^n (y_i - \hat{y}_i)^2}{\sum_{i=1}^n (y_i - \bar{y})^2} \quad (5.4)$$

where  $y_i$  was the observed water temperature;  $\hat{y}_i$  was the simulated water temperature at time  $i$ ,  $\bar{y}$  was the mean observed water temperature and  $n$  was the number of samples.

Data analysis was carried out using R (R Core Team, 2020). For each forecast, the MAE was calculated for each forecast ensemble compared to observed water temperature profile data and then mean of the ensemble was calculated. The MAE was averaged in time and depth for each forecast date to generate a time series of MAE for each forecast throughout the period. MAE over the forecast period were calculated by averaging all the forecasts for each lake status (stratified and isothermal) for each day of the forecast starting at day 1 and ending at day 14 for each lake. MAE was calculated for the lake profile for each lake status. Density distributions were plotted showing the distribution of MAE for each forecast during each lake status and the mean RMSE for the free run. Improvements in forecasts were calculated as a percentage reduction in MAE relative to the model NDA run.

#### 5.4. Results

Feeagh was stratified throughout six months of the study year from late March (2007-03-26) until early September (2007-09-10) (Figure 5.4 A). Maximum surface temperature of 20.6 °C occurred in May while the maximum bottom temperatures (15.3 °C) occurred during autumn overturn (2007-09-12) in September. The minimum surface temperature of 6.0 °C occurred at the end of December 2007. Stratification within Feeagh was relatively weak compared to the other two sites, with the largest temperature difference between top and bottom temperatures during the stratified period being 11 °C on 2007-04-06 (mean temperature difference: 3.6 °C, SD: 1.6 °C, n =180). As a result of its weak stratification, a small metalimnion developed during stratification between 15.0 m and 15.6 m.

Langtjern was the only lake in this study to have ice cover, which occurred from 2014-11-23 until 2015-05-09 and from 2015-11-12 until 2016-05-09 (Figure 5.4 B). It was isothermal for approximately a two-month period following the breakdown of summer stratification in both years, from 2014-10-08 until 2014-12-11 (64 days) and 2015-10-02 until 2015-12-08 (67 days). In comparison, a relatively short 18-day isothermal period occurred following ice-off in 2015 (2015-04-26 to 2015-05-13). The maximum surface temperature of 23.3 °C occurred on 2015-07-05 while the minimum surface temperature of 0 °C coincided with the period of ice cover. During the summer stratification period, bottom temperatures were very stable (mean 6.1 °C; SD: 0.6 °C, n=178) with a maximum bottom temperature of 8.6 °C occurring on 2015-10-03 following autumn turnover. There was a relatively large temperature differential between top and bottom during summer stratification (mean: 7.6 °C, SD: 3.5 °C, n=178) which resulted in a metalimnion between 2.1 m and 4.0 m.

The sub-tropical lake, Kinneret, had a slightly different temperature structure when compared to the other two sites. It had long periods of stratification with a stable thermal structure from 2010-04-08 until 2011-01-12. Throughout the study period bottom temperatures were much higher than either of the other lakes and remained

relatively stable (mean: 16.6 °C; SD: 0.1 °C, n=267), while surface temperatures underwent large diel fluctuations (up to 6 °C). The maximum surface temperature was 32.1 °C on 2010-09-07 and the minimum surface temperature was 22.8 °C on 2011-02-06. The lake was isothermal for very short periods in January and February 2011 but there were no long continuous isothermal periods (maximum continuous period of 9 days, 2011-01-30 to 2011-02-08) (Figure 5.4 C). The metalimnion occurred at depths between 14.1 m and 21.2 m and was stable until turnover occurred.

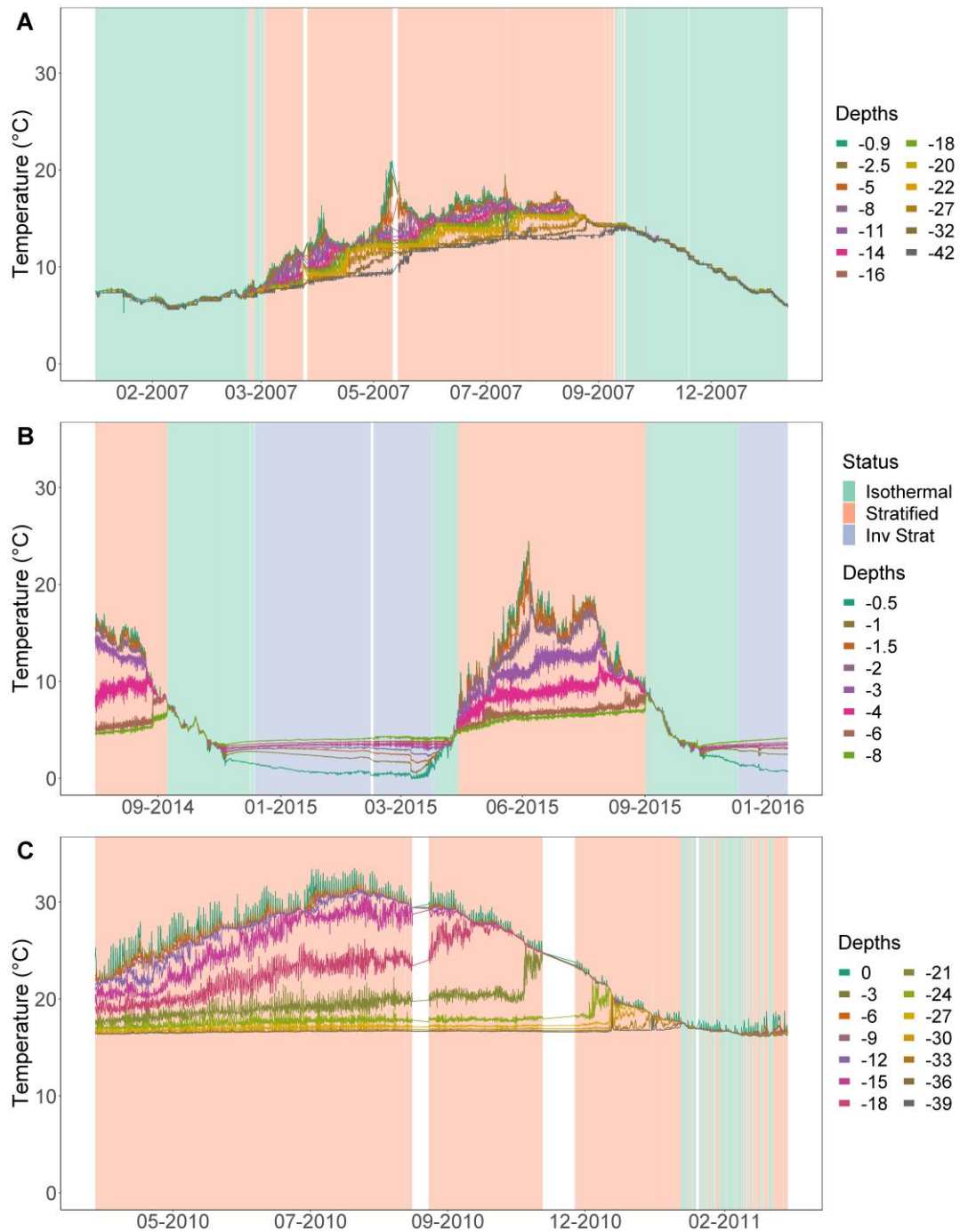


Figure 5.4 Observed water temperature at different depths for the three study lakes: A) Feeagh B) Langtjern and C) Kinneret. Green background indicates periods when the lake was isothermal, red for when the lake was stratified and blue for when the lake was inversely stratified (only Langtjern). White spaces indicate time periods where observation data were missing.

Following model calibration, the model simulated the entire study time period with the best calibrated parameters for each site. Model performance statistics were calculated for the overall time period and both the stratified and isothermal time periods. For the overall time period, GOTM simulated the seasonal dynamics for each lake with a reasonable degree of accuracy. The simulations for Feeagh had the smallest MAE (0.53 °C) and highest NSE (0.96), followed by those for Langtjern (MAE: 0.76, NSE: 0.94) and then those for Kinneret (MAE: 1.38, NSE: 0.86) (Table 5.1). Simulations for Feeagh and Langtjern had a negative bias during the isothermal period (-0.05 °C and -0.28) while those for Kinneret had a warm bias (+0.40 °C). During the stratified period the output for Langtjern had a larger negative bias (-0.47 °C) while that for Feeagh and Kinneret had a warm bias (+0.39 °C and +0.40 °C) respectively).

Table 5.1 Model performance over the entire study period for each lake comparing modelled temperatures to observed temperatures at corresponding depths.

	<b>Feeagh</b>	<b>Langtjern</b>	<b>Kinneret</b>
<b>Bias (°C)</b>			
Overall	0.18	-0.38	0.47
Isothermal	-0.05	-0.28	0.89
Stratified	0.39	-0.47	0.40
<b>MAE (°C)</b>			
Overall	0.53	0.76	1.38
Isothermal	0.31	0.54	0.89
Stratified	0.74	0.96	1.46
<b>RMSE (°C)</b>			
Overall	0.68	1.02	1.79
Isothermal	0.37	0.72	1.00
Stratified	0.88	1.23	1.89
<b>NSE</b>			
Overall	0.96	0.94	0.87
Isothermal	0.98	0.79	-2.97
Stratified	0.90	0.89	0.86

The range in MAE values for the forecasts when no observational data were assimilated (NDA) was much larger for Kinneret (mean: 0.90 °C, SD: 1.05 °C) than for Feeagh (mean: 0.35 °C, SD: 0.34 °C) or Langtjern (mean: 0.64 °C, SD: 0.59 °C) (Figure 5.5). For all three lakes, there was a similar pattern in error values throughout the annual lake cycle, with the largest MAE values occurring during summer months when the lake was stratified, and lowest values occurring when it was isothermal. The mean difference in simulated temperatures between the NDA runs and the runs with the longest interval between re-initialization and the start of the forecast (four weeks: T672) was largest for Kinneret (1.2 °C), followed by Langtjern (1.0 °C) and then Feeagh (0.5 °C) (Figure 5.5). The error estimates for the multiple sequential 14-day forecasts for Feeagh were variable over the study time, with six noticeable peaks in error which were related to mixing events (arrows: 1, 4, 5) (Figure 5.5 A) and warming events (2, 3). The error for Langtjern was variable over the annual cycle, with eight distinct peaks in error. As with Feeagh, these eight peaks again coincided with discrete events related in this case to warming events (arrows: 1, 2, 6) (Figure 5.5 B), changes in the lake thermal structure: offset of summer stratification (7), cooling events (4, 8) and mixing events (3, 5). For Kinneret, there were two smaller peaks in error: one was a result of the missing data (1) and the other was related to a mixing event (2) (Figure 5.5 C; 1, 2). The width and height of these peaks in error increased as the time period between the assimilation of the measured profile and the start of the forecast became longer for all sites. However, the NDA simulations had the tallest and widest peaks in error for all three sites (Figure 5.5).

For each of the three study lakes, there was very little difference in MAE values between the T000 and T024 simulations throughout the entire study period. During isothermal periods, there were smaller differences between the error for the NDA simulations and those for each of the forecast datasets where observational data were assimilated (T000 – T672) for both Kinneret and Feeagh. The NDA had slightly lower MAE values than the runs in which data were assimilated during the month of December 2007 for Feeagh. For Langtjern, a site where the periods during which the lake was isothermal were much shorter, there were large peaks in error associated with

two sudden events: a warming event in October 2014 and rapid cooling event in October 2015 (2, 8) (Figure 5.5 B).

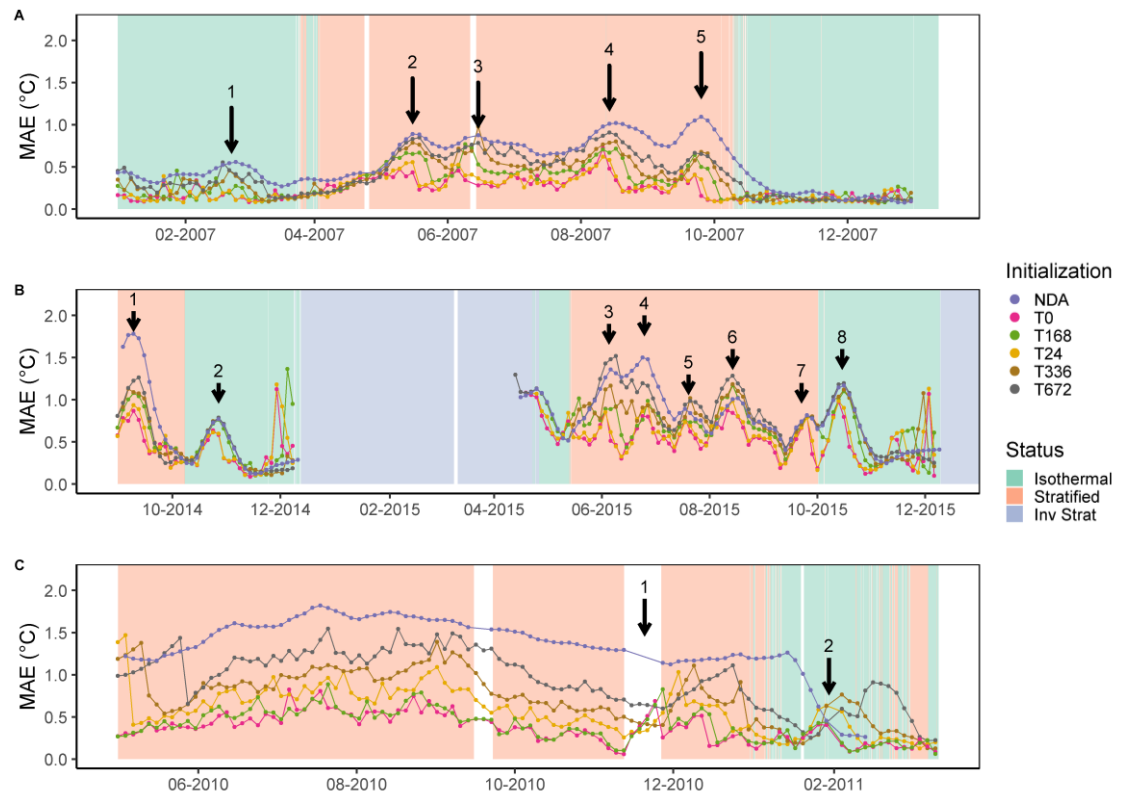


Figure 5.5 Impact of the length of time between data assimilation and start of the forecast on the mean absolute error (MAE) for forecast water temperature for the three lakes: A) Feeagh, B) Langtjern and C) Kinneret during stratified and isothermal conditions. Each dot represents the mean absolute error of the 14-day ensemble forecast on that day for the entire water column. The numbered arrows highlight peaks where notable events occurred.

In general, the MAE values increased over the time period of the 14 day forecasts for all three lakes for runs with assimilated data, while the NDA simulations had a relatively consistent range of error throughout the 14-day forecast period (Figure 5.6). During the stratified period, the T000 and T024 simulations had noticeably lower MAE values across all 3 lakes in both the epilimnion and hypolimnion, but these increased with forecast length. After day eight of the forecast for Langtjern during the

stratified period and for the epilimnion, the MAE estimate for all datasets for Langtjern converged around a value of 0.8 °C. The simulations for Kinneret had a larger error for temperature in the epilimnion during periods of stratification compared to those in the hypolimnion (mean MAE epilimnion: 1.2 °C; mean MAE hypolimnion 0.2 °C). The MAE for NDA was consistently much higher in the Kinneret hypolimnion (mean: 1.5 °C) while the MAE of the assimilated datasets remained below 0.5 °C even after 14 days.

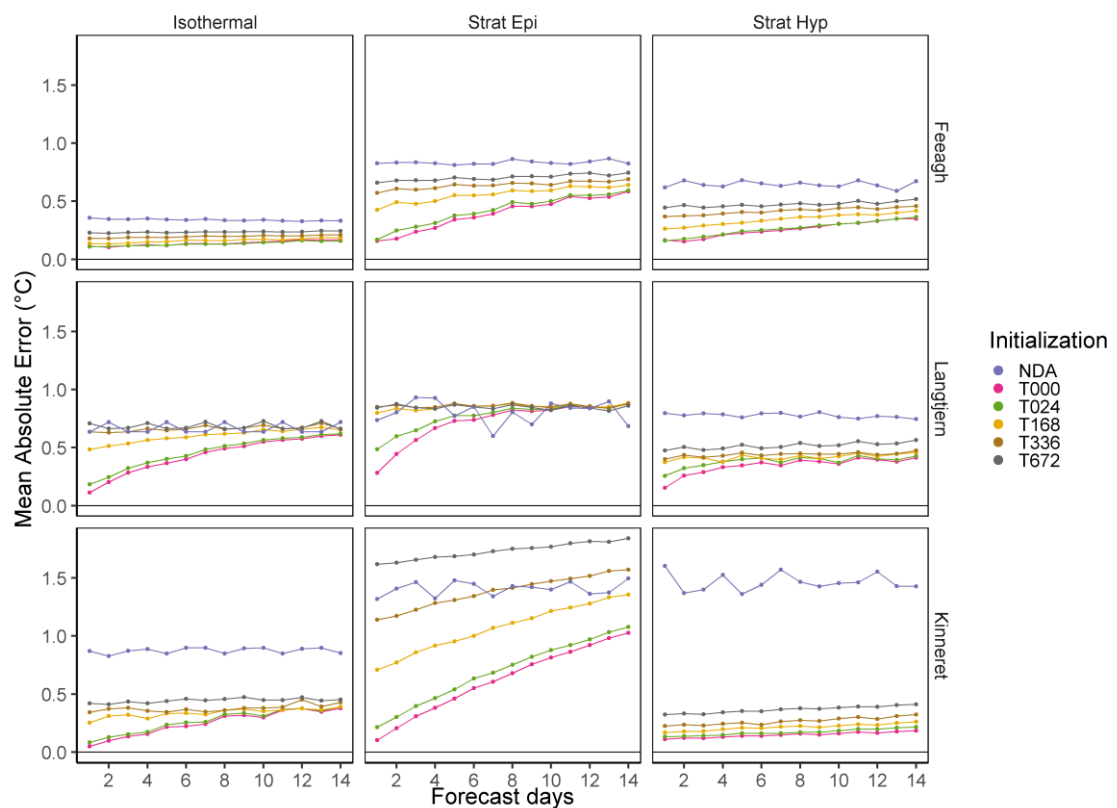


Figure 5.6 MAE averaged across the 14-day forecasts of water temperature in three lakes: Langtjern, Kinneret and Feeach. The colours of the lines represent the length of time between data assimilation and start of the forecast. Forecasts during isothermal (left panel) and epilimnion and hypolimnion water during stratified periods (middle and right panels) are presented separately. Each line represents the MAE of all the forecasts generated during each thermal period (Feeach-Isothermal:  $n=86$ ; Feeach-Stratified:  $n=53$ ; Kinneret-Isothermal:  $n=28$ ; Kinneret-Stratified:  $n=104$ ; Langtjern-Isothermal:  $n=62$ ; Langtjern-Stratified:  $n=66$ ).

The forecasts for Kinneret and Feeagh had higher error values for temperatures in the epilimnion and lower error values for the hypolimnion (Figure 5.7). However, the NDA simulations had much larger errors for simulations of temperatures in the metalimnion for Kinneret (depths between 14 m and 21 m) and Langtjern (depths between 1m and 4m). The range in MAE values for the forecast epilimnetic temperatures across the different assimilation runs for Feeagh (0 - 15 m), Kinneret (0 - 15 m) and Langtjern (0 - 1.8 m) were 0.4 - 0.8 °C, 0.6 - 2.1 °C and 0.8 - 1.0 °C respectively. For forecasts of metalimnetic temperatures in Feeagh (15 - 15.6 m), the range in MAE values was lower compared to the epilimnion (0.2 - 0.45 °C). For Kinneret (14 - 21 m) this range was 0.6 - 1.3 °C while for Langtjern (2.1 - 4.8 m) it was 0.45 - 0.9 °C. Forecast MAE for the hypolimnion for Feeagh had a range of 0.2 - 0.5 °C and for Kinneret (22 - 30 m) the range was 0.25 - 0.5 °C but this reduced to 0.05 - 0.2 °C for the bottom depths (30 - 41 m) (Figure 5.7). For the hypolimnion in Langtjern (4.8 - 9 m) the MAE range was 0.25 - 0.8 °C.

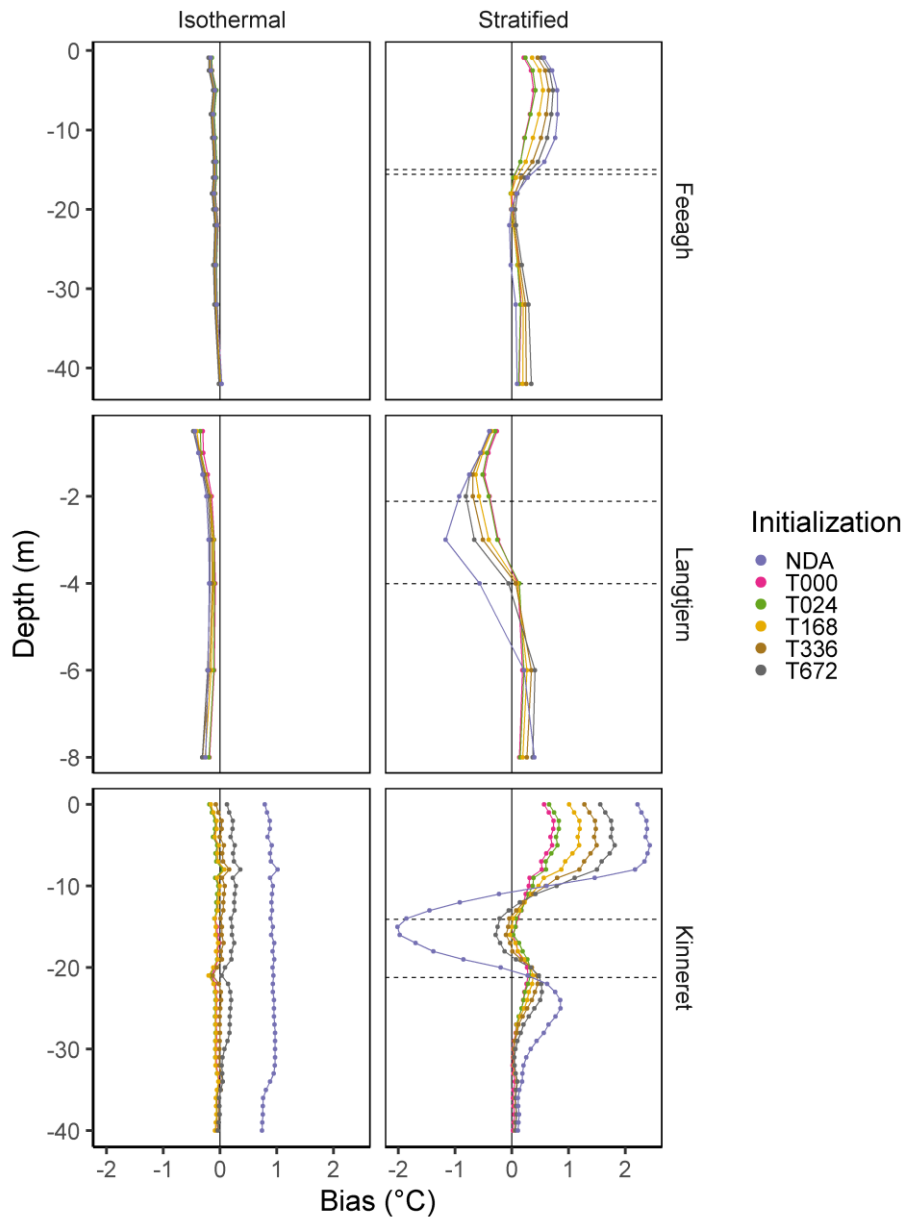


Figure 5.7 Mean bias of water temperature profiles in three lakes Feeagh, Langtjern and Kinneret for forecasts averaged across the isothermal (Feeagh:  $n=73$ ; Langtjern:  $n=64$ ; Kinneret:  $n=31$ ) and stratified periods (Feeagh:  $n=69$ ; Langtjern:  $n=64$ ; Kinneret:  $n=104$ ). The colours of the lines represent the length of time between data assimilation and start of the forecast. Forecasts during stratified and isothermal conditions are presented separately in each panel. Each line represents the bias of all the 14-day forecasts generated during that thermal period. Dashed horizontal lines indicate the mean top and bottom of the metalimnion during the stratification period.

Overall, the NDA run had a larger MAE values throughout the water column compared to all the assimilation datasets for all the three sites, during both the isothermal and stratified periods (Feeagh: 0.53 °C, Langtjern: 0.75 °C and Kinneret: 1.17 °C). An exception were specific depths during the stratified period at Kinneret and at Feeagh (Table 5.2). During the stratified period each forecast where observational data were assimilated had a bias in the epilimnion, but this was a positive bias for Feeagh and Kinneret and a negative bias for Langtjern. For Kinneret during the stratified period, the NDA run had a large warm bias in the epilimnion, a large negative bias in the metalimnion and slight warm bias in the hypolimnion. During the isothermal period it had a consistent warm bias throughout the water column (+1 °C). There were slight negative biases near the surface for both Feeagh and Langtjern (mean: -0.17 °C, -0.4 °C respectively).

Density plots of the distributions of the MAE for the temperature profile for all 14-day forecasts showed that the range of the errors was largest during the stratified period for all three lakes (Figure 5.8). For both Kinneret and Feeagh, during the isothermal period (Jan – Mar 2011; and Jan – Apr 2007 and Oct – Dec 2007 respectively), there was a distinct difference between all the forecasts that had observational data assimilated compared to the NDA run while there was little to no difference between the assimilated datasets. The mean values of the distributions during this period for Feeagh ranged between 0.13 and 0.22 °C (mean MAE: T000: 0.14 °C; T024: 0.13 °C; T168: 0.16 °C; T336: 0.18 °C; T672: 0.22 °C) for the assimilated datasets while for the NDA run it was 0.31 °C. Similarly, for Kinneret there was a range in the mean values of 0.27-0.48 °C for the datasets where observational data were assimilated, while the mean was 0.9 °C for NDA. For simulations during the isothermal period for Kinneret, the NDA simulation had a distinctly different error distribution (mean: 0.90 °C; SD: 0.44 °C) than those with observational data assimilation, with both a larger mean error and wider range (mean: 0.22– 0.46 °C; SD: 0.24 - 0.37°C). In contrast, the distribution of the errors for Langtjern had a similar distribution for all runs, including for the NDA run.

During the stratified period, there was a distinct separation between each of the forecasting datasets (i.e. the differing reinitialization times) for all three lakes, with the mean error and range in the errors increasing as the time interval for reinitialization prior to the forecast became longer (Figure 5.8). However, the NDA run had the largest range in error values. For all three lakes, there were very small differences in the distributions of MAE between T000 and T024 forecasts. There was a larger difference in errors between T024 and T168. For Langtjern, there was a large increase in the distribution of MAE as the time of assimilation increased with the largest difference between T024 and T168, while for Kinneret, the distribution of MAE values only showed large increases for the T336 and T672 runs.

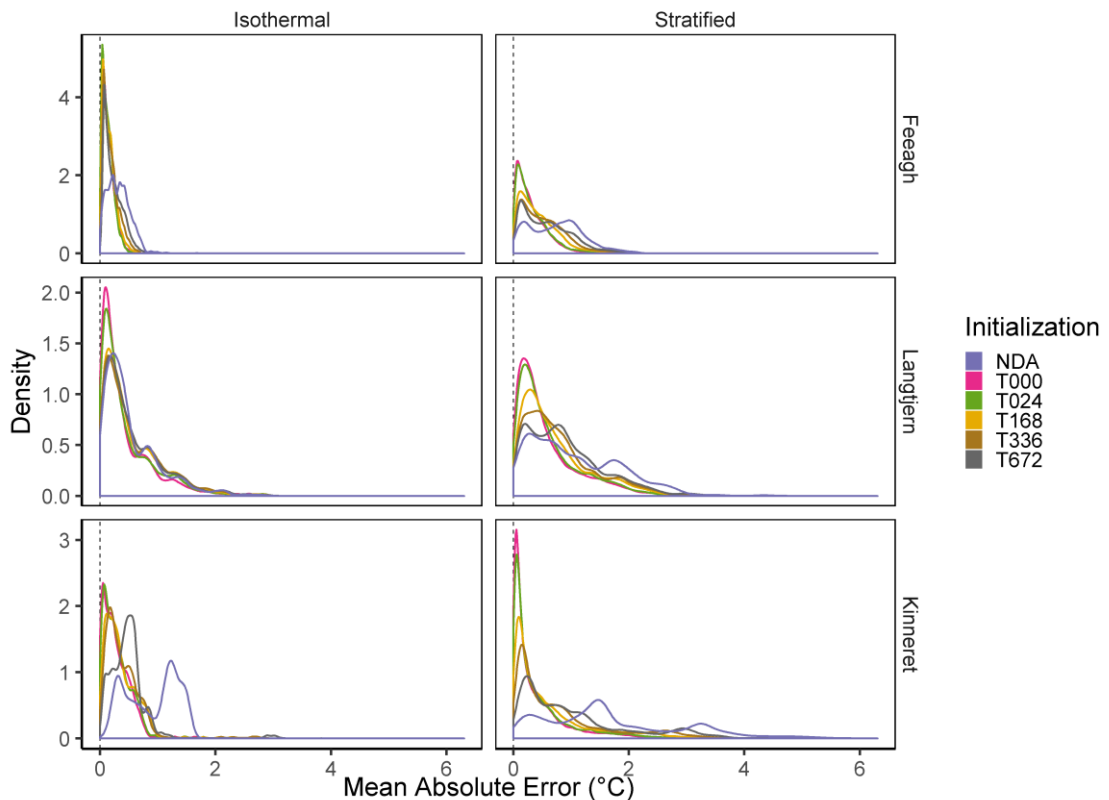


Figure 5.8 Density plots of the distribution of the mean absolute error for all 14-day forecasts for the three lakes: Feeagh (Isothermal:  $n=114$ ; Stratified:  $n=71$ ); Langtjern (Isothermal:  $n=62$ ; Stratified:  $n=66$ ), and Kinneret (Isothermal:  $n=28$ ; Stratified:  $n=104$ ) with panels for the different thermal periods. Colours represent the length of time between data assimilation and start of the forecast.

Overall, assimilating observational data into the model nearly always reduced the forecast error when compared to the NDA simulations (Table 5.2). The forecasts for Kinneret had the greatest improvement score across both the isothermal and stratified periods, with the percentage improvement in the MAE values ranging from 41 % (Stratified: T672) to 77 % (Stratified; T000) (Table 5.2). The simulations for Feeagh had similar levels of improvement during the stratified period (23 - 59 %) and the isothermal period (31 - 56 %). For Langtjern, only the T000 and T024 forecasts

for the isothermal period had a better percentage increase in performance compared to the NDA runs (20 and 31 % respectively). In contrast, the T168 forecasts showed no improvement (0 %) while the T336 and T672 runs both had a decrease in performance (-4 % for both).

Table 5.2 Data assimilation performance for the different temporal frequencies showing the percentage improvement in forecast compared to the model run without data assimilation.

	<b>T000</b>	<b>T024</b>	<b>T168</b>	<b>T336</b>	<b>T672</b>	<b>NDA</b>
<b>Feeagh</b>						
MAE (°C)						
Overall	0.23	0.24	0.30	0.36	0.41	0.51
Isothermal	0.14	0.13	0.16	0.18	0.22	0.32
Stratified	0.31	0.33	0.44	0.52	0.58	0.75
Improvement (%)						
Overall	55	53	41	29	20	-
Isothermal	56	59	50	44	31	-
Stratified	59	56	41	31	23	-
<b>Langtjern</b>						
MAE (°C)						
Overall	0.50	0.54	0.64	0.68	0.74	0.69
Isothermal	0.43	0.47	0.54	0.56	0.56	0.54
Stratified	0.57	0.61	0.73	0.79	0.89	1.06
Improvement (%)						
Overall	28	22	7	1	-7	-
Isothermal	20	13	0	-4	-4	-
Stratified	46	42	31	25	16	-
<b>Kinneret</b>						
MAE (°C)						
Overall	0.38	0.42	0.59	0.75	0.97	1.60
Isothermal	0.27	0.29	0.36	0.39	0.48	0.90
Stratified	0.39	0.43	0.62	0.79	1.01	1.70
Improvement (%)						
Overall	76	74	63	53	39	-
Isothermal	70	68	60	57	47	-
Stratified	77	75	64	54	41	-

## 5.5. Discussion

Water quality and water security are two of the key areas of concern within the Sustainable Development Goals (United Nations General Assembly, 2015). Early-warning forecasts in lakes and reservoirs that are used for drinking water and recreational needs have the potential to play a key role in supporting water management and public health authorities. Lake ecosystems are underpinned by an evolving physical and thermal structure. When modelling lake ecosystems it is imperative, therefore, to simulate lake physics with a high degree of accuracy as physical characteristics of the thermal regime control the process rates of many biogeochemical variables of lake biota (Trolle *et al.*, 2012; Bruggeman and Bolding, 2014; Hu *et al.*, 2016). The occurrence of algal blooms, for example, is largely governed by the internal dynamics of a lake (Paerl and Huisman, 2008; Paerl *et al.*, 2011). Temperature and the seasonal pattern of thermal stratification are some of the most important variables affecting lake ecosystems (Dunham *et al.*, 2003; Magnuson *et al.*, 1979) because temperature affects many biogeochemical processes, for example cyanobacterial blooms (Chen *et al.*, 2014). Being able to forecast lake water temperature to a high degree of accuracy in the near-term future (14 days) would be of enormous benefit to water resource managers.

Our study is the first, as far as we know, to examine the effects of assimilating observational data by direct insertion on the performance of a lake hydrodynamic model. We did this for three lakes that have differing seasonal patterns of stratification. We found that even the assimilation of data collected one month before the forecast (T672) reduced the forecast error when compared to a free run (NDA) of the lake model. The greatest improvement in forecasting ability occurred during periods when all three study lakes were stratified (33-45 %, Table 5.2), a time that is critical for many biogeochemical processes such as horizontal oxygen mixing (Couture *et al.*, 2015), calcite crystallization (Katz and Nishri, 2013) or distribution of zooplankton (Pinel-Alloul *et al.*, 2004). In fact, assimilating observational data at any timestep up to one month prior to the forecasts reduced forecast error compared

to making the forecast without data assimilation. The improvement when data were assimilated is partly due to a reduction in error related to accumulation of a cold bias in the lower depths, which can carry forward through the simulation if no data assimilation is carried out (Thiery *et al.*, 2014b). By inserting observed temperature profile data, the model state variables were corrected and brought back in line with observed data for each run thus reducing MAE in the first number of days (e.g. Figure 5.3). Data assimilation of observed lake surface temperature from satellite measurements has previously been found to improve the characterisation of changing lake surface state (Rontu *et al.*, 2012) and lake water surface temperature (Kourzeneva, 2014). This agrees with our finding that even assimilation of observational data measured four weeks before the forecast resulted in a lower error and more accurate forecast. As might be expected, however, the lowest error of all was obtained by assimilating data collected in the 0 to 24-hour period before the start of the forecasts. This was particularly apparent when a specific in-lake event occurred, such as a warming or mixing event in the 14-day forecast period. During these periods, the error peaked but then showed rapid return to pre-event levels, particularly for shorter assimilation lead in times.

The error in the epilimnion was much higher in the largest lake Kinneret than in the other two lakes. This was likely owing to large fluctuations in daily surface temperature and the presence of large-scale internal waves (Laval *et al.*, 2003; Gómez-Giraldo *et al.*, 2006; Ji and Jin, 2006). The presence of large internal waves can be a source of error when using a 1-dimensional lake model as a result of the model structure (Hodges *et al.*, 2000b). This influences the accuracy of the forecast in trying to capture the depth of the epilimnion, which is clearly seen in Figure 5.7 where the largest errors for the NDA simulations were at the surface and at the metalimnion. Since Kinneret is in the sub-tropics, surface water temperature fluctuations during the summer period can be as large as 6 °C, a range which our model simulations did not always capture (Figure 5.4). This suggests that the error during stratified periods was mainly related to model structural error, where the model cannot replicate some of the 3-dimensional internal processes in the lake, for example,

the occurrence of multiple internal seiche modes (Antenucci *et al.*, 2000). When observational data were assimilated, the biases in the forecast was reduced.

Model errors were less substantial, for the shallow and thermally stable lake in our study, Langtjern. Although, during the isothermal period, and in the epilimnion during the stratified period, we only found improvements in forecasts for the T000 and T024 runs and for the first 8-10 days before it had the same MAE as T168 (Figure 5.6). This could be a result of the lake being more stable and shallower therefore making the initial conditions of the lake model more sensitive to atmospheric disturbances. Where after 8 days, the sensitivity to the initial conditions has dissipated. This is important in the context of short-term episodic events which can have a large impact on in-lake conditions (Jennings *et al.*, 2012; Kuha *et al.*, 2016). Therefore, higher frequency data would be needed to accurately forecast during and immediately after the event occurred. In contrast, for Feeagh, a lake with weak thermal stability, differences in errors resulting from varying data assimilation times remained, even after 14 days, The mean depth of Feeagh is much larger than Langtjern and mean depth is a key factor with regards lake stability (Kraemer *et al.*, 2015).

There was also a clear distinction in the magnitude of error between those times when the lakes were stratified compared to when the lakes were isothermal, highlighting the challenges of modelling water temperature during these different lake conditions (Kourzeneva, 2014). Assimilation of measured data reduced error by accurately simulating the depth of the epilimnion and metalimnion during the stratified period, the zones of the lake that govern biotic processes for zooplankton and phytoplankton (Pilati and Wurtsbaugh, 2003; Twiss *et al.*, 2012). It would therefore be particularly beneficial for forecasts when a lake is stratified, or for deep large lakes which have large internal dynamics such as internal waves. For the deep and strongly stratified Kinneret, the main reduction in error was for the surface temperatures and around the depth of the metalimnion, suggesting that the assimilation of measured data was particularly useful in correcting errors related to prediction of the thermocline depth (Baracchini *et al.*, 2019). There were slight biases for simulated temperatures in the hypolimnion during the stratified period. This is an

important depth zone when modelling water quality, especially for simulating periods of hypoxia or anoxia, as temperature is a strong regulator (Stefan *et al.*, 1996). Our results showed that reinitializing the model using measured profile data can reduce biases in temperature forecasts for the hypolimnion.

The overall aim of any forecast system for lake management should be that it is easy to use, computationally efficient and of low financial cost (Coulibaly, 2010). Environmental models are often not employed in the context of decision support or policy management, however, due to the large uncertainty associated with such predictions (Omlin *et al.*, 2001; Reichert and Vanrolleghem, 2001). If lake model forecasts are to be used to aid management decisions, then error between the model simulations and observed conditions must be reduced as much as possible. Our study has demonstrated a simple method of reducing forecast error for lake hydrodynamics. We also found that using the hot-start functionality in GOTM to assimilate observational had a low computational demand (0.78 – 1.36 s across all lakes, Table 5.3) and therefore a shorter time needed to forecast water temperature profiles. This would have implications, for example, when running model ensemble forecasts, which is known to have a large computational burden (Raso *et al.*, 2014). Our workflow for observational data assimilation allows forecasts to be consistently updated as soon as new weather forecast data became available. The hot-start functionality is a noteworthy software development that can be used to reduce model computational time and has been included in the newest versions of other lake models Simstrat (EAWAG, 2020; Goudsmit *et al.*, 2002) and the General Lake Model (GLM) (Hipsey *et al.*, 2017; UWA, 2020).

Table 5.3 Run time (in seconds) for GOTM for the spin-up period and for each of the forecast periods and the free model run (NDA).

<b>Lake</b>	<b>Spin-up</b>	<b>T000</b>	<b>T024</b>	<b>T168</b>	<b>T336</b>	<b>T672</b>	<b>NDA</b>
Feeagh	2.54	1.28	1.26	1.2	1.33	1.36	5.76
Langtjern	1.4	0.78	0.78	0.84	0.86	0.93	2.1
Kinneret	2.82	1.04	1.03	1.06	1.11	1.13	3.7

Our results suggest that having knowledge about the thermal regime of a lake can inform the sampling frequency that would likely be required to setup a lake profile forecasting framework. Near-real time data acquisition brings challenges for water managers as data collection is costly, resource intensive and weather dependent. Automatic HFM offers several advantages. It can be collected remotely, irrespective of weather conditions, and at a temporal resolution that is appropriate to rapidly changing water conditions (i.e. sub-daily). It can be streamed online and automatically quality controlled (Marcé *et al.*, 2016). HFM is critical for capturing short-term trends, extreme events and sub-daily in-lake variability (Aguilera *et al.*, 2016). We recommend that for lakes in sub-tropical climates with large surface temperature fluctuations and strong internal dynamics such as Kinneret that the sampling frequency to inform lake forecasts would need to be at least daily to reduce the MAE to less than 0.5 °C overall. A similar frequency would be needed for a small, very shallow dimictic lake like Langtjern given its susceptibility to undergo rapid changes in physical state in response to sudden changes in atmospheric conditions. Since this study was carried out, GOTM now has an ice model which would allow for predictions in ice formation and ice off. Forecasting of this phenology change could be of great importance for spring phytoplankton blooms (Katz *et al.*, 2015; Weyhenmeyer *et al.*, 1999). For a medium-sized lake in terms of surface area and depth, such as Feeagh, that undergoes relatively small changes in surface temperature,

in contrast, monthly sampling may be enough to improve forecasts and keep the MAE at a similar level.

### *5.6. Conclusion*

We have shown that assimilating observational data using direct insertion into a hydrodynamic model can reduce forecast error by up to 1 °C (60 % improvement) compared to running the model with estimated values for initialization and a one-year spin-up period with no updates to the state variables. Although the largest decreases in forecast error came with assimilation of near-real time observational data (i.e. today or yesterday), we also showed that assimilation of observational data from low frequency monitoring (monthly: T672) still greatly reduces error compared to no assimilation (34 % improvement). This simple methodology could be easily adapted and used to generate forecasts on many lakes, even those with low-frequency monitoring data. Our study used a multi-lake comparison from different climates, lake type, size and depth and the results therefore should be applicable to other sites. An even greater advantage would most likely be obtained from assimilation of observational data into a biogeochemical model, which would allow improved water quality forecasts to be generated.

## **CHAPTER 6. ENSEMBLE MODELLING OF FUTURE CLIMATE IMPACTS ON LAKE THERMAL DYNAMICS**

### **Note on the collaborative nature of the work described here:**

The work described in this chapter is part of a large collaborative project, the Lake Sector of ISIMIP (ISIMIP, 2020). Scientists who worked on this part of the project include **Tadhg Moore** (TM), Robert Ladwig (RL), Elvira de Eyto (EdeE), Oaxana Erina (OE), Gideon Gal (GiG), Gosia Golub (GoG), Sean Kelly (SK), Madeline Magee (MM), Rafael Marce (RM), Donald C. Pierson (DP), Noam Shachar (NS), Wim Thiery (WT), R. Iestyn Woolway (RIW) and Eleanor Jennings (EJ).

RM, DP and WT are the ISIMIP Lake Sector managers. GoG is the ISIMIP Lake Sector Coordinator who collated all the observed lake data. **TM** was model leader for the GOTM model and co-leader for GLM with RL within the ISIMIP Lake Sector - Local. This involved developing a modelling protocol, which included calibration and simulation procedures. **TM**, DP, GiG, NS ran the GOTM calibration procedure on the 60 study lakes. **TM**, RL, OE, GiG, NS, MM ran the GLM calibration procedure on the 60 study lakes. **TM**, GiG, NS and DP ran the climate change simulations for GOTM. **TM** and RL ran the climate change simulations for GLM. **TM** analysed the data presented in this chapter and wrote the draft with feedback from SK, EdeE, RIW, EJ.

## 6.1. Abstract

Global lakes and reservoirs are a critical natural resource and are vulnerable to the effects of climate change. These effects will vary depending on lake location and morphometry. Projected impacts can also vary, however, depending on the general circulation model (GCM) and lake model used. To best quantify and understand the wide and variable response of lakes to climate change, an ensemble modelling approach is best practice. The Inter-Sectoral Impact Model Intercomparison Project (ISIMIP) is a cross-sectoral network of climate impact modellers using a common approach and set of future projections to gain a consensus on global impacts. Here, we describe the protocol used for two lake impact models: the General Ocean Turbulence Model (GOTM) and the General Lake Model (GLM), and simulate projected thermodynamic changes in 46 lakes. We found that we achieved a good fit (RMSE:  $< 2$  °C and NSE:  $> 0.5$ ) of modelled to observed water temperatures for 77 % of the lakes in the study (46/60) for both models. Future simulations of climate change impacts under three different emissions scenarios, representative concentration pathways (RCP), which showed unequivocal warming in surface temperatures by 2069-2099 (RCP 2.6: +1.3 °C; RCP 6.0: +2.4 °C; RCP 8.5: +3.7 °C) and increases in stratification duration (RCP 2.6: +11.3 days; RCP 6.0: +21.2 days; RCP 8.5: +32.1 days). Changes in summer thermocline depth were sensitive to the choice of lake model used, with large variability by 2069-2099 for RCP 6.0 when all GCMs, sites and years in that time period were included (GLM:  $+0.4$  m  $\pm$  2.5 m; GOTM:  $+0.2$  m  $\pm$  2.0 m). The projected changes in thermal dynamics highlight that lakes and reservoirs are highly vulnerable to warming and will experience changes in stratification patterns, and an increased strength of stratification and therefore changes in habitat availability for lake biota under each of the different climate scenarios. We demonstrated in this study the steps necessary for approaching ensemble climate change modelling across multiple lakes and highlighted the key changes that are likely to occur in lakes under RCP 6.0. This knowledge will help to manage these fragile ecosystems as we move into a future of climate adaptation.

## 6.2. Introduction

### 6.2.1. Importance of lakes in the global context.

Lakes are an important environmental resource globally. They provide drinking, water food and have cultural significance. In an ecological sense, lakes provide habitats for a range of species that differs with latitude. Lakes influence the local climate through air-water fluxes (Bogomolov *et al.*, 2016; Heiskanen *et al.*, 2015; Mironov *et al.*, 2010). They also have a latent response to changes in the climate and, therefore, can integrate long-term climatic signals (Adrian *et al.*, 2009).

There have been significant trends in water quality degradation for lakes on a global scale as a result of direct and indirect anthropogenic activities (Mueller *et al.*, 2016; Shadkam *et al.*, 2016). At the same time, there has been quantifiable but highly variable increases in lake surface temperatures globally, and also in metrics of lake stratification (Kraemer *et al.*, 2015; O'Reilly *et al.*, 2015). Increases in lake water temperature and resultant changes in stratification can have large impacts on these ecosystems. Changes to the thermal profile of the lake can shift how fish and zooplankton interact. For example, daphnids inhabit surface waters for longer during periods of extended stratification, making them less accessible to deep water predators such as coregonids (Helland *et al.*, 2007). There has also been an increase in reporting of extreme climatic events which can affect lakes, such as high precipitation events which can reduce gross primary productivity (de Eyto *et al.*, 2016) or extended droughts which cause strong hypolimnetic oxygen depletion (Jankowski *et al.*, 2006). The trophic status of lakes can also affect the response of lake zooplankton communities to climate change, where high nutrient load can make the lake more sensitive (Alric *et al.*, 2013). Water temperature and incident irradiance are two of the main variables which explain global productivity in lakes, while the extent and duration of ice cover plays an important role in some regions (Lewis, 2011). Lake water temperature is recognised as a master environmental variable as it influences

many different processes within lakes (Magnuson *et al.*, 1979). Understanding the potential changes in lake temperature under different climate change scenarios will aid in developing robust adaptation strategies for lakes and reservoirs across lake physical, chemical and biological domains (Jeppesen *et al.*, 2009; Ogutu-Ohwayo *et al.*, 2016; Paukert *et al.*, 2016; Trolle *et al.*, 2019).

### 6.2.2. Ensemble modelling of anthropogenic perturbations on lakes

Lake water temperature is largely controlled by a combination of climatic drivers that contribute to the lake surface energy budget. Climatic variables including cloud cover, wind speed, atmospheric humidity and air temperature are the main drivers of this energy budget (Edinger *et al.*, 1968). Changes in any of these drivers can influence lake temperature through multiple feedbacks in the surface energy balance. To accurately project lake temperature responses to future climate change, process-based numerical models that can compute complex air-water thermodynamic fluxes are needed. A number of such process-based models have been developed in recent decades, including those developed from parameterization schemes based on similarity theory (Mironov, 2008), mixed-layer concept (Goyette *et al.*, 2000), eddy-diffusion (Hostetler and Bartlein, 1990), energy balance (Hipsey *et al.*, 2019), and turbulence closure (Goudsmit *et al.*, 2002). However, most studies to date that have simulated future climate change impacts on lake temperature have utilised only a single mechanistic model (e.g. Shatwell *et al.*, 2019; Woolway and Merchant, 2019). Whilst such studies have merit, the advantage of applying more than one independently developed model (i.e., an ensemble approach), is that some of the inherent uncertainties in the individual models can be reduced by conveying the mean and standard deviation of the simulations, thus enabling increased robustness of future projections. Such coordinated modelling experiments of independently developed multi-model projections have become the de facto standard in climate science including, for example, the Coupled Model Intercomparison Project (Eyring *et al.*,

2016). However, ensemble modelling of lake physical responses to future climate change has not yet been undertaken.

Uncertainty is a crucial characteristic that must be taken into account in any modelling study, including studies on lake thermal dynamics, due to the number of unknowns that are an inherent part of model structure (Smith and Stern, 2011). This includes uncertainty related to the general circulation models (GCM) used, uncertainty in human behaviour that will drive change in greenhouse gas emissions used for those global simulations, and uncertainty inherent to the lake model used, as well as variation in lake response that will be linked to local lake characteristics. The selection of a given GCM for an impact study can affect results obtained, particularly if the chosen lake model is sensitive to a parameter that is simulated with a large degree of uncertainty by that GCM, for example precipitation (McSweeney and Jones, 2016). There is also uncertainty related to estimations of future fossil fuel production. It has been estimated that the Inter-governmental Panel on Climate Change (IPCC) high emissions scenario is highly unlikely due to an overestimation of global fossil fuel resources (Capellán-Pérez *et al.*, 2016; Mohr *et al.*, 2015). Accounting for such different sources of uncertainty, with some linked to model structure and others linked to human behaviour, is particularly important for any study of future climate projections. Ensuring that this uncertainty is communicated effectively is essential if climate research is to inform global policy (Stainforth *et al.*, 2007). Future projections using GCMs are also inherently uncertain due to the fact they are trying to predict a never seen system, and historical skill for the model does not translate into future skill (Collins *et al.*, 2006; Murphy *et al.*, 2004), possibly because of the non-stationarity of the feedback processes within the models (Reifen and Toumi, 2009). There are many ways of characterising and accounting for uncertainty. For models of lake thermal structure there are four main sources of uncertainty: 1) initial condition uncertainty; 2) boundary conditions uncertainty; 3) process uncertainty and 4) parameter uncertainty. Kiktev *et al.* (2007) found that a multi-GCM ensemble means produced more accurate simulations than use of a single GCM, in the context of air temperature and precipitation outputs from GCMs. Ensemble modelling is regarded as best

practice particularly when trying to gauge the variable impacts of climate change (Collins *et al.*, 2006). This is because it allows for the biases between differing models to be balanced out and accounts for uncertainties associated with the GCM forcing data and process error within for example the lake models used.

### 6.2.3. ISIMIP Approach

There have been many modelling studies undertaken to assess the impacts of projected climate change on lake thermal structure at a local and regional spatial scale (e.g. Schmid *et al.*, 2014; Sahoo *et al.*, 2016; Schmid and Koster, 2016; Magee and Wu, 2017b; Woolway *et al.*, 2017a; Råman Vinnå *et al.*, 2018; Woolway and Merchant, 2019). It has been highlighted that when summarising potential impacts of climate change in one sector, such as the lake sector, there can be a mis-characterization of the response to climate change due to a lack of accounting for complex interdependencies that exist between sectors (Harrison *et al.*, 2016). The ISIMIP project is unique because it adopts a cohesive global approach across many different sectors, for example agriculture, forests, fisheries, terrestrial biodiversity and hydrology (Frieler *et al.*, 2017; ISIMIP, 2020). It provides a common simulation protocol which allows for the separation of historical warming from pre-industrial conditions, quantifies the impact of global air temperature warming by 1.5 °C in accordance with the Conference of Parties 21 (COP21) agreement in Paris (UNFCCC, 2015) and allows for further comparisons across different potential future emission scenarios (Frieler *et al.*, 2017). Representative Concentration Pathways (RCPs) have been developed to represent potential future greenhouse gas emission (GHG) scenarios representing differing levels of global action to mitigate the effects of anthropogenic induced climate change. General circulation models provide consistent atmospheric and oceanic forcing data representing each of the different RCPs on a global scale. Sector impact modelling use these datasets, along with projected socio-economic conditions, to project the potential impacts. The use of common forcing data also

allows impacts to be quantified across sectors and therefore through cross-sectoral analysis. All the ISIMIP output data are publicly available.

Prior to the initiation of the ISIMIP Lake sector, there was a group which set up a lake model intercomparison project (LakeMIP; Stepanenko *et al.*, 2010). The purpose of LakeMIP was to evaluate the individual performance of various lake models at different sites (Perroud *et al.*, 2009; Thiery *et al.*, 2014a), couple a lake model with an atmospheric model (Goyette and Perroud, 2012; Perroud and Goyette, 2012) and accurately simulate energy fluxes and thermal stratification (Stepanenko *et al.*, 2014). This project built up a network of researchers who work with many different lake models (Stepanenko *et al.*, 2010). The focus of the LakeMIP group was on short-term lake thermal dynamics, while the current ISIMIP Lake sector built on this to start focusing on investigating long-term multi-decadal and centennial changes in lake variables.

Within the current ISIMIP lake sector, six models were used to simulate the effects of climate change on lake water temperature, which included Simstrat, Freshwater Lake Model (FLake), Advanced Lake Biogeochemical Model (ALBM), Multi-year Lake model (MyLake), and the two models used in this study: the General Lake Model (GLM) and the General Ocean Turbulence Model (GOTM). These simulations were carried out in line with the protocol of ISIMIP2b (Frieler *et al.*, 2017). ISIMIP2b is the latest round of global climate simulations and was designed to complement the IPCC scheduled report which focused on reflecting the impacts of the 1.5 °C target (Frieler *et al.*, 2017). There were two distinct simulation approaches used within the Lake Sector which have been termed 1) global and 2) local. The global approach used a global lakes database based on a 0.5° x 0.5° gridded map of the world (Figure 6.1 A). A percentage value per grid was calculated using data from ~13 000 freshwater lakes for lake area, mean depth and maximum depth which was then mapped onto a global grid with a resolution of 30 arc sec (Kourzeneva *et al.*, 2010). The models were run uncalibrated using boundary conditions (forcing data) from four GCMs. The aim of this approach was to capture the geographical response and variability of a 'typical' or generic lake to different climate conditions based on

different carbon emission scenarios. Simulated lake variables included lake surface temperature, lake stratification and ice cover regime shifts. Given the generic approach and assumptions of the global lake sector methodology, a complimentary local lake sector group was formed with the purpose of examining individual lake responses to climate change which used specific detail from each individual site (Figure 6.1 B). The local lake sector, which the work presented in this chapter was part of, used high-frequency, long-term *in situ* data from some of the world's best-studied lakes, which allowed full calibration and validation of model performance for each individual site prior to simulating climate change projections.

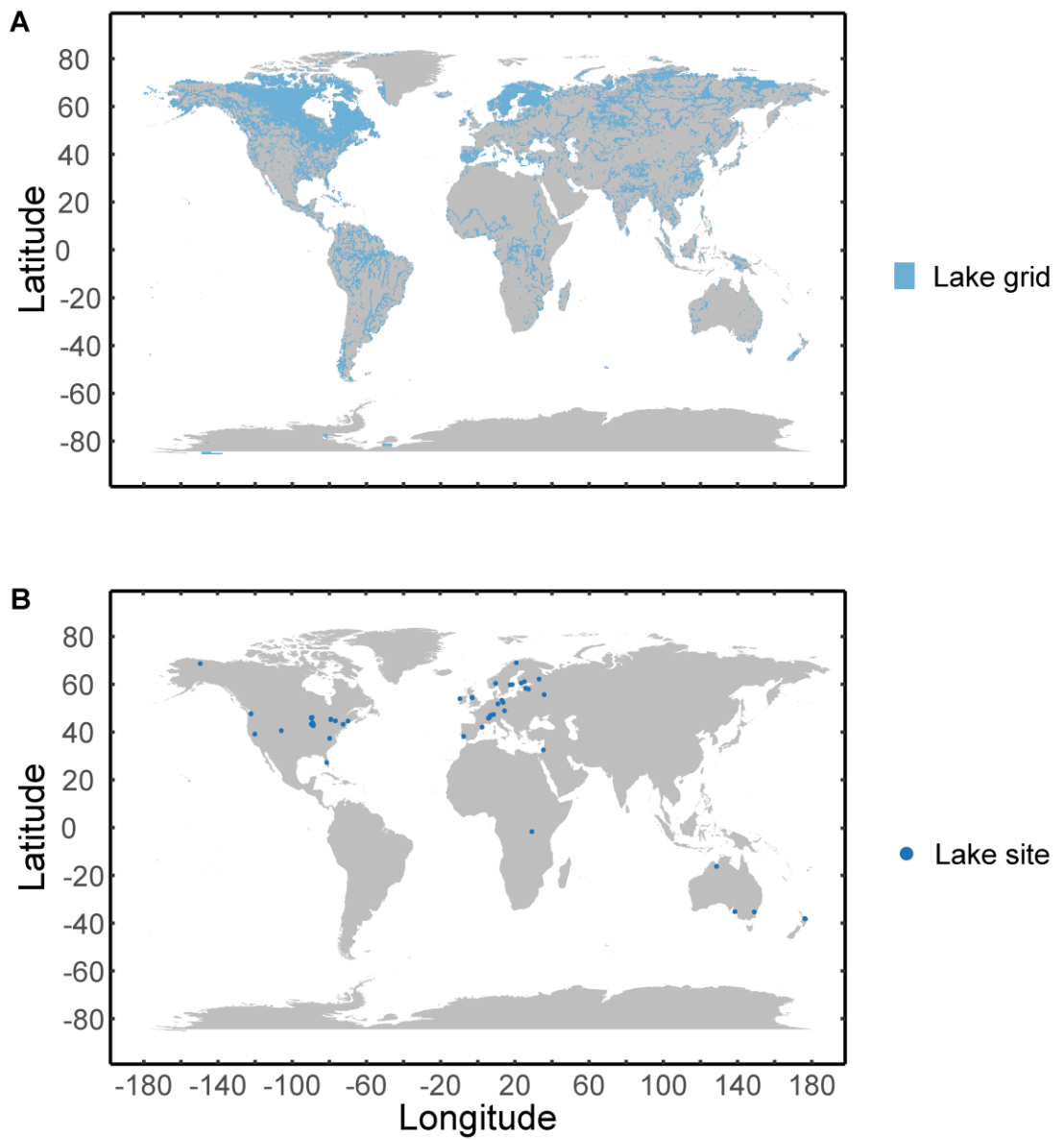


Figure 6.1 Distribution of lakes that are included in the global (A) and local (B) ISIMIP lake study. The data for the global lakes comes from the Global Lake Data Base (Kourzeneva *et al.*, 2010).

#### 6.2.4. Previous global lake studies

Global studies of the historical response of lakes to change in climate have found key trends and identified potential explanatory variables. O'Reilly *et al.* (2015) showed that the response of lake summer surface temperatures to contemporary (1985 to 2009) climate change in 235 globally distributed lakes was highly variable using *in-situ* and satellite measured data. The main drivers for these trends were increases in air temperature and downwelling solar radiation and decreases in cloud cover. A separate study of 26 lakes across the world demonstrated that historical (1970 to 2010) changes in lake stratification varied depending on lake average temperature and morphometry (Kraemer *et al.*, 2015). In a regional study of 160 monitored lakes in the north-eastern and midwestern United States from 1981 to 2010, local drivers combined with regional scales strongly influenced lake sensitivity to climate change (McCullough *et al.*, 2019). Relationships between water clarity and lake warming were found to be highly non-linear in a climate change modelling study (Shatwell *et al.*, 2019). Previous global lake modelling studies have applied uncalibrated and simple lake models to characterise regional scale responses to climate change (Woolway and Merchant, 2019; Woolway *et al.*, 2019). Some case-studies have used model calibration to reduce the uncertainty in the model output and accounts for biases present in the climate forcing data (Ayala *et al.*, 2019; Sahoo *et al.*, 2016; Shatwell *et al.*, 2019).

#### 6.2.5. Aim of this study

This chapter describes the protocol used to undertake impact modelling for the “local” lake sector of ISIMIP using two one-dimensional (1-D) lake models: The General Lake Model (GLM) and the General Ocean Turbulence Model (GOTM), which has been adapted for lakes. Simulations of projected climate change impacts on lake thermal dynamics were forced using data from four GCMs. An introduction and

summary for the GCMs, the RCPs and both lake models are described along with model configuration and calibration workflows that were developed as part of this project and applied across the 60 sites. A general overview of the results from these simulations is presented in the context of the different RCP scenarios, with a key focus on the impacts on lake thermodynamic properties under RCP 6.0 for the period 2069 to 2099. The discussion of this local lake study is framed in the context of the global lake sector simulations, with the key benefits of each study approach being highlighted. Recommendations for future approaches and developments are outlined in anticipation of the next round of simulations, ISIMIP3, which has recently been launched.

### 6.3. Simulation protocol and data sources

Here we describe the components of the modelling workflow as per the ISIMIP protocol (ISIMIP, 2019) and captured in the schematic Figure 6.2.

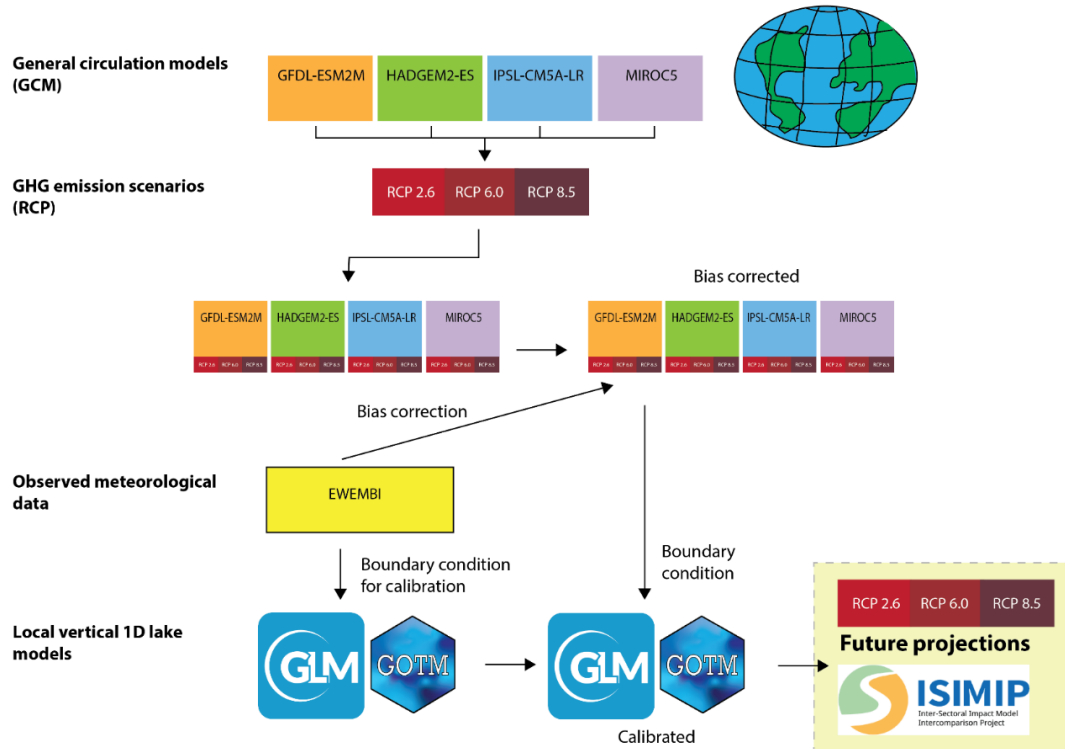


Figure 6.2 Schematic of the ISIMIP workflow, detailing how the GCMs are bias corrected with EWEMBI, the lake models are calibrated with EWEMBI and then are both used to simulate future lake thermal states under different greenhouse gas (GHG) emission scenarios which are the RCPs.

### 6.3.1. General Circulation Models

General circulation models are numerical models that have been developed to simulate climatic processes, and are used in weather and climate prediction and to investigate atmospheric dynamics (Mechoso and Arakawa, 2015). They simulate the processes within the atmosphere, ocean, troposphere, land surface and cryosphere and the many complex interactions between them (Manabe *et al.*, 1965; Coppin and Bony, 2017) and have even been applied to other planetary bodies such as Mars (Mooring *et al.*, 2019). They provide geographically and physically based consistent projections on a global scale as they operate in a three-dimensional grid that covers the globe. They can have varying degrees of horizontal ( $0.5 - 3.75^\circ$ ) and vertical resolution in the atmosphere (20-40 layers) and in the ocean (10-50 layers). Parameterisation of the GCMs allows for the integration over large spatial areas. The temporal resolution of GCMs is usually daily to monthly, to minimise computational run time and the quantity and magnitude of output data. To capture the influence that humans have on the future global atmosphere and environment, the GCMs operate on large time scales, stretching back to the pre-industrial period 1661-1860, which means the use of GCMs can disentangle the historical influence of anthropogenic activity, particularly the industrial revolution on the climate system.

Due to their relatively coarse spatial resolution, GCMs contain systematic biases across many variables when compared with observations, as a result of the neglect of sub-grid scale orography (Cattiaux *et al.*, 2013; Sillmann *et al.*, 2013; Kumar *et al.*, 2014; Mueller and Seneviratne, 2014). Systematic biases refer to distinct differences in distributions of the variables, such as precipitation, compared to observed distributions. GCM output can be corrected for these biases by applying empirical or statistical bias correction techniques and the most widely used is quantile mapping (Cannon, 2016, 2018; Cannon *et al.*, 2015; Eden *et al.*, 2012). This method maps quantiles from a source distribution, the GCM output, to a target distribution which is the historical observations (Wilcke *et al.*, 2013). Bias correction allows for a more direct comparison between observed and projected states, accounts for threshold

related behaviour, for example, between air temperature and precipitation, incorporates more detailed observational data and improves simulation of variance. On the other hand, it significantly alters the consistency of the data and can potentially change the trend (Piani *et al.*, 2010).

Four general circulation models (GCM) were selected for the ISIMIP protocol (Figure 6.2; Table 6.1), based on whether they could provide the required atmospheric variables (i.e. boundary conditions) needed to force each lake model and that they covered the following time periods: 1) 200 pre-industrial control years (1661-1860); 2) the entire historical period (1861-2005); 3) RCP 2.6, RCP 6.0 and RCP 8.5 from 2006 to 2099. The four GCMs used were Geophysical Fluid Dynamics Laboratory (GFDL) Earth System Model with Modular Ocean Model version 4 (MOM4) component (ESM2M) (GFDL-ESM2M), Met Office Hadley Centre Earth System Model (HadGEM2-ES), Institut Pierre-Simon Laplace Climate Model 5A - Low Resolution (IPSL-CM5A-LR) and Model for Interdisciplinary Research on Climate (MIROC5) (Table 6.1). The atmospheric variables provided are listed in Table 6.2.

Table 6.1 Summary of General Circulation Models used for the Inter-Sectorial Inter-Model Intercomparison Project (ISIMIP).

Name	Abbreviation	Atmosphere Spatial resolution	Ocean Spatial resolution	Atmospheric levels	Ocean levels	Components	Reference
Geophysical Fluid Dynamics Laboratory Earth System Model (GFDL) with Modular Ocean Model version 4 (MOM4) component (ESM2M)	GFDL-ESM2M	2° x 2.5°	1° x 1°	24	50	Ocean, atmosphere, land, sea-ice	Dunne <i>et al.</i> , 2012, 2013
Met Office Hadley Centre Earth System Model	HADGEM2-ES	1.875° x 1.25°	1° x 1°	38	40	Land-surface scheme, large scale hydrology module, river model, tropospheric chemistry, aerosols, terrestrial carbon cycle, ocean carbon cycle	Collins <i>et al.</i> , 2011; Jones <i>et al.</i> , 2011
Institut Pierre-Simon Laplace Climate Model 5A - Low Resolution	IPSL-CM5A-LR	1.9° x 3.75°	Varies	39	31	ORCHIDEE land-surface model, NEMOV3.2 oceanic module, sea-ice model LIM-2 and ocean biogeochemistry mode PISCES	Dufresne <i>et al.</i> , 2013; Hourdin <i>et al.</i> , 2013
Model for Interdisciplinary Research on Climate	MIROC5	1.4° x 1.4°	1.4° x 1.4°	40	49	Atmosphere and ocean model	Watanabe <i>et al.</i> , 2010

Table 6.2 Climate variables provided by each General Circulation Model (GCM).

<b>Variable</b>	<b>Short name</b>	<b>Unit</b>
Near-Surface Relative Humidity	hurs	%
Near-Surface Specific Humidity	huss	kg kg <sup>-1</sup>
Precipitation (rainfall + snowfall)	pr	kg m <sup>-2</sup> s <sup>-1</sup>
Snowfall Flux	prsn	kg m <sup>-2</sup> s <sup>-1</sup>
Sea-level Air Pressure	ps	Pa
Surface Air Pressure	psl	Pa
Surface Downwelling Longwave Radiation	rlds	W m <sup>-2</sup>
Surface Downwelling Shortwave Radiation	rsds	W m <sup>-2</sup>
Near-Surface Wind Speed	sfcWind	m s <sup>-1</sup>
Near-Surface Air Temperature	tas	K
Daily Maximum Near-Surface Air Temperature	tasmax	K
Daily Minimum Near-Surface Air Temperature	tasmin	K

### 6.3.2. Representative Concentration Pathways

Potential future scenarios are based on anticipated and projected changes in the climate system based on fluctuations in greenhouse gases (GHGs), aerosols and incorporating land use and land cover changes (Parson *et al.*, 2007). These scenarios are representative of pathways of changes in global radiative forcing and are referred to as representative concentration pathways (RCPs). Radiative forcing is the overall change in the net radiative flux at the top of the atmosphere. These are the inputs used to force the GCMs to project future climate. The scenarios are not exact methods to capture precise changes, but represent different potential futures all of which are equally feasible under different scenarios (Moss *et al.*, 2008). Not only do they capture shifts in radiative forcing, but they also project the trajectory at which such shifts can potentially occur (Moss *et al.*, 2010).

RCPs are the result of collaboration between climate modellers, emission inventory experts, terrestrial ecosystem experts and integrated assessment modellers (Moss *et al.*, 2010) (Figure 6.3). They include variables such as technological advancements, land use changes, population growth, air pollutants, socio-economic changes and greenhouse gas emissions (van Vuuren *et al.*, 2011). Four scenarios were selected to capture the potential range of responses dependent on human mitigation measures with representative pathways that capture a potential way in which those response may occur in relation to CO<sub>2</sub> equivalent emissions (Moss *et al.*, 2010). These accounted for radiative forcing increases of 2.6 W m<sup>-2</sup> (RCP 2.6), 4.5 W m<sup>-2</sup> (RCP 4.5), 6.0 W m<sup>-2</sup> (RCP 6.0) and 8.5 W m<sup>-2</sup> (RCP 8.5) (Table 6.3). For the ISIMIP project only three of the RCPs were selected: RCP 2.6, RCP 6.0 and RCP 8.5 with the focus being RCP 2.6, the scenario where global temperature rise is limited to 1.5 °C.

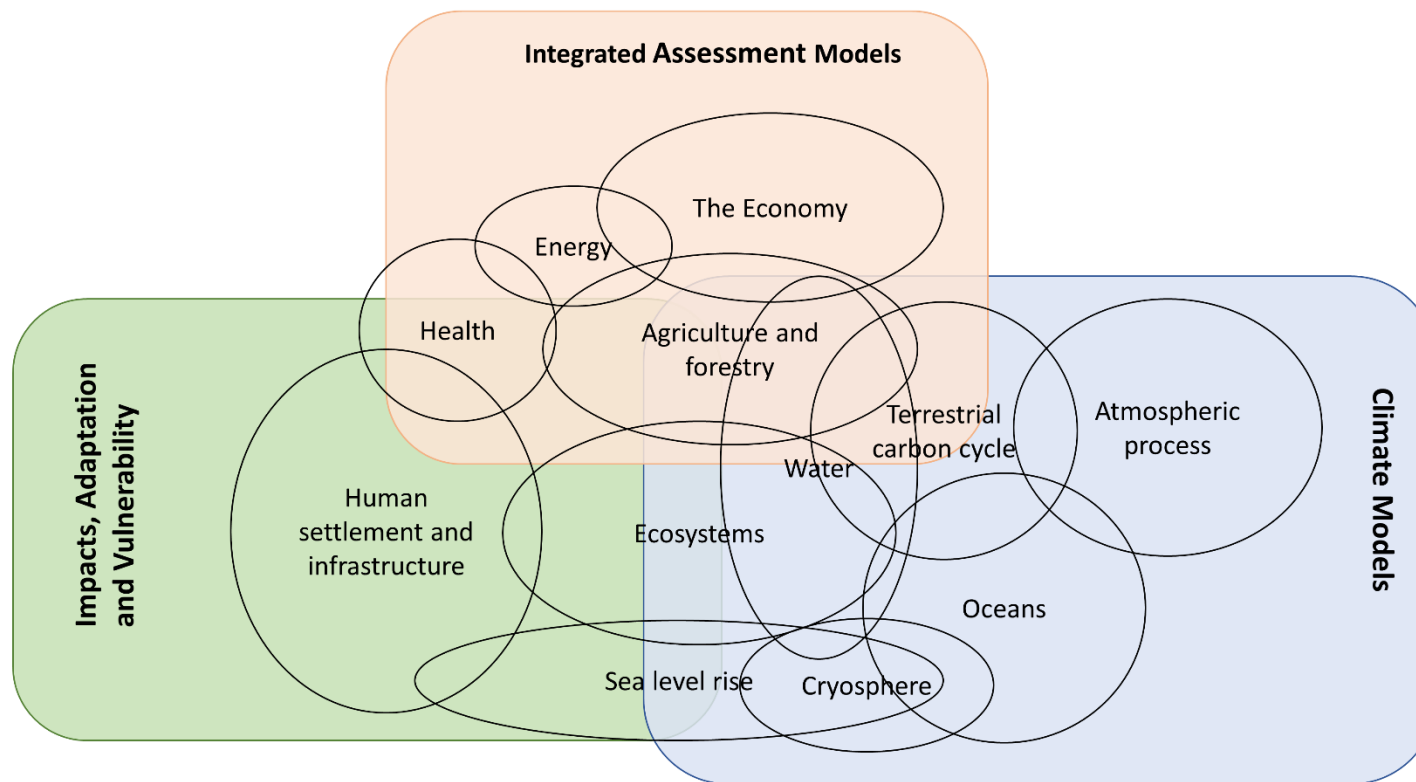


Figure 6.3 Development of RCPs. Scenarios are generated and used by three broad types of models and analytic frameworks in climate change research: integrated assessment models, climate models and other approaches used to help assess impacts, adaptation and vulnerability. (Adapted from Moss *et al.*, 2010).

Table 6.3 The four Regional Concentration Pathways (RCPs) (adapted from Moss *et al.*, 2010).

<b>Name</b>	<b>Radiative forcing</b>	<b>Concentration (p.p.m)</b>	<b>Pathway</b>	<b>Reference</b>
RCP 2.6	Peak at $\sim 3 \text{ W m}^{-2}$ before 2100 and then declines	Peak at $\sim 490 \text{ CO}_2$ equivalent before 2100 and then declines	Peak and decline	(van Vuuren <i>et al.</i> , 2006)
RCP 4.5	$\sim 4.5 \text{ W m}^{-2}$	$\sim 650 \text{ CO}_2$ equivalent (at stabilization after 2100)	Stabilization without overshoot	(Smith and Wigley, 2006)
RCP 6.0	$\sim 6 \text{ W m}^{-2}$	$\sim 850 \text{ CO}_2$ equivalent (at stabilization after 2100)	Stabilization without overshoot	(Fujino <i>et al.</i> , 2016)
RCP 8.5	$> 8.5 \text{ W m}^{-2}$ in 2100	$> 1370 \text{ CO}_2$ equivalent in 2100	Rising	(Riahi <i>et al.</i> , 2007)

### 6.3.3. EWEMBI

The output data from each of the GCMs were interpolated with a first-order conservative remapping scheme (Jones, 1999) on a regular  $0.5^\circ \times 0.5^\circ$  grid. To correct for biases within each GCM, a standardised reanalysis dataset based on global observations (EWEMBI) was used (Frieler *et al.*, 2017) (Figure 6.2). The Earth2Observe WATCH forcing data methodology was applied to ERA-Interim reanalysis data (WFDEI) and ERA-Interim data Merged and Bias-corrected for ISIMIP (EWEMBI) datasets, which temporally ranged from 1979-2016 on a daily timestep, and were at a spatial resolution of  $0.5^\circ \times 0.5^\circ$  (Lange *et al.*, 2019). This dataset was created by merging data from the ERA-Interim reanalysis data (ERA-Interim; Dee *et al.*, 2011), WATCH forcing data, (Weedon *et al.*, 2014), earth2Observe forcing data (E2OBS; Calton *et al.*, 2016) and NASA/GEWEX Surface Radiation Budget data (SRB) (Stackhouse Jr. *et al.*, 2011).

Although some bias could be introduced by selection of a subset of GCMs, it has been shown that use of a subset is representative of the full range of GCM outputs, particularly for air temperature although the overall uncertainty would be underestimated (McSweeney and Jones, 2016).

### 6.3.4. Lake models

In this part of the ISIMIP Lake sector project, the two 1D physical lake models used to simulate water temperature: GLM and GOTM are described. A general overview and references of each model is presented in section 2.3.5. We used the General Lake Model (v3.0.0 beta12) for this study, the most up-to-date version of the model at the outset of the ISIMIP project. For this study, the General Ocean Turbulence Model (GOTM) (v5.1 – lake branch) was used for the simulations. This was the most up-to-date version of the model at the outset of the ISIMIP project, although currently (2020) there is a version 5.4 which has a new integrated ice model.

### 6.3.5. Collation of lake data

A data request was distributed by email throughout the collaborative networks of ISIMIP participants. Announcements were also made at several international conferences and workshops, aimed at data providers with access to *in situ* lake data. For a candidate lake site to be included in the project, one of two separate criteria had to be met: 1) at least two years of high-frequency water temperature profiles (sub-daily) or 2) at least five years of low-frequency water temperature profiles. For both conditions, the data had to be within the time period 1979-01-01 and 2016-12-31 as this was the period covered by the meteorological dataset used to calibrate the model (section 6.3.7). Hypsograph data were provided from each site. Additional metadata were also requested, including latitude, longitude, elevation, maximum depth, lake surface area, watershed area, influence of hydrology, trophic state, light extinction coefficient and/or Secchi depth. In total, we were able to collect data from 60 lakes around the world (Figure 6.1).

### 6.3.6. Model configuration

#### 6.3.6.1. General Lake Model

To resolve the vertical density profile, the minimum layer thickness in GLM was set to be 0.5 m and the maximum layer thickness to be 1.5 m. GLM uses a light extinction coefficient to capture the depth of light penetration into the water column and we used the setting where 45 % of incident solar radiation is photosynthetically active radiation (PAR) and follows Beer-Lambert law (Swinehart, 1962):

$$\phi_{PAR}[z] = f_{PAR}\phi_{SW_0} \exp[-K_w z], \quad (6.1)$$

where  $z$  is the depth of any layer from the surface,  $\phi_{PAR}[z]$  is the incident PAR at depth  $z$ , where  $f_{PAR}$  is the PAR fraction of incident solar radiation and  $K_w$  is the light extinction coefficient in  $\text{m}^{-1}$ . The default surface heat exchange parameters were used as defined from (Fischer *et al.*, 1979) and mixing parameters similarly to (Bruce *et al.*, 2018).

Basin length and basin width were calculated by assuming an elliptical lake shape with a length which is twice the width:

$$bsn_{wid} = \sqrt{\frac{2 * A_0}{\pi}} \quad (6.2)$$

$$bsn_{len} = 2 * bsn_{wid} \quad (6.3)$$

where  $A_0$  is the surface area,  $bsn_{wid}$  is the basin width and  $bsn_{len}$  is the basin length. When daily forcing data are supplied to GLM, it is disaggregated internally to a sub-daily time-step according to the calculation in Hamilton and Schladow (1997), which distributes the daily solar flux over a diurnal cycle based on the latitude, day of the year and time of day. Short-wave albedo was estimated using equations from Hamilton and Schladow (1997).

Sedimentary heat flux parameterisations in GLM were also switched off to ensure that model setups were coherent across sites between lake models. No inflows and outflows were configured because we did not have inflow or outflow data for all the sites. When running long term simulations this can lead to issues such as decreasing water level over time (Winslow *et al.*, 2017b). To deal with this, Winslow *et al.* (2017b) increased precipitation by 170 mm during the summer months and excess water was allowed to overflow over the lake surface thus reducing the impact on mixing within the model. In this study, we assumed a fixed water level by switching off the mass loss associated with evaporation. However, the thermal energy fluxes associated with evaporation were still calculated. To prevent lakes from over filling we ensured there was overflow if the lake volume increased beyond basin carrying capacity.

### 6.3.6.2. General Ocean Turbulence Model

The number of depth levels used to discretise the water column for lakes shallower than 50 m in depth was:

$$nlev = \frac{z_{max}}{0.5} \quad (6.4)$$

where  $nlev$  is the number of layers in the model and  $z_{max}$  is the maximum depth. Surface zooming is a feature in GOTM that allows inclusion of an adjusted grid and an increase in the number of layers at different depths of the water column. For lakes deeper than 50 m, the number of layers was set to 100 and surface zooming was switched on. The layer depth in the model is determined by:

$$h_i = D \frac{\tanh\left((d_l + d_u) \frac{i}{nlev} - d_l\right) + \tanh(d_l)}{\tanh(d_l) + \tanh(d_u)} \quad (6.5)$$

where  $h_i$  is discretization depth from the bottom for layer  $i$ ,  $d_l$  is the bottom zooming factor,  $d_u$  is the surface zooming factor and  $nlev$  is the number of layers for discretisation, see Figure 6.4 for an example of discretized depths in three lakes of varying depths. For lakes with a depth greater than 50 m and less than 100 m, the surface zooming factor ( $d_u$ ) was set to 1.5 and the bottom zooming factor ( $d_l$ ) was set to 0 and lakes with a depth greater than 100m the surface zooming factor ( $d_u$ ) was set to 3 and the bottom zooming factor ( $d_l$ ) was set to 0.

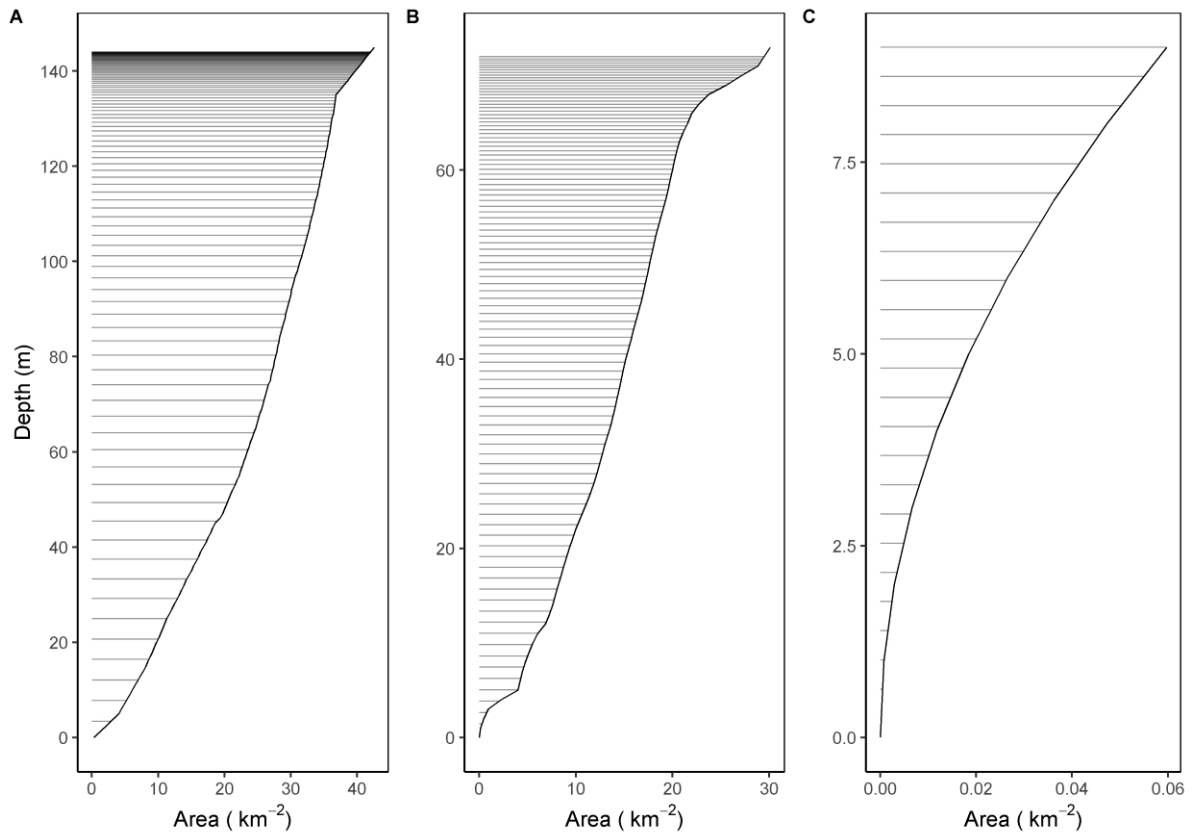


Figure 6.4 Examples of discretization depths of layers within GOTM for three example study lakes A) Bourget, FR (145 m; 100 layers), B) Green Lake, US (73 m; 100 layers) and C) Langtjern, NO (9 m; 24 layers).

GOTM has a wide variety of turbulence models that can be utilised within its structure. For our study we used a second-order turbulence closure model. These models result from the approximate or full solution of transport equations for turbulent fluxes, which are strongly influenced by the Navier-Stokes equations (Sander, 1998).

Whilst the meteorological driving data provided were on a daily timestep, the internal timestep for model integration was set to 3600 s. GOTM resolves internal processes more accurately when run at a sub-daily time step (Ayala *et al.*, 2019). When model input data is at a lower temporal resolution, GOTM performs internal interpolation of the input data to match the integration timestep.

The method for calculating net longwave radiation was the method developed by Clark *et al.* (1974). Within GOTM, we used the Fairall *et al.* (1996) method for calculating the heat fluxes between the lake surface and atmosphere. GOTM requires

cloud cover as a driving variable so this was calculated using the method from Martin and McCutcheon (1999) which uses air temperature, relative humidity, short-wave radiation, latitude, longitude and elevation. Light was separated into visible and non-visible components with the visible component accounting for 45 % and the non-visible was 55 %. The *e*-folding depth (light attenuation) for each lake was included in the calibration parameters. Incoming short-wave radiation was disaggregated from mean daily values using a calculation that uses time, latitude and longitude from Simpson and Paulson (1979).

#### *6.3.7. Calibration procedure*

The aim of the calibration process for each lake model simulation was to correct the model for potential biases in the meteorological forcing data and internal model processes. For example, the use of daily meteorological data as forcing data does not accurately represent the influence of wind speed, which can sometimes have pronounced diurnal patterns. Light attenuation is a state variable that can have large temporal variation (Yacobi, 2006; Gerea *et al.*, 2017; Lisi and Hein, 2019) and uncertainty around the value due to Secchi depth approximations. As a result of these uncertainties it was also included in calibration. For each lake, GLM and GOTM were calibrated by forcing the models with meteorological data extracted from the appropriate EWEMBI grid square (Figure 6.2). Model simulations were then compared to observed data, and a calibration procedure applied. This calibration procedure differed with lake model and is described below.

### 6.3.7.1. GLM Calibration

For GLM calibrations, we ensured there was a two-year spin-up period. The model was initialized using a ‘typical’ profile at a time of year when the lake was isothermal. For GLM the parameters selected for calibration were a wind scaling factor (wind\_factor) and light attenuation (Kw). GLM uses incoming long-wave radiation as a forcing variable so we also included a scaling factor for this (lw\_factor). We used similar ranges to ensure parameters stayed within realistic ranges (Table 6.4).

Table 6.4 Parameters used in the GLM calibration with their default values and ranges.

Long name	Short name	Set value	Range	
			Min	Max
Long wave radiation scaling factor	lw_factor	1	0.5	1.5
Wind speed scaling factor	wind_factor	1	0.5	2.0
Light attenuation	Kw	$K_{W_{obs}}$	$0.1 * K_{W_{obs}}$	$1.9 * K_{W_{obs}}$

A Covariance Matrix Adaptive Evolutionary Strategy (CMA-ES) algorithm (Hansen and Ostermeier, 2001; Hansen *et al.*, 2003) was used to calibrate the model. The aim of CMA-ES is to fit the multi-variate normal distributions of the mutations to the contour of the objective function. The cost function used for GLM was the root mean square error (RMSE).

$$RMSE = \sqrt{\frac{1}{n} \sum_{i=1}^n (\hat{y}_i - y_i)^2} \quad (6.6)$$

where  $n$  was the number of samples,  $y_i$  was the observed and  $\hat{y}_i$  was the simulated water temperatures at time  $i$ . Root mean square error was chosen because it is widely used to assess the goodness of fit for lake models. This differed from GOTM due to the ACPy tool being hard coded to use just log likelihood. Due to computational and time constraints we limited the calibration to 500 iterations which for most lakes allowed for convergence. The ‘best’ parameter set was the one with the lowest RMSE. There was a significant variability in sensitivity to the different parameters across the lakes. Each lake’s calibration value was inspected following the completion of calibration to ensure that it was in a reasonable range and that the model performance was reasonable.

#### 6.3.7.2. GOTM Calibration

A minimum two-year spin-up period was used to ensure there was no influence on the simulation related to the initial water temperature conditions. The parameters used for calibrating GOTM were scaling factors for wind speed (*wind\_factor*), total downwelling short-wave radiation (*swr\_factor*) and surface heat fluxes (*shf\_factor*) (Table 6.5). The parameters which affect light attenuation:  $e$ -folding depth for visible (*g2*) and non-visible light (*g1*), and the minimum turbulent kinetic energy (*k\_min*) were also included. These were the main parameters identified in a preliminary investigation as being an important part of GOTM calibration (Ayala *et al.*, 2019).

Table 6.5 Parameters used in the GOTM calibration with their default values and ranges.

Long name	Short name	Set value	Range	
			Min	Max
Surface heat-flux factor	shf_factor	1	0.5	1.5
Short wave radiation factor	swr_factor	1	0.5	(1200 / SWR <sub>max</sub> )
Wind factor	wind_factor	1	0.5	2.0
Minimum turbulent kinetic energy	k_min	3.6e <sup>-6</sup>	1.4e <sup>-7</sup>	1e <sup>-5</sup>
e-folding depth for non-visible fraction	g1	0.54	0.01	2
e-folding depth for visible fraction	g2	7.18	(0.1 * g2 <sub>obs</sub> )	(1.9 * g2 <sub>obs</sub> )

The program used to calibrate GOTM was ACPy (Auto calibration utility for GOTM written in Python, now renamed parsac), developed by Bolding and Bruggeman Aps and the code is available on GitHub (Bolding and Bruggeman, 2020). ACPy uses a differential evolution (DE) algorithm which calculates a log likelihood function based on comparing the modelled water temperature to the observed temperature (Storn and Price, 1997).

In this study, for each calibration run, the model was run for 84 generations which allowed for ~5000 iterations. The cost function used for the calibration routine was the calculation of log likelihood (*lnlikelihood*) for each parameter set, comparing modelled to observed:

$$lnlikelihood = \sum_{i=1}^n -0.5(\log_e(\pi)) - \log_e(\sigma_{obs}) - 0.5\left(\frac{y_i - \hat{y}_i}{\sigma_{obs}}\right) \quad (6.7)$$

where  $\sigma_{obs}$  was the standard deviation of observed values,  $y_i$  was the observed and  $\hat{y}_i$  was the simulated water temperatures at time  $i$ , and  $n$  was the number of samples. The ‘best’ parameters selected were the ones that had the highest log likelihood.

Issues were encountered for individual scaling factor calibration whenever the best-fit parameter would approach the upper or lower limit of the pre-set value range. We recognised that this demonstrated that the parameters could potentially improve by increasing the limit range, but the limits were selected to ensure that the parameters stayed within a realistic range to prevent the potential for the model to achieve the best fit for the wrong reasons. The best parameter set was then used for all the historical and future simulations.

### 6.3.8. Simulating projections

For initialising the model, we selected a period where the lake was isothermal and initialised each simulation with this profile and on this day of year. To counteract the influence of the initial conditions we used a three-year spin-up period (Hodges, 2014). This period was created by repeating the first three years in the driving data and then removed this from the simulated output. For initial conditions we used an observed temperature profile from when the lake was isothermal and initialised each simulation with a three-year spin-up period.

For simulations using GOTM, daily averaged data was extracted, while for GLM daily point values at 8:00 every day were extracted. This was because of

differences in the model outputs: GOTM has the functionality to save mean daily output while GLM only has the capacity to save point values. Outputting hourly values for GLM would have exponentially increased model runtime and handling of model output files particularly for the very deep sites. The differences between daily averaging hourly model output and extracting data at 8:00 were compared for IE\_Fee over a 10-year period with a mean difference of 0.01 °C (SD: 0.06 °C) (Figure 6.5), This showed that this method did not influence the results to a large degree.

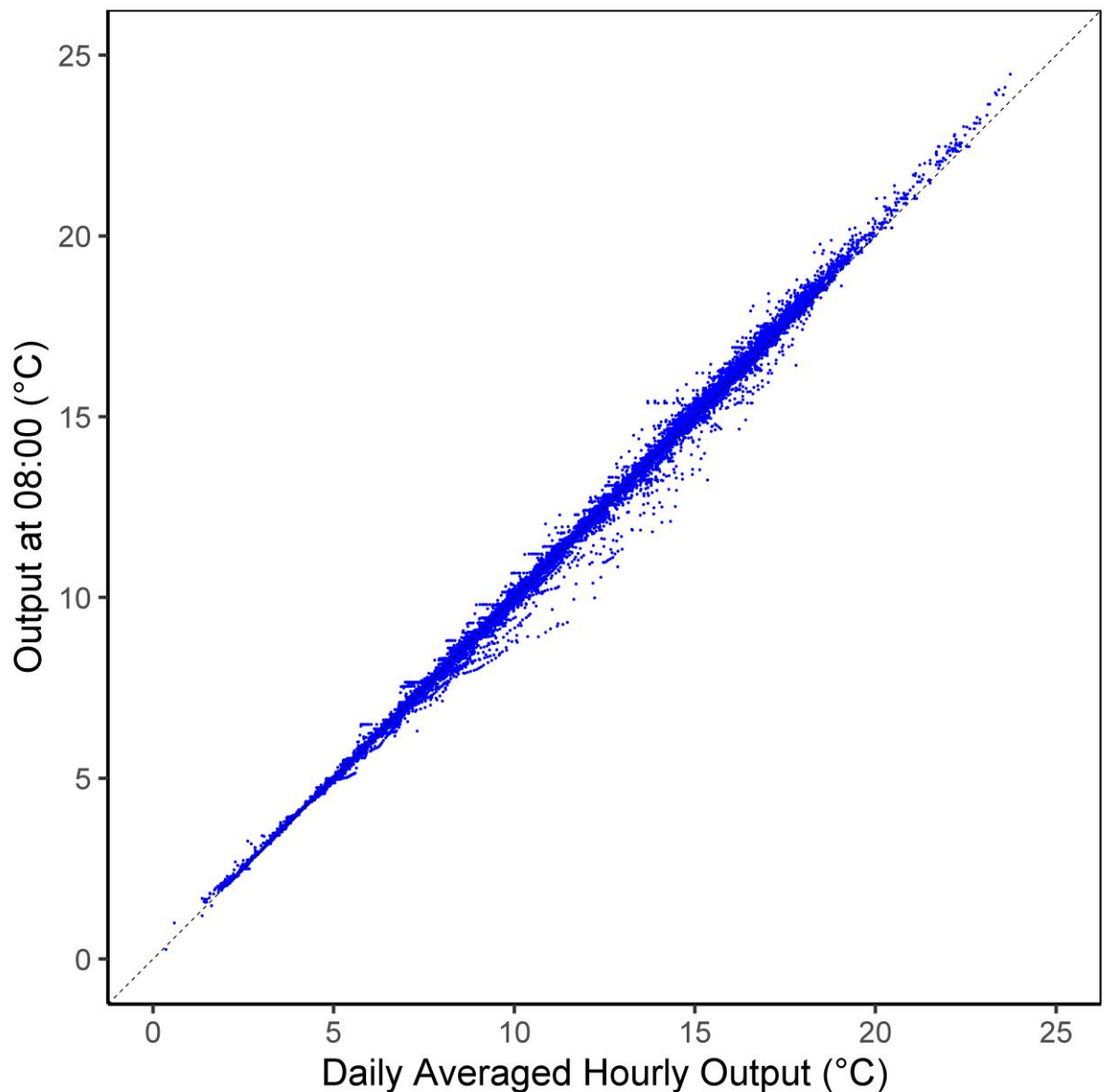


Figure 6.5 Daily averaged hourly GLM output versus output at 08:00 every day for the time period 2005-2014.

### 6.3.9. Data analysis

For each lake, the variables analysed were surface and bottom temperature, volumetrically averaged whole lake temperature, the duration, start and end of stratification, density differences between surface and bottom, and summer thermocline depth. Throughout this chapter, each of the variables were analysed as anomalies relative to the historical period of 1970 to 2005 annual and monthly mean values for each GCM.

Lake stratification was defined as when there was a density difference of greater than  $0.1 \text{ kg m}^{-3}$  between the surface and the bottom (ISIMIP, 2019). The start of stratification was defined as the first day of stratification for the longest continuous period of stratification each year, while the end was the end of that period. Thermocline depth was calculated using the calculations in the '*rLakeAnalyzer*' developed for R by Read *et al.* (2011) (R Core Team, 2020).

Model output was extracted and saved into a standardised format which has been defined by the overall ISIMIP project. NetCDF files was used as the output file type to preserve file size, allow the inclusion of metadata and facilitate easier analysis.

The overall trends for the three RCPs are described below. For comparisons across lakes, we focus solely on RCP 6.0. Similarly, when describing monthly anomalies, it is for the period 2069-2099 for RCP 6.0.

## 6.4. Results

### 6.4.1. Lake observations

Data from 46 lakes met the requirements for this simulation experiment which were that the RMSE had to be less than 2 °C and the NSE was greater than 0.5 for both models. Lakes were classified into regions according to the IPCC classification used in Seneviratne *et al.* (2012) from Giorgi and Francisco (2000). Regions and lakes are shown in Figure 6.6 and characteristics for each lake are presented in Table 6.6. The study sites were dominated by lakes in the Northern Europe region (NEU) (11), Central Europe region (CEU) (10) and Central North America region (CNA) (10). There were five lakes in the Southern Hemisphere, one in the North Australia region (NAU) and four in the South Australia region (SAU). The lakes represented a wide range of morphometry. Most of the lakes were between 10 – 90 m deep and 1 – 50 km<sup>2</sup> in area. There were five very deep lakes (depth greater than 100 m) and six very large lakes (surface area greater than 100 km<sup>2</sup>). Out of these lakes three were both very deep and very large (Table 6.6).

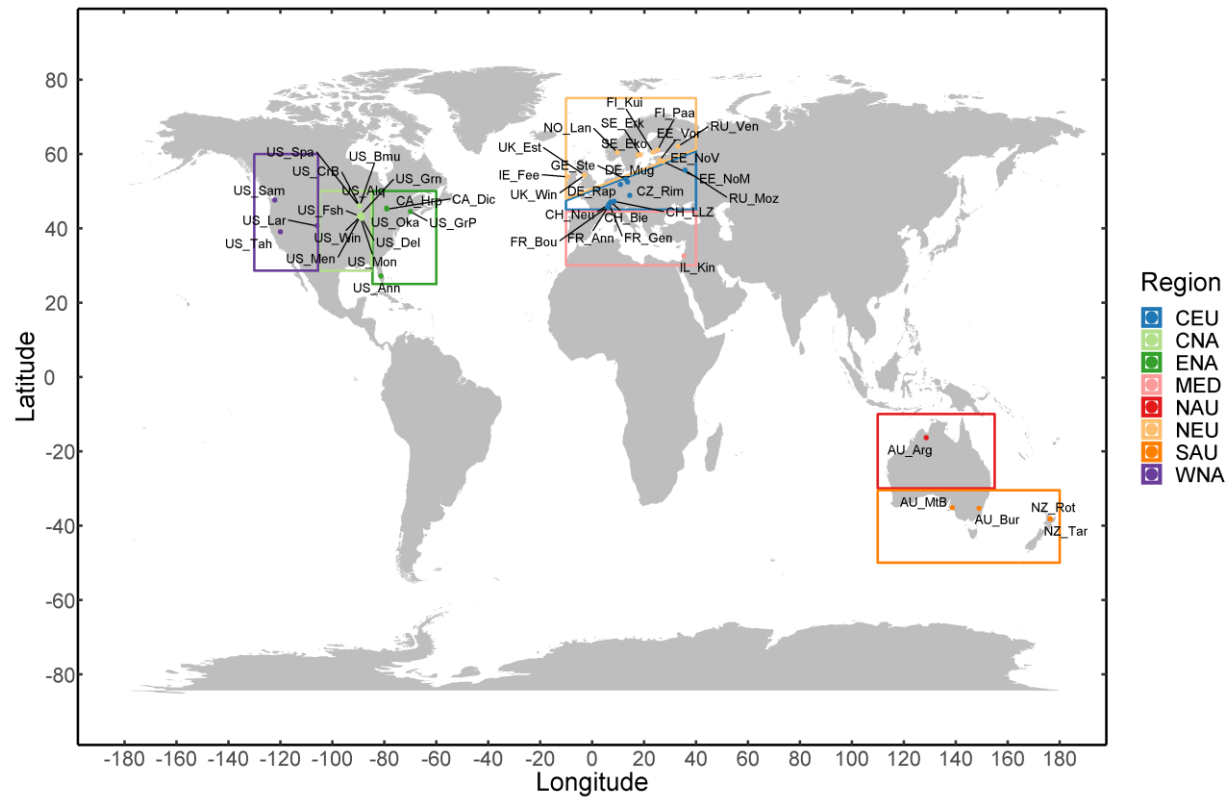


Figure 6.6 Global distribution of calibrated lakes that are included in the local study with associated shorthand labels. Regions are outlined as described in Seneviratne *et al.* (2012): CEU = Central Europe, CNA = Central North America, ENA = East North America, MED = Mediterranean, NAU = North Australia, SAU = South Australia and New Zealand, WNA = Western North America. See Table 6.6 for site reference names.

Table 6.6 Description of the location, characteristics and climates of each of the 60 sites. Lakes which did not meet the criteria for being included in this study are denoted by being in **bold** with an asterisk (\*) next to the name. The criteria were that the RMSE had to be less than 2 °C and the NSE was greater than 0.5 for both models. Regions are outlined as described in Seneviratne *et al.* (2012): CEU = Central Europe, CNA = Central North America, ENA = East North America, EAF = East Africa, MED = Mediterranean, NAU = North Australia, SAU = South Australia and New Zealand, WNA = Western North America.

ISIMIP Name	Short Name	Region	Latitude (°N)	Longitude (°W)	Elevation (m)	Area (km <sup>2</sup> )	Max depth (m)	Mean depth (m)	GLM RMSE (°C)	GOTM RMSE (°C)	GLM NSE	GOTM NSE
Allequash Lake	US_Alq	CNA	46.04	-89.62	494.00	0.58	8.00	5.53	1.43	1.75	0.96	0.91
Annecy	FR_Ann	CEU	45.87	6.17	447.00	26.51	65.00	42.53	0.66	0.64	0.98	0.98
Annie	US_Ann	ENA	27.21	-81.35	33.70	0.34	68.00	8.05	1.30	1.33	0.91	0.91
Argyle	AU_Arg	NAU	-16.31	128.68	100.00	1013.8	51.00	11.37	1.15	0.99	0.79	0.84
Biel	CH_Bie	CEU	47.08	7.16	429.00	39.30	74.00	29.57	1.45	1.30	0.90	0.92
Big Muskellunge Lake	US_Bmu	CNA	46.02	-89.61	500.00	3.87	21.30	8.18	1.57	1.48	0.94	0.93
<b>Black Oak Lake*</b>	US_Bla	CNA	46.16	-89.32	521.51	2.25	25.91	12.85	<b>3.94</b>	1.08	0.59	0.97

Bourget	FR_Bou	CEU	45.76	5.86	231.00	42.60	145.00	81.99	0.72	0.76	0.95	0.95
Burley Griffin	AU_Bur	SAU	-35.30	149.07	556.00	6.05	17.00	4.22	1.49	1.11	0.90	0.95
<b>Crystal Bog*</b>	US_CrB	CNA	46.00	-89.61	503.00	0.01	20.40	1.48	<b>3.47</b>	<b>2.93</b>	0.72	0.76
Crystal Lake	US_Cry	CNA	46.01	-89.61	502.00	0.37	2.50	11.51	1.71	1.78	0.92	0.90
Delavan	US_Del	CNA	42.61	-88.60	282.55	6.96	16.46	7.72	1.43	1.47	0.96	0.94
Dickie Lake	CA_Dic	ENA	45.15	-79.09	341.00	0.94	12.00	5.00	1.14	1.35	0.96	0.94
<b>Eagle Lake*</b>	CA_Eag	ENA	44.68	-76.70	419.00	6.86	35.00	13.69	1.69	<b>2.16</b>	0.93	0.88
Ekoln basin of Malaren	SE_Eko	NEU	59.75	17.62	0.70	20.18	50.00	16.92	1.33	1.57	0.94	0.86
Erken	SE_Erk	NEU	59.84	18.63	10.00	23.67	21.00	9.03	1.25	1.18	0.94	0.91
Esthwaite Water	UK_Est	NEU	54.37	-2.99	65.00	0.96	16.00	7.02	0.94	1.09	0.95	0.93
<b>Falling Creek Reservoir*</b>	US_Fal	ENA	37.31	-79.84	507.00	0.12	9.30	2.68	<b>4.81</b>	<b>2.36</b>	<b>0.41</b>	0.79
Feeagh	IE_Fee	NEU	53.90	-9.50	15.00	3.93	44.00	16.05	0.75	0.80	0.95	0.95
Fish Lake	US_Fsh	CNA	43.29	-89.65	261.00	0.87	18.90	5.98	1.42	1.72	0.95	0.92
Geneva	FR_Gen	CEU	46.45	6.59	372.00	580.10	309.70	156.15	0.78	0.62	0.91	0.94

Great Pond	US_GrP	ENA	44.53	-69.89	81.00	32.55	21.00	6.04	0.96	1.19	0.97	0.95
Green Lake	US_Grn	CNA	43.81	-89.00	243.00	30.12	72.00	33.83	1.20	1.03	0.96	0.97
Harp Lake	CA_Hrp	ENA	45.38	-79.13	327.00	0.71	37.50	13.33	0.94	0.69	0.96	0.98
<b>Kilpisjarvi*</b>	FI_Kil	NEU	69.03	20.77	473.00	30.83	57.00	19.67	<b>2.98</b>	<b>5.17</b>	<b>-0.05</b>	<b>-2.40</b>
Kinneret	IL_Kin	MED	32.49	35.35	-210.00	167.00	45.00	24.17	1.62	1.65	0.87	0.87
<b>Kivu*</b>	RW_Kiv	EAF	-1.73	29.24	1463.00	2488.3	485.00	221.51	0.35	0.26	<b>0.45</b>	0.61
Kuivajarvi	FI_Kui	NEU	60.47	23.51	130.00	0.64	13.20	4.87	1.40	1.36	0.95	0.92
Langtjern	NO_Lan	NEU	60.37	9.73	510.00	0.06	12.00	3.02	1.38	1.59	0.86	0.83
Laramie Lake	US_Lar	WNA	40.62	-105.8	2843.80	0.14	6.40	2.19	1.05	0.51	0.91	0.98
Lower Zurich	CH_LLZ	CEU	47.28	8.58	406.00	66.60	136.00	50.14	1.09	0.73	0.95	0.98
Mendota	US_Men	CNA	43.10	-89.41	259.00	39.40	25.30	12.44	1.39	1.39	0.95	0.94
Monona	US_Mon	CNA	43.06	-89.36	258.00	13.67	22.50	8.24	1.42	1.43	0.95	0.93
Mozhaysk	RU_Moz	CEU	55.59	35.82	183.00	23.67	23.00	9.03	1.39	1.06	0.87	0.92
Mt Bold	AU_MtB	SAU	-35.12	138.71	242.90	3.22	45.40	13.74	1.68	1.59	0.81	0.83
Mueggelsee	DE_Mug	CEU	52.43	13.65	32.30	7.66	7.70	4.77	0.75	0.63	0.99	0.99

Neuchatel	CH_Neu	CEU	46.54	6.52	429.00	217.90	152.00	63.29	1.32	1.07	0.92	0.95
Nohipalo Mustjarv	EE_NoM	NEU	57.93	27.34	61.00	0.21	8.90	4.06	1.56	1.23	0.93	0.95
Nohipalo Valgejarv	EE_NoV	NEU	57.94	27.35	62.00	0.07	12.50	4.75	1.31	1.77	0.95	0.92
Okauchee Lake	US_Oka	CNA	43.13	-88.43	269.00	4.63	28.65	13.69	1.35	1.67	0.96	0.94
Paajarvi	FI_Pää	NEU	61.07	25.13	102.00	13.44	85.00	14.90	1.23	0.92	0.91	0.95
Rappbode Reservoir	DE_Rap	CEU	51.74	10.89	415.00	4.34	89.00	25.14	0.61	0.54	0.97	0.98
Rimov	CZ_Rim	CEU	48.85	14.49	471.48	2.11	44.00	16.02	1.70	1.59	0.89	0.89
Rotorua	NZ_Rot	SAU	-38.08	176.28	280.00	79.31	52.90	10.36	0.75	0.72	0.97	0.97
Sammamish	US_Sam	WNA	47.59	-122.1	9.00	20.00	32.00	17.43	0.74	0.82	0.99	0.96
<b>Sau Reservoir*</b>	ES_Sau	MED	41.97	2.40	425.00	6.00	65.00	27.49	<b>2.99</b>	<b>2.46</b>	0.69	0.79
Sparkling Lake	US_Spa	CNA	46.01	-89.70	495.00	0.58	20.00	11.03	1.25	1.27	0.97	0.96
Stechlin	GE_Ste	CEU	53.17	13.03	59.80	4.23	69.50	23.52	0.91	0.84	0.97	0.98
<b>Sunapee*</b>	US_Sun	ENA	43.23	-72.50	333.00	16.93	34.00	12.24	<b>2.50</b>	1.26	0.87	0.94
Tahoe	US_Tah	WNA	39.09	-120.0	1897.00	465.97	501.00	339.40	0.49	0.48	0.94	0.94

Tarawera	NZ_Tar	SAU	-38.21	176.43	300.00	40.97	87.50	55.93	0.65	0.59	0.92	0.94
<b>Toolik Lake*</b>	US_Too	ALA	68.63	-149.6	720.00	1.49	26.00	7.36	<b>3.76</b>	1.31	<b>-0.14</b>	0.83
<b>Trout Bog*</b>	US_TrB	CNA	46.04	-89.69	499.00	0.01	7.90	6.10	1.60	<b>2.40</b>	0.93	0.85
<b>Trout Lake*</b>	US_Tro	CNA	46.03	-89.67	492.00	160.79	35.70	15.09	<b>2.07</b>	1.66	0.86	0.91
<b>Two Sisters Lake*</b>	US_Two	CNA	45.77	-89.53	481.00	2.83	19.20	9.82	<b>3.12</b>	1.36	0.67	0.94
Vendyurskoe	RU_Ven	NEU	62.10	33.10	131.00	10.40	13.40	5.36	1.30	1.19	0.96	0.94
Vortsjarv	EE_Vor	NEU	58.31	26.01	33.00	270.60	6.10	2.79	1.33	0.98	0.97	0.97
<b>Washington*</b>	US_Was	WNA	47.64	- 122.27	5.00	87.62	65.20	33.03	<b>4.39</b>	0.82	<b>-0.17</b>	0.96
Windermere	UK_Win	NEU	54.31	-2.95	39.00	6.72	64.00	16.78	0.86	0.65	0.95	0.97
Wingra	US_Win	CNA	43.05	-89.43	259.00	1.40	6.70	2.09	1.39	1.53	0.96	0.94

---

Based on observed historical data, all lakes in NEU experienced annual variations in water temperature of 0 – 24 °C and all had ice cover during winter except for the three lakes which are strongly influenced by the Atlantic Ocean (UK\_Est, IE\_Fee, and UK\_Est). There were three lakes in sub-tropical areas IL\_Kin in MED, US\_Ann in ENA and AU\_Arg which all had annual water temperature variations of 14 – 32 °C. Lakes in CNA had a slightly larger range in temperatures (0 – 26 °C) compared with lakes in CEU and NEU (0 – 22 °C). The sites in NAU had a small range with higher observed temperatures (22 – 30 °C), while sites in SAU was at a slightly lower range (10-26 °C) (Figure 6.7). Most lakes in NEU and CEU had very low surface temperature during winter (less than 4 °C), except for the lakes in the western NEU (IE\_Fee, UK\_Win and UK\_Est) and the deep alpine lakes (depth greater than 50 m) in CEU (FR\_Ann, CH\_Bie, FR\_Bou, FR\_Gen, CH\_LLZ) which had slightly warmer surface temperatures from December through to March (6 to 10 °C).

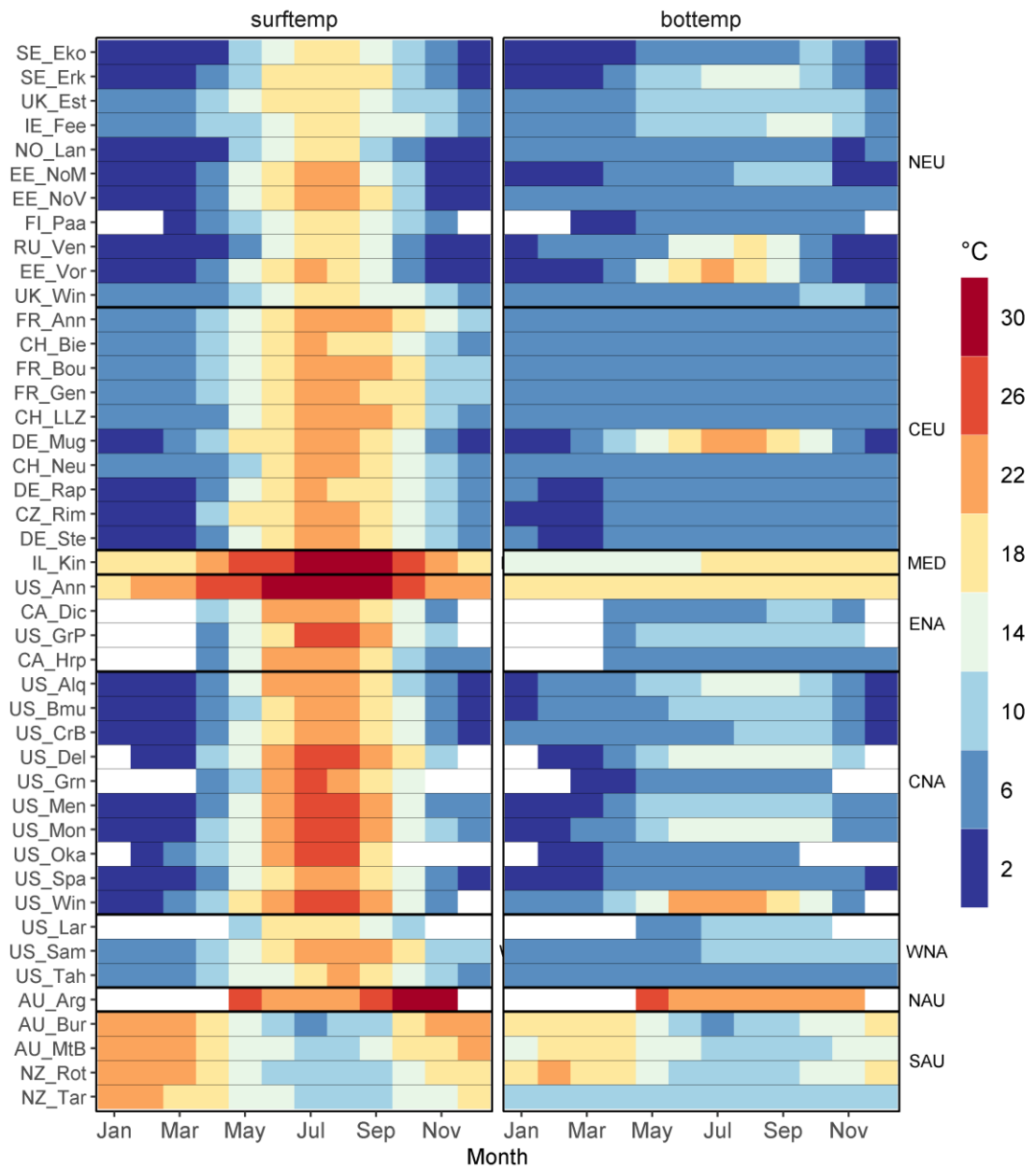


Figure 6.7 Mean observed surface (surftemp) and bottom temperature (bottemp) for 46 calibrated lakes. Sites are ordered according to regions with labels on the right side, separated by a bold line. White blocks indicate no recorded data from that period. See Table 6.6 for site reference names.

Two of the lakes in sub-tropical areas (IL\_Kin and US\_Ann) had the largest observed density difference ( $-3.5 \text{ kg m}^{-3}$ ) between surface and bottom temperatures and the longest period of strong density differences ( $>200$  days) (Figure 6.8). Some of the shallower and polymictic lakes, EE\_Vor, DE\_Mug, US\_Win, had small ( $-0.5 \text{ kg m}^{-3}$ ) to no density differences between surface and bottom, indicating that they did not

continuously stratify during the year. A known monomictic lake, IE\_Fee, also had a very low-density difference between top and bottom indicating that it stratified very weakly in comparison to other sites.

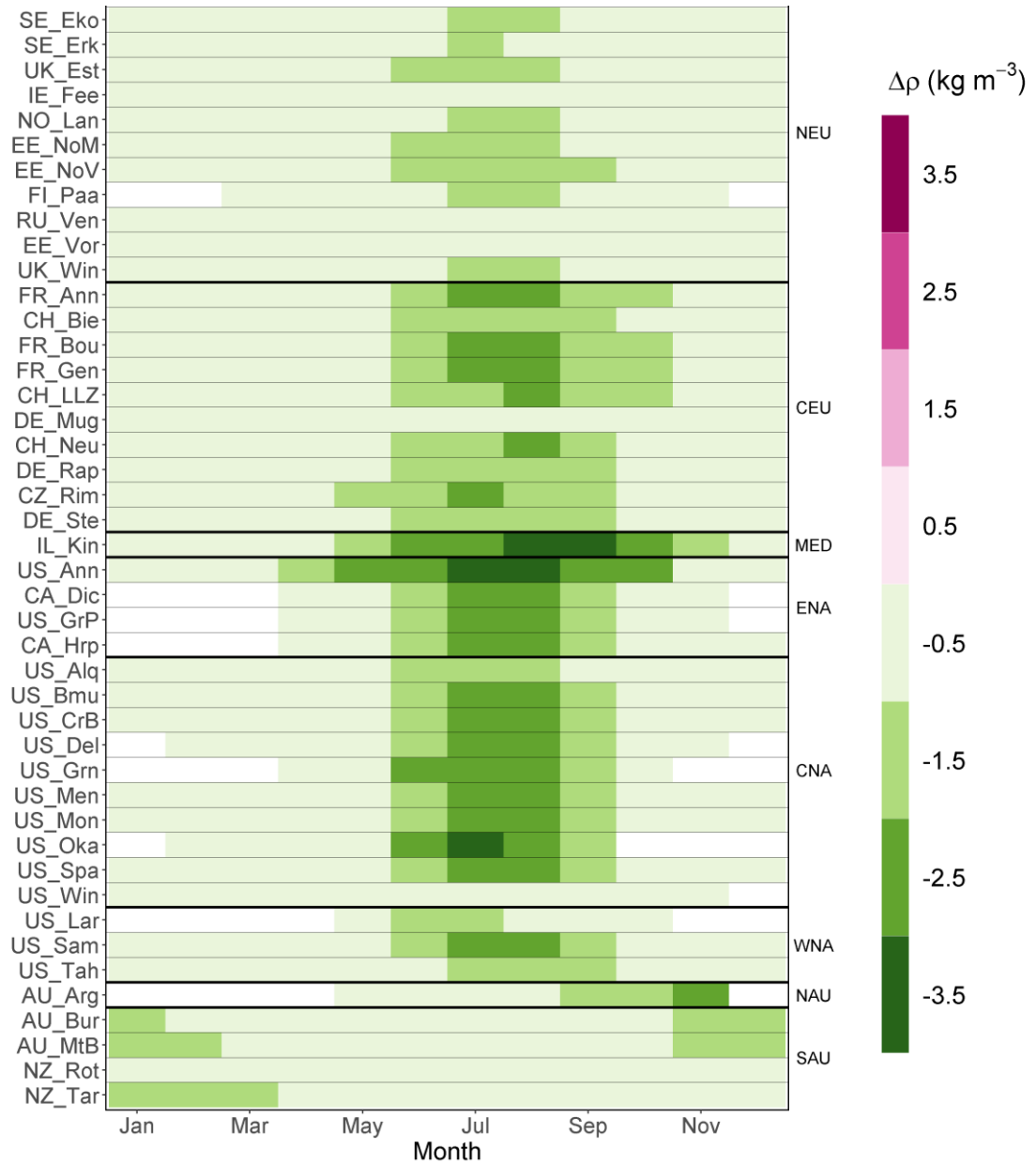


Figure 6.8 Monthly mean observed density difference between surface and bottom for 46 calibrated lakes. Sites are ordered according to regions with labels on the right side, separated by a bold line. White blocks indicate no recorded data from that period. See Table 6.6 for site reference names.

### 6.4.2. Calibration results

Following calibration, 77 % of the lakes (46/60) had a RMSE below the threshold of 2 °C and a Nash-Sutcliffe efficiency greater than 0.5 for both GOTM and GLM (Figure 6.9; Table 6.6). Possible reasons for some lakes not meeting the calibration threshold criteria were because they had large lake level fluctuations (e.g. US\_FCR, ES\_Sau and US\_TrB), highly irregular morphometry (e.g. CA\_Eag), or were meromictic (e.g. RW\_Kiv). For some lakes (e.g. US\_Too) the reasons for poor calibration were unclear.

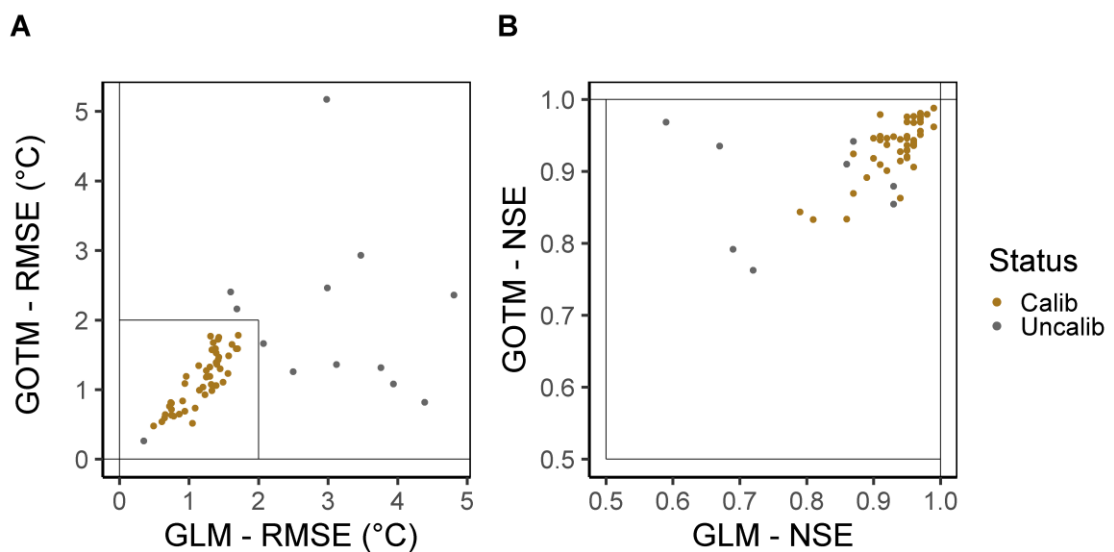


Figure 6.9 Root mean square error (RMSE) results from calibration of the General Ocean Turbulence Model (GOTM) and the General Lake Model (GLM) (A). Nash-Sutcliffe Efficiency (NSE) results from calibration of the General Ocean Turbulence Model (GOTM) and the General Lake Model (GLM) (B). Lakes with a RMSE greater than 2 and NSE less than 0.5 are coloured grey and referred to as uncalibrated (Uncalib). See Table 6.6 for values corresponding to each site.

Two common parameters which were calibrated in both models were wind scaling factor and the light extinction coefficient ( $K_w$ ). The log transform of  $K_w$  had a relatively strong correlation between both models (0.62) while the wind scaling factor had a weak correlation (0.32) (Figure 6.10).

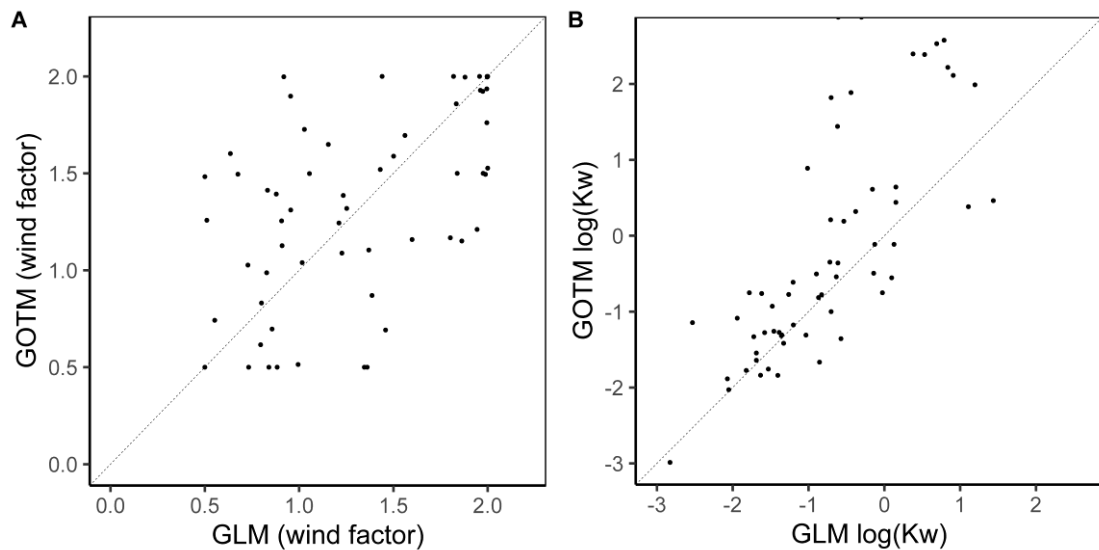


Figure 6.10 Calibrated values for wind scaling factor (A) and light attenuation (Kw) (B), the two common parameters which were calibrated for the two lake models: GLM and GOTM. Kw values have been log transformed. Dashed line is the 1:1. See Table 6.6 for actual values.

#### 6.4.3. GCM projections

Annual mean air temperature anomalies across all sites displayed an unequivocal increase for RCP 6.0 for the period 2006 – 2099 relative to the historical anomaly which was calculated from 1970-2005 (Figure 6.11). There were strong regional coherencies for regions where sites are relatively close together such as Northern Europe (NEU) (EE\_Vor, EE\_NoM, EE\_NoV, FI\_Kui, SE\_Erk, FI\_Paa, SE\_Eko), which were projected to warm by +3 to +5 °C (SD: 1 - 3 °C; n=1460) by 2069-2099. The western sites in NEU (UK\_Est, IE\_Fee and UK\_Win) had a smaller projected increase by the same time period of +1 to +3 °C (SD: 1 °C). Central Europe (CEU) (DE\_Rap, DE\_Ste, DE\_Mug, CH\_BIE, FR\_Ann, CH\_LLZ, CH\_Neu, FR\_Bou, FR\_Gen) had a positive increase of +3 to +4 °C (SD: 1 °C), while Eastern North America (ENA) and Central North America (CNA) followed a similar pattern but had a larger increase of +4 to +6 °C (SD: 1 – 2 °C). Lakes in the NAU had a slightly warmer increase of +3 to +5 °C (SD: 1 °C) compared to those in SAU, which had an increase of +2 to +4 °C (SD: 1 °C). The variation between GCMs was below 1 °C throughout the entire period for all lakes except for a few years.

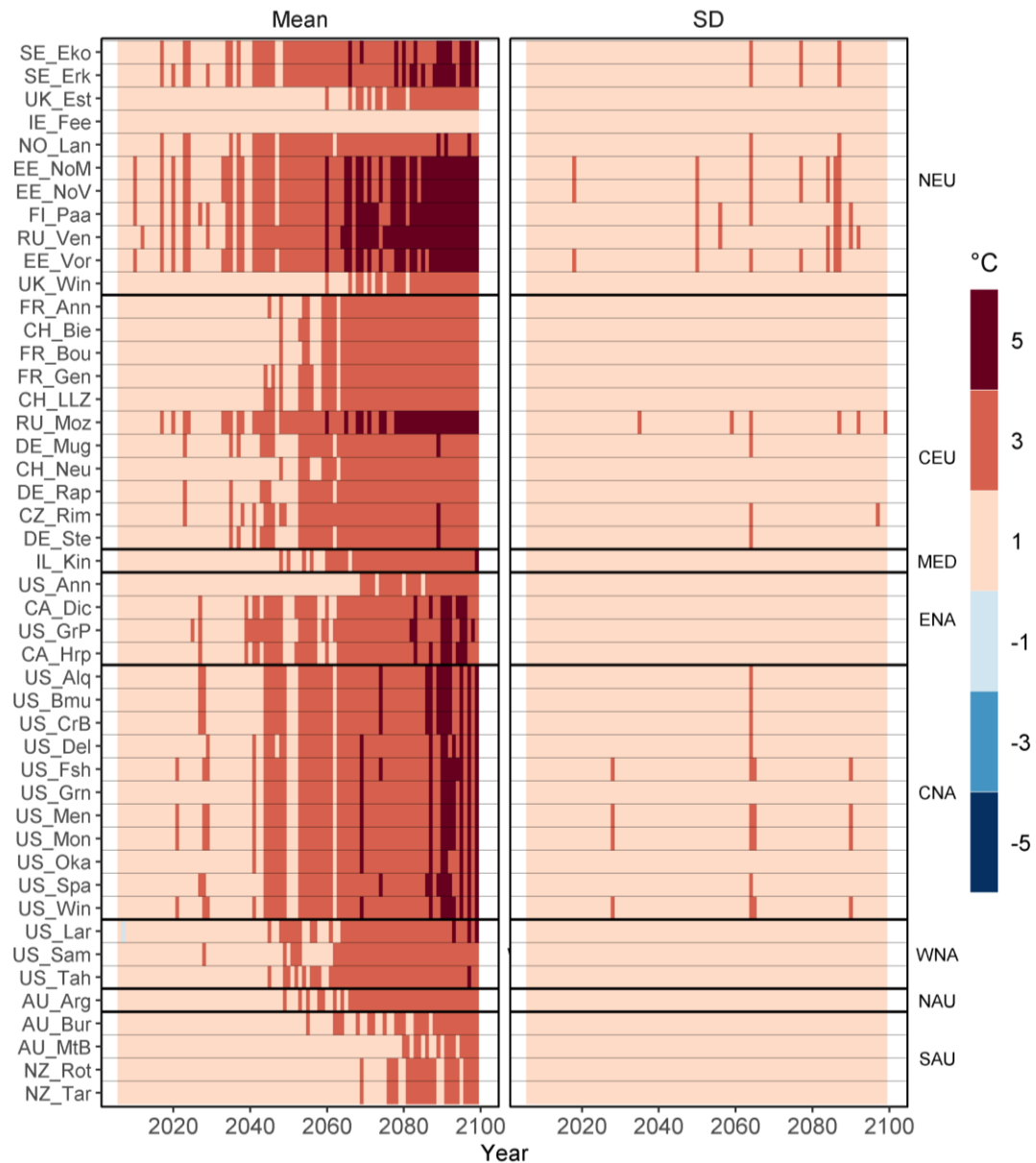


Figure 6.11 Mean and standard deviation (SD) of the annual anomaly for air temperature for 46 lakes across four GCMs for RCP 6.0 for the time period 2006 – 2099 (n =1460). Sites are ordered according to regions with labels on the right side, separated by a bold line. See Table 6.6 for site reference names.

Mean annual wind speed anomalies were more variable within regions compared to air temperature from 2006 – 2099 (Figure 6.12). There was a strong coherence among some of the NEU sites (EE\_Vor, EE\_NoM, EE\_NoV, FI\_Kui) which had a projected increase in wind speed by 2069-2099 from +0.2 to +0.6 m s<sup>-1</sup> but with large variability (SD: 0.7 to 1.1 m s<sup>-1</sup>; n =1460). Site RU\_Moz in CEU had a strong decrease in the wind speed throughout the entire time period 2006-2099, with a mean anomaly which ranged

from  $-0.1$  to  $-0.4 \text{ m s}^{-1}$  with a SD of  $0.1 - 0.5 \text{ m s}^{-1}$ . The western sites in NEU (UK\_Est, IE\_Fee and UK\_Win) all had slight decreases in wind speed by 2069-2099 with mean anomalies that ranged from of  $-0.1$  to  $-0.4 \text{ m s}^{-1}$  (SD:  $0.7$  to  $1.1 \text{ m s}^{-1}$ ). In the CEU region, there was a slight increase in wind speeds of  $+0.1$  to  $+0.3 \text{ m s}^{-1}$  (SD:  $0.1$  to  $0.3 \text{ m s}^{-1}$ ). Wind speed showed a coherent decrease in projected values across sites in ENA (US\_Win, US\_Fsh, US\_Del, US\_Mon, US\_Men, US\_Oka, US\_Grn) by the later period of 2069-2099, with mean decreases of  $-0.1$  to  $-0.2 \text{ m s}^{-1}$  (SD:  $0.1 - 0.3 \text{ m s}^{-1}$ ). Sites further north in ENA (CA\_Dic and CA\_Hrp) had a slight projected increase in wind speed by 2069-2099 of  $+0.1$  to  $+0.3 \text{ m s}^{-1}$  (SD:  $0.1 - 0.5 \text{ m s}^{-1}$ ). In the CNA region, there was a regional decrease in wind speed by 2069- 2099 of  $-0.1$  to  $-0.2 \text{ m s}^{-1}$  (SD:  $0.1 - 0.3 \text{ m s}^{-1}$ ).

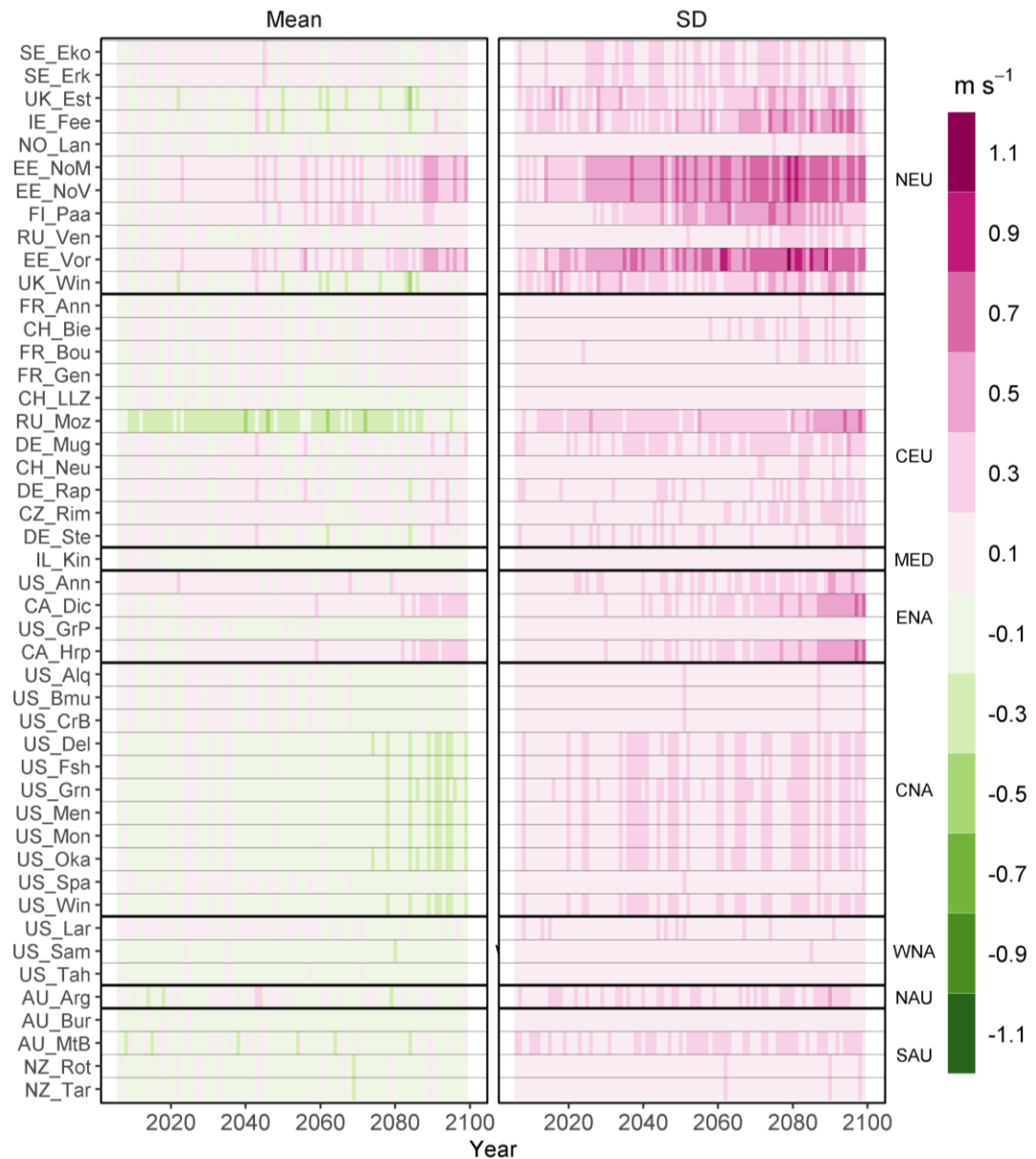


Figure 6.12 Mean and standard deviation (SD) of the annual anomaly for wind speed for 46 lakes across four GCMs for RCP 6.0 for the time period 2006 – 2099 (n =1460). Sites are ordered according to regions with labels on the right side, separated by a bold line. See Table 6.6 for site reference names.

Mean annual short-wave radiation was projected to increase across all sites except for one site, AU\_Arg in Northern Australia (NAU) of -4 to +4 W m<sup>-2</sup> (SD: 4 – 12 W m<sup>-2</sup>; n =1460) (Figure 6.13). Sites in NEU and CEU showed the largest projected increase by 2050 of +4 to +20 W m<sup>-2</sup> (SD: 4 – 12 W m<sup>-2</sup>). Sites in CEU had the largest increase by 2069-2099 which ranged from +12 to +20 W m<sup>-2</sup> (SD: 4 – 12 W m<sup>-2</sup>). Sites

across ENA, CNA and WNA had a more gradual increase and smaller magnitude by 2069-2099 of +4 to +12 W m<sup>-2</sup> (SD: 4 – 12 W m<sup>-2</sup>).

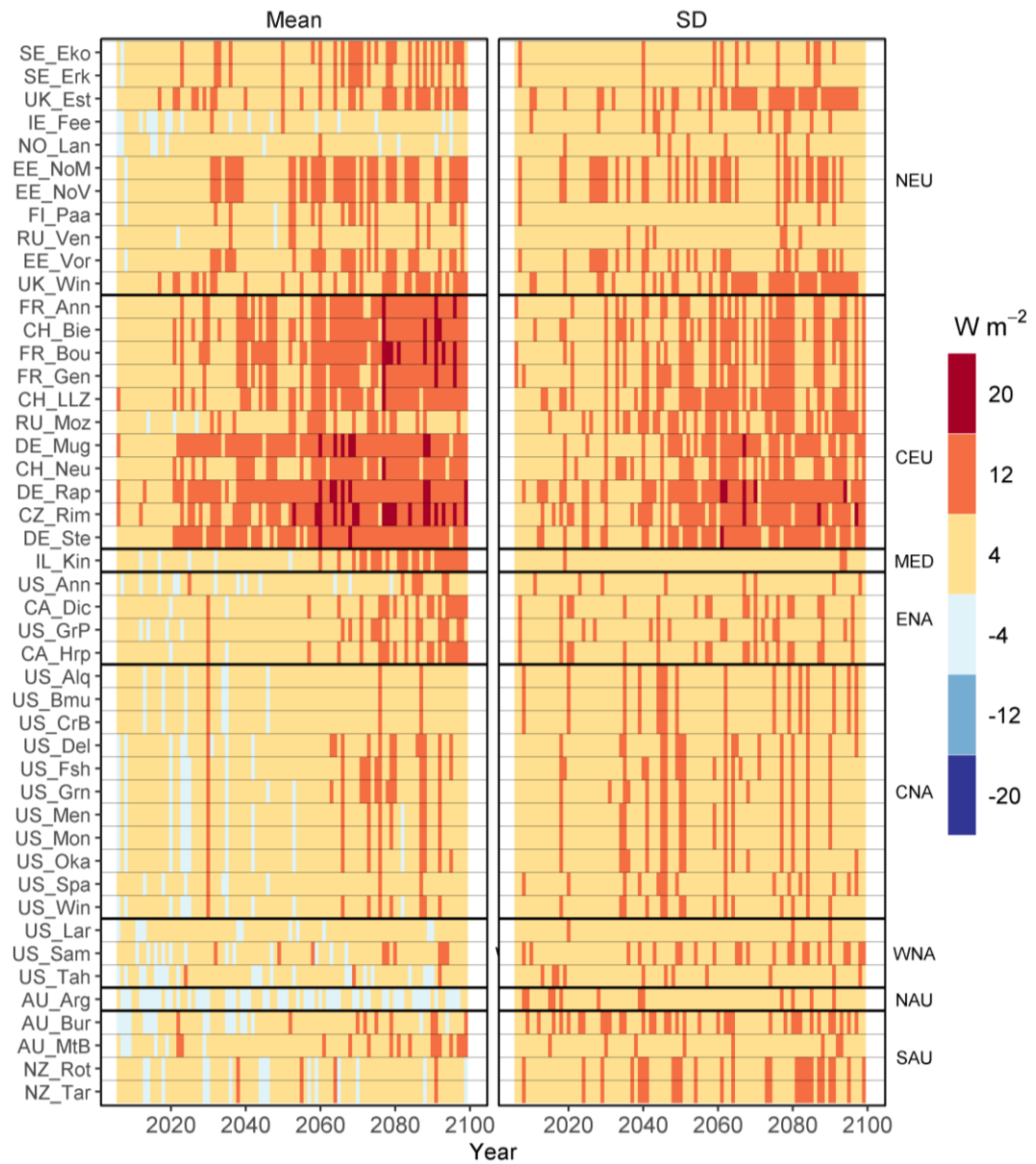


Figure 6.13 Mean and standard deviation (SD) of the annual anomaly for short-wave radiation for 46 lakes across four GCMs for RCP 6.0 for the time period 2006 – 2099 (n =1460). Sites are ordered according to regions with labels on the right side, separated by a bold line. See Table 6.6 for site reference names.

The mean monthly anomalies for 2069-2099 showed a general regional coherence for air temperature (Figure 6.14). Site RU\_Ven in the NEU region had the largest projected anomaly for mean monthly air temperature anomaly from November through February of +5 to +7 °C (SD: 1 – 2 °C; n=3600). The sites in western NEU

(UK\_Est, IE\_Fee, UK\_Win) had a smaller magnitude in the range of anomalies of +3 to +4 °C (SD: 1 – 2 °C). Site in CEU had the largest anomaly for the month of August (FR\_Ann, CH\_Bie, FR\_Bou, FR\_Gen) of +5 °C (SD: 2 °C), with a higher anomaly in June to September across all sites of +5 °C (SD: 2 °C). The ENA region has a larger anomaly of +5 °C in the months of January, February, August and September, while it was +4 °C (SD: 2 °C) in that same region for the other months. Sites in NAU and SAU had a smaller projected anomaly for air temperature generally, but with a larger anomaly in summer November through March of +3 °C (SD: 1 °C) compared to winter which was +2 °C (SD: 1-2 °C).

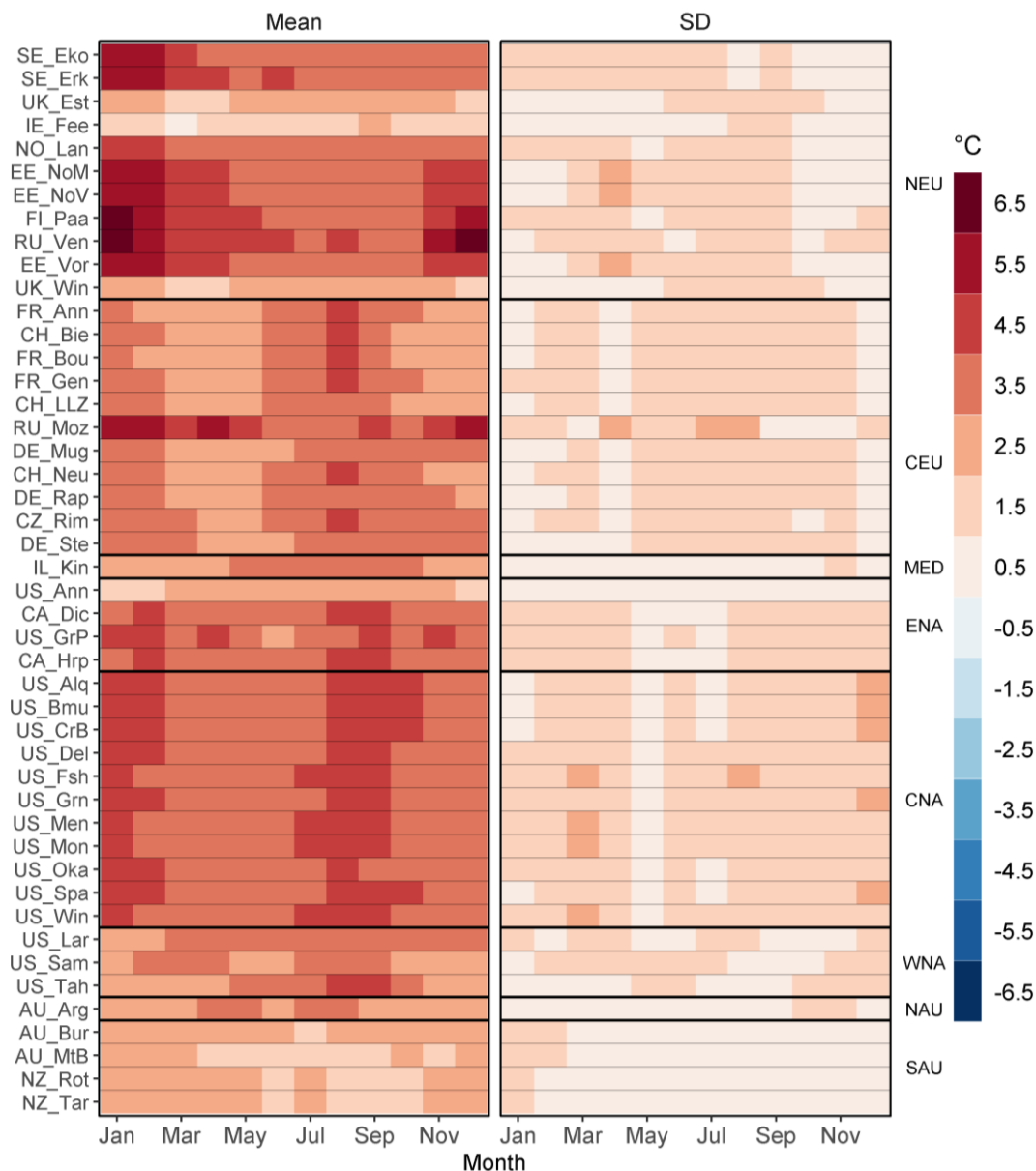


Figure 6.14. Mean and standard deviation (SD) of the monthly anomaly for air temperature, for 46 lakes across four GCMs for RCP 6.0 for the time period 2069-2099 (n=3600). Sites are ordered according to regions with labels on the right side, separated by a bold line. See Table 6.6 for site reference names.

The projected mean monthly wind speed anomaly was negative in March, April and May for sites in the western NEU, with values of  $-0.2$  to  $-0.1$   $\text{m s}^{-1}$  (SD:  $0.1 - 0.5$   $\text{m s}^{-1}$ ; n=3600) (Figure 6.15). In the CNA region, there were coherent decreases in projected windspeeds across seven of the sites, ranging from  $-0.3$  to  $-0.1$   $\text{m s}^{-1}$  (SD:  $0.1 - 0.3$   $\text{m s}^{-1}$ ) from March to November, with values in the month of June having the largest decrease of  $-0.3$   $\text{m s}^{-1}$  (SD:  $0.1$   $\text{m s}^{-1}$ ). The three sites in Estonia (EE\_NoM, EE\_NoV and EE\_Vor)

had the same mean monthly anomaly for September through February of  $+0.1$  to  $+0.3$   $\text{m s}^{-1}$  (SD:  $0.5 - 0.9$   $\text{m s}^{-1}$ ).

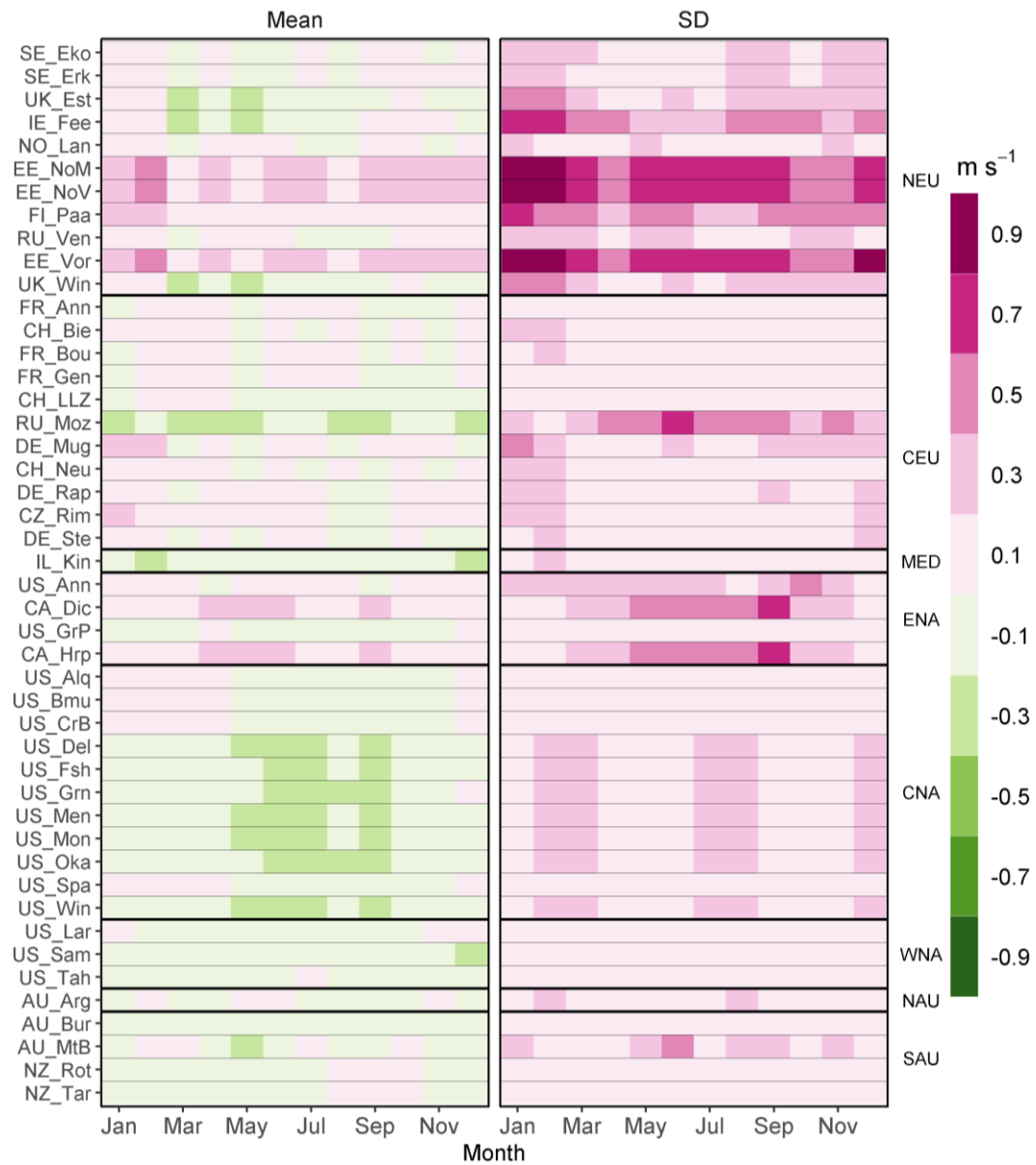


Figure 6.15 Mean and standard deviation (SD) of the monthly anomaly for wind speed for 46 lakes across four GCMs for RCP 6.0 for the time period 2069-2099 ( $n=3600$ ). Sites are ordered according to regions with labels on the right side, separated by a bold line. See Table 6.6 for site reference names.

Sites in CEU had a relatively large increase in the monthly mean SWR anomaly particularly in June, July and August of  $+25$  to  $+35$   $\text{W m}^{-2}$  (SD:  $5 - 25$   $\text{W m}^{-2}$ ;  $n=3600$ ) (Figure 6.16). These months showed increases for each of the sites in the Northern Hemisphere  $+10$  to  $+35$   $\text{W m}^{-2}$  (SD:  $5 - 25$   $\text{W m}^{-2}$ ) except for the two sub-tropical lakes

IL\_Kin and US\_Ann. Each had smaller increases in February through May of +10 to +20  $\text{W m}^{-2}$  (SD: 5 – 15  $\text{W m}^{-2}$ ). IE\_Fee and NO\_Lan had much smaller increases throughout the entire year of +5 to +10  $\text{W m}^{-2}$  (SD: 5 – 15  $\text{W m}^{-2}$ ). The sites in NAU and SAU had small increases of +5 to +15  $\text{W m}^{-2}$  (SD: 5 – 15  $\text{W m}^{-2}$ ) throughout the whole year.

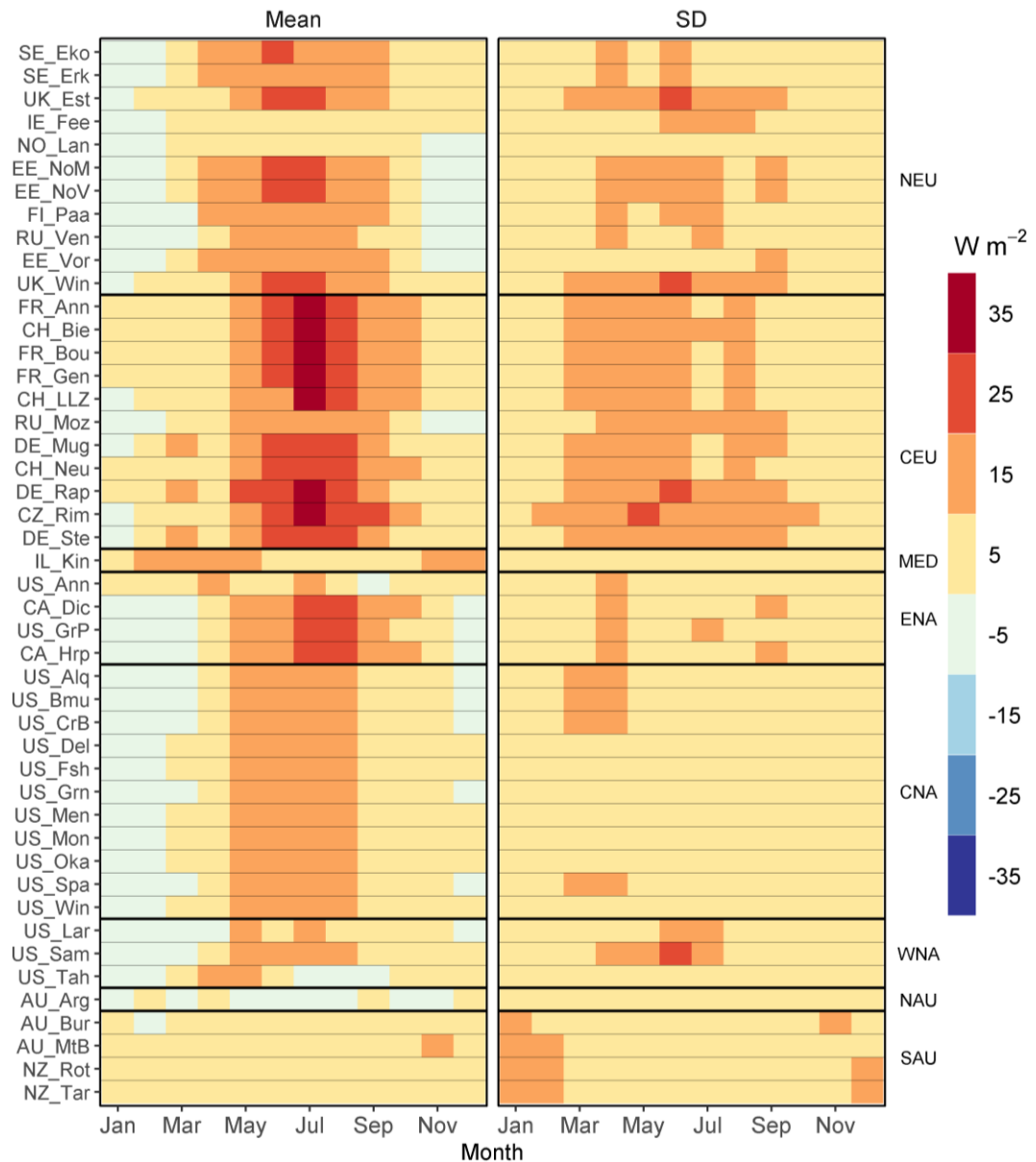


Figure 6.16 Mean and standard deviation (SD) of the monthly anomaly for short-wave radiation for 46 lakes across four GCMs for RCP 6.0 for the time period 2069-2099 (n=3600). Sites are ordered according to regions with labels on the right side, separated by a bold line. See Table 6.6 for site reference names.

#### 6.4.4. Overall simulations

Overall there was an increase in the mean annual lake surface water temperature anomaly under each of the RCP scenarios averaged across all lakes, with the simulations using RCP 8.5 having the largest increase by 2099 (overall mean anomaly for all sites of +4.5 °C; n=134320) (Figure 6.17). The anomaly was calculated relative to the 1970-2005 historical period. These RCP 8.5 simulations also had the largest degree of variability when all 46 sites were included (SD: 1.8 °C). The simulations using RCP 2.6 and RCP 6.0 followed similar increases until 2050 (+1.3 °C). After 2050, the projected increase for the RCP 2.6 simulations levelled off before decreasing slightly towards the 2069-2099 (mean anomaly +1.6 °C) while RCP 6.0 continued to increase at a relatively constant rate with a mean anomaly of +2.7 °C by 2099.

The increase in projected mean annual bottom lake water temperature was not as large when compared to the surface temperature (RCP 2.6: +0.6 °C; RCP 6.0: +1 °C; RCP 8.5: +2 °C) (Figure 6.17). Simulations using RCP 2.6 and RCP 6.0 also diverged from each other later (~2060) than those for the surface temperature. There was also a much larger variability in the anomalies for the mean lake bottom temperature across the 46 sites, likely reflecting the differences in depth across the study sites (RCP 2.6: +0.8 °C; RCP 6.0: +1.0 °C; RCP 8.5: +1.4 °C), than was observed for the surface temperature (RCP 2.6: +1.0 °C; RCP 6.0: +0.9 °C; RCP 8.5: +1.5 °C).

Volumetrically averaged lake temperature follows a similar upward trajectory, but the increase was not as steep as the surface temperature, with a lower projected mean anomaly by 2099 (RCP 2.6: +1.3 °C; RCP 6.0: +2.0 °C; RCP 8.5: +3.4 °C) (Figure 6.17). The standard deviation was all within the positive anomaly, signifying that under all scenarios there would be an increase in water temperature and in most lakes.

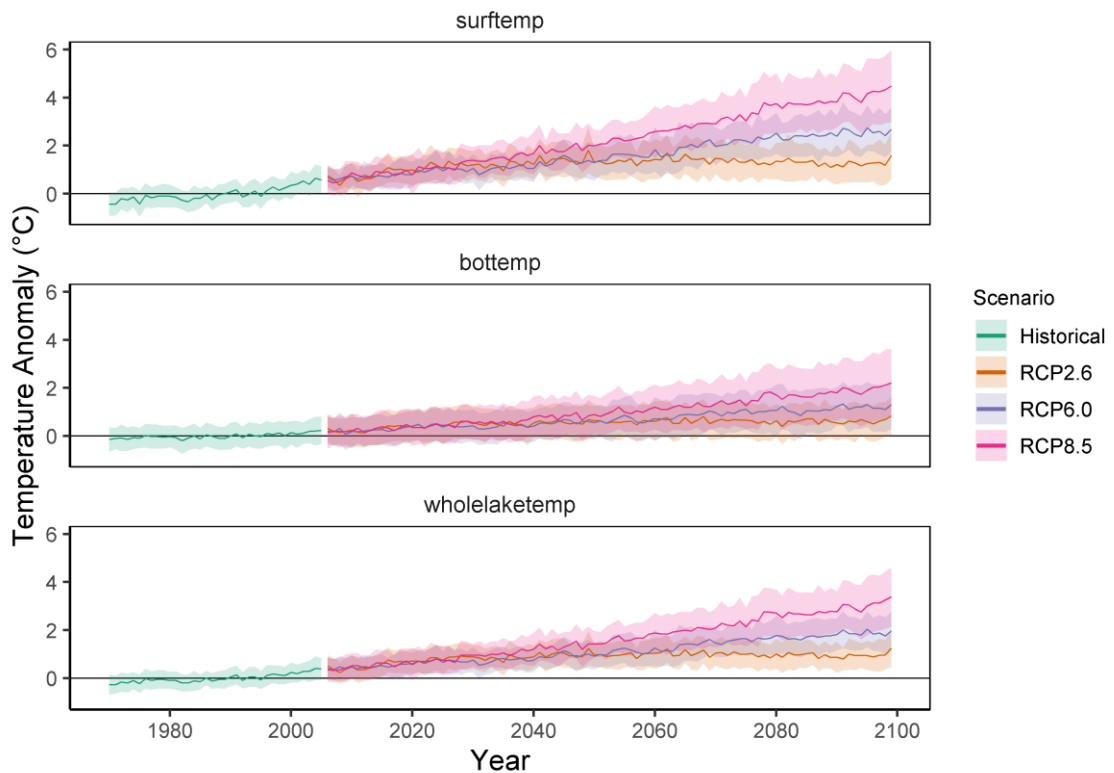


Figure 6.17 Mean surface (surftemp), bottom (bottemp) and volumetrically averaged lake temperature (wholelaketemp) anomaly across 46 lakes, four GCMs and two lake models ( $n=134320$ ), under the historical, RCP 2.6, RCP 6.0 and RCP 8.5 scenarios from 1970-2100. Shaded areas represent one standard deviation from the mean.

The mean number of stratified days for the 46 lakes was projected to increase at a relatively consistent rate until 2040 for each of the three emissions scenarios (+5 to +15 days;  $n=368$ ) (Figure 6.18). Following this, the number of stratified days increased at a higher rate for RCP 8.5 compared to either of the other scenarios (RCP 2.6: +10 days; RCP 6.0: +22 days; RCP 8.5: +35 days). Stratified days for the RCP 2.6 and RCP 6.0 simulations continued to follow a similar trajectory until ~2065 at +14 days. After this period the number of days for the RCP 2.6 simulations declined while in contrast, for the RCP 6.0 the projections for the mean number of days stratified continued to increase.

There was large variability around the mean values for each of the scenarios until 2050 (SD: 20 days) which increased further towards the 2069-2099 period particularly for the simulations using RCP 8.5 (SD: 30 days) (Figure 6.18). This observed increase in the number of stratified days was driven by both a projected earlier start of stratification and a later end of stratification. There was a larger shift to an earlier timing

for onset of stratification by the period 2069-2099, with a mean anomaly for RCP 8.5 of -15 days. The mean timing of the offset of stratification was projected to be later by +8 days. There was also a larger variation around the onset of stratification (SD: 25 to 30 days) compared to offset (SD: 15 to 25 days).

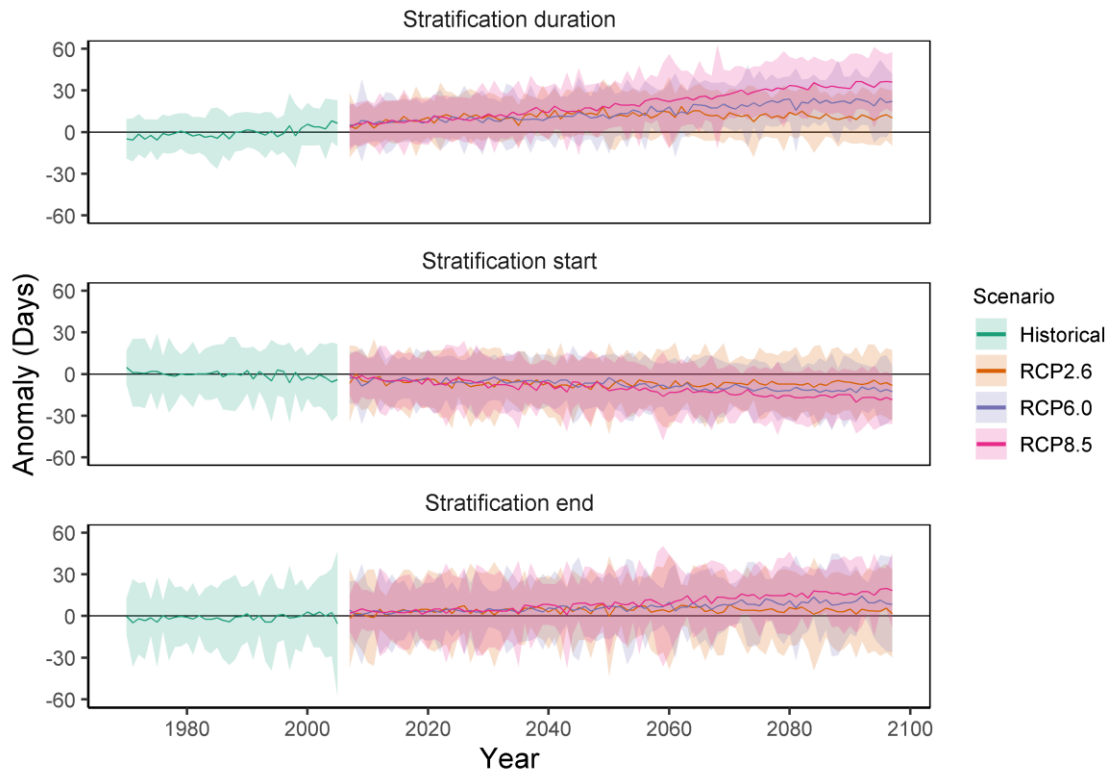


Figure 6.18 Mean anomaly of the duration, start and end of stratification each year across 46 lakes, four GCMs and two lake models (n=368) under the historical, RCP 2.6, RCP 6.0 and RCP 8.5 scenarios from 1970 to 2100. Shaded errors represent one standard deviation from the mean.

#### 6.4.5. Lake simulations

For the simulations using RCP 6.0, there were unambiguous projected warming of water temperatures across all sites studied, strongest for the surface temperatures (Figure 6.19). Surface temperatures increased by between +0.5 and +1.5 °C (SD: 0.5 – 1.5 °C; n=2920) by 2050 and continuing to increase up to a range of +2.5 to +3.5 °C (SD: 1.5 – 1.5 °C) by 2069-2099. However, there were some sites which did not show the same rate of

projected increase, such as IE\_Fee, NO\_Lan, US\_Ann, US\_Lar and AU\_MtB with increases of +0.5 to +1.5 °C (SD: 0.5 – 1.5 °C) by 2069-2099 (Figure 6.19). The highest increases were in CEU and CNA with increases of +1.5 to +3.5 °C (SD: 0.5 – 1.5 °C) with one site, US\_Oka having an increase of +1.5 to +3.5 °C (SD: 0.5 – 1.5 °C).

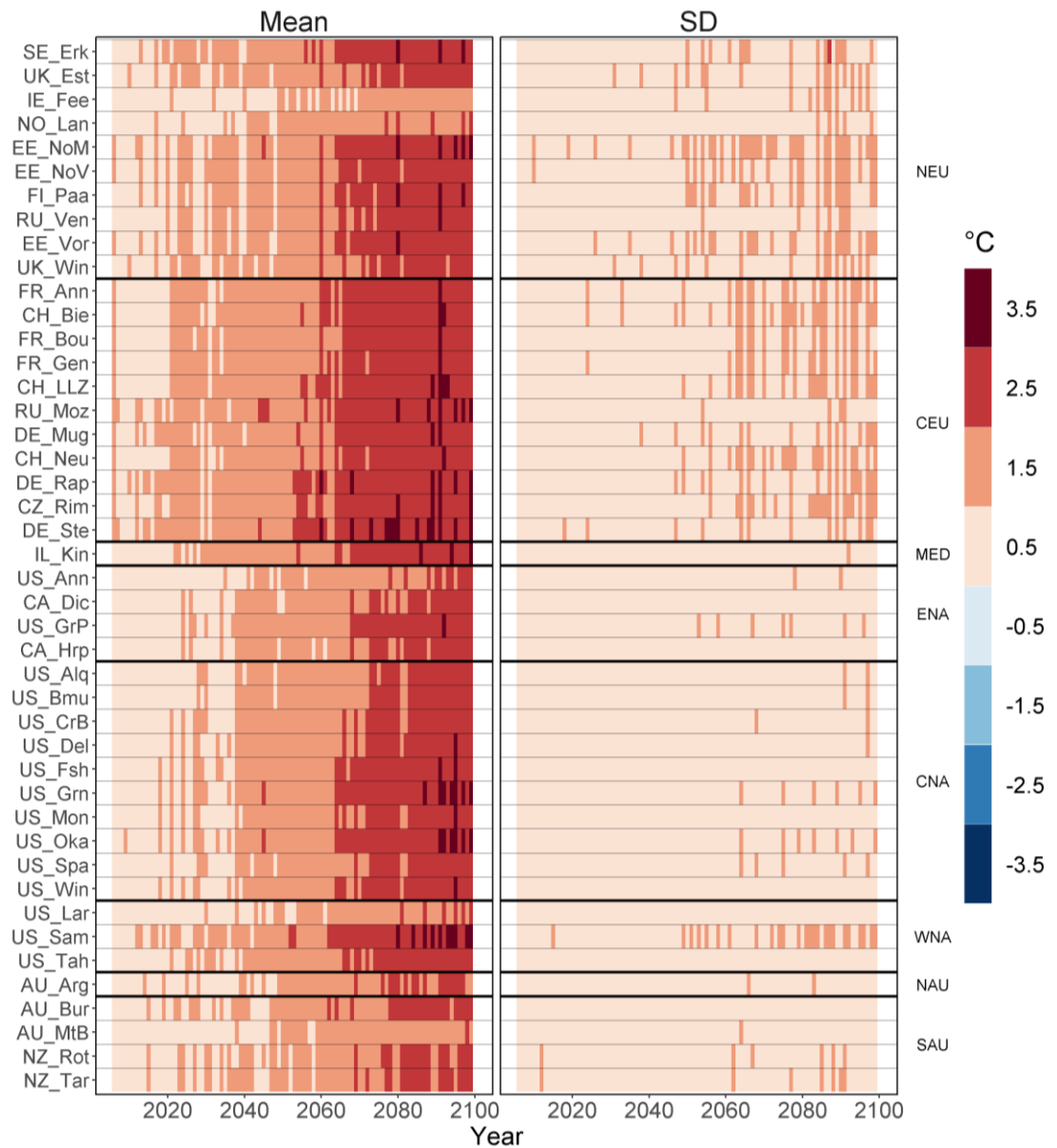


Figure 6.19 Mean and standard deviation (SD) of the annual surface temperature anomaly for 46 lakes across four GCMs and two lake models (n=2920) for RCP 6.0. Sites are ordered according to regions with labels on the right side, separated by a bold line. See Table 6.6 for site reference names.

For bottom temperatures there was a projected increase in mean annual temperature across all sites, but the change was much more variable between sites than that seen for surface water temperature (Figure 6.20). The sites which exhibited the greatest increase by 2069-2099 were three of the sites which have relatively small mean depths US\_Win (2.1 m) of +2 to +3 °C (SD: 0.5 – 1.5 °C), EE\_Vor (2.8 m) +2 to +3 °C (SD: 0.5 – 1.5 °C) and DE\_Mug (4.8 m) +2 to +3 °C (SD: 0.5 – 1.5 °C). Some sites with relatively large mean depths were also projected to have an increase in bottom temperatures by 2069-2099: NZ\_Tar (56.0 m) +1 to +2 °C (SD: 0.5 – 1.5 °C), CH\_Neu (63.3 m) +1 to +2 °C (SD: 0.5 – 1.5 °C), FR\_Bou (82.0 m) +1 to +2 °C (SD: 0.5 – 1.5 °C) and FR\_Gen (156.0 m) +0.5 to +1.5 °C (SD: 0.5 – 1.5 °C). Most of the lakes in NEU and CNA had a small increase of 0.5 to +1.5 °C (SD: 0.5 – 1.5 °C).

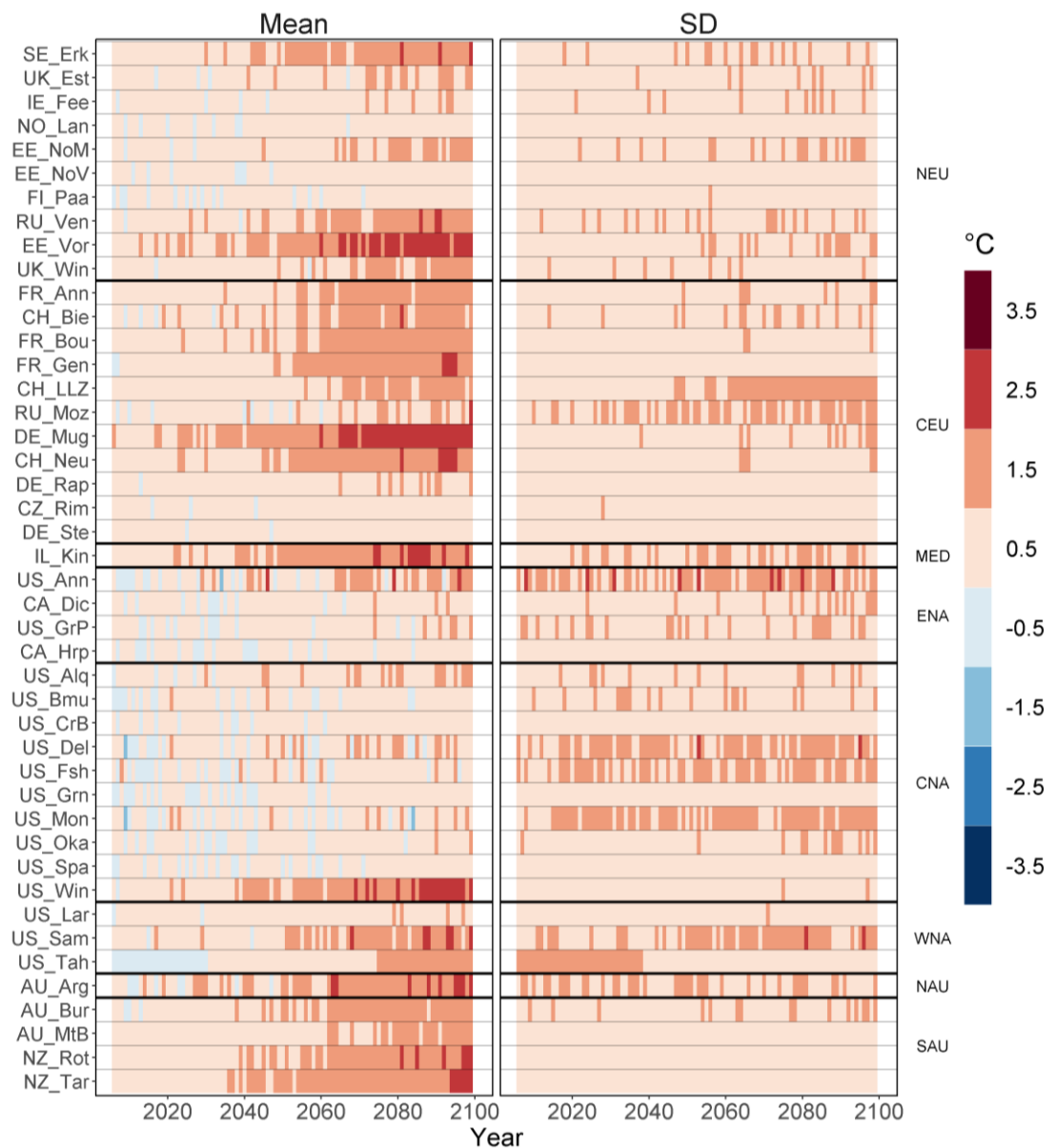


Figure 6.20 Mean and standard deviation (SD) of the annual bottom temperature anomaly for 46 lakes across four GCMs and two lake models (n=2920) for RCP 6.0 for the time period 2006-2099. Sites are ordered according to regions with labels on the right side, separated by a bold line. See Table 6.6 for site reference names.

Increases in projected mean annual whole lake temperature were greater for sites with a smaller mean depth for example US\_Win (mean depth 2.1 m, +2 to +3 °C) and EE\_Vor (mean depth 2.8 m, +1.5 to +2.5 °C) and DE\_Mug (mean depth 4.8 m, +2.5 to +3.5 °C) (Figure 6.21). Two other sites which also had a large projected increase were US\_Sam and IL\_Kin (+1.5 to +2.5 °C). Some of the sites had relatively small projected

increases across the time period IE\_Fee, NO\_Lan, CA\_Hrp and US\_Grn (+0.5 to +1.5 °C).

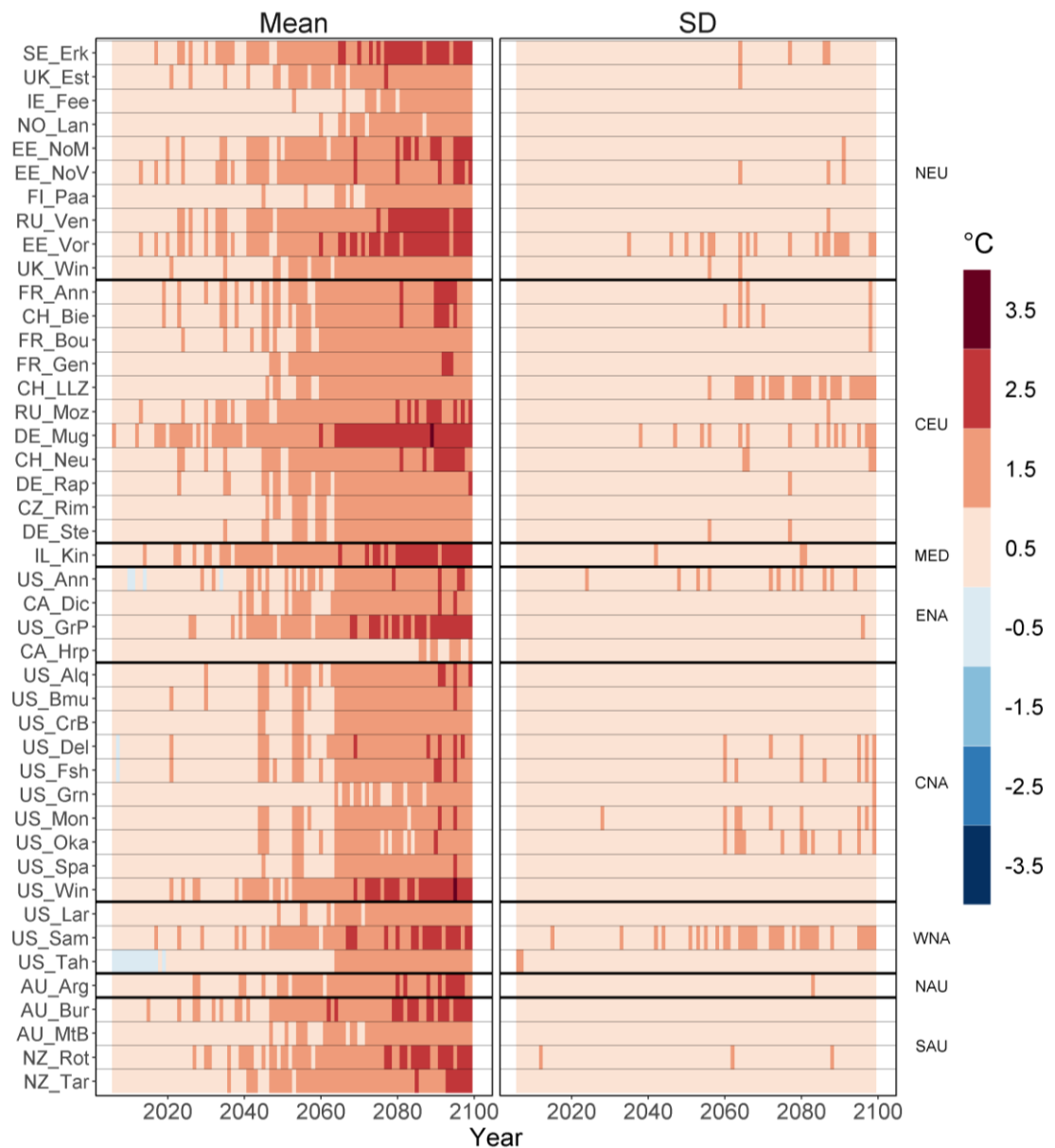


Figure 6.21 Mean and standard deviation (SD) of the annual volumetrically averaged whole lake temperature anomaly for 46 lakes across four GCMs and two lake models (n=2920) for RCP 6.0 for the time period 2006-2099. Sites are ordered according to regions with labels on the right side, separated by a bold line. See Table 6.6 for site reference names.

For the period 2069-2099, surface temperature for sites in the northern hemisphere had large projected positive anomaly during the months April through

October while southern hemisphere sites had an increase across all months (Figure 6.22). The largest positive anomalies were for sites NO\_Lan, RU\_Moz, EE\_NoM, EE\_NoV, FI\_Paa, and EE\_Vor between April to June of +2.5 to +5.5 °C (SD: 0.5 – 2.5 °C; n=7200). Sites in the CEU region had consistent warming from November through to February of +1.5 to +2.5 °C (SD: 0.5 – 1.5 °C) across all sites, with a slightly larger increase in summer of +3 to +4 °C (SD: 0.5 – 1.5 °C). Sites in ENA and CNA had both small decreases and increases for January and February of -0.5 to +1.5 °C (SD: 0.5 °C) with relatively large increases in April through November of +3.5 to +4.5 °C (SD: 0.5 – 1.5 °C).

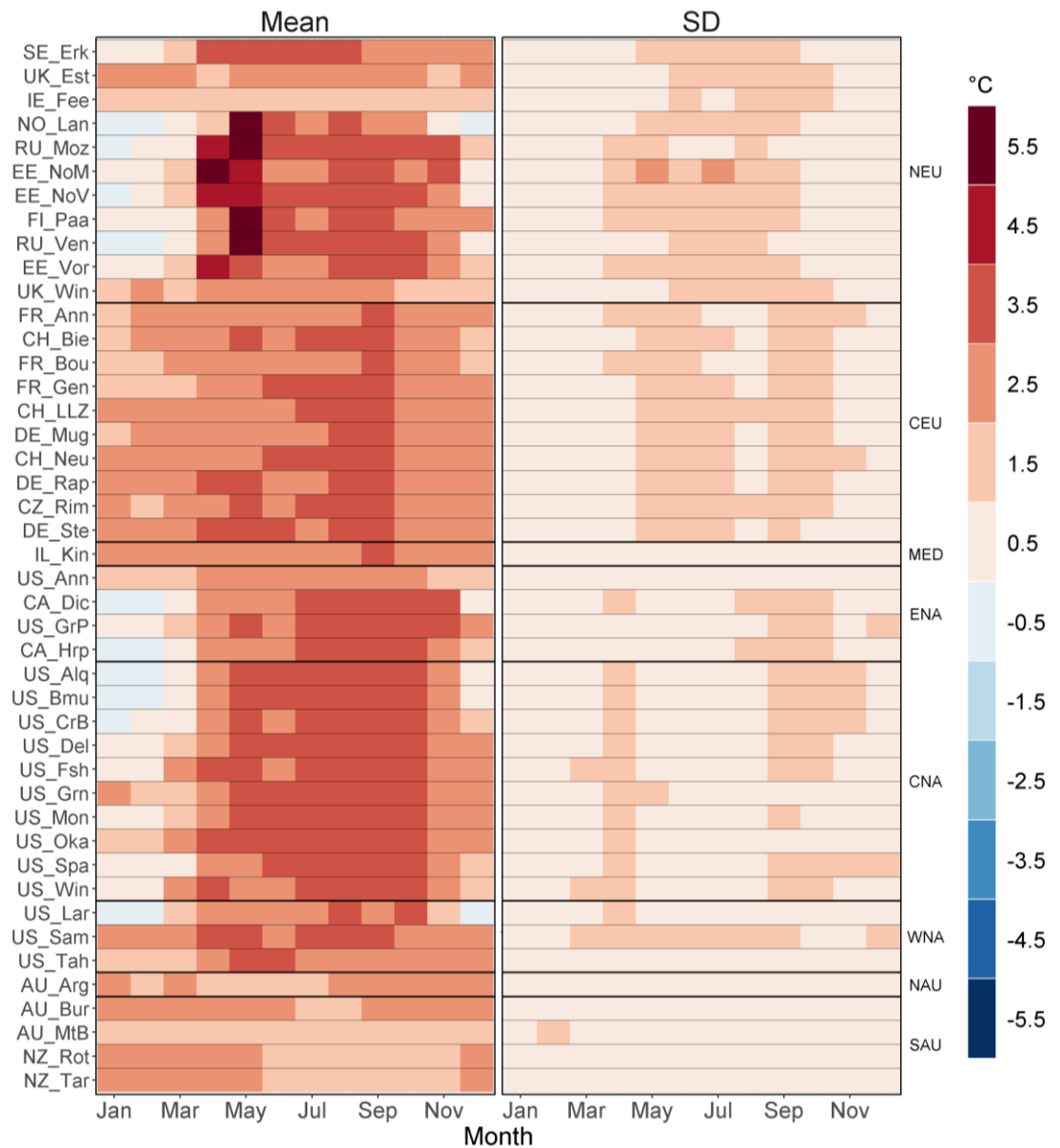


Figure 6.22 Mean and standard deviation (SD) of the monthly surface temperature anomaly for 46 lakes across four GCMs and two lake models ( $n=7200$ ) for RCP 6.0 for the time period 2069-2099. Sites are ordered according to regions with labels on the right side, separated by a bold line. See Table 6.6 for site reference names.

There were large projected increases in bottom temperatures at two sites, RU\_Ven, EE\_Vor, which both had anomalies of  $+3.5$  °C in May and April respectively (Figure 6.23). In the CEU region, there was an increase in bottom temperature throughout the entire year of  $+1.5$  °C (SD:  $0.5$  °C) with the exception of for site DE\_Mug which had a larger projected increase than for other lakes of  $+1.5$  to  $+2.5$  °C (SD:  $0.5 - 1.5$  °C). In ENA and CNA there were only increases projected for bottom temperature in March,

April and for September through to December, all of which were between +1 and +3 °C (SD: 0.5 – 1.5 °C). An exception were the two relatively shallow lakes US\_Win and US\_Lar (mean depth: 2.1 m and 2.2 m respectively) which had increases from March through to November of +0.5 to +3.5 °C (SD: 0.5 – 1.5 °C). For each of the sites in the NAU and SAU regions, there were positive projected anomalies throughout the whole year of +1 to +2 °C (SD: 0.5 °C).

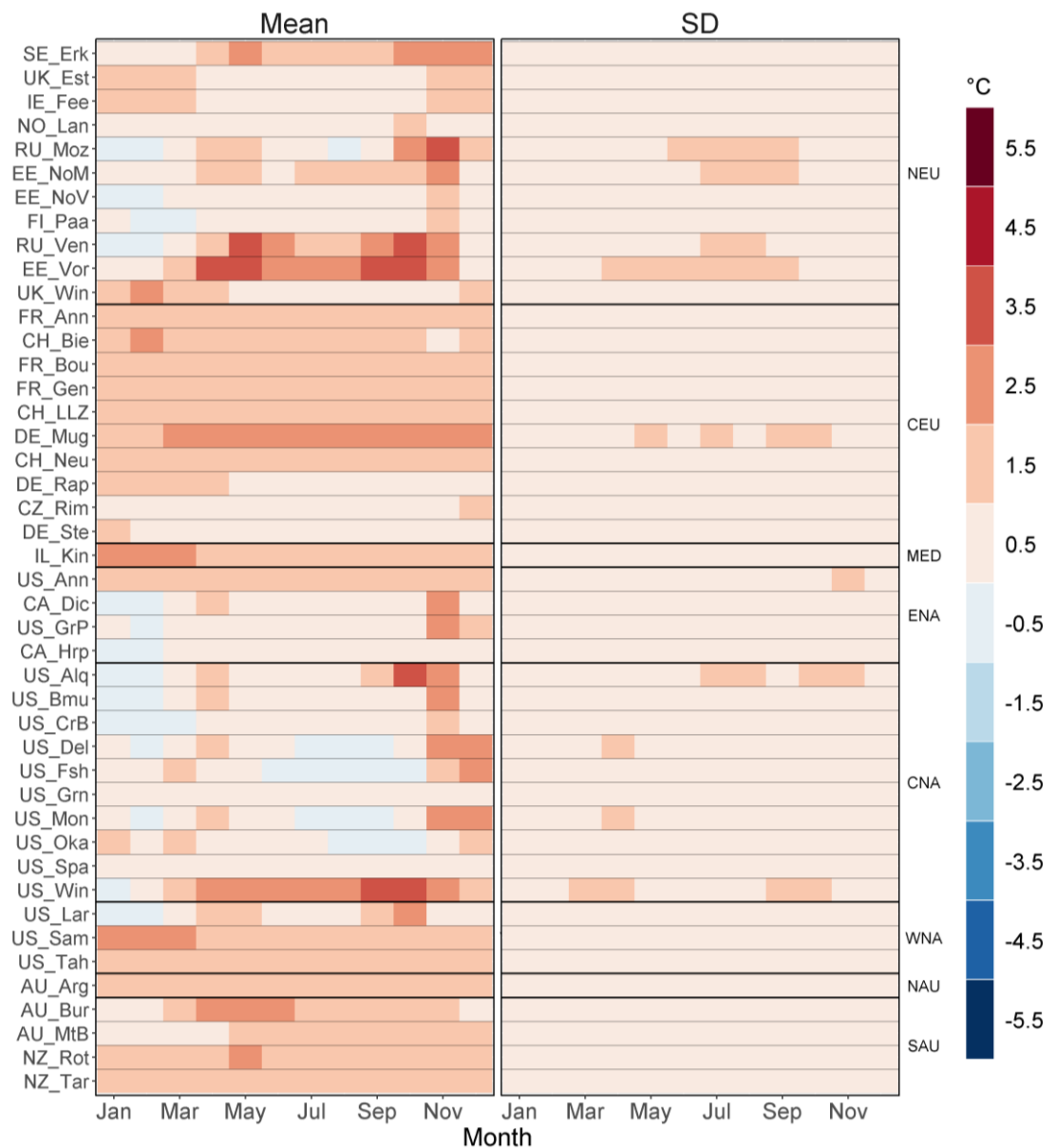


Figure 6.23 Mean and standard deviation (SD) of the monthly bottom temperature anomaly for 46 lakes across four GCMs and two lake models (n=7200) for RCP 6.0 for the time period 2069-2099. Sites are ordered according to regions with labels on the right side, separated by a bold line. See Table 6.6 for site reference names.

Volumetrically averaged water temperature was projected to increase from March to November in the NEU region by +1 to +6 °C (SD: 0.5 – 1.5 °C) (Figure 6.24). There was a consistent positive anomaly across four of the lakes in CEU (FR\_Ann, CH\_Bie, FR\_Bou and FR\_Gen) of +2 °C (SD: 0.5 – 1.5 °C). In ENA and CNA, April through November had increases of +1.5 to +3.5 °C (SD: 0.5 – 1.5 °C).

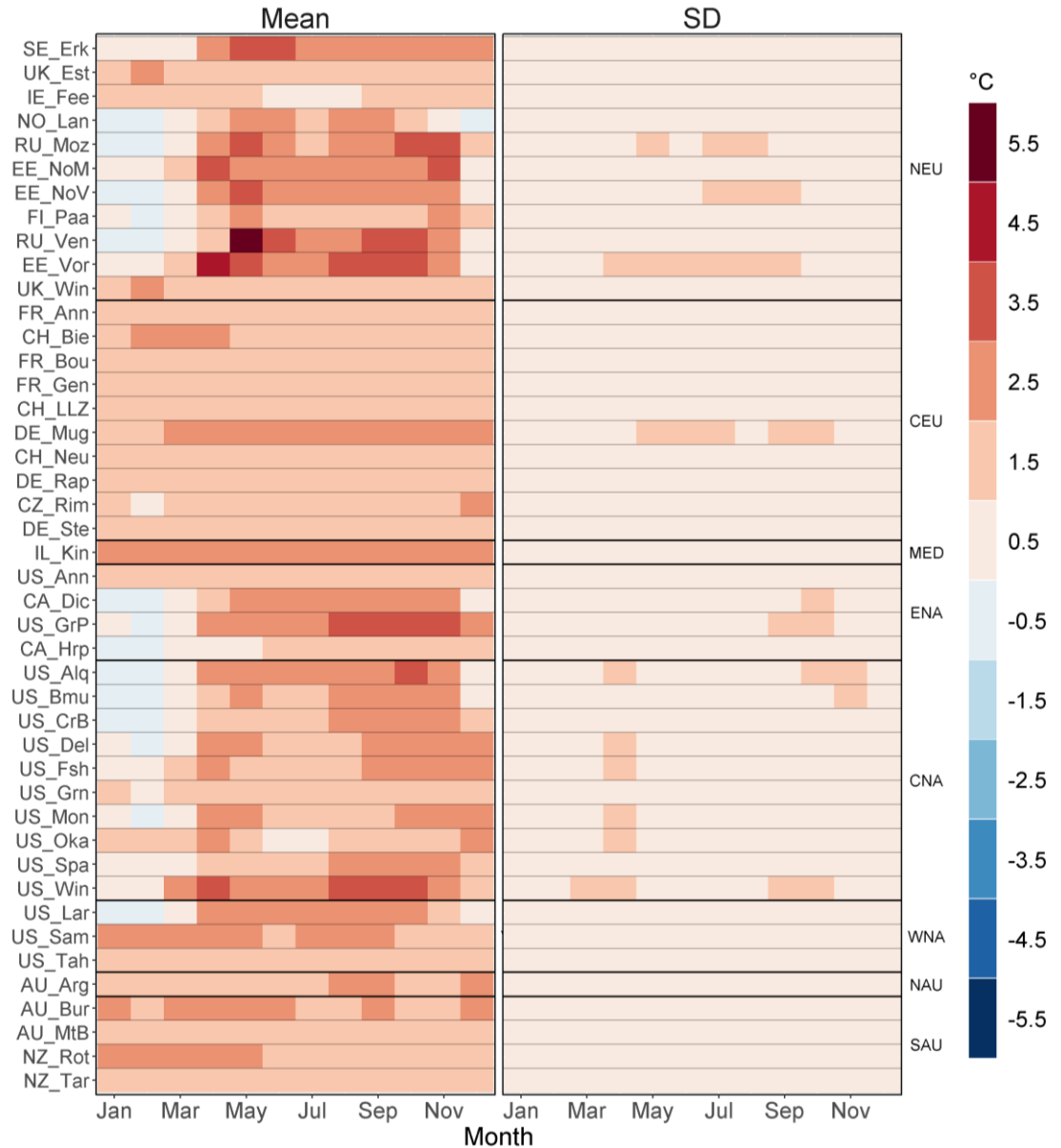


Figure 6.24 Mean and standard deviation (SD) of the monthly volumetrically averaged whole lake temperature anomaly for 46 lakes across four GCMs and two lake models (n=7200) for RCP 6.0 for the time period 2069-2099. Sites are ordered according to regions with labels on the right side, separated by a bold line. See Table 6.6 for site reference names.

The overall increase in the number of stratified days, described above, was apparent across most of the individual sites (Figure 6.25). The lakes that had the largest increase in the total number of stratified days by 2069-2099 for RCP 6.0 were in CEU (DE\_Rap and DE\_Ste) of +25 to +35 days (SD: 5 – 15 days; n=8) and WNA (US\_Tah) with increases of +25 to greater than +35 days (SD: 15 – 35 days). Each of these sites had similar changes in stratification starting earlier and finishing later throughout the period. There were four sites in NEU (NO\_Lan, EE\_NoM, EE\_NoV and FI\_Paa) where the increase in stratification duration of +15 to + 35 (SD: 15 – 25 days) days was influenced more by stratification starting earlier by -15 days (SD: 5 – 15 days) (Figure 6.26) days more so than stratification ending later +5 to +15 days (SD: 5 – 15 days) (Figure 6.27). In ENA and CNA, from 2006-2050 there were more occurrences of stratification starting earlier by -5 to -15 days (SD: 5 – 15 days) than ending later by +5 to +15 days (SD: 5 – 15 days). The warm tropical lake IL\_Kin had the smallest increase in stratified days by 2069-2099 of +5 to +15 days (SD: 5 – 15 days).

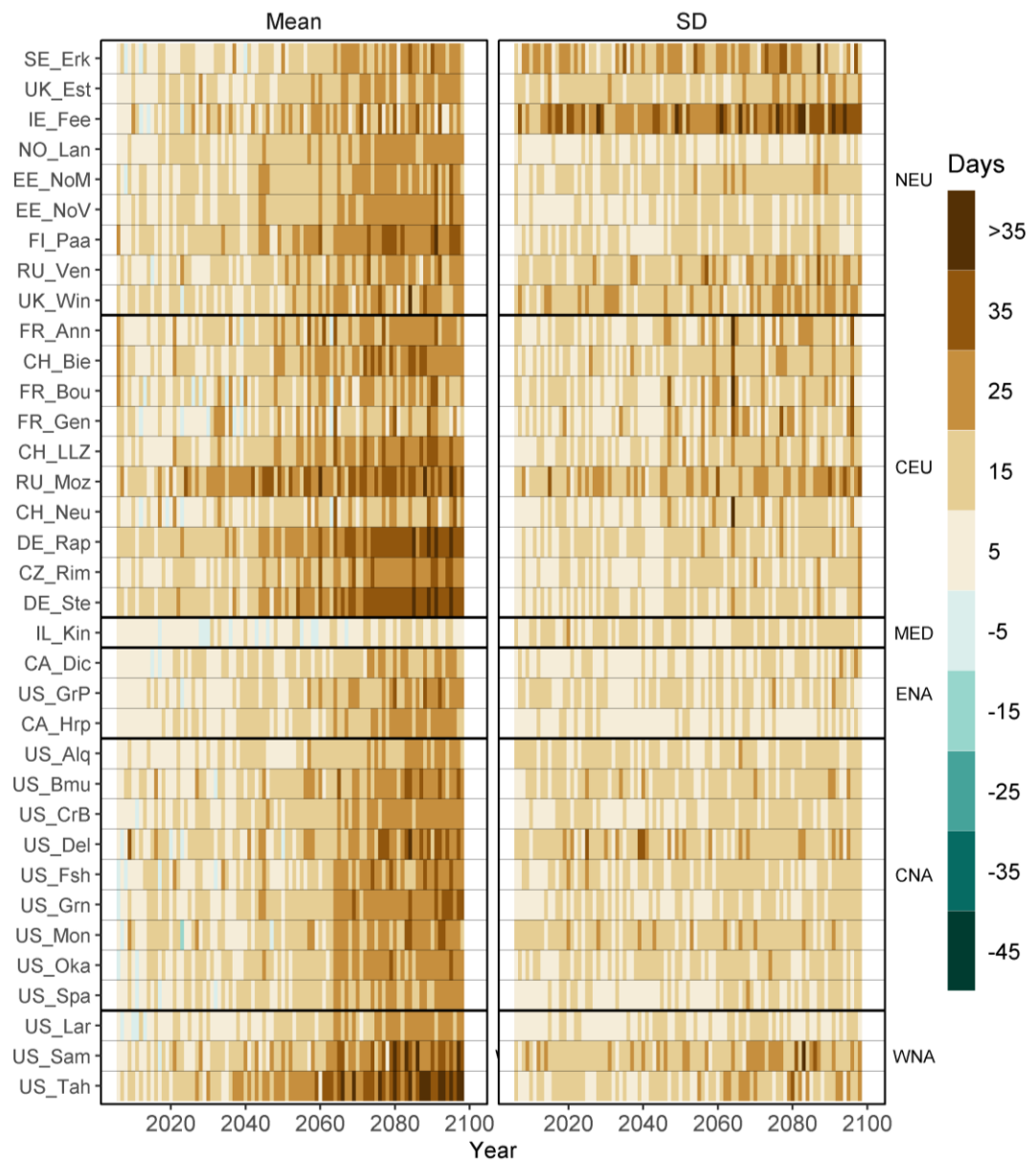


Figure 6.25 Mean and standard deviation (SD) of the anomaly for duration of stratification across the four GCMs and two lake models for 35 lakes (n=8) for RCP 6.0. Only dimictic and monomictic lakes are shown. Sites are ordered according to regions with labels on the right side, separated by a bold line. See Table 6.6 for site reference names.

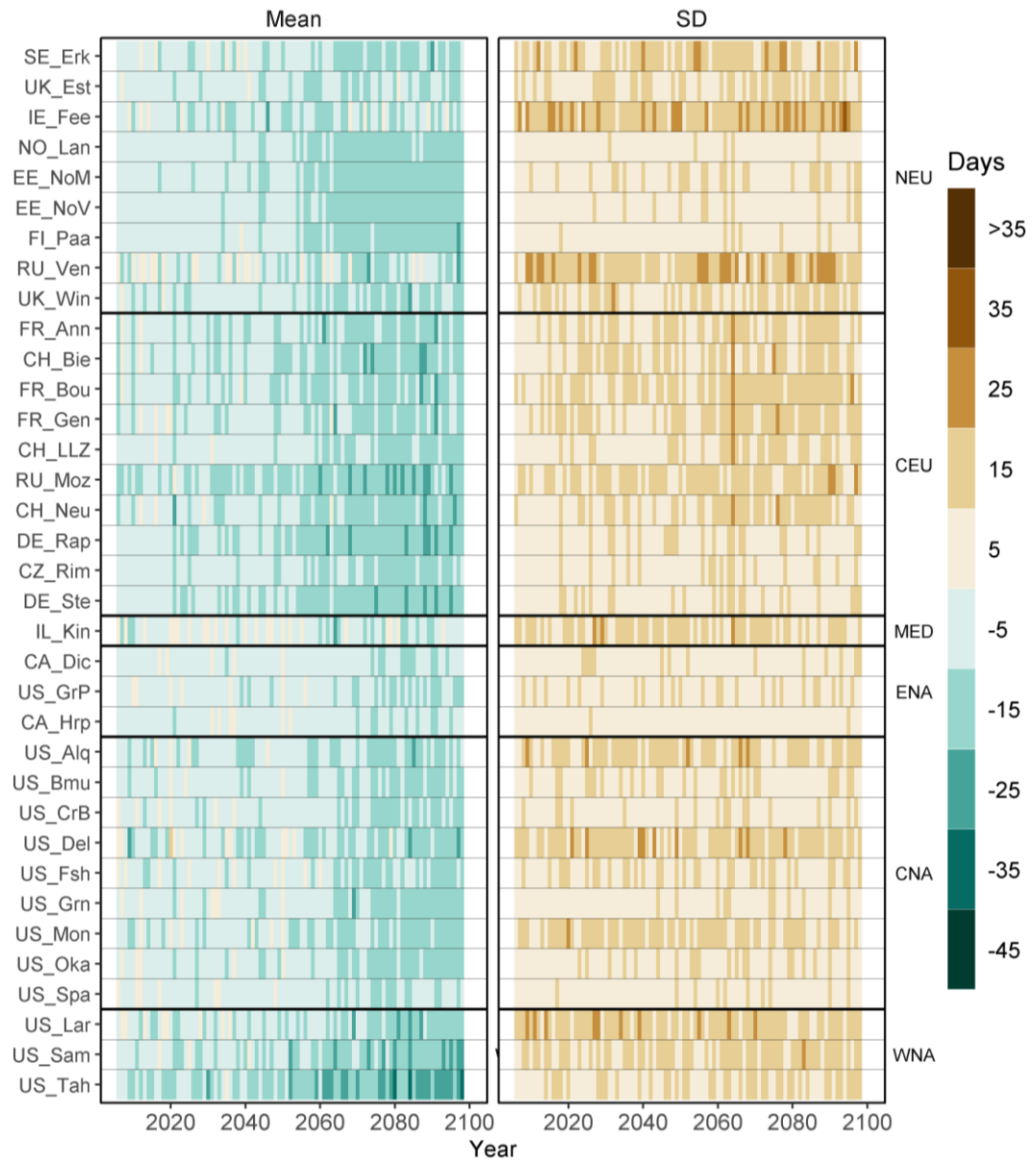


Figure 6.26 Mean and standard deviation (SD) of the anomaly for the start of stratification across the four GCMs and two lake models for 35 lakes (n=8) for RCP 6.0 for the time period 2006-2099. Only dimictic and monomictic lakes are shown. See Table 6.6 for site reference names.

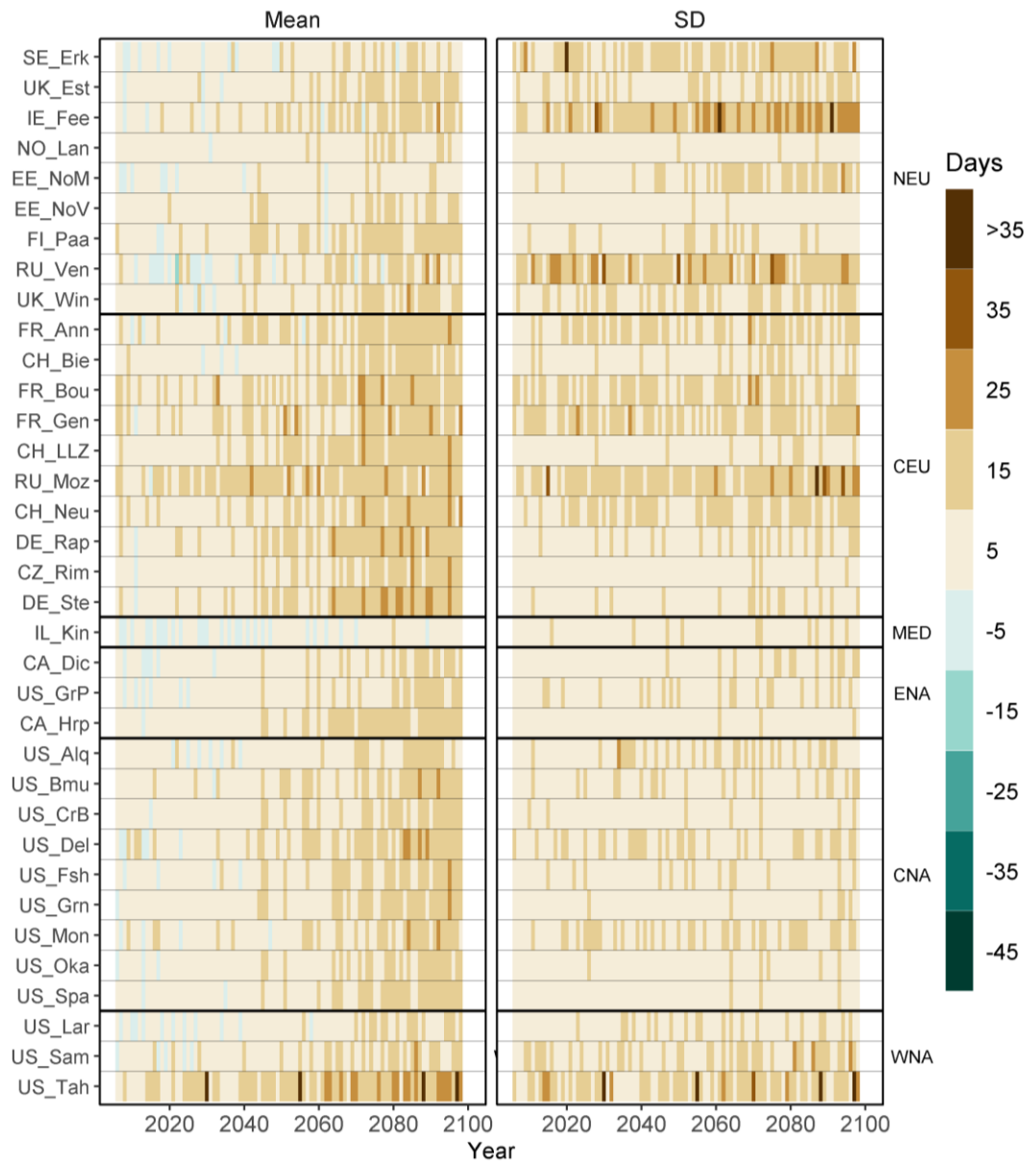


Figure 6.27 Mean and standard deviation (SD) of the anomaly for the end of stratification across the four GCMs and two lake models for 35 lakes (n=8) for RCP 6.0 for the time period 2006-2099. Only dimictic and monomictic lakes are shown. Sites are ordered according to regions with labels on the right side, separated by a bold line. See Table 6.6 for site reference names.

The magnitude of the density difference between the surface and bottom increased for all lakes throughout 2006-2099 for RCP 6.0 (Figure 6.28). There were four lakes in ENA (US\_Fsh, US\_Grn, US\_Mon and US\_Oka) which had the largest changes

of  $-0.3$  to  $-0.5 \text{ kg m}^{-3}$  (SD:  $0.1 - 0.3 \text{ kg m}^{-3}$ ;  $n=2920$ ). Shallow polymictic lakes (EE\_Vor, DE\_Mug and US\_Win) had no change to annual mean density difference between surface and bottom of  $+0.1 \text{ kg m}^{-3}$  (SD:  $0.1 \text{ kg m}^{-3}$ ). While monomictic lakes which had weak stratification (IE\_Fee and RU\_Ven) had a very slight changes in density difference by 2069-2099 of  $-0.1$  to  $-0.3 \text{ kg m}^{-3}$  (SD:  $0.1 \text{ kg m}^{-3}$ ). For the sites in the Southern hemisphere the changes were not as large by 2069-2099 of  $-0.1$  to  $-0.3 \text{ kg m}^{-3}$  (SD:  $0.1-0.3 \text{ kg m}^{-3}$ ). The rest of the sites all had changes of  $-0.1$  to  $-0.5 \text{ kg m}^{-3}$  by 2069-2099 (SD:  $0.1 - 0.3 \text{ kg m}^{-3}$ ) with US\_Ann having a larger SD ( $0.3 - 0.5 \text{ kg m}^{-3}$ ).

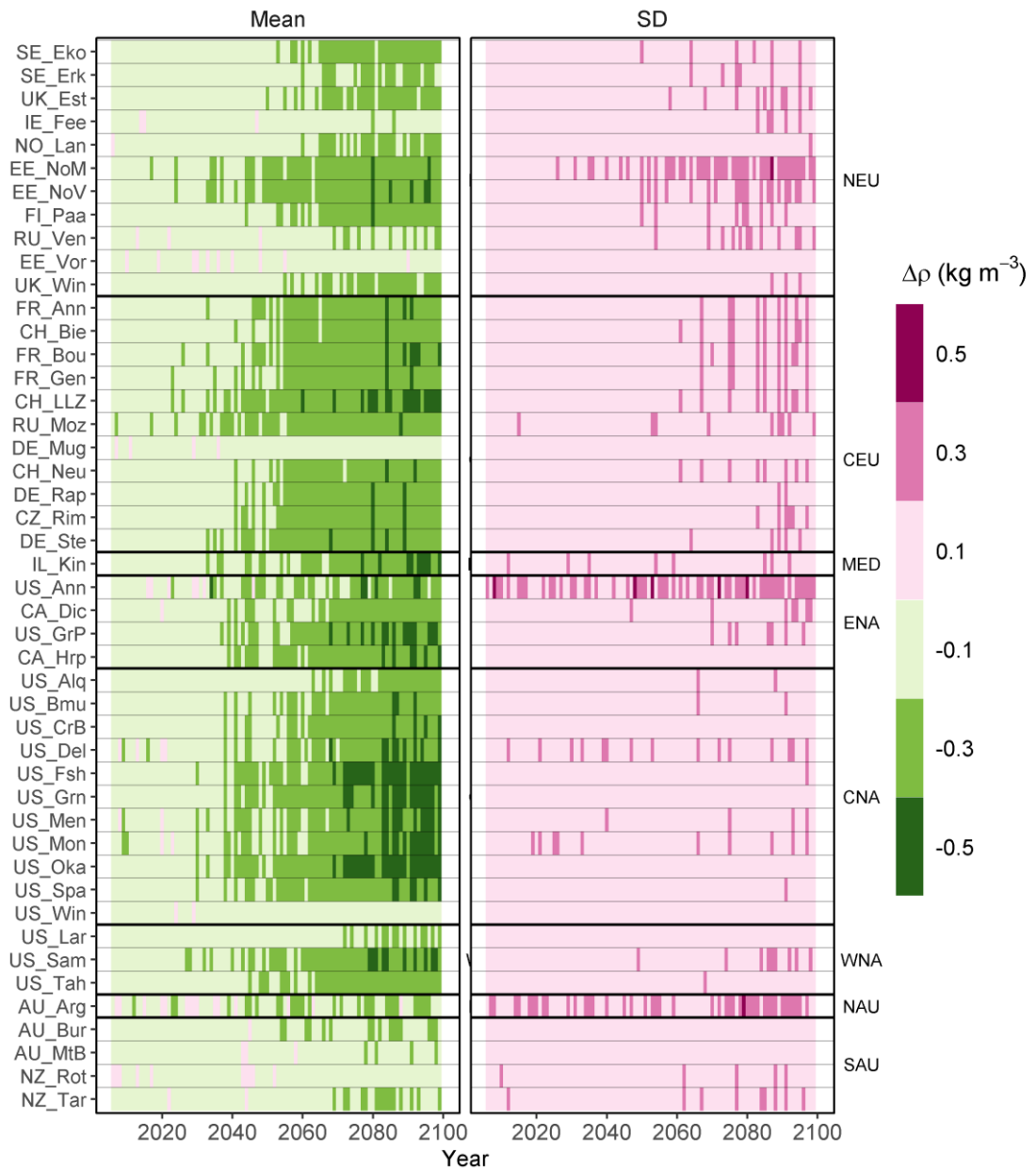


Figure 6.28 Mean and standard deviation (SD) of the annual anomaly for density difference of stratification averaged across the four GCMs and two lake models ( $n=2920$ ) for 46 lakes for RCP 6.0 for the time period 2006-2099. Sites are ordered according to regions with labels on the right side, separated by a bold line. See Table 6.6 for site reference names.

For the period of 2069-2099, the mean monthly anomalies showed a large change in the projected density difference from April to October for lakes in the Northern Hemisphere (Figure 6.29). RU\_Moz had the largest mean anomaly in June through

August of  $-0.9 \text{ kg m}^{-3}$  (SD:  $0.1 \text{ kg m}^{-3}$ ;  $n=7200$ ). Sites in ENA and CNA all had increases of  $-0.3$  to  $-0.5 \text{ kg m}^{-3}$  (SD:  $0.1 - 0.3 \text{ kg m}^{-3}$ ) from June through September. The shallow and polymictic lakes (EE\_Vor, DE\_Mug and US\_Win) had very small changes in density difference  $+0.1 \text{ kg m}^{-3}$ .

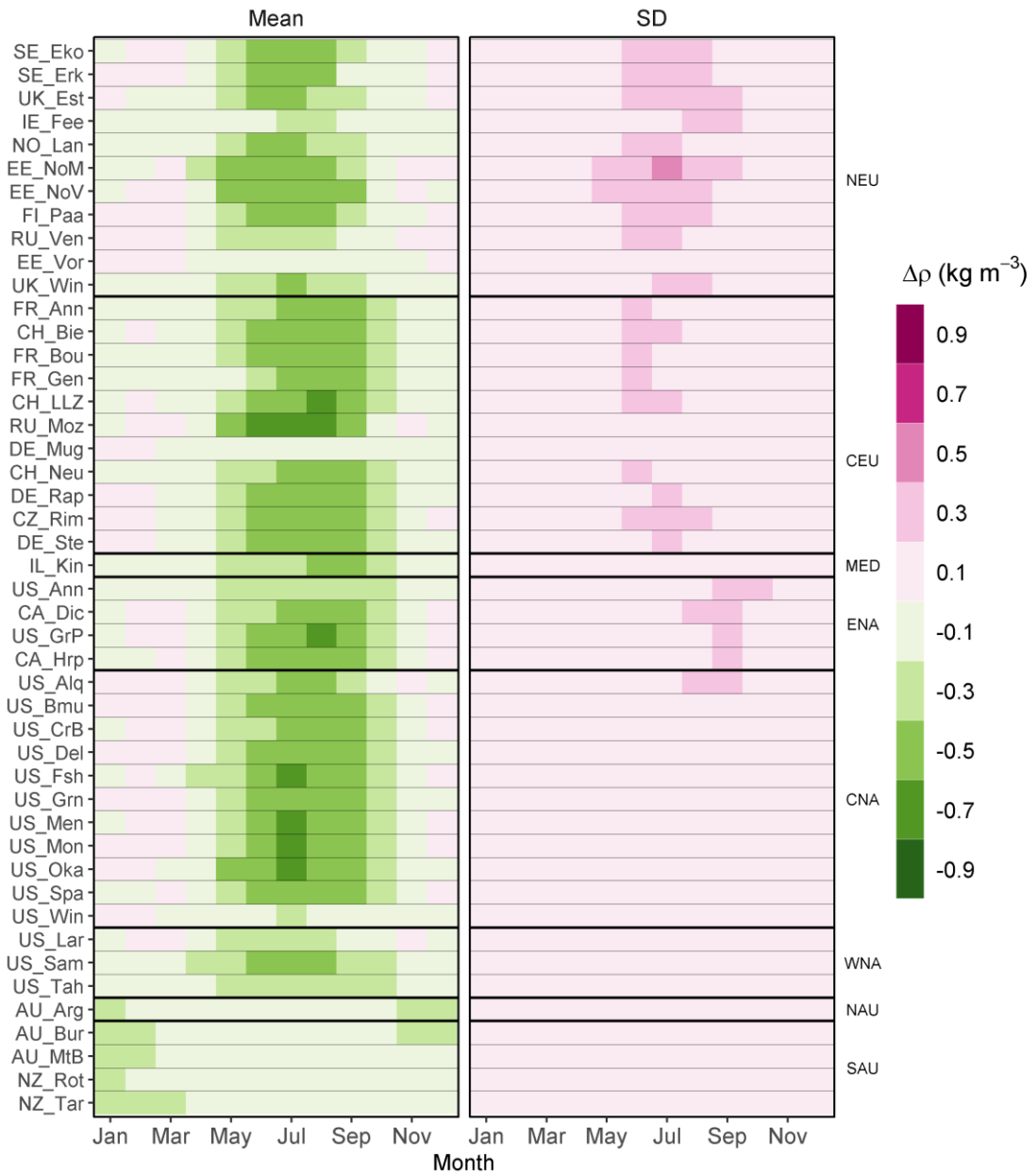


Figure 6.29 Mean and standard deviation (SD) of the monthly anomaly for density difference of stratification averaged across the four GCMs and two lake models ( $n=7200$ ) for 46 lakes for RCP 6.0 for the time period 2069-2099. Sites are ordered according to regions with labels on the right side, separated by a bold line. See Table 6.6 for site reference names.

Thermocline depth was found to be very sensitive to the lake model, so the results were separated by model. Due to the variability between the GCMs, a rolling 30-year mean was used to remove this noise and extract the climatic signal from 2036 to 2099. The changes in projected thermocline depth was much larger and variable for simulations using GLM (Figure 6.30) compared to GOTM (Figure 6.31), mainly for the sites with a larger mean depth. Sites with relatively small mean depths did not show any large shifts in projected thermocline depth based on simulations using GOTM, while the GLM simulations for sites AU\_Bur, EE\_NoV and US\_GrP all projected a deepening of the thermocline (Figure 6.30). The inter-model divergence was most apparent for AU\_Arg (GLM: -0.25 to -0.75 m; GOTM: +0.25 to +.75 m), FI\_Paa (GLM: +0.25 to +1.75 m; GOTM: -0.25 to -1.25 m) and US\_Grn (GLM: +0.25 to -0.25 m; GOTM: -0.75 to -2.75 m).

Overall, the projections based on GLM indicated a stronger deepening of the thermocline depth than those using GOTM. For GOTM, three of the sites with large mean depth in the CEU region (FR\_Ann, CH\_LLZ, CH\_Neu, CH\_Bie) had a consistent deepening of thermocline depth of +0.25 to +1.25 m (SD: 0.25 –0.75 m; n=14400). In contrast, for simulations using GLM, only site FR\_Ann projected a similar deepening of the thermocline while the other lakes projected thermocline shallowing (CH\_Bie) or larger magnitudes in thermocline deepening (CH\_LLZ). The site US\_Tah was the deepest lake in the study (max depth: 501 m). It was projected to have a large deepening of the thermocline based on simulations using GOTM of greater than 3m (SD: >3 m) while for GLM it showed slight shallowing of -0.25 to -0.75 m (SD: 0.75 – 1.25 m).

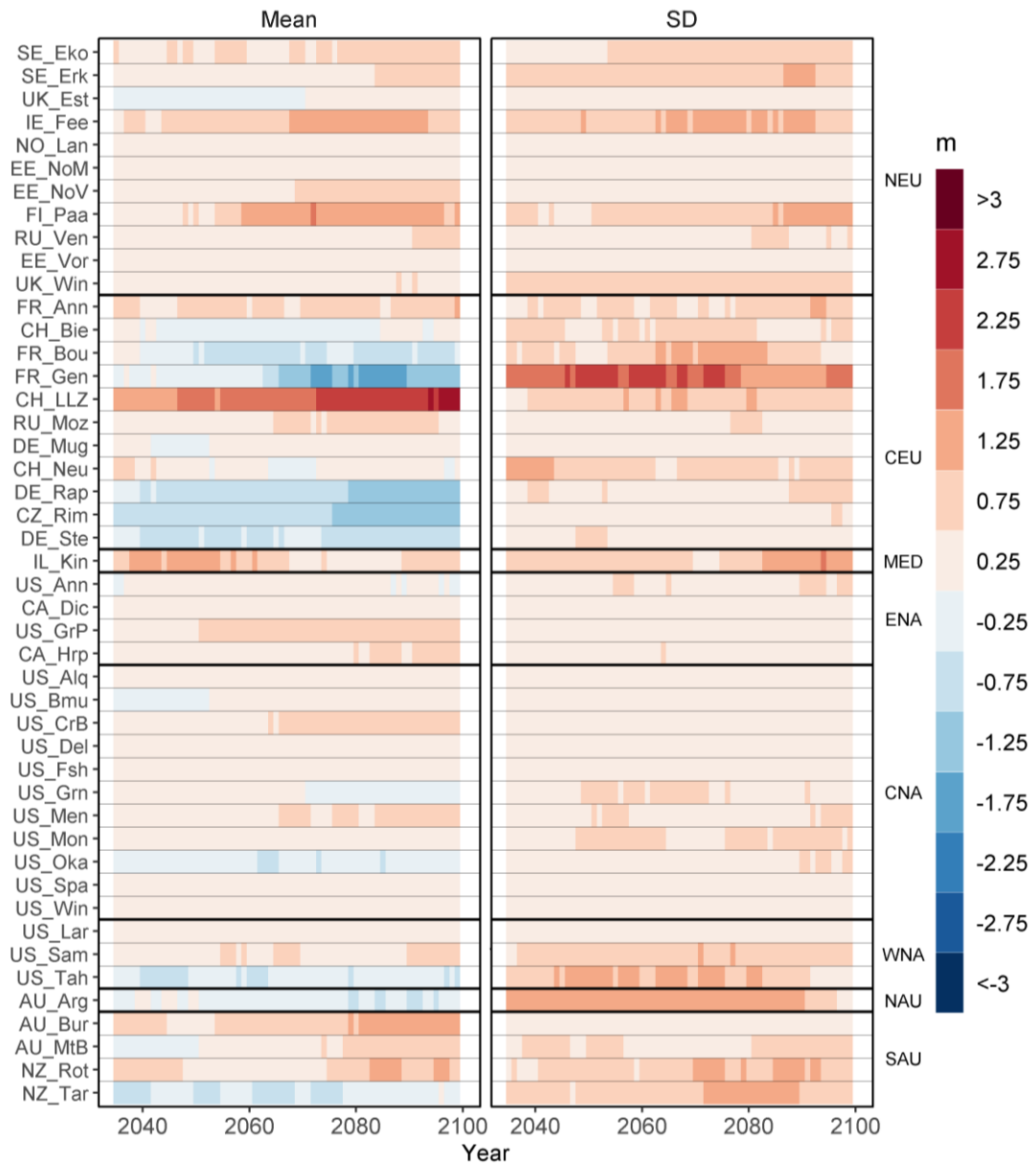


Figure 6.30 30-year rolling mean of the annual summer anomaly for thermocline depth for 46 lakes simulated using GLM, averaged across four GCMs (n=14400) for RCP 6.0 for the time period 2036-2099. Sites are ordered according to regions with labels on the right side, separated by a bold line. See Table 6.6 for site reference names. Positive values indicate that the thermocline is getting deeper while negative indicates it is getting shallower.

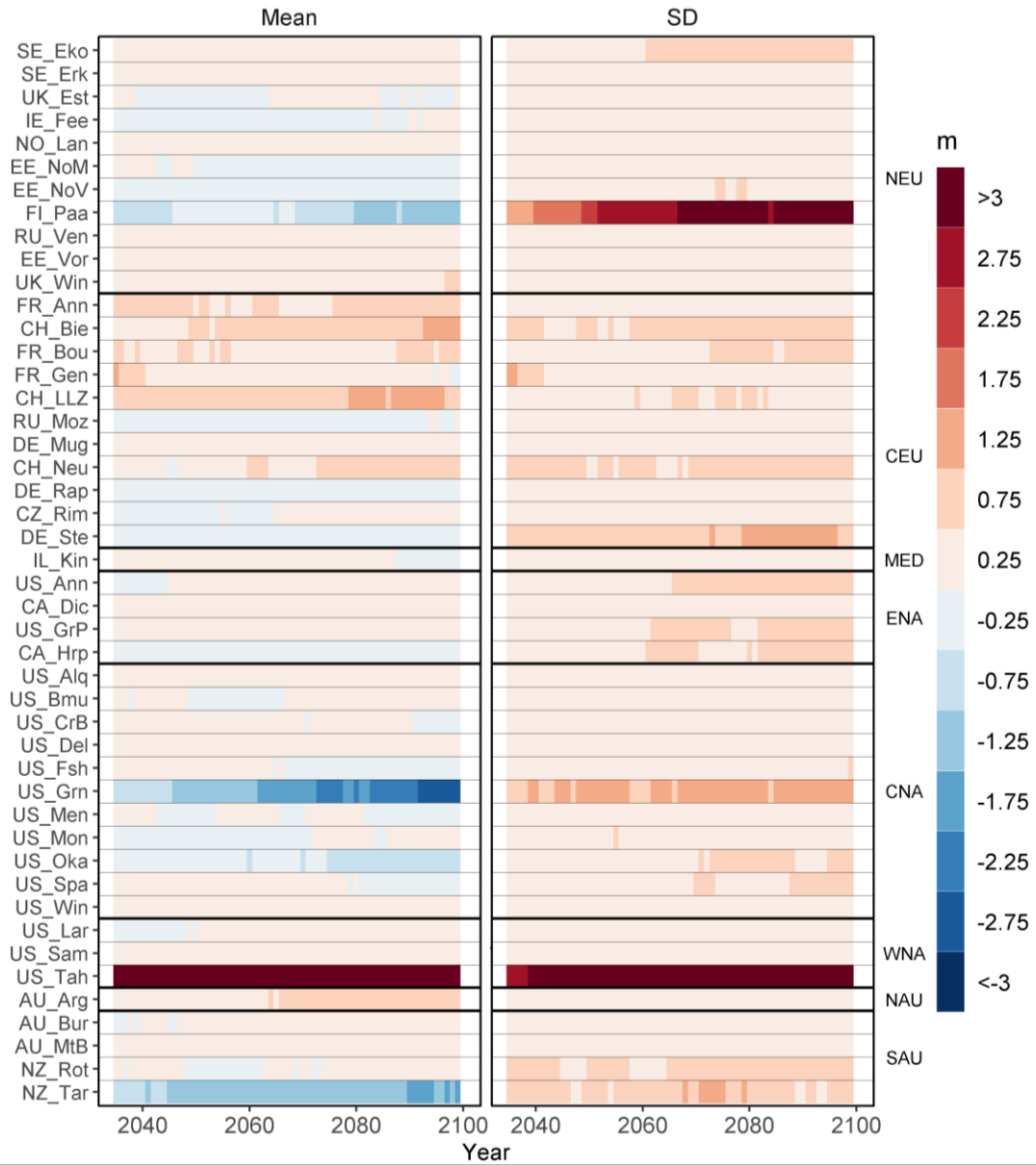


Figure 6.31 30-year rolling mean of the annual anomaly for thermocline depth for 46 lakes simulated using GOTM averaged across four GCMs (n=14400) for RCP 6.0 for the time period 2036-2099. Sites are ordered according to regions with labels on the right side, separated by a bold line. See Table 6.6 for site reference names. Positive values indicate that the thermocline is getting deeper while negative indicates it is getting shallower.

#### 6.4.6. Comparison of global and local

Data from the GOTM global simulations were retrieved from the grid squares where six of the study lakes were located (Golub, personal communication). The lakes were chosen to represent shallow and small (NO\_Lan), medium (IE\_Fee) and deep (FR\_Bou) lakes, sub-tropical (US\_Ann and AU\_Arg) and large surface area (US\_GrP). The anomalies for surface and bottom temperature for the Local and Global study projections followed very similar distributions for the six sites for which we made comparisons (Figure 6.32). The Local study values for NO\_Lan had a smaller range in distribution for bottom temperatures than those for the same site in the Global study, while for site US\_Ann the opposite was true, and the Local study projected anomalies had a wider distribution than those from the Global study.

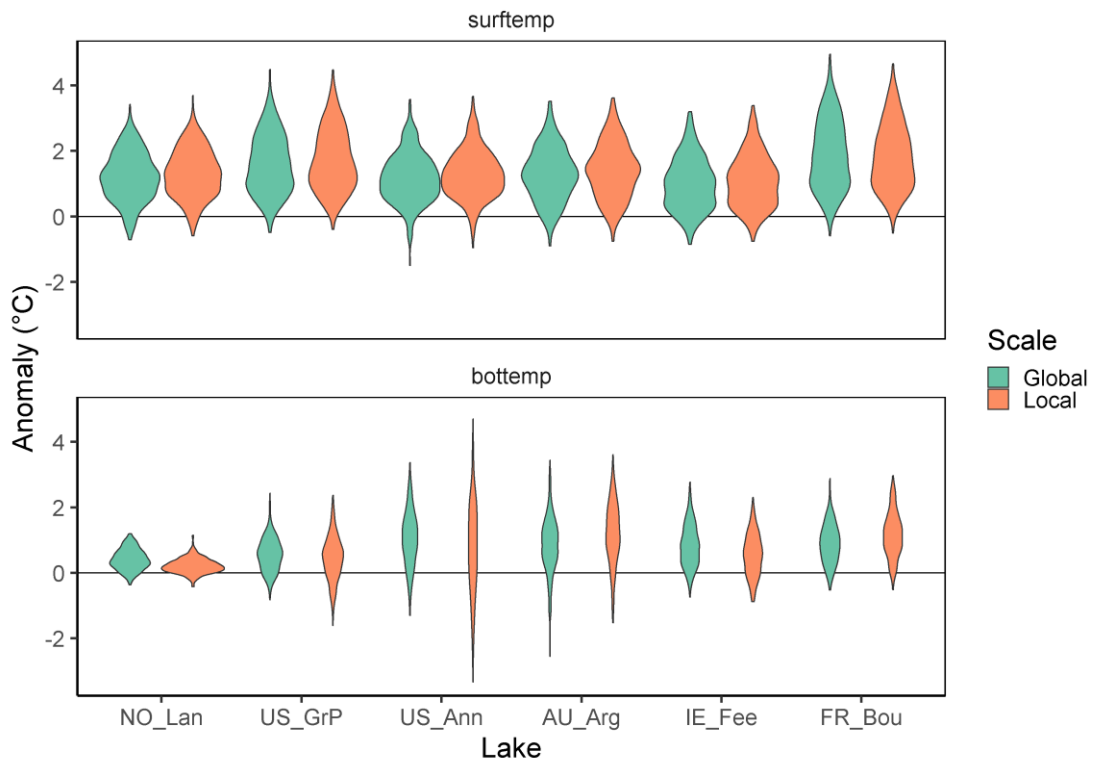


Figure 6.32 Distribution of anomalies for 4 GCM for GOTM (n=122640) for six lakes from the local and global simulations for RCP 6.0 for the time period 2015-2099 for surface and bottom temperature. See Table 6.6 for site reference names.

## 6.5. Discussion

Understanding the effects of directional climate change on lake temperature and thermal dynamics is essential for the future management of these systems and the services that they provide. This is the largest scale study that was been carried out, comparing multiple lakes, using a calibrated ensemble of hydrodynamic models and forced with an ensemble of GCMs under three prescribed climate change scenarios. We found that there was an unequivocal increase in surface, bottom and whole-lake water temperature across all 46 lakes under all scenarios. Both the duration of the stratification period and the density difference between the surface and bottom waters also increased for most lakes. The consistency in these results indicates that these shifts will be part of a global phenomenon that will likely affect lakes in all the regions where our study sites were located (Woolway and Merchant, 2019). Moreover, the data from these simulations of lake physical responses can be used to inform on biogeochemical and biological responses. For example, water temperature has been empirically linked to metabolic rates (Kraemer *et al.*, 2017) and decreases in thermocline depth coupled with increased light attenuation can potentially mitigate the potential for thermal shocks to cold-water fish species (Warren *et al.*, 2017).

This is also the first study of this scale that allows detailed insights into site specific responses. The study included lakes of varying morphometry which allowed further insights into what characteristics can influence the vulnerability of the lakes, as we had clusters of lakes which had regionally coherent forcing data but had divergent response in the lake variables (Butcher *et al.* (2015). For example, EE\_Vor in NEU, DE\_Mug in CEU and US\_Win in CNA all had relatively large increases in bottom temperature (+2.5 °C) by the end of the century, which was a result of them being relatively shallow (mean depths: 2.8 m, 4.8 m and 2.1 m respectively) compared to the other lakes in the same region. In CEU, surface lake temperatures are projected to increase at a similar rate to most lakes in NEU and CNA despite air temperature increases being lower (+3 °C) than in the other regions (+5 °C). This could be explained by the increase in downwelling solar radiation experienced in CEU (+12 to +20 W m<sup>-2</sup>) which has been shown to account for up to 40 % of surface water temperature increases in CEU (Schmid and Koster, 2016). Five lakes in CNA (US\_Fsh, US-Grn, US\_Men, US\_Mon

and US\_Oka) had the largest increase in density difference between surface and bottom (-0.5 kg ) by 2069-2099 (Figure 6.28). There were decreases in wind speed (-0.3 m s<sup>-1</sup>) experienced at these sites, potentially attributed to atmospheric stilling (Vautard *et al.*, 2010), during the summer months of May to September (Figure 6.15). This phenomena has been shown to significantly prolong stratification dynamics for EE\_Vor from 1982 – 2010 (Woolway, *et al.*, 2017a).

We found that the mean annual surface temperature anomaly increase was relatively similar across most of the lakes by the end of the century and this was explained by increases in air temperature and incoming short-wave radiation. These results are similar to the changes reported for observed summer surface temperature trends in a study of lakes in many global locations by O'Reilly *et al.* (2015). For all lakes that thermally stratified in summer, the current study found that there was an increase in stratification duration under the RCP 6.0 scenario of on average +20 days This increase was highly variable for the CEU region, despite most of the lakes there showing a relatively consistent increase in surface temperature. This difference in the patterns for these surface temperature and stratification duration can be attributed to the lakes in this region having distinctly varying morphometry, particularly with regards mean depth and surface area, which Kraemer *et al.* (2015) previously highlighted as being more important in explaining differences in stratification patterns than increased surface warming. Two of the lakes which had the largest projected increase in stratification duration, DE\_Ste and DE\_Rap, are lakes with historically low-density differences (Figure 6.8), which was similar results reported by Kraemer *et al.* (2015).

Wind speed has a large effect on lake thermal dynamics and a decrease in wind speed has been shown to reduce average whole-lake water temperature (Tanentzap *et al.*, 2008), increase the length of stratification (Woolway *et al.*, 2017a) and potentially alter lake mixing regimes (Woolway and Merchant, 2019). Sites in the ENA and CNA regions were projected to experience reductions in wind speed, but all our simulations indicated that all these sites would have increases in whole lake temperature and increases in stratification duration. This result indicates that the increases in air temperature and downwelling shortwave radiation have a stronger influence than a possible cooling effect caused by decreases in wind speed. Seasonal and monthly variability are highly important when quantifying climate change impacts (Shatwell *et al.*, 2019; Toffolon *et*

*al.*, 2020; Winslow *et al.*, 2017a). In the NEU region, there was a large positive anomaly in air temperature from November through to April, which led to a large increase in surface temperature in April and May, This then contributed to large increases in the density difference between surface and bottom water while also contributing to the start of stratification becoming earlier.

The multi-model ensemble approach used in this chapter was very powerful, particularly for ascertaining levels of uncertainty associated with each output. The key benefit of using ensembles is that the non-predictable aspects of the simulation can be removed through averaging, and uncertainty information can be gauged from the range of ensemble members (Duan *et al.*, 2007). In this climate impact study for lake thermal dynamics, the ensemble represents the range of uncertainty across all the four GCMs and the two lake models. A multi-model ensemble approach brings with it risks of underestimating uncertainty due to correlation between models that share input data and parameterization (Riccio *et al.*, 2007). However, using a diversity of input data (e.g. in our study forcing data from four GCMs) improves estimations of uncertainty as they account for many different possible futures (Diallo *et al.*, 2012; Kendon *et al.*, 2010; Shatwell *et al.*, 2019). There was a noticeable lack of agreement between GCMs for the wind speed anomalies (Figure 6.34), while in contrast downwelling short-wave radiation anomalies and air temperature anomalies were highly correlated between GCMs (Figure 6.33, Figure 6.35).

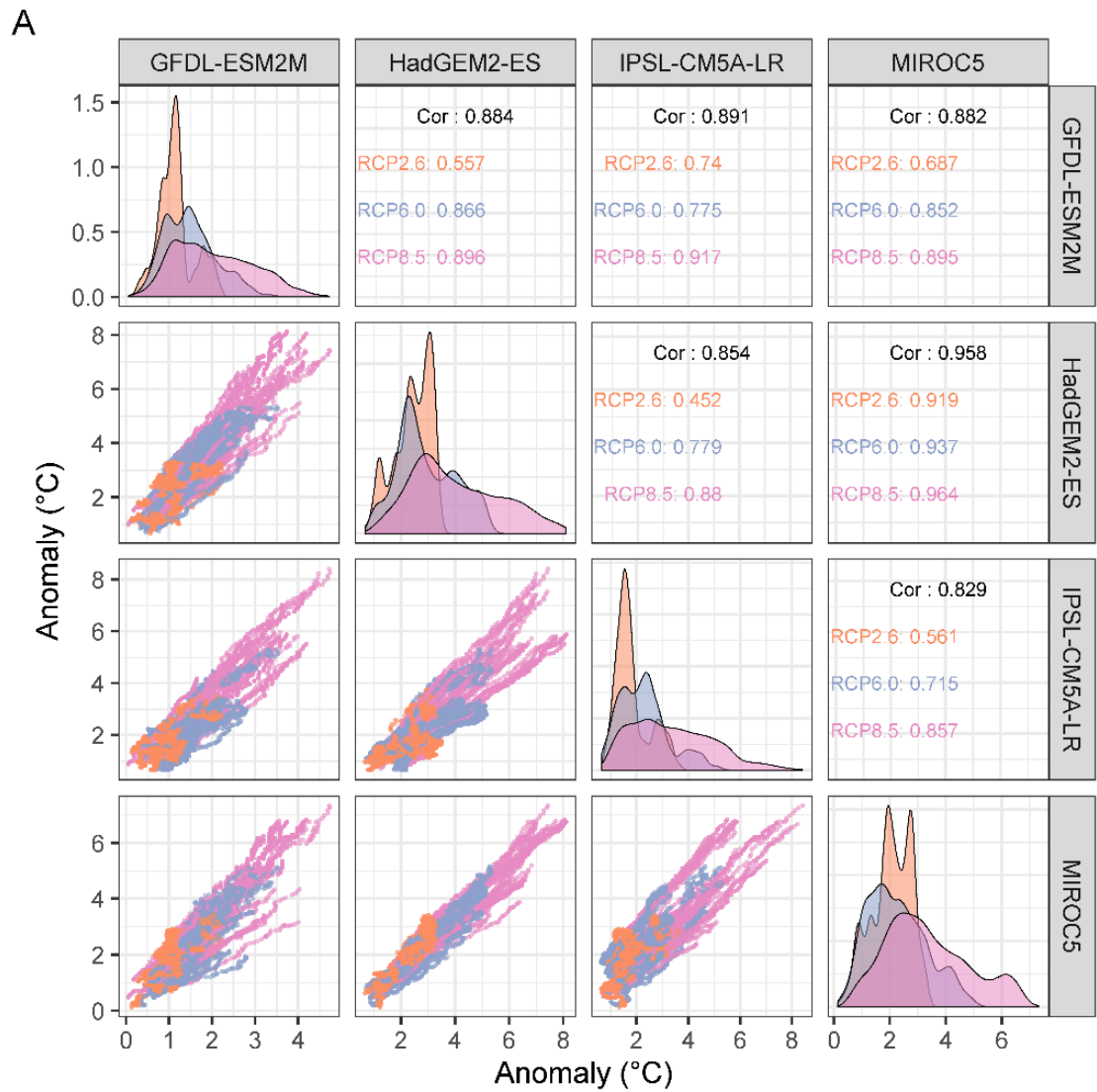


Figure 6.33 Paired scatter plot, distributions and correlations of the 30-year rolling mean anomaly for air temperature (A) the four GCMs across all 46 lakes from 2036-2099.

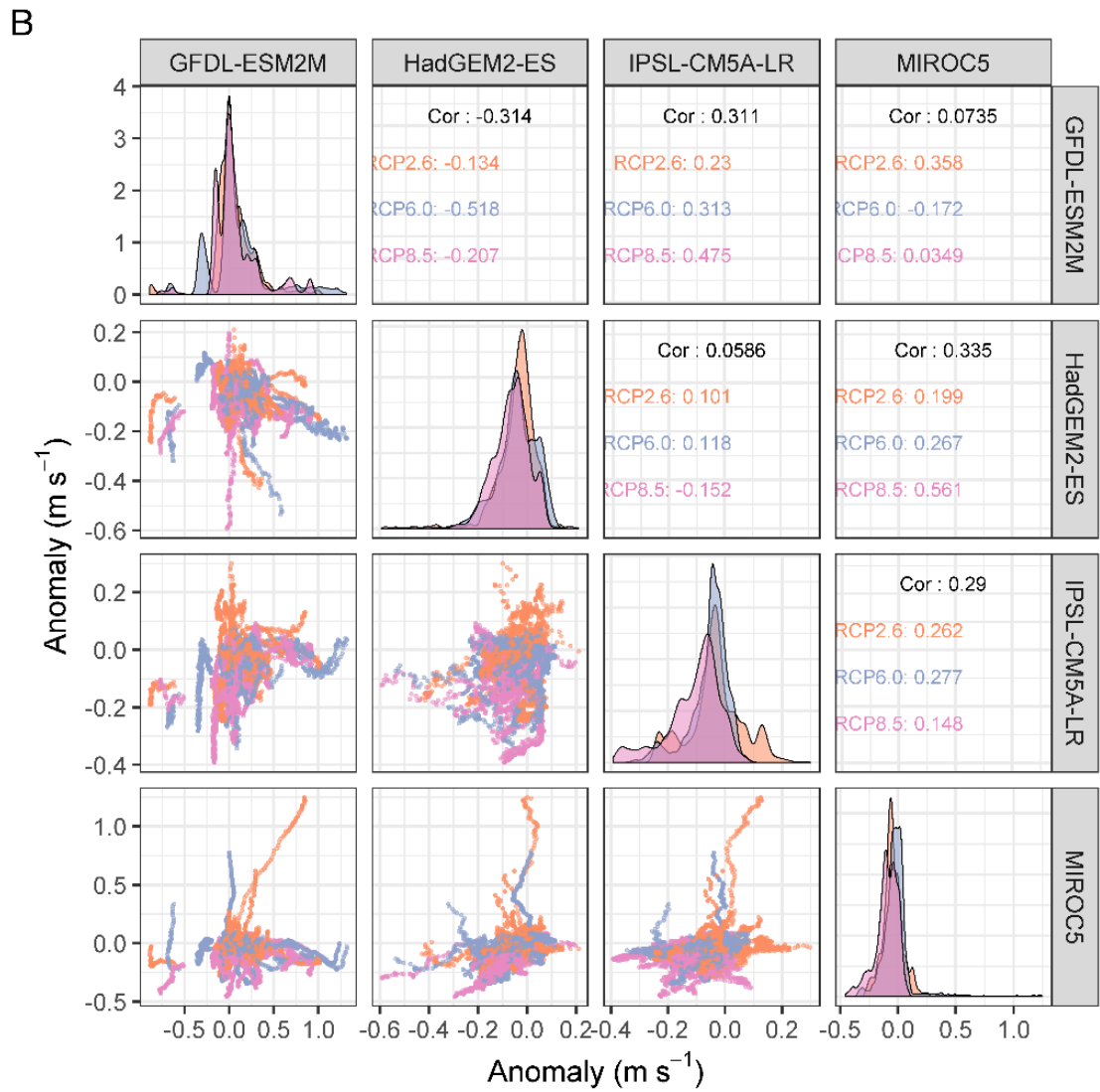


Figure 6.34 Paired scatter plot, distributions and correlations of the 30-year rolling mean anomaly for wind speed for the four GCMs across all 46 lakes from 2036-2099.



biogeochemical models are to produce reliable projections. Overall, these results highlighted that projections of lake temperature anomalies have relatively low uncertainty, while the uncertainty around thermocline depth is still quite large and will require further investigation and model refinement. Further research will be carried out in this area when all the simulations for all lake models for ISIMIP2b have been completed.

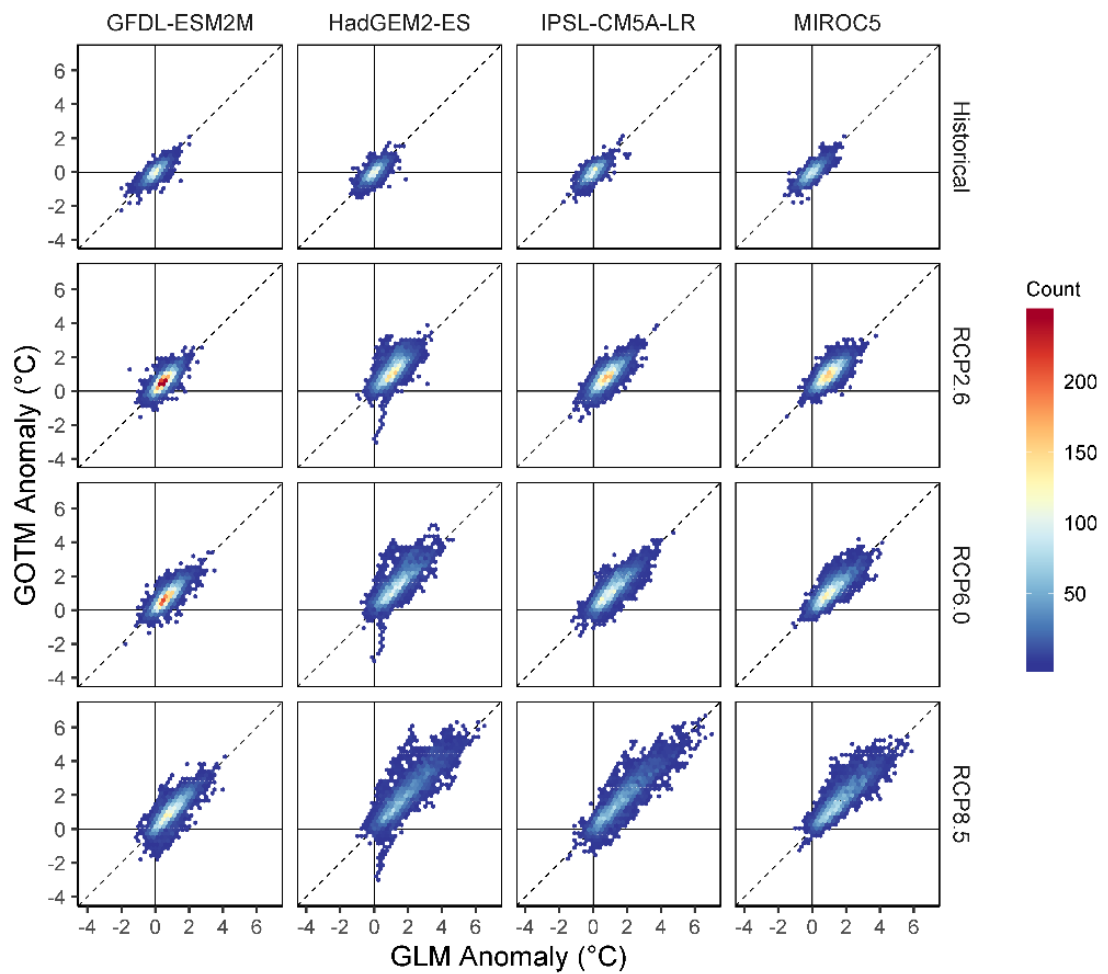


Figure 6.36 Hexagon density scatterplot of annual GOTM anomaly versus GLM anomaly for the four GCMs and for the four scenarios for volumetrically averaged temperature for 46 lakes.

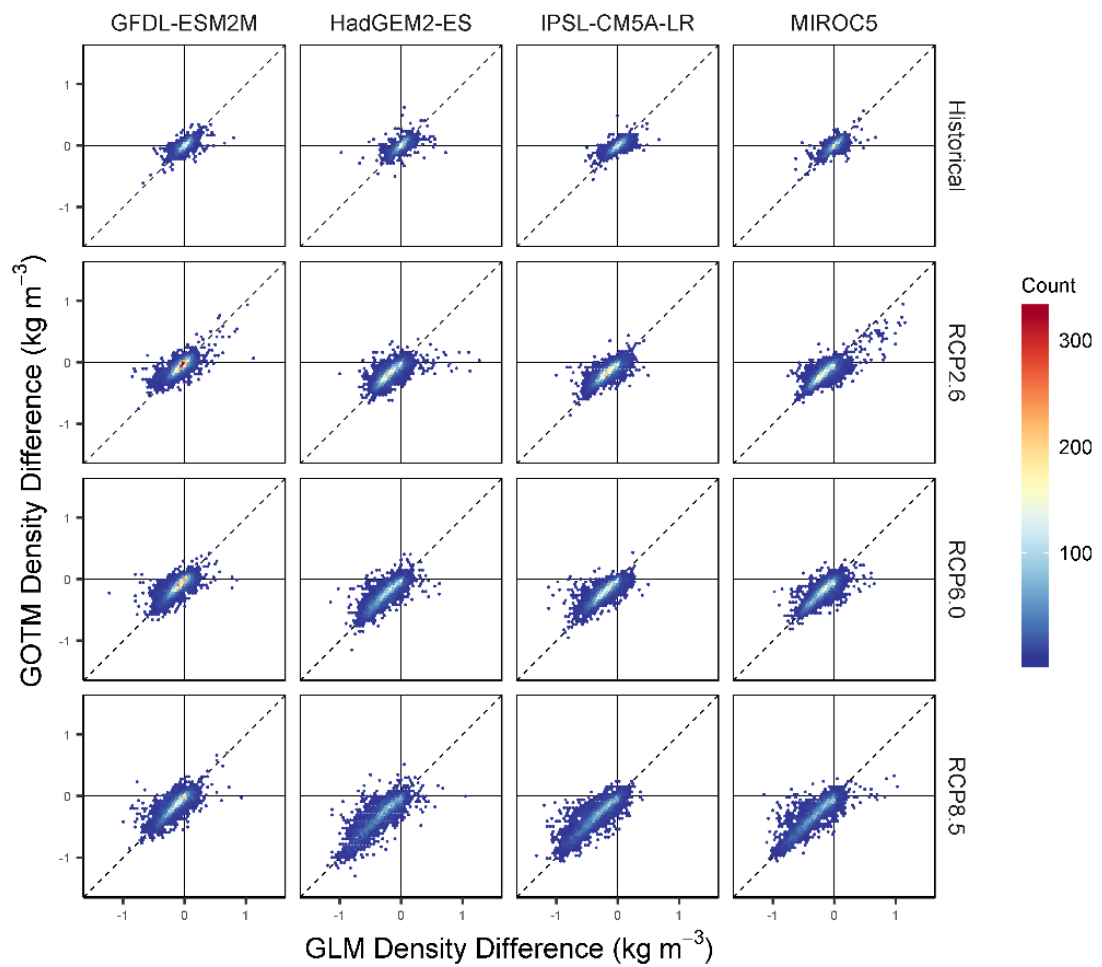


Figure 6.37 Hexagon density scatterplot of annual GOTM anomaly versus GLM anomaly for the four GCMs and for the four scenarios for density difference between the surface and bottom for 46 lakes.

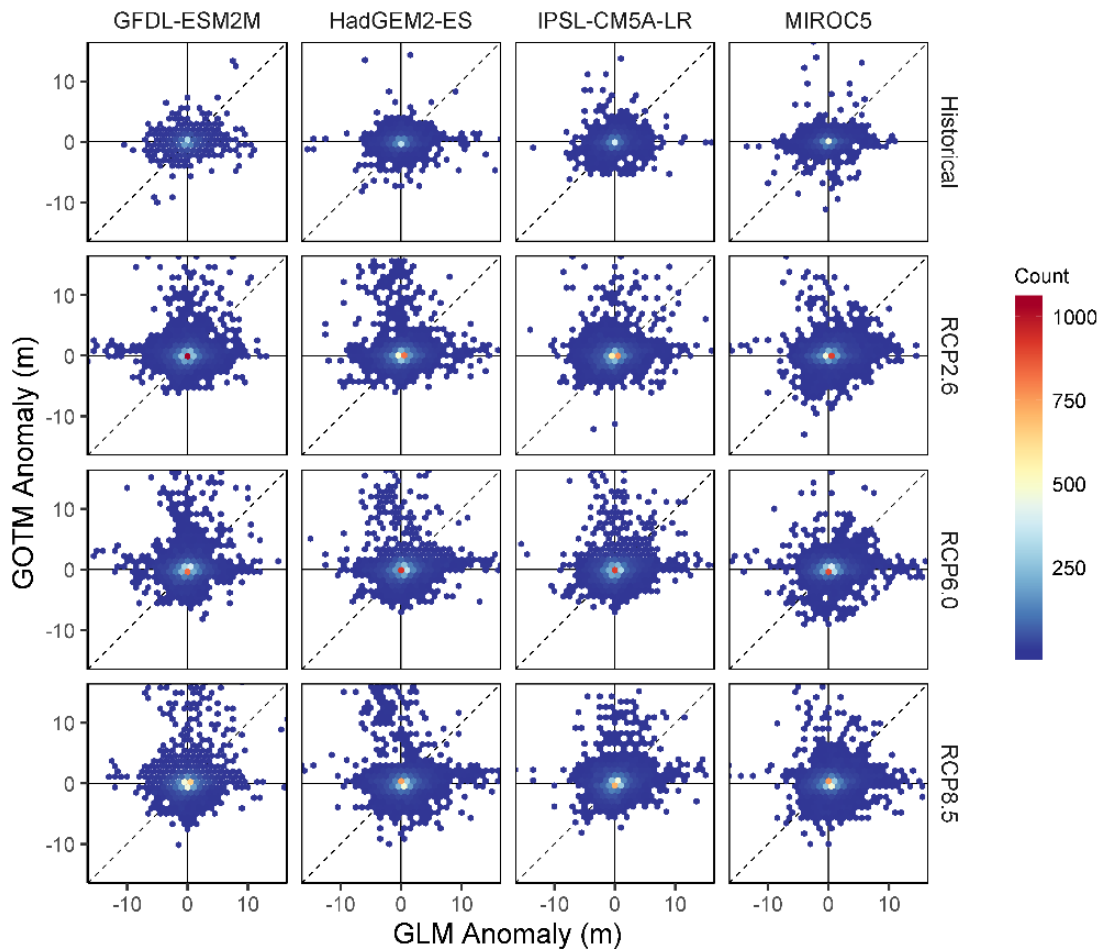


Figure 6.38 Hexagon density scatterplot of annual GOTM anomaly versus GLM anomaly for the four GCMs and for the four scenarios for thermocline depth for 46 lakes.

The Global and Local lake simulations had very similar distributions of annual anomalies for surface and bottom temperatures for six lakes (Figure 6.32). This result, while preliminary, is promising for the Global simulations ability to accurately replicate thermal conditions to a similar degree of accuracy as the local. When working on a global scale, it is imperative that simulations are ‘ground-truthed’ to ensure that the assumptions made e.g. cylinder bathymetry, do not lead to unrealistic results as has been shown for global modelling studies in hydrology (Vörösmarty *et al.*, 1998) and the carbon cycle (Carvalhais *et al.*, 2008). Further comparison between the Global and Local models will

be carried out in the future across other variables, such as stratification, to investigate if there are any potential biases in the global dataset.

It is envisaged that the output from the ISIMIP project will be used to help design policies which affect stakeholders such as lake or reservoir managers for managing hydropower production (Jahandideh-Tehrani *et al.*, 2014), flood risk (Eum *et al.*, 2012) and water supplies (Georgakakos *et al.*, 2012; Sidiropoulos *et al.*, 2013). It is important to remind these potential end-users that the projections within the ISIMIP project are for specific prescribed scenarios which represent potential different changes to radiative forcing on our planet (Moss *et al.*, 2010). While there is uncertainty with regards the trajectory within these scenarios, historical climate models have been shown to be skilful in predicting global mean surface temperature changes, even when accounting for the differences between observed changes in forcing and prescribed changes (Hausfather *et al.*, 2020). The skill of our historical simulations indicates that the model projections produced in our study are highly likely, if there are no concerted global efforts made to reduce emissions (IPCC, 2013). Increases in the strength and duration of stratification pose significant challenges to water resource largely due to increases in the risk of hypoxia at lower depths, internal loading of nutrients and increases in cyanobacteria blooms (Butcher *et al.*, 2015; North *et al.*, 2014). This can particularly affect the quality of drinking water (Delpla *et al.*, 2009) and has led to the development and increased deployment of technologies to aerate and de-stratify lakes and thus reduce these risks (Gerling *et al.*, 2014; Hanh *et al.*, 2017; Smith *et al.*, 2018). This would be a highly expensive mitigation measure that could potentially need to be introduced at sites if the anticipated changes in stratification pose such a threat at sites. Fundamental changes in the lake thermal structure could also drastically reduce the availability of thermal habitat for certain species of cold-water fish (Guzzo and Blanchfield, 2017). This could lead to a shift in habitat range and subsequently a loss of some fish species in some lakes (Hein *et al.*, 2012).

For ISIMIP3, the next round of climate impact modelling projections, there are several recommendations arising from this study that would increase confidence in projections of lake thermal structure. We would strongly recommend against the inclusion of light attenuation as a parameter for calibration because 1) it changes the light regime of the lake and 2) reduces the ability to do a fair comparison between models if

the light attenuation used for the same lake but different models is quite different (Figure 6.10). There are notable dynamic feedbacks that occur between lake biogeochemistry and light where light can decrease as a result of establishment of macrophytes (Su *et al.*, 2019) or increase as a result of nutrient loading, for example phosphorus or nitrogen (Søndergaard *et al.*, 2017). Model parameters used in the calibration protocol should be selected that do not have a large impact on the energy budget of the lake. This would mean not including variables such as scaling factors on incoming short-wave radiation and net surface heat fluxes. Usage of such scaling factors could impact and potentially alter the climate signal. Therefore, an area for future research would be to analyse and quantify the potential impact including such factors has on how climatic trends are transferred into an in-lake response. Ideally, we suggest that incorporating as few model adjustments as necessary would be the best approach. Many of these lake sites have measured meteorological data on-site. Development of a bias-correction method for each site to be applied to each GCM would allow further reduction in uncertainty rather than using EWEMBI as was carried out by Shatwell *et al.* (2019). We also assumed a fixed water level for each of the lakes which potentially was one of the reasons for poor calibration for some lakes but also it is an unrealistic assumption to neglect the flow of water in these systems. We would recommend that, particularly for lakes which have large water level fluctuations and/or short residence times, that a protocol for inflow and outflow calculation is developed which could be a relatively simple format of having inflow equal the outflow, or to introduce a seasonal fluctuation if that is strongly pronounced in the lake. It would be of even higher impact if there was a cross-sectoral integration of the ISIMIP regional hydrological modelling group to produce inflows for the lake simulations, otherwise using a simple lumped hydrological model could be driven by the GCM's to produce scenario relevant inflows.

## 6.6. Conclusion

This study is the first to apply multiple complex dynamic models to project global lake thermal responses to climate change. The ensemble modelling approach has been used for decades for weather forecasting and climate modelling, and is common practise when, for example, in IPCC reports on the potential effects of anthropogenic activities on future

climate. Furthermore, the meteorological and climate modelling communities have, over many years, built up a strong history for observation and model-data sharing hence facilitating ensemble modelling. This can to a large degree be explained by the fact the national meteorological institutes are all members of the World Meteorological Organization and data exchanges are built into the organization charter. The same is not the case for lake-modelling. Sharing of observations and model results is mostly done on a bi-lateral basis through direct/individual contact. Providing an open forum for exchange of observations, numerical models, model configurations and model results is of prime interest to the entire lake-modelling community and is necessary to adequately convey uncertainties in model projections to the wider community. This is even more importance as we aim to mitigate and manage the impacts of climate change on lake ecosystems.

## CHAPTER 7. SYNTHESIS

Inland water bodies are a crucial resource globally with approximately over 50 % of the global population living within 3 km of a freshwater body (Kummu *et al.*, 2011). They hold cultural, recreational, economical and functional importance (Rees, 1997; Sobek *et al.*, 2012; Gallina *et al.*, 2017). Water security is a constant issue in some parts of the world (White *et al.*, 2007; Xia *et al.*, 2007). Provision of potable water and water for irrigation purposes are two fundamental purposes of lakes and reservoirs (Goff and Crow, 2014; Torabi Haghighi and Kløve, 2017). Historical mismanagement of water courses has led to significant degradation of aquatic habitat to a degree where it is highly unlikely they will be able to recover, for example the Aral Sea (Micklin, 2007), the Great Lakes in Africa (Fryer, 1972; Chen *et al.*, 2018) and the Great Lakes in North America (Sproule-Jones, 1999; Kling *et al.*, 2003). Currently, humanity is having to deal with the resultant impacts its actions have left on the Earth's environment, such that we have now entered the Anthropocene (Crutzen, 2006; Lewis and Maslin, 2015). The biosphere is increasingly under pressure as humans disrupt the hydrological cycle (Tapiador *et al.*, 2016; Szilagy, 2018), creating imbalances in the carbon cycle (Curtis and Gough, 2018; Kirschbaum *et al.*, 2019), phosphorus cycle (Filippelli, 2008; Vaccari, 2009) and the nitrogen cycle (Vitousek *et al.*, 1997; Fields, 2004). A rigorous scientific approach which seeks to understand and predict future trajectories in a rapidly changing world is required to meet these management challenges and ensure water security for future generations. Hydrodynamic modelling is central to this effort.

Aquatic ecosystems are particularly sensitive to short-term and long-term meteorological changes (Adrian *et al.*, 2009). One of the reasons is because of water's high specific heat capacity and the non-linear relationship between water temperature and density. This causes water bodies to warm slowly and retain heat for longer periods of time and as water temperature increases, the decrease in density becomes greater. This influences the length and strength of stratification in lakes and reservoirs and governs ecosystem structure. The ability, therefore, to accurately simulate the physical structure of lakes is fundamental to any development of automated predictions of in-lake processes including short-term forecasts or decadal-scale projections (Peng *et al.*, 2019; Shatwell *et al.*, 2019). Such automated workflows are central to the future managements of

precious freshwater resources. The work described in this thesis addresses some of the key issues associated with implementing automated modelling workflows, including efficiency, coverage, uncertainty and accuracy. While gridded climate products have been used as forcing data for 1D hydrodynamic models in several previous studies (e.g. Woolway *et al.*, 2017b), the limitations and uncertainties associated with such an approach have not been rigorously compared against a common benchmark, such as locally observed meteorological data. This was explored in chapter 4. Increased availability of real-time monitoring data offers an opportunity to assimilate observed data into modelling workflows to improve accuracy, and this was demonstrated in chapter 5. Finally, knowledge and modelling expertise gained through the work described in chapters 4 and 5 enabled the work described in chapter 6, a multi-model ensemble approach toward accurately simulating future climate impacts across multiple lake sites on a global scale, which has never been carried out before.

## *7.1. Summary of findings*

### *7.1.1. Temporal and spatial expansion of modelling sites*

The work in chapter 3 of this thesis showed that gridded meteorological datasets, which are freely obtainable on-line, can be used in an uncalibrated model setup to simulate observed water temperature profiles with a high degree of accuracy. The use of gridded data offers many benefits for lake modellers. Firstly, it allows hydrodynamic modelling to be carried out for large areas where there is sparse meteorological data and a large numbers of lake, for example Northern Canada, the Tibetan plateau or Northern Europe (Verpoorter *et al.*, 2014). Secondly, gridded meteorological datasets can be used as a complimentary dataset for occasions when meteorological instrumentation malfunctions and creates gaps in the forcing dataset. Finally, the ECMWF datasets currently cover a relatively long time period from 1979 to the present and it is expected in the near future, that the ERA5 dataset will cover the period 1950 to the present (Copernicus Climate Change Service, 2017). This will present increased opportunities for accurate hindcasting of lake conditions, as in order to understand the implications of future possible changes,

it is necessary to understand the historic state of any site (Hadley *et al.*, 2014; Moras *et al.*, 2019; Piccolroaz *et al.*, 2020). If lake models which have been forced with these gridded datasets simulate lake thermal structure and related physical processes accurately for present day conditions (as demonstrated in chapter 3), it gives greater confidence that a similar degree of accuracy will be obtained for historical time periods using the same forcing data. The work described in chapters 5 and 6 also adds confidence that short term forecasts and future climate projections can accurately simulate in lake dynamics, as they are also generated using gridded meteorological datasets.

This thesis covers research from site specific to large-scale global work. This provided key insights into the trade-offs when approaching such studies. Site specific modelling studies allow for higher levels of detail towards accounting for site specific processes such as inflows, outflows and water level fluctuations as was seen in chapters 4 and 5. While for large global studies, assumptions must be made to reduce the dimensions of complexity which is seen in chapter 6. It is critical, that such assumptions are designed and approached in a way that ensures that the robustness of the study is not compromised. Justification of assumptions is critically important and also having clear and well-defined boundaries to ensure that simulations which fall below a certain level of quality are excluded to prevent spurious and suspect results as was done in chapter 6 through the exclusion of lakes which did not meet a certain criteria. Further research into ways to overcome some of the assumptions made would be hugely beneficial in reducing some sources of uncertainty in large global modelling studies and lend more weight/credibility to such findings.

### *7.1.2. Global limnology*

Global ecology was a term that brought ecological matters to the forefront on a global scale. Global limnology is the effort to build understanding around the processes that affect lakes beyond site-specific in-lake events (Downing, 2009). Efforts have been made to simplify understanding and provide classifications according to a lake type e.g. based on mixing regime or surface water temperature (Lewis, 1983; Maberly *et al.*, 2020b), these generalisations allow for projecting upwards based on lake “type”. Use of such

classifications can be problematic as it goes against the concept of general ecological theory and can introduce further limitations (Kraemer, 2020). Lakes play an important role in many key global cycles e.g. hydrological and carbon cycles. However, many limnological studies are focused on one case study or a small selection of lakes. The ISIMIP Lake Sector is the first globally inter-connected network focused on characterising global impacts of climatic change on lakes *via* a dual-layered approach i.e. global and local simulations (section 6.2.3). Currently, the Lake Sector is in a developmental stage, but this will be an important network to maintain and build upon recent research in global limnology. Expansion of the study focus of that group to include as many lakes as possible is crucially important through inclusion of sites from areas which were not included in this study, for example South America, Central and South East Asia and the African Great Lakes. Also the inclusion of small lakes and ponds is critical because it has been shown that their contribution to the global carbon cycle has been largely underestimated (Downing, 2010).

In chapter 6 the potential applications of this project at a global scale were clearly demonstrated. The use of an ensemble of lake models and GCMs allowed the determination of sources of uncertainty, and therefore levels of confidence, in predictions. While there were differing responses in the meteorological variables, there was a strong cohesive global response for key lake variables e.g. lake surface water temperatures and length of stratification were projected to increase unequivocally under the emissions scenario RCP 6.0. These results highlight that management needs to target both emissions and effects in lakes as resource managers seek to mitigate the negative changes that were identified in this study. The uncertainties related to some lake physical variables (e.g. thermocline depth) and the unmeasured uncertainties as a result of some assumptions (e.g. fixed water levels, unchanging light attenuation, no inflows or outflows) need to be the focus of the next round of simulations. While it can be gleaned from the current results that responses for surface temperatures are relatively clear-cut, further research is needed to reduce the uncertainties in the projected change in lake physical thermal structure.

### 7.1.3. Foundations of predictive limnology

The aim of forecasting is to predict what is probably going to occur in the near future. Unsurprisingly, research in clairvoyancy has so far yielded little to no results. The goal of using a mechanistic model for forecasting is based on the understanding that the model can simulate observed processes. In chapter 5 a simple data assimilation methodology was applied to varying systems and showed how effective it was at reducing error in short-term simulations. For forecasting, predicting the future needs to be communicated in a probabilistic manner to represent the inherent uncertainties that are integrated within (Grounds *et al.*, 2017). Managing these uncertainties is crucially important if the forecasts are to be actionable and to build trust between the end-user and the forecaster. In tandem with this, forecast need is dependent on the service a water body provides, although in these early stages of water temperature forecasts they should be deployed at sites with highly instrumented sites to develop the fundamental principles of lake forecasting.

In contrast to meteorological forecasting, limnological forecasting is not dominated by the “initial conditions” problems that dominates meteorological forecasting. Lakes and reservoirs are well constrained and follow a relatively predictable seasonal cycle. The key benefits of a forecast are the ability to accurately predict episodic events. While this was not the focus of this study, the results highlighted that with high-frequency data the short-term forecasts are extensively improved with such data. Actual observed meteorological data was used in this study, for an actual forecast there will be increased uncertainty when this propagate through this framework. Accuracy in meteorological forecasts has been consistently improving throughout the last 90-years of research. This has been through a combined approach of increases in synoptic weather observations combined with advances in model development with improved data assimilation techniques (Simmons and Hollingsworth, 2002). Therefore, it is important to understand that predictive limnology still must grow and develop. This will allow for: the principles of predictive limnology to develop, identification of research bottlenecks and the expansion of knowledge in this field. At the same time, predictive limnology can utilise the insights from the almost 90-year journey that numerical weather prediction has already been on (Shuman, 1989). This includes the development of strong

collaborative networks to facilitate data and knowledge sharing while also harnessing the power of open source and freely available tools.

## 7.2. An Irish context

This thesis sets the groundwork for establishing a comprehensive regional monitoring and modelling programme which could be part of a more comprehensive management program for lakes and reservoirs. For example, in Ireland 226 lakes are included in the national monitoring program run by the Irish EPA (<https://www.epa.ie/water/wm/lakes/>). This includes all lakes larger than 50 ha (0.5 km<sup>2</sup>) monitored in accordance with the European Commission's WFD 2000/60/EC (European Council, 2000), several of which are used for drinking water. Many of these sites are monitored at a relatively low frequency. It is envisioned that the workflows developed within this study could allow for scaling up and integration of lake modelling into the monitoring of Irish lakes. Setting up of models for monitoring sites has become easier through the development of open-source and well documented tools such as the newly developed open-source R package "*LakeEnsemblR*" which has been collaboratively developed with colleagues in the Aquatic Ecosystem Modelling Network – Junior (AEMON-J) (Moore *et al.*, 2020). This toolset allows the user to set up a modelling study with five different lake models (FLake, GLM, GOTM, Simstrat and MyLake) using a standardised format of model inputs (a prototype of which was used in chapter 4). Using measured historical data (even low frequency as described in chapter 5) models could be calibrated for each Irish lake of interest. If meteorological data are not measured on site, then freely available gridded reanalysis data could be used as forcing data for the model such as ERA5 or ERAI (as demonstrated in chapter 4). A hindcasting experiment using data from ERA5 could provide an extensive resource to accurately recreate the recent historical period in Ireland.

Developing a regional-scale forecasting framework for the above-mentioned 226 Irish lakes could potentially be implemented using the forecasting system described in chapter 5. It would be able to provide forecasts daily across all lakes and the data collected from the monitoring programme could be assimilated at its current collection

frequency to reduce uncertainty around the forecasts. To further understand potential threats and vulnerabilities in a changing climate, long-term multi-decadal projections can be used. These have already been used to produce adaptive management scenarios (Ladwig *et al.*, 2018; Page *et al.*, 2018; Mi *et al.*, 2019; Feldbauer *et al.*, 2020). The expansion of such a network would provide an environmental monitoring body such as the EPA with unprecedented information about past, present and future conditions in Irish lakes. This would allow for more targeted management plans for lakes which are potentially more vulnerable and allow a more cost-efficient allocation of restoration and conservation efforts. Modelling studies at a regional scale have been carried out elsewhere. For example, thousands of lakes across the US Midwest were modelled using GLM for contemporary and future time periods (Read *et al.*, 2014; Winslow *et al.*, 2017a). There is no doubt that the tools described here, including the use of consistent, openly available meteorological data, calibration of models using observed data and projections using an ensemble of lake models, make these regional scale studies more accurate, and computationally efficient.

The Irish EPA have recently released the latest round of global climate simulations as part of the Coupled Model Intercomparison Project phase 6 (CMIP6) (Nolan and McKinstry, 2020). This has been integrated into the Coordinated Regional Downscaling Experiment (CORDEX) Model Intercomparison Project (MIP). This provides high resolution, temporal (6-hourly) and spatial (~79 km horizontal grid spacing) data and could be used to model lakes across Ireland, using a similar framework as described in chapter 6. The impact of climate change could be quantified across lake types. For example, Arctic Char (*Salvelinus alpinus* L.) have been shown to be particularly sensitive to shifts in climate change due to warming water temperatures and shifts in predator-prey interactions (Hein *et al.*, 2012; Jonsson and Setzer, 2015), and are confined to only a small number of Irish lakes (Igoe *et al.*, 2003; Igoe and Hammar, 2004). Modelling future habitat changes in Irish lakes would help to inform the management of this species.

As previously highlighted, the integration of hydrological information into lake modelling workflows is likely to increase their usefulness. Previous hydrological research has been carried out across 37 catchments on the island of Ireland (Broderick *et al.*, 2016) which could potentially be expanded upon using the extensive network of

hydrometric stations around the country maintained by the Office of Public Works (OPW) (OPW, 2020). This could be interconnected with the lake network in Ireland to allow for modelling from catchment to sea. Such a system has been demonstrated in a boreal catchment in Southern Finland and allows for improved estimations of dissolved organic carbon export (Holmberg *et al.*, 2014).

### 7.3. Future research

There are several gaps in the knowledge which have been highlighted by the works in this thesis that warrant further research. The influence of uncertainty in inflow volumes when forecasting was not included in chapter 4 despite one of the sites having a relatively short residence time (Langtjern, NO: ~ 80 days). Inflows and outflows were also not included in the ISIMIP modelling workflow described in chapter 6. Lake inflows can play an important role in determining lake physical structure (Fenocchi *et al.*, 2017; Råman Vinnå *et al.*, 2018). The coupling of open source hydrology modules could significantly increase the accuracy of model simulations in certain lake types. An area of interest would be the integration of hydrology models from the ISIMIP hydrology sector in future lake simulations carried out within the ISIMIP framework. This is of particular importance in geographic areas where water security is an identified risk (Paton *et al.*, 2013; Paton *et al.*, 2014).

Characterising each of the model's sensitivity to lake bathymetry is another area which would benefit from some attention, particularly if models are going to be used for many lakes on a regional scale. Detailed lake bathymetry is only available for a very small proportion of the global lake population, only detailed bathymetry from 2,434 sites globally were included in Messenger *et al.* (2016) from an estimated 1.42 million lakes on the planet. Potentially some of the current generation of 1D models are more sensitive than others to a lack of this data. For example, the FLake model does not require bathymetry, as it uses mean depth. While it has been demonstrated that FLake simulates observed surface data relatively well (Thiery *et al.*, 2014;b Woolway *et al.*, 2017b; Shatwell *et al.*, 2019; Woolway and Merchant, 2019; Woolway *et al.*, 2019), the work

described in this thesis indicates that it has reduced performance at simulating water temperatures at lower depths (chapter 4).

A key area of interest would be the coupling of biogeochemical models with the physical lake models using a forecasting framework as described in chapter 5. Information regarding water quality such as fluxes of dissolved organic carbon and algal blooms is of key importance for water quality managers. Whilst accurate prediction of lake thermodynamics is central to water quality management, detailed information in relation to in-lake biogeochemical processes is also required. Coupling of lake hydrodynamic models with process-based biogeochemical models can be a difficult and onerous task due to the large quantities of data that are required (Janssen *et al.*, 2019). These data, such as inflowing nutrient concentrations of total nitrogen and total phosphorus, may have lower temporal resolution (weekly to monthly) and have a higher uncertainty due to the higher potential for large fluctuations (Nielsen *et al.*, 2014). Despite these limitations, several studies have successfully simulated important biological processes such as phytoplankton dynamics across lakes of varying trophic states (Copetti *et al.*, 2006), biogeochemical variations during floods (Romero *et al.*, 2004), timing of biogeochemical processes (Kara *et al.*, 2012), phytoplankton succession (Kerimoglu *et al.*, 2017), in-lake carbon dynamics (Benoy *et al.*, 2007; Couture *et al.*, 2012), oxygen dynamics (Couture *et al.*, 2015) and methane emissions (Tan and Zhuang, 2015; Tan *et al.*, 2018). The results of these studies indicate that many biogeochemical and ecological dynamics can be modelled successfully, with the next step to include them in the types of forecasting future climate frameworks described in chapters 4 and 5. During the PROGNOS project a Simple EcoLogical Model for the Aquatic environment (SELMA) was developed, which can be used to simulate abundance of zooplankton and phytoplankton groups. A sub-module DOMCAST was also developed for the simulation of the fate of DOM in the lake. Further testing of these models with high resolution data collected at the test sites in chapter 3 would allow for potential application at these sites.

A final area that is currently rapidly evolving is the subject of ecological forecasting. A quick and efficient data assimilation method which considerably reduces the model error in short-term forecasts is described in chapter 5. Further development of a water forecasting framework that accounts for more sources of uncertainty and a more thorough approach to data assimilation than simple direct insertion would be desirable.

The benefits of using Ensemble Kalman filters (EnKF) in modelling has been clearly demonstrated for lake carbon dynamics (Zwart *et al.*, 2019), three-dimensional hydrodynamics (Baracchini *et al.*, 2019), sediment transport modelling (Stroud *et al.*, 2010) and forecasting phytoplankton communities (Page *et al.*, 2018). Such methods allow for partitioning out and quantification of different sources of uncertainty. Uncertainty quantification is crucially important if forecasts are to be actionable (Kirchhoff *et al.*, 2013).

#### *7.4. Personal development*

Lake modelling is a rapidly evolving area of science due to its multitude of applications. A key driver in this field is the emphasis on open-source software, collaborative and networked science. Using these three approaches I was able to advance my own research and contribute back to the community through the development of new methods and tools built using open-source software that are freely available. Emphasis in this regard is key to driving further developments and is critical for science to be reproducible. Through collaborative research I have been able to work with scientists across Europe, North America and Australia as part of the PROGNOSE and WateXr projects. This was critical to helping shape my approach to critical thinking when approaching scientific problems and developing skills in project management. Being part of the Global Lake Ecological Observation Network (GLEON) and AEMON-J helped to integrate myself into networks which are at the forefront of research developments within lake science. I would argue that these three pillars; open-source software, collaborative research and networked science are instrumental in advancing science, but also the fundamental unit that is needed for the field of science to tackle many of the issues facing the world today.

### *7.5. Concluding remarks*

Across the world the ecological status of aquatic ecosystems and particularly lakes are in decline. This thesis has shown how the power of using collaborative open source science is critical in addressing future problems as a result of the unequivocal changes to our climate. Hydrodynamic models can: forecast lake temperature accurately on short-time scales with assimilation of observation data, expand modelling efforts for sites which do not have measured meteorological data and project the potential impacts of future climate conditions on lake thermal structure.

## REFERENCES

- Abatzoglou, J. T. and Williams, A. P. (2016) ‘Impact of anthropogenic climate change on wildfire across western US forests’, *Proceedings of the National Academy of Sciences of the United States of America*, 113(42), pp. 11770–11775. doi: 10.1073/pnas.1607171113.
- Acosta, M., Anguita, M., Fernández-Baldomero, F. J., Ramón, C. L., Schladow, S. G. and Rueda, F. J. (2015) ‘Evaluation of a nested-grid implementation for 3D finite-difference semi-implicit hydrodynamic models’, *Environmental Modelling and Software*, 64, pp. 241–262. doi: 10.1016/j.envsoft.2014.10.015.
- Adrian, R., O’Reilly, C. M., Zagarese, H., Baines, S. B., Hessen, D. O., Keller, W., Livingstone, D. M., Sommaruga, R., Straile, D., Van Donk, E., Weyhenmeyer, G. A., Winderl, M. and A (2009) ‘Lakes as sentinels of climate change’, *Limnology and Oceanography*, 54(6), pp. 2283–2297. doi: 10.4319/lo.2000.45.3.0591.
- Afshar, A., Kazemi, H. and Saadatpour, M. (2011) ‘Particle Swarm Optimization for Automatic Calibration of Large Scale Water Quality Model (CE-QUAL-W2): Application to Karkheh Reservoir, Iran’, *Water Resources Management*, 25(10), pp. 2613–2632. doi: 10.1007/s11269-011-9829-7.
- AghaKouchak, A., Norouzi, H., Madani, K., Mirchi, A., Azarderakhsh, M., Nazemi, A., Nasrollahi, N., Farahmand, A., Mehran, A. and Hasanzadeh, E. (2015) ‘Aral Sea syndrome desiccates Lake Urmia: Call for action’, *Journal of Great Lakes Research*. International Association for Great Lakes Research., 41(1), pp. 307–311. doi: 10.1016/j.jglr.2014.12.007.
- Aguilera, R., Livingstone, D. M., Marcé, R., Jennings, E., Piera, J. and Adrian, R. (2016) ‘Using dynamic factor analysis to show how sampling resolution and data gaps affect the recognition of patterns in limnological time-series’, *Inland Waters*, 6(3), pp. 284–294. doi: 10.5268/IW-6.3.948.
- Albergel, C., Dutra, E., Munier, S., Calvet, J. C., Munoz-Sabater, J., De Rosnay, P. and Balsamo, G. (2018) ‘ERA-5 and ERA-Interim driven ISBA land surface model simulations: Which one performs better?’, *Hydrology and Earth System Sciences*, 22(6), pp. 3515–3532. doi: 10.5194/hess-22-3515-2018.

- Alric, B., Jenny, J. P., Berthon, V., Arnaud, F., Pignol, C., Reyss, J. L., Sabatier, P. and Perga, M. E. (2013) 'Local forcings affect lake zooplankton vulnerability and response to climate warming', *Ecology*, 94(12), pp. 2767–2780. doi: 10.1890/12-1903.1.
- Andersen, M. R., de Eyto, E., Dillane, M., Poole, R. and Jennings, E. (2020) '13 years of storms: An analysis of the effects of storms on lake physics on the Atlantic fringe of Europe', *Water (Switzerland)*, 12(2), pp. 1–21. doi: 10.3390/w12020318.
- Anderson, W. L., Robertson, D. M. and Magnuson, J. J. (1996) 'Evidence of climatic change and projected future change', *Science*, 41(5), pp. 815–821.
- Antenucci, J. P., Imberger, J. and Saggio, A. (2000) 'Seasonal evolution of the basin-scale internal wave field in a large stratified lake', *Limnology and Oceanography*, 45(7), pp. 1621–1638. doi: 10.4319/lo.2000.45.7.1621.
- Arhonditsis, G. B. and Brett, M. T. (2005) 'Eutrophication model for Lake Washington (USA): Part I. Model description and sensitivity analysis', *Ecological Modelling*, 187(2–3), pp. 140–178. doi: 10.1016/j.ecolmodel.2005.01.040.
- Arhonditsis, G. B., Recknagel, F. and Jöhnk, K. D. (2017) 'Process-Based Modeling of Nutrient Cycles and Food-Web Dynamics', in *Ecological Informatics: Data Management and Knowledge Discovery: Third Edition*, pp. 1–482. doi: 10.1007/978-3-319-59928-1.
- Arritt, R. W. (1987) 'The effect of water surface temperature on lake breezes and thermal internal boundary layers', *Boundary-Layer Meteorology*, 40(1–2), pp. 101–125. doi: 10.1007/BF00140071.
- Arvola, L., George, G., Livingstone, D. M., Järvinen, M., Dokulil, M. T., Jennings, E. and Aonghusa, C. N. (2010) 'The Impact of Climate Change on European Lakes', *The Impact of Climate Change on European Lakes*, (June 2014). doi: 10.1007/978-90-481-2945-4.
- Ascough II, J. C., Maier, H. R., Ravalico, J. K. and Strudley, M. W. (2008) 'Future research challenges for incorporation of uncertainty in environmental and ecological decision-making', *Ecological Modelling*, 219, pp. 383–399. doi: 10.1016/j.ecolmodel.2008.07.015.

Auer, M. T., Auer, N. A., Barkdoll, B. B., Bornhorst, T. J., Brooks, C., Dempsey, D., Doskey, P. V., Green, S. A., Hyslop, M. D., Kerfoot, W. C., Mayer, A. S., Perlinger, J. A., Shuchman, R., Urban, N. R. and Watkins, D. W. (2013) *The Great Lakes: Foundations of Physics, Hydrology, Water Chemistry, and Biodiversity, Comprehensive Water Quality and Purification*. Elsevier Ltd. doi: 10.1016/B978-0-12-382182-9.00092-X.

Avila, R., Horn, B., Moriarty, E., Hodson, R. and Moltchanova, E. (2018) 'Evaluating statistical model performance in water quality prediction', *Journal of Environmental Management*. Elsevier Ltd, 206, pp. 910–919. doi: 10.1016/j.jenvman.2017.11.049.

Ayala, A. I., Moras, S. and Pierson, D. C. (2019) 'Simulations of future changes in thermal structure of Lake Erken: Proof of concept for ISIMIP2b lake sector local simulation strategy', *Hydrology and Earth System Sciences Discussions*, (July), pp. 1–25. doi: 10.5194/hess-2019-335.

Bakker, M., Vreeburg, J. H. G., van Schagen, K. M. and Rietveld, L. C. (2013) 'A fully adaptive forecasting model for short-term drinking water demand', *Environmental Modelling and Software*. Elsevier Ltd, 48, pp. 141–151. doi: 10.1016/j.envsoft.2013.06.012.

Balon, E. K. and Coche, A. G. (1974) 'Thermal Properties of Lake Kariba', in *Lake Kariba*. Springer, Dordrecht, pp. 131–163. doi: 10.1007/978-94-010-2334-4\_11.

Balvanera, P. (2019) 'Societal burdens of nature loss', *Science*, 366(6462), pp. 184–185. doi: 10.1126/science.aaz1433.

Baracchini, T., Chu, P. Y., Šukys, J., Lieberherr, G., Wunderle, S., Wüest, A. and Bouffard, D. (2019) 'Data assimilation of in-situ and satellite remote sensing data to 3D hydrodynamic lake models', *Geoscientific Model Development Discussions*, (March), pp. 1–31. doi: 10.5194/gmd-2019-47.

Bardina, J. E., Huang, P. G. and Coakley, T. J. (1997) 'Turbulence modeling validation testing and development', *NASA Technical Memorandum 110446*, (April 1997).

Bastola, S., Murphy, C. and Sweeney, J. (2011) 'The sensitivity of fluvial flood risk in Irish catchments to the range of IPCC AR4 climate change scenarios', *Science of the*

- Total Environment*. Elsevier B.V., 409(24), pp. 5403–5415. doi: 10.1016/j.scitotenv.2011.08.042.
- Bates, B., Kundzewicz, Z., Wu, S. and Palutikof, J. (2008) *Climate change and water. Technical paper of the Intergovernmental Panel on Climate change*. IPCC Secretariat, Geneva. doi: 10.1093/nq/s10-IX.235.507-c.
- Bauer, P., Thorpe, A. and Brunet, G. (2015) ‘The quiet revolution of numerical weather prediction’, *Nature*, 525(7567), pp. 47–55. doi: 10.1038/nature14956.
- Bennington, V., McKinley, G. A., Kimura, N. and Wu, C. H. (2010) ‘General circulation of Lake Superior: Mean, variability, and trends from 1979 to 2006’, *Journal of Geophysical Research: Oceans*, 115(12), pp. 1–14. doi: 10.1029/2010JC006261.
- Benoy, G., Cash, K., McCauley, E. and Wrona, F. (2007) ‘Carbon dynamics in lakes of the boreal forest under a changing climate’, *Environmental Reviews*, 15(NA), pp. 175–189. doi: 10.1139/A07-006.
- Benson, B. J., Magnuson, J. J., Jensen, O. P., Card, V. M., Hodgkins, G., Korhonen, J., Livingstone, D. M., Stewart, K. M., Weyhenmeyer, G. A. and Granin, N. G. (2012) ‘Extreme events, trends, and variability in Northern Hemisphere lake-ice phenology (1855-2005)’, *Climatic Change*, 112(2), pp. 299–323. doi: 10.1007/s10584-011-0212-8.
- Beven, K. J. (2006) ‘A manifesto for the equifinality thesis’, *Journal of Hydrology*, 320, pp. 18–36. doi: 10.1016/j.jhydrol.2005.07.007.
- Beven, K. J. (2012) ‘Causal models as multiple working hypotheses about environmental processes’, *Comptes Rendus - Geoscience*. Academie des sciences, 344(2), pp. 77–88. doi: 10.1016/j.crte.2012.01.005.
- Bhagowati, B. and Ahamad, K. U. (2019) ‘A review on lake eutrophication dynamics and recent developments in lake modeling’, *Ecohydrology and Hydrobiology*. European Regional Centre for Ecohydrology of the Polish Academy of Sciences, 19(1), pp. 155–166. doi: 10.1016/j.ecohyd.2018.03.002.
- Blois, J. L., Zarnetske, P. L., Fitzpatrick, M. C. and Finnegan, S. (2013) ‘Climate change and the past, present, and future of biotic interactions’, *Science*, 341, pp. 499–504. doi: 10.1126/science.1237184.

- Bloom, D. E. and Cadarette, D. (2019) ‘Infectious disease threats in the twenty-first century: Strengthening the global response’, *Frontiers in Immunology*, 10(MAR), pp. 1–12. doi: 10.3389/fimmu.2019.00549.
- Boegman, L., Loewen, M. R., Hamblin, P. F. and Culver, D. A. (2001) ‘Application of a two-dimensional hydrodynamic reservoir model to Lake Erie’, *Canadian Journal of Fisheries and Aquatic Sciences*, 58(5), pp. 858–869. doi: 10.1139/cjfas-58-5-858.
- Boehrer, B. and Schultze, M. (2008) ‘Stratification of lakes’, *Reviews of Geophysics*, 46(2), pp. 1–27. doi: 10.1029/2006RG000210.
- Bogomolov, V., Stepanenko, V. M. and Volodin, E. (2016) ‘Development of lake parametrization in the INMCM climate model’, *IOP Conference Series: Earth and Environmental Science*, 48(1), p. 12005. doi: 10.1088/1755-1315/48/1/012005.
- Bolding, K. and Bruggeman, J. (2020) *parsac: Parallel Sensitivity Analysis and Calibration*. Available at: <https://github.com/BoldingBruggeman/parsac> (Accessed: 7 April 2020).
- Bosilovich, M. G., Chen, J., Robertson, F. R. and Adler, R. F. (2008) ‘Evaluation of global precipitation in reanalyses’, *Journal of Applied Meteorology and Climatology*, 47(9), pp. 2279–2299. doi: 10.1175/2008JAMC1921.1.
- Branco, B. F. and Torgersen, T. (2009) ‘Predicting the onset of thermal stratification in shallow inland waterbodies’, *Aquatic Sciences*, 71(1), pp. 65–79. doi: 10.1007/s00027-009-8063-3.
- Broderick, C., Matthews, T., Wilby, R. L., Bastola, S. and Murphy, C. (2016) ‘Transferability of hydrological models and ensemble averaging methods between contrasting climatic periods’, *Water Resources Research*, 52, pp. 8243–8373. doi: 10.1111/j.1752-1688.1969.tb04897.x.
- Bruce, L. C. *et al.* (2018) ‘A multi-lake comparative analysis of the General Lake Model (GLM): Stress-testing across a global observatory network’, *Environmental Modelling & Software*, 102, pp. 274–291. doi: 10.1016/j.envsoft.2017.11.016.
- Bruesewitz, D. A., Carey, C. C., Richardson, D. C. and Weathers, K. C. (2015) ‘Under-ice thermal stratification dynamics of a large, deep lake revealed by high-frequency data’,

*Limnology and Oceanography*, 60(2), pp. 347–359. doi: 10.1002/lno.10014.

Bruggeman, J. and Bolding, K. (2014) ‘A general framework for aquatic biogeochemical models’, *Environmental Modelling and Software*, 61(November), pp. 249–265. doi: 10.1016/j.envsoft.2014.04.002.

Bucak, T., Trolle, D., Tavşanoğlu, N., Çakıroğlu, A. İ., Özen, A., Jeppesen, E. and Beklioğlu, M. (2018) ‘Modeling the effects of climatic and land use changes on phytoplankton and water quality of the largest Turkish freshwater lake: Lake Beyşehir’, *Science of the Total Environment*, 621, pp. 802–816. doi: 10.1016/j.scitotenv.2017.11.258.

Bueche, T., Hamilton, D. P. and Vetter, M. (2017) ‘Using the General Lake Model (GLM) to simulate water temperatures and ice cover of a medium-sized lake: a case study of Lake Ammersee, Germany’, *Environmental Earth Sciences*. Springer Berlin Heidelberg, 76(13). doi: 10.1007/s12665-017-6790-7.

Bueche, T. and Vetter, M. (2014) ‘Simulating water temperatures and stratification of a pre-alpine lake with a hydrodynamic model: Calibration and sensitivity analysis of climatic input parameters’, *Hydrological Processes*, 28(3), pp. 1450–1464. doi: 10.1002/hyp.9687.

Bullock, T. H. (1955) ‘Compensation for Temperature in the Metabolism and Activity of Poikilotherms’, *Biological Reviews*, 30(3), pp. 311–342. doi: 10.1111/j.1469-185X.1955.tb01211.x.

Bunting, L., Leavitt, P. R., Simpson, G. L., Wissel, B., Laird, K. R., Cumming, B. F., St. Amand, A. and Engstrom, D. R. (2016) ‘Increased variability and sudden ecosystem state change in Lake Winnipeg, Canada, caused by 20th century agriculture’, *Limnology and Oceanography*, 61(6), pp. 2090–2107. doi: 10.1002/lno.10355.

Burchard, H. and Baumert, H. Z. (1995) ‘On the performance of a mixed-layer model based on the  $k$ - $\epsilon$  turbulence closure’, *Journal of Geophysical Research*, 100(C5), pp. 8523–8540. doi: 10.1029/94JC03229.

Burchard, H., Bolding, K., Kühn, W., Meister, A., Neumann, T. and Umlauf, L. (2006) ‘Description of a flexible and extendable physical-biogeochemical model system for the

water column’, *Journal of Marine Systems*, 61, pp. 180–211. doi: 10.1016/j.jmarsys.2005.04.011.

Burchard, H., Bolding, K. and Ruiz-Villarreal, M. (1999) *GOTM, a general ocean turbulence model. Theory, implementation and test cases, Technical Report*.

Butcher, J. B., Nover, D., Johnson, T. E. and Clark, C. M. (2015) ‘Sensitivity of lake thermal and mixing dynamics to climate change’, *Climatic Change*, 129, pp. 295–305. doi: 10.1007/s10584-015-1326-1.

Butterwick, C., Heaney, S. I. and Talling, J. F. (2005) ‘Diversity in the influence of temperature on the growth rates of freshwater algae, and its ecological relevance’, *Freshwater Biology*, 50(2), pp. 291–300. doi: 10.1111/j.1365-2427.2004.01317.x.

Calton, B., Schellekens, J. and la Torre, A. (2016) ‘Water Resource Reanalysis V1: Data Access And Model Verification Results’. Zenodo. doi: 10.5281/ZENODO.57760.

Cannon, A. J. (2016) ‘Multivariate bias correction of climate model output: Matching marginal distributions and intervariable dependence structure’, *Journal of Climate*, 29(19), pp. 7045–7064. doi: 10.1175/JCLI-D-15-0679.1.

Cannon, A. J. (2018) ‘Multivariate quantile mapping bias correction: an N-dimensional probability density function transform for climate model simulations of multiple variables’, *Climate Dynamics*. Springer Berlin Heidelberg, 50(1–2), pp. 31–49. doi: 10.1007/s00382-017-3580-6.

Cannon, A. J., Sobie, S. R. and Murdock, T. Q. (2015) ‘Bias correction of GCM precipitation by quantile mapping: How well do methods preserve changes in quantiles and extremes?’, *Journal of Climate*, 28(17), pp. 6938–6959. doi: 10.1175/JCLI-D-14-00754.1.

Cantin, A., Beisner, B. E., Gunn, J. M., Prairie, Y. T. and Winter, J. G. (2011) ‘Effects of thermocline deepening on lake plankton communities’, *Canadian Journal of Earth Sciences*, 68(2), pp. 260–276. doi: 10.1139/F10-138.

Capellán-Pérez, I., Arto, I., Polanco-Martínez, J. M., González-Eguino, M. and Neumann, M. B. (2016) ‘Likelihood of climate change pathways under uncertainty on fossil fuel resource availability’, *Energy and Environmental Science*, 9(8), pp. 2482–

2496. doi: 10.1039/c6ee01008c.

Carmack, E. C. (1979) 'Combined influence of inflow and lake temperatures on spring circulation in a riverine lake', *Journal of Physical Oceanography*, pp. 422–434. doi: 10.1175/1520-0485(1979)009<0422:CIOIAL>2.0.CO;2.

Carmack, E. C. and Weiss, R. F. (1991) 'Convection in Lake Baikal: An Example of Thermobaric Instability', *Elsevier Oceanography Series*, 57, pp. 215–228.

Carmack, E. C., Wiegand, R. C., Daley, R. J., Gray, C. B. J., Jasper, S. and Pharo, C. H. (1986) 'Mechanisms influencing the circulation and distribution of water mass in a medium residence-time lake', (2), pp. 249–265.

Carpenter, S. R., Caraco, N. F., Correll, D. L., Howarth, R. W., Sharpley, A. N. and Smith, V. H. (1998) 'Nonpoint Pollution of Surface Waters with Phosphorus and Nitrogen', *Ecological Applications*, 8(3), p. 559. doi: 10.2307/2641247.

Carpenter, S. R., Cole, J. J., Pace, M. L., Batt, R., Brock, W. A., Cline, T., Coloso, J., Hodgson, J. R., Kitchell, J. F., Seekell, D. A., Smith, L. and Weidel, B. (2011) 'Early warnings of regime shifts: A whole-ecosystem experiment', *Science*, 332(6033), pp. 1079–1082. doi: 10.1126/science.1203672.

Carvalhais, N., Reichstein, M., Seixas, J., Colltaz, G. J., Pereira, J. S., Berbigier, P., Carrara, A., Granier, A., Montagnani, L., Papale, D., Rambal, S., Sanz, M. J. and Valentini, R. (2008) 'Implications of the carbon cycle steady state assumption for biogeochemical modeling performance and inverse parameter retrieval', *Global Biogeochemical Cycles*, 22(2), pp. 1–16. doi: 10.1029/2007GB003033.

Castelletti, A., Zaiacomo, M. De, Galelli, S., Restelli, B. M., Sanavia, P., Soncini-Sessaa, R. and Antenucci (2009) 'An emulation modelling approach to reduce the complexity of a 3D hydrodynamic- ecological model of a reservoir', *Proceedings of the 8th International Symposium on Environmental Software Systems 2009*, 8(1), pp. 13–23.

Cattiaux, J., Douville, H. and Peings, Y. (2013) 'European temperatures in CMIP5: Origins of present-day biases and future uncertainties', *Climate Dynamics*, 41(11–12), pp. 2889–2907. doi: 10.1007/s00382-013-1731-y.

Chen, J., Brissette, F. P. and Leconte, R. (2011) 'Uncertainty of downscaling method in

quantifying the impact of climate change on hydrology', *Journal of Hydrology*. Elsevier B.V., 401(3–4), pp. 190–202. doi: 10.1016/j.jhydrol.2011.02.020.

Chen, M., Ye, T. R., Krumholz, L. R. and Jiang, H. L. (2014) 'Temperature and cyanobacterial bloom biomass influence phosphorous cycling in eutrophic lake sediments', *PLoS ONE*, 9(3). doi: 10.1371/journal.pone.0093130.

Chen, X., Zheng, T. and Shuang, C. (2018) 'Analysis of Water Environmental Quality and Monitoring Management in the Great Lakes Basin of East Africa', *Journal of Water Resources Research*, 07(03), pp. 251–258. doi: 10.12677/jwrr.2018.73027.

Cheng, R. T., Powell, T. M. and Dillon, T. M. (1976) 'Numerical models of wind-driven circulation in lakes', *Applied Mathematical Modelling*, 1(3), pp. 141–159. doi: 10.1016/0307-904X(76)90035-4.

Cheung, W. W. L., Jones, M. C., Reygondeau, G., Stock, C. A., Lam, V. W. Y. and Frölicher, T. L. (2016) 'Structural uncertainty in projecting global fisheries catches under climate change', *Ecological Modelling*. Elsevier B.V., 325, pp. 57–66. doi: 10.1016/j.ecolmodel.2015.12.018.

Chung, E. G., Schladow, S. G., Perez-Losada, J. and Robertson, D. M. (2008) 'A linked hydrodynamic and water quality model for the Salton Sea', *Hydrobiologia*, 604, pp. 57–75. doi: 10.1007/978-1-4020-8806-3.

Ciglencečki, I., Janeković, I., Marguš, M., Bura-Nakić, E., Carić, M., Ljubešić, Z., Batistić, M., Hrustić, E., Dupčić, I. and Garić, R. (2014) 'Impacts of extreme weather events on highly eutrophic marine ecosystem (Rogoznica Lake, Adriatic coast)', *Continental Shelf Research*, 108, pp. 144–155. doi: 10.1016/j.csr.2015.05.007.

Clark, N. E., Eber, L., Laurs, R. M., Renner, J. a. and Saur, J. F. T. (1974) 'Heat exchange between ocean and atmosphere in the eastern North Pacific for 1961-71', *NOAA Tech. Rep. NMFS SSRF*, pp. 632–682.

Coats, R., Perez-Losada, J., Schladow, G., Richards, R. and Goldman, C. (2006) 'The warming of Lake Tahoe', *Climatic Change*, 76(1–2), pp. 121–148. doi: 10.1007/s10584-005-9006-1.

Cohn, T. A., Caulder, D. L., Gilroy, J., Zynjuk, L. D. and Summers, R. M. (1992) 'The

Validity of a Simple Statistical Model for Estimating Fluvial Constituent Loads: An Empirical Study Involving Nutrient Loads Entering Chesapeake Bay', *Water Resources Research*, 28(9), pp. 2353–2363.

Collins, M., Booth, B. B. B., Harris, G. R., Murphy, J. M., Sexton, D. M. H. and Webb, M. J. (2006) 'Towards quantifying uncertainty in transient climate change', *Climate Dynamics*, 27(2–3), pp. 127–147. doi: 10.1007/s00382-006-0121-0.

Collins, W. J., Bellouin, N., Doutriaux-Boucher, M., Gedney, N., Halloran, P., Hinton, T., Hughes, J., Jones, C. D., Joshi, M., Liddicoat, S., Martin, G., Connor, F., Rae, J., Senior, C., Sitch, S., Totterdell, I., Wiltshire, A. and Woodward, S. (2011) 'Development and evaluation of an Earth-system model – HadGEM2', *Geoscientific Model Development Discussions*, 4(2), pp. 997–1062. doi: 10.5194/gmdd-4-997-2011.

Copernicus Climate Change Service (2017) *ERA5: Fifth generation of ECMWF atmospheric reanalyses of the global climate*. Copernicus Climate Change Service Climate Data Store (CDS). Available at: <https://cds.climate.copernicus.eu/cdsapp#!/home> (Accessed: 2 February 2020).

Copetti, D., Tartari, G., Morabito, G., Oggioni, A., Legnani, E. and Imberger, J. (2006) 'A biogeochemical model of Lake Pusiano (North Italy) and its use in the predictability of phytoplankton blooms: First preliminary results', *Journal of Limnology*, 65(1), pp. 59–64. doi: 10.4081/jlimnol.2006.59.

Coppin, D. and Bony, S. (2017) 'Internal variability in a coupled general circulation model in radiative-convective equilibrium', *Geophysical Research Letters*, 44(10), pp. 5142–5149. doi: 10.1002/2017GL073658.

Cortés, A., Fleenor, W. E., Wells, M. G., de Vicente, I. and Rueda, F. J. (2014) 'Pathways of river water to the surface layers of stratified reservoirs', *Limnology and Oceanography*, 59(1), pp. 233–250. doi: 10.4319/lo.2014.59.1.0233.

Coulibaly, P. (2010) 'Reservoir Computing approach to Great Lakes water level forecasting', *Journal of Hydrology*. Elsevier B.V., 381(1–2), pp. 76–88. doi: 10.1016/j.jhydrol.2009.11.027.

Coulter, G. W. (1963) 'Hydrology and Biological Production in Lake Tanganyika',

*Limnology and Oceanography*, 8(4), pp. 463–477.

Couture, R. M., de Wit, H. A., Tominaga, K., Kiuru, P. and Markelov, I. (2015) ‘Oxygen dynamics in a boreal lake responds to long-term changes in climate, ice phenology, and DOC inputs’, *Journal of Geophysical Research G: Biogeosciences*, 120(11), pp. 2441–2456. doi: 10.1002/2015JG003065.

Couture, S., Houle, D. and Gagnon, C. (2012) ‘Increases of dissolved organic carbon in temperate and boreal lakes in Quebec, Canada.’, *Environmental science and pollution research international*, 19(2), pp. 361–71. doi: 10.1007/s11356-011-0565-6.

Crawford, T. M. and Duchon, C. E. (1999) ‘An improved parameterization for estimating effective atmospheric emissivity for use in calculating daytime downwelling longwave radiation’, *Journal of Applied Meteorology*, 38(4), pp. 474–480. doi: 10.1175/1520-0450(1999)038<0474:AIPFEE>2.0.CO;2.

Crutzen, P. J. (2006) ‘The anthropocene’, *Earth System Science in the Anthropocene*, pp. 13–18. doi: 10.1007/3-540-26590-2\_3.

Cuddington, K., Fortin, M. J., Gerber, L. R., Hastings, A., Liebhold, A., O’connor, M. and Ray, C. (2013) ‘Process-based models are required to manage ecological systems in a changing world’, *Ecosphere*, 4(2), pp. 1–12. doi: 10.1890/ES12-00178.1.

Curtis, P. S. and Gough, C. M. (2018) ‘Forest aging, disturbance and the carbon cycle’, *New Phytologist*, 219(4), pp. 1188–1193. doi: 10.1111/nph.15227.

Dake, J. M. K. (1972) ‘Evaporative Cooling of a Body Water’, *Water Resources Research*, 8(4), pp. 1087–1091.

Dake, J. M. K. and Harleman, D. R. F. (1969) ‘Thermal stratification in lakes: Analytical and laboratory studies’, *Water Resources Research*, 5(2), pp. 484–495. doi: 10.1029/WR005i002p00484.

Dalton, C., O’Dwyer, B., Taylor, D., de Eyto, E., Jennings, E., Chen, G., Poole, R., Dillane, M. and McGinnity, P. (2014) ‘Anthropocene environmental change in an internationally important oligotrophic catchment on the Atlantic seaboard of western Europe’, *Anthropocene*. Elsevier B.V., 5, pp. 9–21. doi: 10.1016/j.ancene.2014.06.003.

- Daly, K. L., Byrne, R. H., Dickson, A. G., Gallagher, S. M., Perry, M. J. and Tivey, M. K. (2004) 'Chemical and biological sensors for time-series research: Current status and new directions', *Marine Technology Society Journal*, 38(2), pp. 121–143. doi: 10.4031/002533204787522767.
- Daniel, C. J., Ter-Mikaelian, M. T., Wotton, B. M., Rayfield, B. and Fortin, M. J. (2017) 'Incorporating uncertainty into forest management planning: Timber harvest, wildfire and climate change in the boreal forest', *Forest Ecology and Management*. Elsevier B.V., 400, pp. 542–554. doi: 10.1016/j.foreco.2017.06.039.
- Darko, D., Trolle, D., Asmah, R., Bolding, K., Adjei, K. A. and Odai, S. N. (2019) 'Modeling the impacts of climate change on the thermal and oxygen dynamics of Lake Volta', *Journal of Great Lakes Research*. International Association for Great Lakes Research, 45(1), pp. 73–86. doi: 10.1016/j.jglr.2018.11.010.
- Dee, D. *et al.* (2011) 'The ERA-Interim reanalysis: Configuration and performance of the data assimilation system', *Quarterly Journal of the Royal Meteorological Society*, 137(656), pp. 553–597. doi: 10.1002/qj.828.
- DeGaetano, A. T. and Belcher, B. N. (2007) 'Spatial interpolation of daily maximum and minimum air temperature based on meteorological model analyses and independent observations', *Journal of Applied Meteorology and Climatology*, 46(11), pp. 1981–1992. doi: 10.1175/2007JAMC1536.1.
- Delpla, I., Jung, A. V., Baures, E., Clement, M. and Thomas, O. (2009) 'Impacts of climate change on surface water quality in relation to drinking water production', *Environment International*. Elsevier Ltd, 35(8), pp. 1225–1233. doi: 10.1016/j.envint.2009.07.001.
- Deng, B., Liu, S., Xiao, W., Wang, W., Jin, J. and Lee, X. (2013) 'Evaluation of the CLM4 lake model at a large and shallow freshwater lake', *Journal of Hydrometeorology*, 14(2), pp. 636–649. doi: 10.1175/JHM-D-12-067.1.
- Diallo, I., Sylla, M. B., Giorgi, F., Gaye, A. T. and Camara, M. (2012) 'Multimodel GCM-RCM ensemble-based projections of temperature and precipitation over West Africa for the Early 21st Century', *International Journal of Geophysics*, 2012. doi: 10.1155/2012/972896.

- Dibike, Y., Prowse, T., Saloranta, T. and Ahmed, R. (2011) 'Response of Northern Hemisphere lake-ice cover and lake-water thermal structure patterns to a changing climate', *Hydrological Processes*, 29, pp. 2942–2953. doi: 10.1002/hyp.8068.
- Dietze, M. C. (2017) 'Prediction in ecology: A first-principles framework', *Ecological Applications*, 27(7), pp. 2048–2060. doi: 10.1002/eap.1589.
- Dietze, M. C. *et al.* (2018) 'Iterative near-term ecological forecasting: Needs, opportunities, and challenges', *Proceedings of the National Academy of Sciences of the United States of America*, 115(7), pp. 1424–1432. doi: 10.1073/pnas.1710231115.
- Dong, F., Mi, C., Hupfer, M., Lindenschmidt, K. E., Peng, W., Liu, X. and Rinke, K. (2020) 'Assessing vertical diffusion in a stratified lake using a three-dimensional hydrodynamic model', *Hydrological Processes*, 34(5), pp. 1131–1143. doi: 10.1002/hyp.13653.
- Dorner, S., Shi, J. and Swayne, D. (2007) 'Multi-objective modelling and decision support using a Bayesian network approximation to a non-point source pollution model', *Environmental Modelling and Software*, 22(2), pp. 211–222. doi: 10.1016/j.envsoft.2005.07.020.
- Dowd, M. (2006) 'Dynamic Modeling: Introduction', in *Encyclopedia of Environmetrics*. Second. John Wiley & Sons, Ltd., pp. 1–4.
- Downing, A. L. and Truesdale, G. A. (1955) 'Some factors affecting the rate of solution of oxygen in water', *Journal of Applied Chemistry*, 5, pp. 570–581. doi: 10.1002/jctb.5010051008.
- Downing, J. A. (2009) 'Global limnology: up-scaling aquatic services and processes to planet Earth', *SIL Proceedings, 1922-2010*, 30(8), pp. 1149–1166. doi: 10.1080/03680770.2009.11923903.
- Downing, J. A. (2010) 'Emerging global role of small lakes and ponds: Little things mean a lot', *Limnetica*, 29(1), pp. 9–24.
- Duan, Q., Ajami, N. K., Gao, X. and Sorooshian, S. (2007) 'Multi-model ensemble hydrologic prediction using Bayesian model averaging', *Advances in Water Resources*, 30(5), pp. 1371–1386. doi: 10.1016/j.advwatres.2006.11.014.

Dufresne, J. L. *et al.* (2013) *Climate change projections using the IPSL-CM5 Earth System Model: From CMIP3 to CMIP5, Climate Dynamics*. doi: 10.1007/s00382-012-1636-1.

Dunham, J., Rieman, B. and Chandler, G. (2003) 'Influences of Temperature and Environmental Variables on the Distribution of Bull Trout within Streams at the Southern Margin of Its Range', *North American Journal of Fisheries Management*, 23(3), pp. 894–904. doi: 10.1577/m02-028.

Dunne, J. P. *et al.* (2012) 'GFDL's ESM2 global coupled climate-carbon earth system models. Part I: Physical formulation and baseline simulation characteristics', *Journal of Climate*, 25(19), pp. 6646–6665. doi: 10.1175/JCLI-D-11-00560.1.

Dunne, J. P., John, J. G., Shevliakova, S., Stouffer, R. J., Krasting, J. P., Malyshev, S. L., Milly, P. C. D., Sentman, L. T., Adcroft, A. J., Cooke, W., Dunne, K. A., Griffies, S. M., Hallberg, R. W., Harrison, M. J., Levy, H., Wittenberg, A. T., Phillips, P. J. and Zadeh, N. (2013) 'GFDL's ESM2 global coupled climate-carbon earth system models. Part II: Carbon system formulation and baseline simulation characteristics', *Journal of Climate*, 26(7), pp. 2247–2267. doi: 10.1175/JCLI-D-12-00150.1.

Durbach, I. N. and Stewart, T. J. (2012) 'Modeling uncertainty in multi-criteria decision analysis', *European Journal of Operational Research*. Elsevier B.V., 223(1), pp. 1–14. doi: 10.1016/j.ejor.2012.04.038.

Dutra, E., Stepanenko, V. M., Balsamo, G., Viterbo, P., Miranda, P. M. A., Mironov, D. and Schär, C. (2010) 'An offline study of the impact of lakes on the performance of the ECMWF surface scheme', *Boreal Environment Research*, 15(2), pp. 100–112.

EAWAG (2020) *GitHub - Eawag-AppliedSystemAnalysis/Simstrat: Simstrat - 1D lake model*. Available at: <https://github.com/Eawag-AppliedSystemAnalysis/Simstrat> (Accessed: 7 March 2020).

ECMWF (2020) *ERA5*. Available at: <https://www.ecmwf.int/en/forecasts/datasets/reanalysis-datasets/era5> (Accessed: 8 February 2020).

Eden, J. M., Widmann, M., Grawe, D. and Rast, S. (2012) 'Skill, correction, and

downscaling of GCM-simulated precipitation’, *Journal of Climate*, 25(11), pp. 3970–3984. doi: 10.1175/JCLI-D-11-00254.1.

Edinger, J. E., Duttweiler, D. W. and Geyer, J. C. (1968) ‘The Response of Water Temperatures to Meteorological Condition’, *Water Resources Research*, 4(5), pp. 1137–1143.

Elçi, Ş. , (2008) ‘Effects of thermal stratification and mixing on reservoir water quality’, *Limnology*, 9(2), pp. 135–142. doi: 10.1007/s10201-008-0240-x.

Elliott, J. A., McElarney, Y. R. and Allen, M. (2016) ‘The past and future of phytoplankton in the UK’s largest lake, Lough Neagh’, *Ecological Indicators*. Elsevier Ltd, 68, pp. 142–149. doi: 10.1016/j.ecolind.2015.07.015.

Elliott, J. A., Persson, I., Thackeray, S. J. and Blenckner, T. (2007) ‘Phytoplankton modelling of Lake Erken, Sweden by linking the models PROBE and PROTECH’, *Ecological Modelling*, 202(3), pp. 421–426. doi: 10.1016/j.ecolmodel.2006.11.004.

Enstad, L. I., Rygg, K., Haugan, P. M. and Alendal, G. (2008) ‘Dissolution of a CO<sub>2</sub> lake, modeled by using an advanced vertical turbulence mixing scheme’, *International Journal of Greenhouse Gas Control*, 2(4), pp. 511–519. doi: 10.1016/j.ijggc.2008.04.001.

Etemad-Shahidi, A. and Imberger, J. (2001) ‘Anatomy of turbulence in thermally stratified lakes’, *Limnology and Oceanography*, 46(5), pp. 1158–1170. doi: 10.4319/lo.2001.46.5.1158.

Eum, H. Il, Vasan, A. and Simonovic, S. P. (2012) ‘Integrated Reservoir Management System for Flood Risk Assessment Under Climate Change’, *Water Resources Management*, 26(13), pp. 3785–3802. doi: 10.1007/s11269-012-0103-4.

European Council (2000) ‘Directive 2000/60/EC of the European Parliament and of the Council of 23 October 2000 establishing a framework for Community action in the field of water policy’, *Official Journal of the European Union*, 56(C 378), pp. 1–44.

Eyring, V., Bony, S., Meehl, G. A., Senior, C. A., Stevens, B., Stouffer, R. J. and Taylor, K. E. (2016) ‘Overview of the Coupled Model Intercomparison Project Phase 6 (CMIP6) experimental design and organization’, *Geoscientific Model Development*, 9(5), pp.

1937–1958. doi: 10.5194/gmd-9-1937-2016.

de Eyto, E., Jennings, E., Ryder, E., Sparber, K., Dillane, M., Dalton, C. and Poole, R. (2016) ‘Response of a humic lake ecosystem to an extreme precipitation event : physical , chemical , and biological implications’, *Inland Waters*, 6, pp. 483–498. doi: 10.5268/IW-6.4.875.

Fabio, P., Aronica, G. T. and Apel, H. (2010) ‘Towards automatic calibration of 2-D flood propagation models’, *Hydrology and Earth System Sciences*, 14(6), pp. 911–924. doi: 10.5194/hess-14-911-2010.

Fairall, C. W., Bradley, E. F., Rogers, D. P., Edson, J. B. and Young, G. S. (1996) ‘Bulk parameterization of air-sea fluxes for Tropical Ocean-Global Atmosphere Coupled-Ocean Atmosphere Response Experiment’, *Journal of Geophysical Research: Oceans*, 101(C2), pp. 3747–3764. doi: 10.1029/95JC03205.

Falconer, I. R. (1996) ‘Potential impact on human health of toxic cyanobacteria’, *Phycologia*, 35(sup6), pp. 6–11. doi: 10.2216/i0031-8884-35-6s-6.1.

Farley, S. S., Dawson, A., Goring, S. J. and Williams, J. W. (2018) ‘Situating ecology as a big-data science: Current advances, challenges, and solutions’, *BioScience*, 68(8), pp. 563–576. doi: 10.1093/biosci/biy068.

Fasham, M. J. ., Ducklow, H. W. and McKelvie, S. M. (1990) ‘Modeling plankton dynamics in oceanic mixed systems’, *Journal of Marine Research*, pp. 591–639.

Feldbauer, J., Kneis, D., Hegewald, T., Berendonk, T. U. and Petzoldt, T. (2020) ‘Managing climate change in drinking water reservoirs: potentials and limitations of dynamic withdrawal strategies’, *Environmental Sciences Europe*. Springer Berlin Heidelberg, 32(1). doi: 10.1186/s12302-020-00324-7.

Fenocchi, A., Rogora, M., Morabito, G., Marchetto, A., Sibilla, S. and Dresti, C. (2019) ‘Applicability of a one-dimensional coupled ecological-hydrodynamic numerical model to future projections in a very deep large lake (Lake Maggiore, Northern Italy/Southern Switzerland)’, *Ecological Modelling*. Elsevier, 392(December), pp. 38–51. doi: 10.1016/j.ecolmodel.2018.11.005.

Fenocchi, A., Rogora, M., Sibilla, S., Ciampittiello, M. and Dresti, C. (2018)

‘Forecasting the evolution in the mixing regime of a deep subalpine lake under climate change scenarios through numerical modelling (Lake Maggiore, Northern Italy/Southern Switzerland)’, *Climate Dynamics*. Springer Berlin Heidelberg, 0(0), pp. 1–16. doi: 10.1007/s00382-018-4094-6.

Fenocchi, A., Rogora, M., Sibilla, S. and Dresti, C. (2017) ‘Relevance of inflows on the thermodynamic structure and on the modeling of a deep subalpine lake (Lake Maggiore, Northern Italy/Southern Switzerland)’, *Limnologica - Ecology and Management of Inland Waters*, 63, pp. 42–56. doi: 10.1016/j.limno.2017.01.006.

Fields, A. (2004) ‘Cycling out of Control’, *Environmental health perspectives*, 112(10), pp. 556–563. doi: 10.1016/S0140-6736(05)66830-4.

Filippelli, G. M. (2008) ‘The global phosphorus cycle: Past, present, and future’, *Elements*, 4(2), pp. 89–95. doi: 10.2113/GSELEMENTS.4.2.89.

Finstad, A. G. and Hein, C. L. (2012) ‘Migrate or stay: Terrestrial primary productivity and climate drive anadromy in Arctic char’, *Global Change Biology*, 18(8), pp. 2487–2497. doi: 10.1111/j.1365-2486.2012.02717.x.

Fischer, H. B., List, J. E., Koh, C. R., Imberger, J. and Brooks, N. H. (1979) *Mixing in Inland and Coastal waters, Mixing in Inland and Coastal Waters*.

Foley, B., Jones, I. D., Maberly, S. C. and Rippey, B. (2012) ‘Long-term changes in oxygen depletion in a small temperate lake: Effects of climate change and eutrophication’, *Freshwater Biology*, 57(2), pp. 278–289. doi: 10.1111/j.1365-2427.2011.02662.x.

Foley, J. A. *et al.* (2011) ‘Solutions for a cultivated planet’, *Nature*, 478(7369), pp. 337–342. doi: 10.1038/nature10452.

Fortino, K., Whalen, S. C. and Johnson, C. R. (2014) ‘Relationships between lake transparency, thermocline depth, and sediment oxygen demand in Arctic lakes’, *Inland Waters*, 4(1), pp. 79–90. doi: 10.5268/iw-4.1.597.

Frassl, M. A., Boehrer, B., Holtermann, P. L., Hu, W., Klingbeil, K., Peng, Z., Zhu, J. and Rinke, K. (2018) ‘Opportunities and limits of using meteorological reanalysis data for simulating seasonal to sub-daily water temperature dynamics in a large shallow lake’,

*Water (Switzerland)*, 10(5), pp. 1–17. doi: 10.3390/w10050594.

Fréville, H., Brun, E., Picard, G., Tatarinova, N., Arnaud, L., Lanconelli, C., Reijmer, C. and Van Den Broeke, M. (2014) ‘Using MODIS land surface temperatures and the Crocus snow model to understand the warm bias of ERA-Interim reanalyses at the surface in Antarctica’, *Cryosphere*, 8(4), pp. 1361–1373. doi: 10.5194/tc-8-1361-2014.

Frieler, K. *et al.* (2017) ‘Assessing the impacts of 1.5°C global warming - Simulation protocol of the Inter-Sectoral Impact Model Intercomparison Project (ISIMIP2b)’, *Geoscientific Model Development*, 10(12), pp. 4321–4345. doi: 10.5194/gmd-10-4321-2017.

Fryer, G. (1972) ‘Conservation of the Great Lakes of East Africa: A lesson and a warning’, *Biological Conservation*, 4(4), pp. 256–262. doi: 10.1016/0006-3207(72)90121-8.

Fujino, J., Nair, R., M, K., Masui, T. and Matsuoka, Y. (2006) ‘Multi-gas Mitigation Analysis on Stabilization Scenarios Using Aim Global Model’, *The Energy Journal Special Issue: Multi-Greenhouse Gas Mitigation and Climate Policy*, pp. 343–353.

Fujiwara, M. *et al.* (2017) ‘Introduction to the SPARC Reanalysis Intercomparison Project (S-RIP) and overview of the reanalysis systems’, *Atmospheric Chemistry and Physics*, 17(2), pp. 1417–1452. doi: 10.5194/acp-17-1417-2017.

Gal, G., Hipsey, M. R., Parparov, A., Wagner, U., Makler, V. and Zohary, T. (2009) ‘Implementation of ecological modeling as an effective management and investigation tool: Lake Kinneret as a case study’, *Ecological Modelling*, 220(13–14), pp. 1697–1718. doi: 10.1016/j.ecolmodel.2009.04.010.

Gal, G., Imberger, J., Zohary, T., Antenucci, J., Anis, A. and Rosenberg, T. (2003) ‘Simulating the thermal dynamics of Lake Kinneret’, *Ecological Modelling*, 162(1), pp. 69–86. doi: 10.1016/S0304-3800(02)00380-0.

Gal, G., Makler-Pick, V. and Shachar, N. (2014) ‘Dealing with uncertainty in ecosystem model scenarios: Application of the single-model ensemble approach’, *Environmental Modelling and Software*. Elsevier Ltd, 61, pp. 360–370. doi: 10.1016/j.envsoft.2014.05.015.

- Gallina, N., Beniston, M. and Jacquet, S. (2017) 'Estimating future cyanobacterial occurrence and importance in lakes: a case study with *Planktothrix rubescens* in Lake Geneva', *Aquatic Sciences*, 79(2), pp. 249–263. doi: 10.1007/s00027-016-0494-z.
- Gaudard, A., Schwefel, R., Råman Vinnå, L., Schmid, M., Wüest, A. and Bouffard, D. (2017) 'Optimizing the parameterization of deep mixing and internal seiches in one-dimensional hydrodynamic models: A case study with Simstrat v1.3', *Geoscientific Model Development*, 10(9), pp. 3411–3423. doi: 10.5194/gmd-10-3411-2017.
- Gauthier, J., Prairie, Y. T. and Beisner, B. E. (2014) 'Thermocline deepening and mixing alter zooplankton phenology, biomass and body size in a whole-lake experiment', *Freshwater Biology*, 59(5), pp. 998–1011. doi: 10.1111/fwb.12322.
- Georgakakos, A. P., Yao, H., Kistenmacher, M., Georgakakos, K. P., Graham, N. E., Cheng, F. Y., Spencer, C. and Shamir, E. (2012) 'Value of adaptive water resources management in Northern California under climatic variability and change: Reservoir management', *Journal of Hydrology*. Elsevier B.V., 412–413, pp. 34–46. doi: 10.1016/j.jhydrol.2011.04.038.
- Gerea, M., Pérez, G. L., Unrein, F., Soto Cárdenas, C., Morris, D. and Queimaliños, C. (2017) 'CDOM and the underwater light climate in two shallow North Patagonian lakes: evaluating the effects on nano and microphytoplankton community structure', *Aquatic Sciences*, 79(2), pp. 231–248. doi: 10.1007/s00027-016-0493-0.
- Gerling, A. B., Browne, R. G., Gantzer, P. A., Mobley, M. H., Little, J. C. and Carey, C. C. (2014) 'First report of the successful operation of a side stream supersaturation hypolimnetic oxygenation system in a eutrophic, shallow reservoir', *Water Research*. Elsevier Ltd, 67, pp. 129–143. doi: 10.1016/j.watres.2014.09.002.
- Giorgi, F. and Francisco, R. (2000) 'Uncertainties in regional climate change prediction: A regional analysis of ensemble simulations with the HADCM2 coupled AOGCM', *Climate Dynamics*, 16(2–3), pp. 169–182. doi: 10.1007/PL00013733.
- Goff, M. and Crow, B. (2014) 'What is water equity? The unfortunate consequences of a global focus on “drinking water”', *Water International*, 39(2), pp. 159–171. doi: 10.1080/02508060.2014.886355.

Goldman, C. R. (1974) *Eutrophication of Lake Tahoe Emphasizing Water Quality.*, *Ecol Res Ser EPA*.

Gómez-Giraldo, A., Imberger, J. and Antenucci, J. P. (2006) ‘Spatial structure of the dominant basin-scale internal waves in Lake Kinneret’, *Limnology and Oceanography*, 51(1 I), pp. 229–246. doi: 10.4319/lo.2006.51.1.0229.

Goudsmit, G.-H., Burchard, H., Peeters, F. and Wüest, A. (2002) ‘Application of k-ε turbulence models to enclosed basins: The role of internal seiches’, *Journal of Geophysical Research C: Oceans*, 107(12), pp. 23–1. doi: 10.1029/2001jc000954.

Goudsmit, G.-H., Peeters, F., Gloor, M. and Wüest, A. (1997) ‘Boundary versus internal diapycnal mixing in stratified natural’, *Journal of Geophysical Research*, 102, pp. 27903–27914.

Goyette, S., McFarlane, N. A. and Flato, G. M. (2000) ‘Application of the Canadian Regional Climate Model to the Laurentian Great Lakes Region: Implementation of a lake model’, *Atmosphere - Ocean*, 38(3), pp. 481–503. doi: 10.1080/07055900.2000.9649657.

Goyette, S. and Perroud, M. (2012) ‘Interfacing a one-dimensional lake model with a single-column atmospheric model: Application to the deep Lake Geneva, Switzerland’, *Water Resources Research*, 48(4), pp. 1–18. doi: 10.1029/2011WR011223.

Griffiths, K., Michelutti, N., Sugar, M., Douglas, M. S. V. and Smol, J. P. (2017) ‘Ice-cover is the principal driver of ecological change in High Arctic lakes and ponds’, *PLoS ONE*, 12(3). doi: 10.1371/journal.pone.0172989.

Grounds, M. A., Joslyn, S. and Otsuka, K. (2017) ‘Probabilistic Interval Forecasts: An Individual Differences Approach to Understanding Forecast Communication’, *Advances in Meteorology*, 2017. doi: 10.1155/2017/3932565.

Guisado-Pintado, E. and Jackson, D. W. T. (2018) ‘Multi-scale variability of storm Ophelia 2017: The importance of synchronised environmental variables in coastal impact’, *Science of the Total Environment*. The Authors, 630, pp. 287–301. doi: 10.1016/j.scitotenv.2018.02.188.

Guisado-Pintado, E. and Jackson, D. W. T. (2019) ‘Coastal Impact From High-Energy

Events and the Importance of Concurrent Forcing Parameters: The Cases of Storm Ophelia (2017) and Storm Hector (2018) in NW Ireland’, *Frontiers in Earth Science*, 7(August), pp. 1–18. doi: 10.3389/feart.2019.00190.

Guzzo, M. M. and Blanchfield, P. J. (2017) ‘Climate change alters the quantity and phenology of habitat for lake trout (*Salvelinus namaycush*) in small boreal shield lakes’, *Canadian Journal of Fisheries and Aquatic Sciences*, 74(6), pp. 871–884. doi: 10.1139/cjfas-2016-0190.

Haddeland, I., Heinke, J., Biemans, H., Eisner, S., Flörke, M., Hanasaki, N., Konzmann, M., Ludwig, F., Masaki, Y., Schewe, J., Stacke, T., Tessler, Z. D., Wada, Y. and Wisser, D. (2014) ‘Global water resources affected by human interventions and climate change’, *Proceedings of the National Academy of Sciences of the United States of America*, 111(9), pp. 3251–3256. doi: 10.1073/pnas.1222475110.

Hadley, K. R., Paterson, A. M., Stainsby, E. A., Michelutti, N., Yao, H., Rusak, J. A., Ingram, R., McConnell, C. and Smol, J. P. (2014) ‘Climate warming alters thermal stability but not stratification phenology in a small north-temperate lake’, *Hydrological Processes*, 28(26), pp. 6309–6319. doi: 10.1002/hyp.10120.

Haese, R. R. (2006) ‘The biogeochemistry of the air-sea interface’, *Marine Geochemistry*, pp. 241–270. doi: 10.1007/3-540-32144-6\_7.

Hakanson, L. and Boulion, V. V (2002) ‘Empirical and dynamical models to predict the cover, biomass and production of macrophytes in lakes’, *Ecological Modelling*, 151, pp. 213–243.

Hallgren, W., Beaumont, L., Bowness, A., Chambers, L., Graham, E., Holewa, H., Laffan, S., Mackey, B., Nix, H., Price, J., Vanderwal, J., Warren, R. and Weis, G. (2016) ‘The Biodiversity and Climate Change Virtual Laboratory: Where ecology meets big data’, *Environmental Modelling and Software*. Elsevier Ltd, 76, pp. 182–186. doi: 10.1016/j.envsoft.2015.10.025.

Hamilton, D. P. *et al.* (2015) ‘A Global lake ecological observatory network (GLEON) for synthesising high-frequency sensor data for validation of deterministic ecological models’, *Inland Waters*, 5(1), pp. 49–56. doi: 10.5268/IW-5.1.566.

- Hamilton, D. P. and Schladow, S. G. (1997) 'Prediction of water quality in lakes and reservoirs. Part I — Model description', *Ecological Modelling*, 96(1–3), pp. 91–110. doi: 10.1016/S0304-3800(96)00062-2.
- Han, X., Li, H., Liu, Q., Liu, F. and Arif, A. (2019) 'Analysis of influential factors on air quality from global and local perspectives in China', *Environmental Pollution*. Elsevier Ltd, 248, pp. 965–979. doi: 10.1016/j.envpol.2019.02.096.
- Hanh, H., Recknagel, F., Meyer, W. and Frizenschaf, J. (2017) 'Modelling the impacts of altered management practices, land use and climate changes on the water quality of the Millbrook catchment- reservoir system in South Australia', *Journal of Environmental Management*. Elsevier Ltd, 202, pp. 1–11. doi: 10.1016/j.jenvman.2017.07.014.
- Hansen, N., Muller, S. D. and Koumoutsakos, P. (2003) 'Reducing the Time Complexity of the Derandomized Evolution Strategy with Covariance Matrix Adaptation (CMA-ES)', *Evolutionary computation*, 11(1), pp. 1–18.
- Hansen, N. and Ostermeier, A. (2001) 'Completely derandomized self-adaptation in evolution strategies.', *Evolutionary computation*, 9(2), pp. 159–195. doi: 10.1162/106365601750190398.
- Hanson, P. C., Weathers, K. C. and Kratz, T. K. (2016) 'Networked lake science: how the Global Lake Ecological Observatory Network (GLEON) works to understand, predict, and communicate lake ecosystem response to global change', *Inland Waters*, 6(4), pp. 543–554. doi: 10.1080/iw-6.4.904.
- Harrison, P. A., Dunford, R. W., Holman, I. P. and Rounsevell, M. D. A. (2016) 'Climate change impact modelling needs to include cross-sectoral interactions', *Nature Climate Change*, 6(9), pp. 885–890. doi: 10.1038/nclimate3039.
- Harsch, E. C. and Rea, D. K. (1982) 'Composition and distribution of suspended sediments in Lake Michigan during summer stratification', *Environmental Geology*. Springer-Verlag, 4(2), pp. 87–98. doi: 10.1007/BF02415763.
- Hasse, L. and Liss, P. S. (1980) 'Gas exchange across the air-sea interface', *Tellus*, 32(5), pp. 470–481. doi: 10.3402/tellusa.v32i5.10602.
- Hatfield, S., Subramanian, A., Palmer, T. and Düben, P. (2018) 'Improving weather

forecast skill through reduced-precision data assimilation', *Monthly Weather Review*, 146(1), pp. 49–62. doi: 10.1175/MWR-D-17-0132.1.

Hausfather, Z., Drake, H. F., Abbott, T. and Schmidt, G. A. (2020) 'Evaluating the Performance of Past Climate Model Projections', *Geophysical Research Letters*, 47(1), pp. 0–3. doi: 10.1029/2019GL085378.

Haylock, M. R., Hofstra, N., Klein Tank, A. M. G., Klok, E. J., Jones, P. D. and New, M. (2008) 'A European daily high-resolution gridded data set of surface temperature and precipitation for 1950-2006', *Journal of Geophysical Research Atmospheres*, 113(20). doi: 10.1029/2008JD010201.

Heathcote, A. J. and Downing, J. A. (2012) 'Impacts of Eutrophication on Carbon Burial in Freshwater Lakes in an Intensively Agricultural Landscape', *Ecosystems*, 15(1), pp. 60–70. doi: 10.1007/s10021-011-9488-9.

Hein, C. L., Öhlund, G. and Englund, G. (2012) 'Future distribution of arctic char *Salvelinus alpinus* in Sweden under climate change: Effects of temperature, lake size and species interactions', *Ambio*, 41(SUPPL.3), pp. 303–312. doi: 10.1007/s13280-012-0308-z.

Heiskanen, J. J., Mammarella, I., Ojala, A., Stepanenko, V. M., Erkkilä, K. M., Miettinen, H., Sandström, H., Eugster, W., Leppäranta, M., Järvinen, H., Vesala, T. and Nordbo, A. (2015) 'Effects of water clarity on lake stratification and lake-atmosphere heat exchange', *Journal of Geophysical Research*, 120(15), pp. 7412–7428. doi: 10.1002/2014JD022938.

Helfer, F., Zhang, H. and Lemckert, C. (2011) 'Modelling of lake mixing induced by air-bubble plumes and the effects on evaporation', *Journal of Hydrology*. Elsevier B.V., 406(3–4), pp. 182–198. doi: 10.1016/j.jhydrol.2011.06.020.

Helland, I. P., Freyhof, J., Kasprzak, P. and Mehner, T. (2007) 'Temperature sensitivity of vertical distributions of zooplankton and planktivorous fish in a stratified lake', *Oecologia*, 151(2), pp. 322–330. doi: 10.1007/s00442-006-0541-x.

Henderson-Sellers, B. (1985) 'New formulation of eddy diffusion thermocline models', *Applied Mathematical Modelling*, 9(6), pp. 441–446. doi: 10.1016/0307-

904X(85)90110-6.

Henderson-Sellers, B. (1986) 'Calculating the surface energy balance for lake and reservoir modeling: A review', *Journal of Physical Oceanography*, 24(3), pp. 625–649.

Herb, W. R. and Stefan, H. G. (2004) 'Temperature stratification and mixing dynamics in a shallow lake with submersed macrophytes', *Lake and Reservoir Management*, 20(4), pp. 296–308. doi: 10.1080/07438140409354159.

Herr, A., Dambacher, J. M., Pinkard, E., Glen, M., Mohammed, C. and Wardlaw, T. (2016) 'The uncertain impact of climate change on forest ecosystems - How qualitative modelling can guide future research for quantitative model development', *Environmental Modelling and Software*. Elsevier Ltd, 76, pp. 95–107. doi: 10.1016/j.envsoft.2015.10.023.

Hetherington, A. L., Schneider, R. L., Rudstam, L. G., Gal, G., DeGaetano, A. T. and Walter, M. T. (2015) 'Modeling climate change impacts on the thermal dynamics of polymictic Oneida Lake, New York, United States', *Ecological Modelling*, 300, pp. 1–11. doi: 10.1016/j.ecolmodel.2014.12.018.

Hilt, S., Henschke, I., Rucker, J. and Nixdorf, B. (2010) 'Can submerged macrophytes influence turbidity and trophic state in deep lakes? Suggestions from a case study.', *Journal of environmental quality*, 39(2), pp. 725–33. doi: 10.2134/jeq2009.0122.

Hingsamer, P., Peeters, F. and Hofmann, H. (2014) 'The consequences of internal waves for phytoplankton focusing on the distribution and production of *Planktothrix rubescens*', *PLoS ONE*, 9(8). doi: 10.1371/journal.pone.0104359.

Hipsey, M. R., Bruce, L. C., Boon, C., Busch, B., Carey, C. C., Hamilton, D. P., Hanson, P. C., Read, J. S., Sousa, E. De, Weber, M. and Winslow, L. A. (2019) 'A General Lake Model (GLM 3 . 0) for linking with high-frequency sensor data from the Global Lake Ecological Observatory Network (GLEON)', *Geoscientific Model Development*, (2009).

Hipsey, M. R., Bruce, L. C., Bruggeman, J., Bolding, K. and Hamilton, D. P. (2012) 'GLM-FABM v0.9a Model Overview and User Documentation', (October), p. 44.

Hipsey, M. R., Bruce, L. C. and Hamilton, D. P. (2013) 'Aquatic Ecodynamics (AED) Model Library Science Manual', p. 34. Available at:

[http://aed.see.uwa.edu.au/research/models/AED/Download/AED\\_ScienceManual\\_v4\\_draft.pdf](http://aed.see.uwa.edu.au/research/models/AED/Download/AED_ScienceManual_v4_draft.pdf).

Hipsey, M. R., Bruce, L. C. and Hamilton, D. P. (2014) *General Lake Model v2.0 $\beta$  - Oct 2014*.

Hipsey, M. R. and Hamilton, D. P. (2008) *Computational Aquatic Ecosystem Dynamics Model: CAEDYM v3, Science Manual*.

Ho, J. Y., Afan, H. A., El-Shafie, A. H., Koting, S. B., Mohd, N. S., Jaafar, W. Z. B., Lai Sai, H., Malek, M. A., Ahmed, A. N., Mohtar, W. H. M. W., Elshorbagy, A. and El-Shafie, A. (2019) 'Towards a time and cost effective approach to water quality index class prediction', *Journal of Hydrology*. Elsevier B.V., 575, pp. 148–165. doi: 10.1016/j.jhydrol.2019.05.016.

Hodges, B. R. (2014) *Hydrodynamical Modeling, Reference Module in Earth Systems and Environmental Sciences*. Elsevier Inc. doi: 10.1016/b978-0-12-409548-9.09123-5.

Hodges, B. R., Imberger, J., Laval, B. and Appt, J. (2000) 'Modeling the Hydrodynamics of Stratified Lakes', *Hydroinformatics 2000 Conference*, (July), pp. 23–27.

Hodges, B. R., Imberger, J., Saggio, A. and Winters, K. B. (2000) 'Modeling basin-scale internal waves in a stratified lake', *Limnology and Oceanography*, 45(7), pp. 1603–1620. doi: 10.4319/lo.2000.45.7.1603.

Holland, P. R. and Kay, A. (2003) 'A review of the physics and ecological implications of the thermal bar circulation', *Limnologica*, 33(3), pp. 153–162. doi: 10.1016/S0075-9511(03)80011-7.

Holmberg, M., Futter, M. N., Kotamäki, N., Fronzek, S., Forsius, M., Kiuru, P., Pirttioja, N., Rasmus, K., Starr, M. and Vuorenmaa, J. (2014) 'Effects of changing climate on the hydrology of a boreal catchment and lake DOC - probabilistic assessment of a dynamic model chain', *Boreal Environment Research*, 19(SUPPL. A), pp. 66–82.

Hondzo, M. and Haider, Z. (2004) 'Boundary mixing in a small stratified lake', *Water Resources Research*, 40(3), p. W03101. doi: 10.1029/2002WR001851.

Hondzo, M. and Stefan, H. G. (1993) 'Lake Water Temperature Simulation Model',

*Journal of Hydraulic Engineering*, 119, pp. 1251–1273.

Horsburgh, J. S., Caraballo, J., Ramírez, M., Aufdenkampe, A. K., Arscott, D. B. and Damiano, S. G. (2019) ‘Low-cost, open-source, and low-power: But what to do with the data?’, *Frontiers in Earth Science*, 7(April), pp. 1–14. doi: 10.3389/feart.2019.00067.

Hostetler, S. W. and Bartlein, P. J. (1990) ‘Simulation of lake evaporation with application to modeling lake level variations of Harney-Malheur Lake, Oregon’, *Water Resources Research*, 26(10), pp. 2603–2612. doi: 10.1029/WR026i010p02603.

Hoteit, I., Luo, X. and Pham, D. T. (2012) ‘Particle kalman filtering: A nonlinear bayesian framework for ensemble kalman filters’, *Monthly Weather Review*, 140(2), pp. 528–542. doi: 10.1175/2011MWR3640.1.

Hourdin, F., Foujols, M. A., Codron, F., Guemas, V., Dufresne, J. L., Bony, S., Denvil, S., Guez, L., Lott, F., Ghattas, J., Braconnot, P., Marti, O., Meurdesoif, Y. and Bopp, L. (2013) ‘Impact of the LMDZ atmospheric grid configuration on the climate and sensitivity of the IPSL-CM5A coupled model’, *Climate Dynamics*, 40(9–10), pp. 2167–2192. doi: 10.1007/s00382-012-1411-3.

Hu, F., Bolding, K., Bruggeman, J., Jeppesen, E., Flindt, M. R., Van Gerven, L., Janse, J. H., Janssen, A., Kuiper, J. J., Mooij, W. M. and Trolle, D. (2016) ‘FABM-PCLake - Linking aquatic ecology with hydrodynamics’, *Geoscientific Model Development*, 9(6), pp. 2271–2278. doi: 10.5194/gmd-9-2271-2016.

Huang, A., Rao, Y. R. and Lu, Y. (2010) ‘Evaluation of a 3-D hydrodynamic model and atmospheric forecast forcing using observations in Lake Ontario’, *Journal of Geophysical Research: Oceans*, 115(2), pp. 1–13. doi: 10.1029/2009JC005601.

Hundey, E. J., Russell, S. D., Longstaffe, F. J. and Moser, K. A. (2016) ‘Agriculture causes nitrate fertilization of remote alpine lakes’, *Nature Communications*. Nature Publishing Group, 7, pp. 1–9. doi: 10.1038/ncomms10571.

Hupet, F. and Vanclooster, M. (2001) ‘Effect of the sampling frequency of meteorological variables on the estimation of the reference evapotranspiration’, *Journal of Hydrology*, 243(3–4), pp. 192–204. doi: 10.1016/S0022-1694(00)00413-3.

Hurkmans, R. T. W. L., Moel, H. De, Aerts, J. C. J. H. and Troch, P. A. (2008) ‘Water

- balance versus land surface model in the simulation of Rhine river discharges', *Water Resources Research*, 44, pp. 1–14. doi: 10.1029/2007WR006168.
- Hutchinson, G. E. (1957) *A Treatise on Limnology. Vol 1: Geography, Physics and Chemistry*. John Wiley & Sons.
- Hutchinson, G. E. and Loffler, H. (1956) 'The Thermal Classification of Lakes', *Proceedings of the National Academy of Sciences*, 42(2), pp. 84–86.
- Iammarino, S., Rodriguez-Pose, A. and Storper, M. (2019) 'Regional inequality in Europe: Evidence, theory and policy implications', *Journal of Economic Geography*, 19(2), pp. 273–298. doi: 10.1093/jeg/lby021.
- Idso, S. B. (1973) 'On the concept of lake stability', *Limnology and Oceanography*, 18, pp. 681–683.
- Igoe, F., Grady, M. F. O., Tierney, D. and Fitzmaurice, P. (2003) 'Arctic Char *Salvelinus alpinus* (L.) in Ireland: A Millennium Review of Its Distribution and Status with Conservation Recommendations', *Biology & Environment: Proceedings of the Royal Irish Academy*, 103(1), pp. 9–22.
- Igoe, F. and Hammar, J. (2004) 'The arctic char *Salvelinus alpinus* (L.) species complex in Ireland: A secretive and threatened ice age relict', *Biology and Environment*, 104(3), pp. 73–92. doi: 10.3318/BIOE.2004.104.3.73.
- Imberger, J. (1985) 'The diurnal mixed layer', *Limnology and Oceanography*, 30(4), pp. 737–770.
- Imberger, J. and Hamblin, P. F. (1982) 'Dynamics of lakes, reservoirs, and cooling ponds.', *Annual review of fluid mechanics, Volume 14*, pp. 153–187. doi: 10.1146/annurev.fl.14.010182.001101.
- Imberger, J., Loh, I. C., Hebbert, B. and Patterson, J. C. (1978) 'Dynamics of Reservoir of Medium Size', *Journal of the Hydraulics Division*, 104(5), pp. 725–743.
- Imberger, J., Marti, C. L., Dallimore, C., Hamilton, D. P., Escriba, J. and Valerio, G. (2017) 'Real-Time, Adaptive, Self-Learning Management Of Lakes', *Proceedings of the 37th IAHR World Congress*, 6865(1), pp. 72–86.

Imberger, J. and Patterson, J. C. (1981) 'A dynamic reservoir simulation model-DYRESM:5', in *Transport Models for Inland and Coastal Waters*. Fischer, H. B., Academic Press, New York, pp. 310–361. doi: 10.1017/CBO9781107415324.004.

Imberger, J. and Patterson, J. C. (1989) *Physical Limnology, Advances in Applied Mechanics*. doi: 10.1016/S0065-2156(08)70199-6.

Imboden, D. M. and Wüest, A. (1995) 'Mixing Mechanisms in Lakes', in *Physics and Chemistry of Lakes*, pp. 83–138. doi: 10.1007/978-3-642-85132-2\_4.

IPCC (2013) *Climate Change 2013: The Physical Science Basis. Contribution of Working Group I to the Fifth Assessment Report of the Intergovernmental Panel on Climate Change, CLIMATE CHANGE 2013 - The Physical Science Basis, Contribution of Working Group I to the Fifth Assessment Report of the Intergovernmental Panel on Climate Change*. doi: 10.1017/CBO9781107415324.Summary.

Irvine, K., Free, G., De Eyto, E., White, J., Allott, N. and Mills, P. (2011) 'The EC Water Framework Directive and monitoring lakes in the Republic of Ireland', *Freshwater Forum*, 16(1), pp. 48–64.

Isaac, J. L. and Williams, S. E. (2013) 'Climate Change and Extinctions', *Encyclopedia of Biodiversity: Second Edition*, 2, pp. 73–78. doi: 10.1016/B978-0-12-384719-5.00310-5.

ISIMIP (2019) *ISIMIP2b Simulation Protocol*. Available at: [https://www.isimip.org/documents/393/ISIMIP2b\\_protocol\\_8Aug2019\\_0\\_GeneralInfo.pdf](https://www.isimip.org/documents/393/ISIMIP2b_protocol_8Aug2019_0_GeneralInfo.pdf).

ISIMIP (2020) *ISIMIP -The Inter-Sectoral Impact Model Intercomparison Project*. Available at: <https://www.isimip.org/> (Accessed: 7 April 2020).

Jahandideh-Tehrani, M., Bozorg Haddad, O. and Loáiciga, H. A. (2014) 'Hydropower Reservoir Management Under Climate Change: The Karoon Reservoir System', *Water Resources Management*, 29(3), pp. 749–770. doi: 10.1007/s11269-014-0840-7.

James, W. F., Best, E. P. and Barko, J. W. (2004) 'Sediment resuspension and light attenuation in Peoria Lake: Can macrophytes improve water quality in this shallow system?', *Hydrobiologia*, 515(1), pp. 193–201. doi:

10.1023/B:HYDR.0000027328.00153.b2.

Jankowski, T., Livingstone, D. M., Bühner, H., Forster, R. and Niederhauser, P. (2006) ‘Consequences of the 2003 European heat wave for lake temperature profiles, thermal stability, and hypolimnetic oxygen depletion: Implications for a warmer world’, *Limnology and Oceanography*, 51(2), pp. 815–819. doi: 10.4319/lo.2006.51.2.0815.

Janssen, A. B. G., Janse, J. H., Beusen, A. H., Chang, M., Harrison, J. A., Huttunen, I., Kong, X., Rost, J., Teurlincx, S., Troost, T. A., van Wijk, D. and Mooij, W. M. (2019) ‘How to model algal blooms in any lake on earth’, *Current Opinion in Environmental Sustainability*. Elsevier B.V., 36, pp. 1–10. doi: 10.1016/j.cosust.2018.09.001.

Jassby, A. and Powell, T. (1975) ‘Vertical patterns of eddy diffusion during stratification in Castle Lake, California’, *Limnology and Oceanography*, 20(4), pp. 530–543. doi: 10.4319/lo.1975.20.4.0530.

Jenkin, P. M. (1942) ‘Seasonal Changes in the Temperature of Windermere (English Lake District)’, *British Ecological Society*, 11(2), pp. 248–269.

Jennings, E., de Eyto, E., Laas, A., Pierson, D., Mircheva, G., Naumoski, A., Clarke, A., Healy, M., Šumberová, K. and Langenhaun, D. (2017) ‘The NETLAKE Metadatabase—A Tool to Support Automatic Monitoring on Lakes in Europe and Beyond’, *Limnology and Oceanography Bulletin*, 26(4), pp. 95–100. doi: 10.1002/lob.10210.

Jennings, E., Jones, S., Arvola, L., Staehr, P. A., Gaiser, E., Jones, I. D., Weathers, K. C., Weyhenmeyer, G. A., Chiu, C. Y. and De Eyto, E. (2012) ‘Effects of weather-related episodic events in lakes: an analysis based on high-frequency data’, *Freshwater Biology*, 57(3), pp. 589–601. doi: 10.1111/j.1365-2427.2011.02729.x.

Jeppesen, E., Kronvang, B., Meerhoff, M., Søndergaard, M., Hansen, K. M., Andersen, H. E., Lauridsen, T. L., Liboriussen, L., Beklioglu, M., Özen, A. and Olesen, J. E. (2009) ‘Climate Change Effects on Runoff, Catchment Phosphorus Loading and Lake Ecological State, and Potential Adaptations’, *Journal of Environmental Quality*, 38(5), pp. 1930–1941. doi: 10.2134/jeq2008.0113.

Ji, Z.-G. and Jin, K.-R. (2006) ‘Gyres and Seiches in a Large and Shallow Lake’, *International Association of Great Lakes Research*. Elsevier, 32, pp. 764–775. doi:

10.3394/0380-1330(2006)32.

Jia, H., Xu, T., Liang, S., Zhao, P. and Xu, C. (2018) 'Bayesian framework of parameter sensitivity, uncertainty, and identifiability analysis in complex water quality models', *Environmental Modelling and Software*, 104, pp. 13–26. doi: 10.1016/j.envsoft.2018.03.001.

Jöhnk, K. D., Huisman, J., Sharples, J., Sommeijer, B., Visser, P. M. and Strooms, J. M. (2008) 'Summer heatwaves promote blooms of harmful cyanobacteria', *Global Change Biology*, 14, pp. 495–512. doi: 10.1111/j.1365-2486.2007.01510.x.

Jöhnk, K. D. and Umlauf, L. (2001) 'Modelling the metalimnetic oxygen minimum in a medium sized alpine lake', *Ecological Modelling*, 136(1), pp. 67–80. doi: 10.1016/S0304-3800(00)00381-1.

Jones, C. D. *et al.* (2011) 'The HadGEM2-ES implementation of CMIP5 centennial simulations', *Geoscientific Model Development*, 4(3), pp. 543–570. doi: 10.5194/gmd-4-543-2011.

Jones, P. W. (1999) 'First- and second-order conservative remapping schemes for grids in spherical coordinates', *Monthly Weather Review*, 127(9), pp. 2204–2210. doi: 10.1175/1520-0493(1999)127<2204:FASOCR>2.0.CO;2.

Jonsson, T. and Setzer, M. (2015) 'A freshwater predator hit twice by the effects of warming across trophic levels', *Nature Communications*. Nature Publishing Group, 6(May 2014), pp. 1–9. doi: 10.1038/ncomms6992.

Jørgensen, S. E. (1995) 'State of the art of ecological modelling in limnology', *Ecological Modelling*, 78(1–2), pp. 101–115. doi: 10.1016/0304-3800(94)00120-7.

Kara, E. L. *et al.* (2012) 'Time-scale dependence in numerical simulations: Assessment of physical, chemical, and biological predictions in a stratified lake at temporal scales of hours to months', *Environmental Modelling and Software*, 35, pp. 104–121. doi: 10.1016/j.envsoft.2012.02.014.

Katz, A. and Nishri, A. (2013) 'Calcium, magnesium and strontium cycling in stratified, hardwater lakes: Lake Kinneret (Sea of Galilee), Israel', *Geochimica et Cosmochimica Acta*, 105, pp. 372–394. doi: 10.1016/j.gca.2012.11.045.

- Katz, S. L., Izmet'eva, L. R., Hampton, S. E., Ozersky, T., Shchapov, K., Moore, M. V., Shimaraeva, S. V. and Silow, E. A. (2015) 'The "Melosira years" of Lake Baikal: Winter environmental conditions at ice onset predict under-ice algal blooms in spring', *Limnology and Oceanography*, 60(6), pp. 1950–1964. doi: 10.1002/lno.10143.
- Kendon, E. J., Jones, R. G., Kjellström, E. and Murphy, J. M. (2010) 'Using and designing GCM-RCM ensemble regional climate projections', *Journal of Climate*, 23(24), pp. 6485–6503. doi: 10.1175/2010JCLI3502.1.
- Kerimoglu, O., Jacquet, S., Vinçon-Leite, B., Lemaire, B. J., Rimet, F., Soullignac, F., Trévisan, D. and Anneville, O. (2017) 'Modelling the plankton groups of the deep, peri-alpine Lake Bourget', *Ecological Modelling*, 359, pp. 415–433. doi: 10.1016/j.ecolmodel.2017.06.005.
- Khaki, M., Hoteit, I., Kuhn, M., Awange, J., Forootan, E., van Dijk, A. I. J. M., Schumacher, M. and Pattiaratchi, C. (2017) 'Assessing sequential data assimilation techniques for integrating GRACE data into a hydrological model', *Advances in Water Resources*. Elsevier Ltd, 107, pp. 301–316. doi: 10.1016/j.advwatres.2017.07.001.
- Kiktev, D., Caesar, J., Alexander, L. V., Shiogama, H. and Collier, M. (2007) 'Comparison of observed and multimodeled trends in annual extremes of temperature and precipitation', *Geophysical Research Letters*, 34(10), pp. 2–6. doi: 10.1029/2007GL029539.
- King, J. R., Shuter, B. J. and Zimmerman, A. P. (1997) 'The response of the thermal stratification of South Bay (Lake Huron) to climatic variability', *Canadian Journal of Fisheries and Aquatic Sciences*, 54(8), pp. 1873–1882. doi: 10.1139/cjfas-54-8-1873.
- Kirchhoff, C. J., Carmen Lemos, M. and Dessai, S. (2013) 'Actionable Knowledge for Environmental Decision Making: Broadening the Usability of Climate Science', *Annual Review of Environment and Resources*, 38(1), pp. 393–414. doi: 10.1146/annurev-environ-022112-112828.
- Kirillin, G. (2003) 'Modelling of the shallow lake response to climate variability', *Proceedings 7th International Workshop on Physical Processes in Natural Waters (PPNW2003)*, p. 5.

- Kirk, J. T. O. (1988) ‘Solar heating of water bodies as influenced by their inherent optical properties’, *Journal of Geophysical Research*, 93, pp. 10897–10908.
- Kirschbaum, M. U. F., Zeng, G., Ximenes, F., Giltrap, D. L. and Zeldis, J. R. (2019) ‘Towards a more complete quantification of the global carbon cycle’, *Biogeosciences*, 16(3), pp. 831–846. doi: 10.5194/bg-16-831-2019.
- Klemeš, V. (1986) ‘Operational testing of hydrological simulation models’, *Hydrological Sciences Journal*, 31(1), pp. 13–24. doi: 10.1080/02626668609491024.
- Kling, G. W., Hayhoe, K., Johnson, L. B., Magnuson, J. J., Polasky, S., Robinson, S. K., Shuter, B. J., Wander, M. W., Wuebbles, D. J., Zak, D. R. and Lindroth, R. L. (2003) *Confronting Climate Change in the Great Lakes Region The Union of Concerned Scientists and, Union of Concerned Scientists Cambridge Massachusetts and Ecological Society of America Washington DC*. Available at: <http://scholar.google.com/scholar?hl=en&btnG=Search&q=intitle:Confronting+Climate+Change+in+the+Great+Lakes+Region#0>.
- Kocsis, O., Prandke, H., Stips, A., Simon, A. and Wüest, A. (1999) ‘Comparison of dissipation of turbulent kinetic energy determined from shear and temperature microstructure’, *Journal of Marine Systems*, 21(1–4), pp. 67–84. doi: 10.1016/S0924-7963(99)00006-8.
- Kondo, J. (1975) ‘Air-sea bulk transfer in diabatic’, *Boundary-Layer Meteorology*, 9, pp. 91–112.
- Kosten, S., Huszar, V. L. M., Bécares, E., Costa, L. S., van Donk, E., Hansson, L. A., Jeppesen, E., Kruk, C., Lacerot, G., Mazzeo, N., De Meester, L., Moss, B., Lürling, M., Nöges, T., Romo, S. and Scheffer, M. (2012) ‘Warmer climates boost cyanobacterial dominance in shallow lakes’, *Global Change Biology*, 18(1), pp. 118–126. doi: 10.1111/j.1365-2486.2011.02488.x.
- Kourzeneva, E. (2014) ‘Assimilation of lake water surface temperature observations using an extended Kalman filter’, *Tellus A: Dynamic Meteorology and Oceanography*, 66(1), p. 21510. doi: 10.3402/tellusa.v66.21510.
- Kourzeneva, E., Alesnsio, H., Martin, E. and Faroux, S. (2010) ‘External data for lake

parameterization in numerical weather prediction and climate modeling', *Boreal Environment Research*, 15(2), pp. 165–177. doi: 10.3402/tellusa.v64i0.15640.

Kraemer, B. M. (2020) 'Rethinking discretization to advance limnology amid the ongoing information explosion', *Water Research*. doi: 10.1016/j.watres.2020.115801.

Kraemer, B. M., Anneville, O., Chandra, S., Dix, M., Kuusisto, E., Livingstone, D. M., Rimmer, A., Schladow, S. G., Silow, E., Sitoki, L. M., Tamatamah, R., Vadeboncoeur, Y. and McIntyre, P. B. (2015) 'Morphometry and average temperature affect lake stratification responses to climate change', *Geophysical Research Letters*, 42, pp. 4981–4988. doi: 10.1002/2015GL064097.

Kraemer, B. M., Chandra, S., Dell, A. I., Dix, M., Kuusisto, E., Livingstone, D. M., Schladow, S. G., Silow, E., Sitoki, L. M., Tamatamah, R. and McIntyre, P. B. (2017) 'Global patterns in lake ecosystem responses to warming based on the temperature dependence of metabolism', *Global Change Biology*, 23(5), pp. 1881–1890. doi: 10.1111/gcb.13459.

Kuha, J., Arvola, L., Hanson, P. C., Huotari, J., Huttula, T., Juntunen, J., Järvinen, M., Kallio, K., Ketola, M., Kuoppamäki, K., Lepistö, A., Lohila, A., Paavola, R., Vuorenmaa, J., Winslow, L. A. and Karjalainen, J. (2016) 'Response of boreal lakes to episodic weather-induced events', *Inland Waters*, 6(4), pp. 523–534. doi: 10.5268/IW-6.4.886.

Kumar, D., Kodra, E. and Ganguly, A. R. (2014) 'Regional and seasonal intercomparison of CMIP3 and CMIP5 climate model ensembles for temperature and precipitation', *Climate Dynamics*, 43(9–10), pp. 2491–2518. doi: 10.1007/s00382-014-2070-3.

Kummu, M., de Moel, H., Ward, P. J. and Varis, O. (2011) 'How close do we live to water? a global analysis of population distance to freshwater bodies', *PLoS ONE*, 6(6). doi: 10.1371/journal.pone.0020578.

Laas, A., Nõges, P., Kõiv, T. and Nõges, T. (2012) 'High-frequency metabolism study in a large and shallow temperate lake reveals seasonal switching between net autotrophy and net heterotrophy', *Hydrobiologia*, 694(1), pp. 57–74. doi: 10.1007/s10750-012-1131-z.

- Ladwig, R., Furusato, E., Kirillin, G., Hinkelmann, R. and Hupfer, M. (2018) ‘Climate change demands adaptive management of urban lakes: Model-based assessment of management scenarios for Lake Tegel (Berlin, Germany)’, *Water (Switzerland)*, 10(2). doi: 10.3390/w10020186.
- Laloyaux, P., Balmaseda, M., Dee, D., Mogensen, K. and Janssen, P. (2016) ‘A coupled data assimilation system for climate reanalysis’, *Quarterly Journal of the Royal Meteorological Society*, 142(694), pp. 65–78. doi: 10.1002/qj.2629.
- Lange, S. (2019) *Earth2Observe, WFDEI and ERA-Interim data Merged and Bias-corrected for ISIMIP (EWEMBI)*, GFZ Data Services. doi: 10.5880/pik.2016.004.
- Langsdale, S., Beall, A., Bourget, E., Hagen, E., Kudlas, S., Palmer, R., Tate, D., Werick, W., Beall, A., Bourget, E., Hagen, E., Kudlas, S., Palmer, R. and Tate, D. (2013) ‘Collaborative Modeling for Decision Support in Water Resources’, *American Water Resources Association*, 49(3), pp. 629–638. doi: 10.1111/jawr.12065.
- Larssen, T., Høgåsen, T. and Cosby, B. J. (2007) ‘Impact of time series data on calibration and prediction uncertainty for a deterministic hydrogeochemical model’, *Ecological Modelling*, 207(1), pp. 22–33. doi: 10.1016/j.ecolmodel.2007.03.016.
- Laval, B., Imberger, J., Hodges, B. R. and Stocker, R. (2003) ‘Modeling circulation in lakes: Spatial and temporal variations’, *Limnology and Oceanography*, 48(3), pp. 983–994. doi: 10.4319/lo.2003.48.3.0983.
- Ledesma, J. L. J. and Futter, M. N. (2017) ‘Gridded climate data products are an alternative to instrumental measurements as inputs to rainfall–runoff models’, *Hydrological Processes*, 31(18), pp. 3283–3293. doi: 10.1002/hyp.11269.
- Lemmin, U. (1989) ‘Dynamics of horizontal turbulent mixing in a nearshore zone of Lake Geneva’, *Limnology and Oceanography*, 34(2), pp. 420–434. doi: 10.4319/lo.1989.34.2.0420.
- Lewis, S. L. and Maslin, M. A. (2015) ‘Defining the Anthropocene’, *Nature*. Nature Publishing Group, 519(7542), pp. 171–180. doi: 10.1038/nature14258.
- Lewis, W. M. (1983) ‘A Revised Classification of Lakes Based on Mixing’, *Canadian Journal of Fisheries and Aquatic Sciences*, 40(10), pp. 1779–1787. doi: 10.1139/f83-

Lewis, W. M. (2011) 'Global primary production of lakes: 19th Baldi Memorial Lecture', *Inland Waters*, 1(1), pp. 1–28. doi: 10.5268/iw-1.1.384.

Li-kun, Y., Sen, P., Xin-hua, Z. and Xia, L. (2017) 'Development of a two-dimensional eutrophication model in an urban lake (China) and the application of uncertainty analysis', *Ecological Modelling*. Elsevier B.V., 345, pp. 63–74. doi: 10.1016/j.ecolmodel.2016.11.014.

Li, R., Dong, M., Zhao, Y., Zhang, L., Cui, Q. and He, W. (2007) 'Assessment of Water Quality and Identification of Pollution Sources of Plateau Lakes in Yunnan (China)', *Journal of Environmental Quality*, 36(1), pp. 291–297. doi: 10.2134/jeq2006.0165.

Lindim, C., Becker, A., Grüneberg, B. and Fischer, H. (2015) 'Modelling the effects of nutrient loads reduction and testing the N and P control paradigm in a German shallow lake', *Ecological Engineering*. Elsevier B.V., 82, pp. 415–427. doi: 10.1016/j.ecoleng.2015.05.009.

Lindsay, R., Wensnahan, M., Schweiger, A. and Zhang, J. (2014) 'Evaluation of seven different atmospheric reanalysis products in the arctic', *Journal of Climate*, 27(7), pp. 2588–2606. doi: 10.1175/JCLI-D-13-00014.1.

Lisi, P. J. and Hein, C. L. (2019) 'Eutrophication drives divergent water clarity responses to decadal variation in lake level', *Limnology and Oceanography*, 64, pp. S49–S59. doi: 10.1002/lno.11095.

Liu, W., Li, S., Bu, H., Zhang, Q. and Liu, G. (2012) 'Eutrophication in the Yunnan Plateau lakes: The influence of lake morphology, watershed land use, and socioeconomic factors', *Environmental Science and Pollution Research*, 19(3), pp. 858–870. doi: 10.1007/s11356-011-0616-z.

Liu, W. T., Katsaros, K. B. and Businger, J. A. (1979) 'Bulk parameterization of air-sea exchanges of heat and water vapor including the molecular constraints at the interface.', *Journal of Atmospheric Sciences*, pp. 1722–1735. doi: 10.1175/1520-0469(1979)036<1722:BPOASE>2.0.CO;2.

Liu, Y., Guo, H. and Yang, P. (2010) 'Exploring the influence of lake water chemistry

on chlorophyll a: A multivariate statistical model analysis', *Ecological Modelling*, 221(4), pp. 681–688. doi: 10.1016/j.ecolmodel.2009.03.010.

Liu, Y., Weerts, A. H., Clark, M., Hendricks Franssen, H. J., Kumar, S., Moradkhani, H., Seo, D. J., Schwanenberg, D., Smith, P., Van Dijk, A. I. J. M., Van Velzen, N., He, M., Lee, H., Noh, S. J., Rakovec, O. and Restrepo, P. (2012) 'Advancing data assimilation in operational hydrologic forecasting: Progresses, challenges, and emerging opportunities', *Hydrology and Earth System Sciences*, 16(10), pp. 3863–3887. doi: 10.5194/hess-16-3863-2012.

Livingstone, D. M. (2003) 'Impact of Secular Climate Change on the Thermal Structure of a Large Temperate Central European Lake', *Climatic Change*, 57(1), pp. 205–225.

Lorke, A. (2007) 'Boundary mixing in the thermocline of a large lake', *Journal of Geophysical Research: Oceans*, 112(9), pp. 1–10. doi: 10.1029/2006JC004008.

Lorke, A., Peeters, F. and Bauerle, E. (2006) 'High-frequency internal waves in the littoral zone of a large lake', *Society, American*, 51(2006), pp. 1935–1939. doi: 10.4319/lo.2006.51.4.1935.

Lowe, P. R. (1976) 'An Approximating Polynomial for the Computation of Saturation Vapor Pressure', *Journal of Applied Meteorology*, 16(3), pp. 100–103. doi: 10.1175/1520-0450(1978)017<0413:coapft>2.0.co;2.

Luo, L., Hamilton, D., Lan, J., McBride, C. G. and Trolle, D. (2018) 'Autocalibration of a one-dimensional hydrodynamic-ecological model (DYRESM 4 .0-CAEDYM 3 .1) using a Monte Carlo approach: simulations of hypoxic events in a polymictic lake', *Geoscientific Model Development*, 11, pp. 903–913.

Luo, Y., Tucker, C., Fei, S., Gao, C., LaDeau, S., Clark, J. and Schimel, D. (2011) 'Ecological forecasting and data assimilation in a data-rich era', *Ecological Applications*, 21(5), pp. 1429–1442. doi: 10.2307/23023092.

Maberly, S. C. (1996) 'Diel, episodic and seasonal changes in pH and concentrations of inorganic carbon in a productive lake', *Freshwater Biology*, 35, pp. 579–598.

Maberly, S. C., Donnell, R. A. O., Woolway, R. I., Cutler, M. E. J., Gong, M., Jones, I. D., Merchant, C. J., Miller, C. A., Politi, E., Scott, E. M., Thackeray, S. J. and Tyler, A.

- N. (2020) 'Global lake thermal regions shift under climate change', *Nature Communications*. Springer US, pp. 1–9. doi: 10.1038/s41467-020-15108-z.
- Maberly, S. C., Pitt, J. A., Davies, P. S. and Carvalho, L. (2020) 'Nitrogen and phosphorus limitation and the management of small productive lakes', *Inland Waters*. Taylor & Francis, 0(0), pp. 1–14. doi: 10.1080/20442041.2020.1714384.
- MacCallum, S. N. and Merchant, C. J. (2012) 'Surface water temperature observations of large lakes by optimal estimation', *Canadian Journal of Remote Sensing*, 38(1), pp. 25–45. doi: 10.5589/m12-010.
- MacIntyre, S., Flynn, K. M., Jellison, R. and Romero, J. R. (1999) 'Boundary mixing and nutrient fluxes in Mono Lake, California', *Limnology and Oceanography*, 44(3), pp. 512–529. doi: 10.4319/lo.1999.44.3.0512.
- MacIntyre, S. and Melack, J. M. (1995) 'Vertical and Horizontal Transport in Lakes: Linking Littoral, Benthic, and Pelagic Habitats', *Journal of the North American Benthological Society*, 14(4), pp. 599–615. doi: 10.2307/1467544.
- Magee, M. R. and Wu, C. H. (2017a) 'Effects of changing climate on ice cover in three morphometrically different lakes', *Hydrological Processes*, 31(2), pp. 308–323. doi: 10.1002/hyp.10996.
- Magee, M. R. and Wu, C. H. (2017b) 'Response of water temperatures and stratification to changing climate in three lakes with different morphometry', *Hydrology and Earth System Sciences*, 21(12), pp. 6253–6274. doi: 10.5194/hess-21-6253-2017.
- Magnuson, J. J. (1990) 'Long-Term Ecological Research and the Invisible Present Uncovering the processes hidden because they occur slowly or because effects lag years behind causes', *BioScience*, 40(7), pp. 495–501. doi: 10.2307/1311317.
- Magnuson, J. J., Crowder, L. B. and Medvick, P. A. (1979) 'Temperature as an ecological resource', *American Zoologist*, 19(1), pp. 331–343. doi: 10.1093/icb/19.1.331.
- Magnuson, J. J., Meisner, J. D. and Hill, D. K. (1990) 'Potential Changes in the Thermal Habitat of Great Lakes Fish after Global Climate Warming', *Transactions of the American Fisheries Society*, 119, pp. 254–264. doi: 10.1577/1548-8659(1990)119<0254.

- Maier, H. R., Guillaume, J. H. A., van Delden, H., Riddell, G. A., Haasnoot, M. and Kwakkel, J. H. (2016) ‘An uncertain future, deep uncertainty, scenarios, robustness and adaptation: How do they fit together?’, *Environmental Modelling and Software*. Elsevier Ltd, 81, pp. 154–164. doi: 10.1016/j.envsoft.2016.03.014.
- Manabe, S., Smagorinsky, J. and Strickler, R. F. (1965) ‘Simulated Climatology of a General Circulation Model With a Hydrologic Cycle’, *Monthly Weather Review*, 93(12), pp. 769–798. doi: 10.1175/1520-0493(1965)093<0769:scoage>2.3.co;2.
- Mantzouki, E., Beklioglu, M., Brookes, J. D., Domis, L. N. de S., Dugan, H. A., Doubek, J. P., Grossart, H. P., Nejtgaard, J. C., Pollard, A. I., Ptacnik, R., Rose, K. C., Sadro, S., Seelen, L., Skaff, N. K., Teubner, K., Weyhenmeyer, G. A. and Ibelings, B. W. (2018) ‘Snapshot surveys for lake monitoring, more than a shot in the dark’, *Frontiers in Ecology and Evolution*, 6(NOV), pp. 1–5. doi: 10.3389/fevo.2018.00201.
- Marcé, R. *et al.* (2016) ‘Automatic High Frequency Monitoring for Improved Lake and Reservoir Management’, *Environmental Science and Technology*, 50(20), pp. 10780–10794. doi: 10.1021/acs.est.6b01604.
- Marti, C. L., Mills, R. and Imberger, J. (2011) ‘Pathways of multiple inflows into a stratified reservoir: Thomson Reservoir, Australia’, *Advances in Water Resources*. Elsevier Ltd, 34(5), pp. 551–561. doi: 10.1016/j.advwatres.2011.01.003.
- Martin, J. L. and McCutcheon, S. C. (1999) *Hydrodynamics and Transport for Water Quality Modeling*, Taylor & Francis. doi: 10.1017/CBO9781107415324.004.
- Matthews, T., Murphy, C., McCarthy, G., Broderick, C. and Wilby, R. L. (2018) ‘Super Storm Desmond: A process-based assessment’, *Environmental Research Letters*, 13(1). doi: 10.1088/1748-9326/aa98c8.
- McCombie, A. M. (1959) ‘Some Relations Between Air Temperatures and the Surface Water Temperatures of Lakes’, *Limnology and Oceanography*, 4(3), pp. 252–258. doi: 10.4319/lo.1959.4.3.0252.
- McCormick, M. J. and Scavia, D. (1981) ‘Calculation of vertical profiles of lake-averaged temperature and diffusivity in Lakes Ontario and Washington’, *Water Resources Research*, 17(2), pp. 305–310. doi: 10.1029/WR017i002p00305.

- McCullough, I. M., Cheruvilil, K. S., Collins, S. M. and Soranno, P. A. (2019) 'Geographic patterns of the climate sensitivity of lakes', *Ecological Applications*, 29(2), pp. 1–14. doi: 10.1002/eap.1836.
- McIntosh, B. S. *et al.* (2011) 'Environmental decision support systems (EDSS) development - Challenges and best practices', *Environmental Modelling and Software*. Elsevier Ltd, 26(12), pp. 1389–1402. doi: 10.1016/j.envsoft.2011.09.009.
- McKay, M. D., Beckman, R. J. and Conover, W. J. (2000) 'A comparison of three methods for selecting values of input variables in the analysis of output from a computer code', *Technometrics*, 42(1), pp. 55–61. doi: 10.1080/00401706.2000.10485979.
- McSweeney, C. F. and Jones, R. G. (2016) 'How representative is the spread of climate projections from the 5 CMIP5 GCMs used in ISI-MIP?', *Climate Services*. Elsevier B.V., 1, pp. 24–29. doi: 10.1016/j.cliser.2016.02.001.
- Mechoso, C. R. and Arakawa, A. (2015) *Numerical Models: General Circulation Models*. Second Edi, *Encyclopedia of Atmospheric Sciences: Second Edition*. Second Edi. Elsevier. doi: 10.1016/B978-0-12-382225-3.00157-2.
- Messenger, M. L., Lehner, B., Grill, G., Nedeva, I. and Schmitt, O. (2016) 'Estimating the volume and age of water stored in global lakes using a geo-statistical approach', *Nature Communications*, 7, pp. 1–11. doi: 10.1038/ncomms13603.
- Mi, C., Sadeghian, A., Lindenschmidt, K. E. and Rinke, K. (2019) 'Variable withdrawal elevations as a management tool to counter the effects of climate warming in Germany's largest drinking water reservoir', *Environmental Sciences Europe*. Springer Berlin Heidelberg, 31(1). doi: 10.1186/s12302-019-0202-4.
- Micklin, P. (2007) 'The Aral Sea Disaster', *Annual Review of Earth and Planetary Sciences*, 35(1), pp. 47–72. doi: 10.1146/annurev.earth.35.031306.140120.
- Mieleitner, J. and Reichert, P. (2006) 'Analysis of the transferability of a biogeochemical lake model to lakes of different trophic state', *Ecological Modelling*, 194(1-3 SPEC. ISS.), pp. 49–61. doi: 10.1016/j.ecolmodel.2005.10.039.
- Mikulski, Z. (1973) 'Polish Studies on the Penetration of Solar Radiation Into Lakes', *Hydrological Sciences Bulletin*, 18(3), pp. 303–309. doi: 10.1080/02626667309494040.

- Mironov, D. (2008) ‘Parameterization of Lakes in Numerical Weather Prediction: Description of a Lake Model’, *Reports - COSMO*, 11, p. 47. doi: 10.1103/PhysRevLett.91.139903.
- Mironov, D., Heise, E., Kourzeneva, E., Ritter, B., Schneider, N. and Terzhevik, A. (2010) ‘Implementation of the lake parameterisation scheme FLake into the numerical weather prediction model COSMO’, *Boreal Environment Research*, 15(2), pp. 218–230.
- Mironov, D., Ritter, B., Schulz, J. P., Buchhold, M., Lange, M. and Machulskaya, E. (2012) ‘Parameterisation of sea and lake ice in numerical weather prediction models of the German Weather Service’, *Tellus, Series A: Dynamic Meteorology and Oceanography*, 64(1). doi: 10.3402/tellusa.v64i0.17330.
- Missaghi, S., Hondzo, M. and Herb, W. (2017) ‘Prediction of lake water temperature, dissolved oxygen, and fish habitat under changing climate’, *Climatic Change*. *Climatic Change*, 141(4), pp. 747–757. doi: 10.1007/s10584-017-1916-1.
- Mohr, S. H., Wang, J., Ellem, G., Ward, J. and Giurco, D. (2015) ‘Projection of world fossil fuels by country’, *Fuel*. Elsevier Ltd, 141, pp. 120–135. doi: 10.1016/j.fuel.2014.10.030.
- Le Moigne, P., Colin, J. and Decharme, B. (2016) ‘Impact of lake surface temperatures simulated by the FLake scheme in the CNRM-CM5 climate model’, *Tellus, Series A: Dynamic Meteorology and Oceanography*, 68(1), pp. 1–21. doi: 10.3402/tellusa.v68.31274.
- Mooij, W. M. *et al.* (2010) ‘Challenges and opportunities for integrating lake ecosystem modelling approaches’, *Aquatic Ecology*. Springer Netherlands, 44(3), pp. 633–667. doi: 10.1007/s10452-010-9339-3.
- Moore, T. N., Mesman, J., Ladwig, R., Feldbauer, J., Read, J. S. and Pilla, R. M. (2020) *Run ensemble of lake models in R: Package LakeEnsemblR, GitHub repository*. Available at: <https://github.com/aemon-j/LakeEnsemblR> (Accessed: 14 May 2020).
- Mooring, T. A., Held, I. M. and Wilson, R. J. (2019) ‘Effects of the mean flow on Martian transient eddy activity: Studies with an idealized general circulation model’, *Journal of the Atmospheric Sciences*, 76(8), pp. 2375–2397. doi: 10.1175/JAS-D-18-0247.1.

- Moras, S., Ayala, A. I. and Pierson, D. C. (2019) 'Historical modelling of changes in Lake Erken thermal conditions', *Hydrology and Earth System Sciences*, 23(12), pp. 5001–5016. doi: 10.5194/hess-23-5001-2019.
- Moss, R. *et al.* (2008) *Towards new scenarios for analysis of emissions, climate change, impacts, and response strategies*, Intergovernmental Panel on Climate Change, Geneva.
- Moss, R. H. *et al.* (2010) 'The next generation of scenarios for climate change research and assessment', *Nature*. Nature Publishing Group, 463(7282), pp. 747–756. doi: 10.1038/nature08823.
- Mueller, B. and Seneviratne, S. I. (2014) 'Systematic land climate and evapotranspiration biases in CMIP5 simulations', *Geophysical Research Letters*, 41(1), pp. 128–134. doi: 10.1002/2013GL058055.
- Mueller, H., Hamilton, D. P. and Doole, G. J. (2016) 'Evaluating services and damage costs of degradation of a major lake ecosystem', *Ecosystem Services*. Elsevier, 22, pp. 370–380. doi: 10.1016/j.ecoser.2016.02.037.
- Mukherjee, B., Mukherjee, D. and Nivedita, M. (2008) 'Modelling carbon and nutrient cycling in a simulated pond system at Ranchi', *Ecological Modelling*, 213, pp. 437–448. doi: 10.1016/j.ecolmodel.2008.01.013.
- Murphy, J. M., Sexton, D. M. H., Barnett, D. N., Jones, G. S., Webb, M. J., Collins, M. and Stainforth, D. A. (2004) 'Quantification of modelling uncertainties in a large ensemble of climate change simulations', *Nature*, 430, pp. 768–772. doi: 10.1038/nature02770.1.
- Najah, A., El-shafie, A. and Karim, O. A. (2013) 'Application of artificial neural networks for water quality prediction', *Neural, Computing & Application*, 22, pp. S187–S201. doi: 10.1007/s00521-012-0940-3.
- Nandalal, K. D. W., Piyasiri, S. and Abeysinghe, K. G. A. M. C. S. (2010) 'Forecasting Thermal Stratification of the Victoria Reservoir using a Hydrodynamic Model', *Engineer: Journal of the Institution of Engineers, Sri Lanka*, 43(3), p. 26. doi: 10.4038/engineer.v43i3.6971.
- Nazeer, M. and Nichol, J. E. (2016) 'Development and application of a remote sensing-

based Chlorophyll-a concentration prediction model for complex coastal waters of Hong Kong', *Journal of Hydrology*. Elsevier B.V., 532, pp. 80–89. doi: 10.1016/j.jhydrol.2015.11.037.

Niedrist, G. H., Psenner, R. and Sommaruga, R. (2018) 'Climate warming increases vertical and seasonal water temperature differences and inter-annual variability in a mountain lake', *Climatic Change*. *Climatic Change*, 151(3–4), pp. 473–490. doi: 10.1007/s10584-018-2328-6.

Nielsen, A., Trolle, D., Bjerring, R., Sondergaard, M., Olesen, J. E., Janse, J. H., Mooij, W. M. and Jeppesen, E. (2014) 'Effects of climate and nutrient load on the water quality of shallow lakes assessed through ensemble runs by PCLake', *Ecological Applications*, 24(8), pp. 1926–1944. doi: 10.1890/13-0790.1.

NIVA (2020) *Langtjern*. Available at: <https://www.niva.no/en/services/environmental-monitoring/langtjern> (Accessed: 10 February 2020).

Nolan, A. P. and McKinstry, A. (2020) *EC-Earth Global Climate Simulations - Ireland's Contributions to CMIP6*.

North, R. P., North, R. L., Livingstone, D. M., Köster, O. and Kipfer, R. (2014) 'Long-term changes in hypoxia and soluble reactive phosphorus in the hypolimnion of a large temperate lake: Consequences of a climate regime shift', *Global Change Biology*, 20(3), pp. 811–823. doi: 10.1111/gcb.12371.

O'Dwyer, B., Crockford, L., Jordan, P., Hislop, L. and Taylor, D. (2013) 'A palaeolimnological investigation into nutrient impact and recovery in an agricultural catchment', *Journal of Environmental Management*. Elsevier Ltd, 124, pp. 147–155. doi: 10.1016/j.jenvman.2013.01.034.

O'Reilly, C. M., Rowley, R. J., Schneider, P., Lenters, J. D., Mcintyre, P. B. and Kraemer, B. M. (2015) 'Rapid and highly variable warming of lake surface waters around the globe', *Geophysical Research Letters*, pp. 1–9. doi: 10.1002/2015GL066235. Received.

Obenour, D. R., Gronewold, A. D., Stow, C. A. and Scavia, D. (2014) 'Using a Bayesian hierarchical model to improve Lake Erie cyanobacteria bloom forecasts', *Water*

*Resources Research*, 50, pp. 7847–7860. doi: 10.1002/2014WR015616.Received.

Ogutuhwayo, R., Natugonza, V., Musinguzi, L., Olokotum, M. and Naigaga, S. (2016) ‘Implications of climate variability and change for African lake ecosystems, fisheries productivity, and livelihoods’, *Journal of Great Lakes Research*. International Association for Great Lakes Research., 42(3), pp. 498–510. doi: 10.1016/j.jglr.2016.03.004.

Omlin, M., Brun, R. and Reichert, P. (2001) ‘Biogeochemical model of Lake Zurich: sensitivity, identifiability and uncertainty analysis’, *Ecological Modelling*, 141(1–3), pp. 105–123. doi: 10.1016/S0304-3800(01)00257-5.

OPW (2020) *Realtime waterlevel*. Available at: <https://waterlevel.ie/> (Accessed: 12 April 2020).

Oreskes, N., Shrader-frechette, K. and Belitz, K. (1994) ‘Verification, Validation, and Confirmation of Numerical Models in the Earth Sciences’, *Science*, 263(5147), pp. 641–646.

Otto, I. M., Reckien, D., Reyer, C. P. O., Marcus, R., Le Masson, V., Jones, L., Norton, A. and Serdeczny, O. (2017) ‘Social vulnerability to climate change: a review of concepts and evidence’, *Regional Environmental Change*, 17(6), pp. 1651–1662. doi: 10.1007/s10113-017-1105-9.

Paerl, H. W., Hall, N. S. and Calandrino, E. S. (2011) ‘Controlling harmful cyanobacterial blooms in a world experiencing anthropogenic and climatic-induced change’, *Science of the Total Environment*. Elsevier B.V., 409(10), pp. 1739–1745. doi: 10.1016/j.scitotenv.2011.02.001.

Paerl, H. W. and Huisman, J. (2008) ‘Climate: Blooms like it hot’, *Science*, 320(5872), pp. 57–58. doi: 10.1126/science.1155398.

Page, T., Smith, P. J., Beven, K. J., Jones, I. D., Elliott, J. A., Maberly, S. C., Mackay, E. B., De Ville, M. and Feuchtmayr, H. (2017) ‘Constraining uncertainty and process-representation in an algal community lake model using high frequency in-lake observations’, *Ecological Modelling*. Elsevier B.V., 357, pp. 1–13. doi: 10.1016/j.ecolmodel.2017.04.011.

- Page, T., Smith, P. J., Beven, K. J., Jones, I. D., Elliott, J. A., Maberly, S. C., Mackay, E. B., De Ville, M. and Feuchtmayr, H. (2018) 'Adaptive forecasting of phytoplankton communities', *Water Research*. Elsevier Ltd, 134, pp. 74–85. doi: 10.1016/j.watres.2018.01.046.
- Palmer, M. A., Reidy Liermann, C. A., Nilsson, C., Flörke, M., Alcamo, J., Lake, P. S. and Bond, N. (2008) 'Climate change and the world's river basins: Anticipating management options', *Frontiers in Ecology and the Environment*, 6(2), pp. 81–89. doi: 10.1890/060148.
- Palmer, T. N., Shutts, G. J., Hagedorn, R., Doblas-Reyes, F. J., Jung, T. and Leutbecher, M. (2005) 'Representing Model Uncertainty in Weather and Climate Prediction', *Annual Review of Earth and Planetary Sciences*, 33(1), pp. 163–193. doi: 10.1146/annurev.earth.33.092203.122552.
- Pannell, D. J. (1997) 'Sensitivity analysis of normative economic models : theoretical framework and practical strategies', *Agricultural Economics*, 16, pp. 139–152.
- Parker, W. S. (2016) 'Reanalyses and observations: What's the Difference?', *Bulletin of the American Meteorological Society*, 97(9), pp. 1565–1572. doi: 10.1175/BAMS-D-14-00226.1.
- Parson, E. A., Burkett, V. R., Fisher-Vanden, K., Keith, D. W., Mearns, L. O., Pitcher, H. M., Rosenzweig, C. E. and Webster, M. D. (2007) *Global Change Scenarios: Their Development and Use; Sub-report 2.1B of Synthesis and Assessment Product 2.1, US Climate Change Science Program and the Subcommittee on Global Change Research*. Department of Energy, Office of Biological & Environmental Research, Washington DC.
- Paton, F. L., Dandy, G. C. and Maier, H. R. (2014) 'Integrated framework for assessing urban water supply security of systems with non-traditional sources under climate change', *Environmental Modelling and Software*. Elsevier Ltd, 60, pp. 302–319. doi: 10.1016/j.envsoft.2014.06.018.
- Paton, F. L., Maier, H. R. and Dandy, G. C. (2013) 'Relative magnitudes of sources of uncertainty in assessing climate change impacts on water supply security for the southern Adelaide water supply system', *Water Resources Research*, 49(3), pp. 1643–1667. doi:

10.1002/wrcr.20153.

Paukert, C. P., Glazer, B. A., Hansen, G. J. A., Irwin, B. J., Jacobson, P. C., Kershner, J. L., Shuter, B. J., Whitney, J. E. and Lynch, A. J. (2016) 'Adapting Inland Fisheries Management to a Changing Climate', *Fisheries*, 41(7), pp. 374–384. doi: 10.1080/03632415.2016.1185009.

Paul, S., Ooppelstrup, J., Thunvik, R., Magero, J. M., Walakira, D. D. and Cvetkovic, V. (2019) 'Bathymetry development and flow analyses using two-dimensional numerical modeling approach for lake Victoria', *Fluids*, 4(4). doi: 10.3390/fluids4040182.

Peeters, F., Livingstone, D. M., Goudsmit, G.-H., Kipfer, R. and Forster, R. (2002) 'Modeling 50 years of historical temperature profiles in a large central European lake', *Limnology and Oceanography*, 47(1), pp. 186–197. doi: 10.4319/lo.2002.47.1.0186.

Peeters, F., Straile, D., Lorke, A. and Livingstone, D. M. (2007) 'Earlier onset of the spring phytoplankton bloom in lakes of the temperate zone in a warmer climate', *Global Change Biology*, 13(9), pp. 1898–1909. doi: 10.1111/j.1365-2486.2007.01412.x.

Peng, Z., Hu, W., Liu, G., Zhang, H., Gao, R. and Wei, W. (2019) 'Development and evaluation of a real-time forecasting framework for daily water quality forecasts for Lake Chaohu to Lead time of six days', *Science of the Total Environment*. Elsevier B.V., 687, pp. 218–231. doi: 10.1016/j.scitotenv.2019.06.067.

Perroud, M. and Goyette, S. (2012) 'Interfacing a one-dimensional lake model with a single-column atmospheric model: 2. Thermal response of the deep Lake Geneva, Switzerland under a 2 x CO<sub>2</sub> global climate change', *Water Resources Research*, 48(6), pp. 1–14. doi: 10.1029/2011WR011222.

Perroud, M., Goyette, S., Martynov, A., Beniston, M. and Anneville, O. (2009) 'Simulation of multiannual thermal profiles in deep Lake Geneva: A comparison of one-dimensional lake models', *Limnology and Oceanography*, 54(5), pp. 1574–1594. doi: 10.4319/lo.2009.54.5.1574.

Persaud, B. D., Whitfield, P. H., Quinton, W. L. and Stone, L. E. (2020) 'Evaluating the suitability of three gridded-datasets and their impacts on hydrological simulation at Scotty Creek in the southern Northwest Territories, Canada', *Hydrological Processes*,

34(4), pp. 898–913. doi: 10.1002/hyp.13663.

Piani, C., Haerter, J. O. and Coppola, E. (2010) ‘Statistical bias correction for daily precipitation in regional climate models over Europe’, *Theoretical and Applied Climatology*, 99(1–2), pp. 187–192. doi: 10.1007/s00704-009-0134-9.

Pianosi, F., Beven, K. J., Freer, J., Hall, J. W., Rougier, J., Stephenson, D. B. and Wagener, T. (2016) ‘Sensitivity analysis of environmental models : A systematic review with practical work flow’, *Environmental Modelling and Software*. Elsevier Ltd, 79, pp. 214–232. doi: 10.1016/j.envsoft.2016.02.008.

Piccolroaz, S. (2016) ‘Prediction of lake surface temperature using the air2water model: Guidelines, challenges, and future perspectives’, *Advances in Oceanography and Limnology*, 7(1), pp. 36–50. doi: 10.4081/aiol.2016.5791.

Piccolroaz, S., Amadori, M., Toffolon, M. and Dijkstra, H. A. (2019) ‘Importance of planetary rotation for ventilation processes in deep elongated lakes: Evidence from Lake Garda (Italy)’, *Scientific Reports*. Springer US, 9(1), pp. 1–11. doi: 10.1038/s41598-019-44730-1.

Piccolroaz, S., Healey, N. C., Lenters, J. D., Schladow, S. G., Hook, S. J., Sahoo, G. B. and Toffolon, M. (2018) ‘On the predictability of lake surface temperature using air temperature in a changing climate: A case study for Lake Tahoe (U.S.A.)’, *Limnology and Oceanography*, 63(1), pp. 243–261. doi: 10.1002/lno.10626.

Piccolroaz, S., Woolway, R. I. and Merchant, C. J. (2020) ‘Global reconstruction of twentieth century lake surface water temperature reveals different warming trends depending on the climatic zone’, *Climatic Change*. Climatic Change. doi: 10.1007/s10584-020-02663-z.

Pilati, A. and Wurtsbaugh, W. A. (2003) ‘Importance of zooplankton for the persistence of a deep chlorophyll layer: A limnocorral experiment’, *Limnology and Oceanography*, 48(1 I), pp. 249–260. doi: 10.4319/lo.2003.48.1.0249.

Pilotti, M., Valerio, G., Giardino, C., Bresciani, M. and Chapra, S. C. (2018) ‘Evidence from field measurements and satellite imaging of impact of Earth rotation on Lake Iseo chemistry’, *Journal of Great Lakes Research*. The Authors, 44(1), pp. 14–25. doi:

10.1016/j.jglr.2017.10.005.

Pinel-Alloul, B., Méthot, G. and Malinsky-Rushansky, N. Z. (2004) ‘A short-term study of vertical and horizontal distribution of zooplankton during thermal stratification in Lake Kinneret, Israel’, *Hydrobiologia*, 526(1 SPEC. ISS.), pp. 85–98. doi: 10.1023/B:HYDR.0000041611.71680.fc.

Pobel, D., Godon, J. J., Humbert, J. F. and Robin, J. (2012) ‘High-frequency monitoring of the genetic diversity and the potential toxicity of a *Microcystis aeruginosa* bloom in a French shallow lake’, *FEMS Microbiology Ecology*, 79(1), pp. 132–141. doi: 10.1111/j.1574-6941.2011.01203.x.

Pope, S. B. (2000) *Free Shear Flows, Turbulent Flows*. Cambridge University Press.

Porter, J., Arzberger, P., Braun, H.-W., Bryant, P., Gage, S., Hansen, T., Hanson, P., Lin, C.-C., Lin, F.-P., Kratz, T., Michener, W., Shapiro, S. and Williams, T. (2005) ‘Wireless Sensor Networks for Ecology’, *BioScience*, 55(June 2014), pp. 323–334. doi: 10.1641/0006-3568(2005)055.

Porter, J. H., Hanson, P. C. and Lin, C. C. (2012) ‘Staying afloat in the sensor data deluge’, *Trends in Ecology and Evolution*. Elsevier Ltd, 27(2), pp. 121–129. doi: 10.1016/j.tree.2011.11.009.

Porter, J. H., Nagy, E., Kratz, T. K., Hanson, P., Collins, S. L. and Arzberger, P. (2009) ‘New Eyes on the World: Advanced Sensors for Ecology’, *BioScience*, 59(5), pp. 385–397. doi: 10.1525/bio.2009.59.5.6.

Posch, T., Köster, O., Salcher, M. M. and Pernthaler, J. (2012) ‘Harmful filamentous cyanobacteria favoured by reduced water turnover with lake warming’, *Nature Climate Change*. Nature Publishing Group, 2(11), pp. 809–813. doi: 10.1038/nclimate1581.

PROGNOS (2020) *Predicting in-lake responses using high frequency data with near real time models*. Available at: <http://www.prognoswater.org/>.

Quintana-Seguí, P., Barella-Ortiz, A., Regueiro-Sanfiz, S. and Miguez-Macho, G. (2019) ‘The Utility of Land-Surface Model Simulations to Provide Drought Information in a Water Management Context Using Global and Local Forcing Datasets’, *Water Resources Management*. doi: 10.1007/s11269-018-2160-9.

R Core Team (2020) 'R: A language and environment for statistical computing.' R Foundation for Statistical Computing, Vienna, Austria. Available at: <http://www.r-project.org/>.

Råman Vinnå, L., Wüest, A., Zappa, M., Fink, G. and Bouffard, D. (2017) 'Tributaries affect the thermal response of lakes to climate change', *Hydrology and Earth System Sciences Discussions*, (January), pp. 1–40. doi: 10.5194/hess-2017-337.

Råman Vinnå, L., Wüest, A., Zappa, M., Fink, G. and Bouffard, D. (2018) 'Tributaries affect the thermal response of lakes to climate change', *Hydrology and Earth System Sciences*, 22(1), pp. 31–51. doi: 10.5194/hess-22-31-2018.

Ramon, J., Lledó, L., Torralba, V., Soret, A. and Doblas-Reyes, F. J. (2019) 'What global reanalysis best represents near-surface winds?', *Quarterly Journal of the Royal Meteorological Society*, 145(724), pp. 3236–3251. doi: 10.1002/qj.3616.

Rao, Y. R., Skafel, M. G. and Charlton, M. N. (2004) 'Circulation and turbulent exchange characteristics during the thermal bar in Lake Ontario', *Limnology and Oceanography*, 49(6), pp. 2190–2200. doi: 10.4319/lo.2004.49.6.2190.

Raso, L., Schwanenberg, D., van de Giesen, N. C. and van Overloop, P. J. (2014) 'Short-term optimal operation of water systems using ensemble forecasts', *Advances in Water Resources*. Elsevier Ltd, 71, pp. 200–208. doi: 10.1016/j.advwatres.2014.06.009.

Read, J. S., Hamilton, D. P., Jones, I. D., Muraoka, K., Winslow, L. A., Kroiss, R., Wu, C. H. and Gaiser, E. (2011) 'Derivation of lake mixing and stratification indices from high-resolution lake buoy data', *Environmental Modelling and Software*, 26(11), pp. 1325–1336. doi: 10.1016/j.envsoft.2011.05.006.

Read, J. S., Jia, X., Willard, J., Appling, A. P., Zwart, J. A., Oliver, S. K., Karpatne, A., Hansen, G. J. A., Hanson, P. C., Watkins, W., Steinbach, M. and Kumar, V. (2019) 'Process-Guided Deep Learning Predictions of Lake Water Temperature', *Water Resources Research*. Blackwell Publishing Ltd, 55(11), pp. 9173–9190. doi: 10.1029/2019WR024922.

Read, J. S. and Rose, K. C. (2013) 'Physical responses of small temperate lakes to variation in dissolved organic carbon concentrations', *Limnology and Oceanography*,

58(3), pp. 921–931. doi: 10.4319/lo.2013.58.3.0921.

Read, J. S., Winslow, L. A., Hansen, G. J. A., Van Den Hoek, J., Hanson, P. C., Bruce, L. C. and Markfort, C. D. (2014) ‘Simulating 2368 temperate lakes reveals weak coherence in stratification phenology’, *Ecological Modelling*. Elsevier B.V., 291, pp. 142–150. doi: 10.1016/j.ecolmodel.2014.07.029.

Rees, S. E. (1997) ‘The historical and cultural importance of ponds and small lakes in Wales, UK’, *Aquatic Conservation: Marine and Freshwater Ecosystems*, 7(2), pp. 133–139. doi: 10.1002/(sici)1099-0755(199706)7:2<133::aid-aqc225>3.3.co;2-5.

Refsgaard, J. C., van der Sluijs, J. P., Højberg, A. L. and Vanrolleghem, P. A. (2007) ‘Uncertainty in the environmental modelling process - A framework and guidance’, *Environmental Modelling and Software*, 22(11), pp. 1543–1556. doi: 10.1016/j.envsoft.2007.02.004.

Reich, S. (2019) ‘Data assimilation: The Schrödinger perspective’, *Acta Numerica*, 28, pp. 635–711. doi: 10.1017/S0962492919000011.

Reichert, P. and Vanrolleghem, P. (2001) ‘Identifiability and uncertainty analysis of the River Water Quality Model No. 1 (RWQM1)’, *Water Science and Technology*, 43(7), pp. 329–338. doi: 10.2166/wst.2001.0442.

Reifen, C. and Toumi, R. (2009) ‘Climate projections: Past performance no guarantee of future skill?’, *Geophysical Research Letters*, 36(13), pp. 1–5. doi: 10.1029/2009GL038082.

Reilly, C. M. O., Alin, S. R. and Plisnier, P. (2003) ‘Climate change decreases aquatic ecosystem productivity of Lake Tanganyika, Africa’, *Nature*, 424(6950), pp. 766–768. doi: 10.1038/nature01833.

Rempfer, J., Livingstone, D. M., Blodau, C., Forster, R., Niederhauser, P. and Kipfer, R. (2010) ‘The effect of the exceptionally mild European winter of 2006-2007 on temperature and oxygen profiles in lakes in Switzerland: A foretaste of the future?’, *Limnology and Oceanography*, 55(5), pp. 2170–2180. doi: 10.4319/lo.2010.55.5.2170.

Ren, L., Nash, S. and Hartnett, M. (2016) ‘Forecasting of surface currents via correcting wind stress with assimilation of high-frequency radar data in a three-dimensional model’,

*Advances in Meteorology*, 2016. doi: 10.1155/2016/8950378.

Reynolds, C. S. (1980) 'Phytoplankton assemblages and their periodicity in stratifying lake systems', *Ecography*, 3(3), pp. 141–159. doi: 10.1111/j.1600-0587.1980.tb00721.x.

Riahi, K., Grübler, A. and Nakicenovic, N. (2007) 'Scenarios of long-term socio-economic and environmental development under climate stabilization', *Technological Forecasting and Social Change*, 74(7), pp. 887–935. doi: 10.1016/j.techfore.2006.05.026.

Riccio, A., Giunta, G. and Galmarini, S. (2007) 'Seeking for the rational basis of the Median Model: The optimal combination of multi-model ensemble results', *Atmospheric Chemistry and Physics*, 7(24), pp. 6085–6098. doi: 10.5194/acp-7-6085-2007.

Robson, B. J., Arhonditsis, G. B., Baird, M. E., Brebion, J., Edwards, K. F., Geoffroy, L., Hébert, M. P., van Dongen-Vogels, V., Jones, E. M., Kruk, C., Mongin, M., Shimoda, Y., Skerratt, J. H., Trevathan-Tackett, S. M., Wild-Allen, K., Kong, X. and Steven, A. (2018) 'Towards evidence-based parameter values and priors for aquatic ecosystem modelling', *Environmental Modelling and Software*, 100, pp. 74–81. doi: 10.1016/j.envsoft.2017.11.018.

Romero, J. R., Antenucci, J. P. and Imberger, J. (2004) 'One- and three-dimensional biogeochemical simulations of two differing reservoirs', *Ecological Modelling*, 174(1–2), pp. 143–160. doi: 10.1016/j.ecolmodel.2004.01.005.

Rontu, L., Eerola, K., Kourzeneva, E. and Vehviläinen, B. (2012) 'Data assimilation and parametrisation of lakes in HIRLAM', *Tellus, Series A: Dynamic Meteorology and Oceanography*, 64(1). doi: 10.3402/tellusa.v64i0.17611.

Rose, K. C., Weathers, K. C., Hetherington, A. L. and Hamilton, D. P. (2016) 'Insights from the Global Lake Ecological Observatory Network (GLEON)', *Inland Waters*, 6(4), pp. 476–482. doi: 10.1080/iw-6.4.1051.

Rose, K. C., Winslow, L. A., Read, J. S. and Hansen, G. J. A. (2016) 'Climate-induced warming of lakes can be either amplified or suppressed by trends in water clarity', *Limnology and Oceanography Letters*, 1(1), pp. 44–53. doi: 10.1002/lol2.10027.

Rothfus, L. P. (1990) *The heat index equation (or, more than you ever wanted to know*

about heat index), *National Weather Service (NWS) Technical Attachment (SR 90-23)*. Available at: [papers://c6bd9143-3623-4d4f-963f-62942ed32f11/Paper/p395](https://papers://c6bd9143-3623-4d4f-963f-62942ed32f11/Paper/p395).

Saber, A., James, D. E. and Hayes, D. F. (2019) 'Long-term forecast of water temperature and dissolved oxygen profiles in deep lakes using artificial neural networks conjugated with wavelet transform', *Limnology and Oceanography*, (9999), pp. 1–21. doi: 10.1002/lno.11390.

Sachse, R., Petzoldt, T., Blumstock, M., Moreira, S., Pätzig, M., Rücker, J., Janse, J. H., Mooij, W. M. and Hilt, S. (2014) 'Extending one-dimensional models for deep lakes to simulate the impact of submerged macrophytes on water quality', *Environmental Modelling and Software*, 61(October), pp. 410–423. doi: 10.1016/j.envsoft.2014.05.023.

Sacket, W. M. (1996) *Physics and chemistry of lakes, Geochimica et Cosmochimica Acta*. Springer, Berlin, Heidelberg. doi: 10.1016/0016-7037(96)83277-7.

Saggio, A. and Imberger, J. (2001) 'Mixing and turbulent fluxes in the metallimnion of a stratified lake', *Limnology and Oceanography*, 46(2), pp. 392–409.

Sahoo, G. B., Forrest, A. L., Schladow, S. G., Reuter, J. E., Coats, R. and Dettinger, M. (2016) 'Climate change impacts on lake thermal dynamics and ecosystem vulnerabilities', *Limnology and Oceanography*, 61(2), pp. 496–507. doi: 10.1002/lno.10228.

Saloranta, T. M. and Andersen, T. (2007) 'MyLake-A multi-year lake simulation model code suitable for uncertainty and sensitivity analysis simulations', *Ecological Modelling*, 207(1), pp. 45–60. doi: 10.1016/j.ecolmodel.2007.03.018.

Samuelsson, P., Kourzeneva, E. and Mironov, D. (2010) 'The impact of lakes on the European climate as simulated by a regional climate model', *Boreal Environment Research*, 15(2), pp. 113–129.

Sánchez, M. L., Rodríguez, P., Torremorell, A. M., Izaguirre, I. and Pizarro, H. (2017) 'Phytoplankton and Periphyton Primary Production in Clear and Turbid Shallow Lakes: Influence of the Light Environment on the Interactions between these Communities', *Wetlands*. *Wetlands*, 37(1), pp. 67–77. doi: 10.1007/s13157-016-0840-x.

Sander, J. (1998) 'Dynamical equations and turbulent closures in geophysics',

*Continuum Mechanics and Thermodynamics*, 10(1), pp. 1–28. doi: 10.1007/s001610050078.

Sanseverino, I., Conduto, D., Pozzoli, L., Dobricic, S. and Lettieri, T. (2016) *Algal bloom and its economic impact*, *Eur 27905 En*. doi: 10.2788/660478.

Sastri, A. R., Gauthier, J., Juneau, P. and Beisner, B. E. (2014) ‘Biomass and productivity responses of zooplankton communities to experimental thermocline deepening’, *Limnology and Oceanography*, 59(1), pp. 1–16. doi: 10.4319/lo.2014.59.1.0001.

Saur, J. F. T. and Anderson, E. R. (1956) ‘The Heat Budget of a Body of Water of Varying Volume1’, *Limnology and Oceanography*, 1(4), pp. 247–251. doi: 10.4319/lo.1956.1.4.0247.

Schallenberg, M., De Winton, M. D., Verburg, P., Kelly, D. J., Hamill, K. D. and Hamilton, D. P. (2013) ‘Ecosystem Services of Lakes’, *Ecosystem services in New Zealand - Conditions and trends*, pp. 203–225.

Schertzer, W., Saylor, J. H., Boyce, F. M., Robertson, D. G. and Rosa, F. (1987) ‘Seasonal Thermal Cycle of Lake Erie’, *Journal of Great Lakes Research*, 4(13), pp. 468–486.

Schindler, D. W. (1974) ‘Eutrophication and recovery in experimental lakes: Implications for lake management’, *Science*, 184(4139), pp. 897–899. doi: 10.1126/science.184.4139.897.

Schindler, D. W. (2012) ‘The dilemma of controlling cultural eutrophication of lakes’, *Proceedings of the Royal Society B: Biological Sciences*, 279(1746), pp. 4322–4333. doi: 10.1098/rspb.2012.1032.

Schladow, S. G. and Hamilton, D. P. (1997) ‘Prediction of water quality in lakes and reservoirs: Part II - Model calibration, sensitivity analysis and application’, *Ecological Modelling*, 96(1–3), pp. 111–123. doi: 10.1016/S0304-3800(96)00063-4.

Schmid, M., Hunziker, S. and Wüest, A. (2014) ‘Lake surface temperatures in a changing climate: A global sensitivity analysis’, *Climatic Change*, 124(1–2), pp. 301–315. doi: 10.1007/s10584-014-1087-2.

Schmid, M. and Koster, O. (2016) 'Excess warming of a Central European lake driven by solar brightening', *Water Resources Research*, 52, pp. 8103–8116. doi: 10.1111/j.1752-1688.1969.tb04897.x.

Schmidt, W. (1928) 'Über Temperatur and Stabilitätsverhältnisse von Seen', *Geographiska Annaler*, 10, pp. 145–177.

Schwab, D. J., Bennett, J. R. and Jessup, A. T. (1981) *A two-dimensional lake circulation modeling system*. Available at: [https://repository.library.noaa.gov/view/noaa/11200/noaa\\_11200\\_DS1.pdf](https://repository.library.noaa.gov/view/noaa/11200/noaa_11200_DS1.pdf).

Seneviratne, S., Nicholls, N., Easterling, D., Goodess, C., Kanae, S., Kossin, J., Luo, Y., Marengo, J., McInnes, K., Rahimi, M., Reichstein, M., Sorteberg, A., Vera, C. and Zhang, X. (2012) 'Changes in climate extremes and their impacts on the natural physical environment. In: Managing the Risk of Extreme Events and Disasters to Advance Climate Change Adaptation.[Field, C.B., V. Barros, T.F. Stocker, D. Qin, D.J. Dokken, K.L. Ebi, M.D. Mastra', *Managing the Risk of Extreme Events and Disasters to Advance Climate Change Adaptation.[Field, C.B., V. Barros, T.F. Stocker, D. Qin, D.J. Dokken, K.L. Ebi, M.D. Mastrandrea, K.J. Mach, G.-K. Plattner, S.K. Allen, M. Tignor, and P.M. Midgley (eds.)]. A Sp*, pp. 109–230. doi: 10.2134/jeq2008.0015br.

Shadkam, S., Ludwig, F., van Oel, P., Kirmit, Ç. and Kabat, P. (2016) 'Impacts of climate change and water resources development on the declining inflow into Iran's Urmia Lake', *Journal of Great Lakes Research*, 42(5), pp. 942–952. doi: 10.1016/j.jglr.2016.07.033.

Shatwell, T., Thiery, W. and Kirillin, G. (2019) 'Future projections of temperature and mixing regime of European temperate lakes', *Hydrology and Earth System Sciences*, 23(3), pp. 1533–1551. doi: 10.5194/hess-23-1533-2019.

Shuman, F. G. (1989) 'History of numerical weather prediction at the National Meteorological Center', *Weather and Forecasting*, 4(3), pp. 286–296.

Shuter, B. J., Minns, C. K. and Fung, S. R. (2013) 'Empirical models for forecasting changes in the phenology of ice cover for Canadian lakes', *Canadian Journal of Fisheries and Aquatic Sciences*, 70(7), pp. 982–991. doi: 10.1139/cjfas-2012-0437.

- Sidiropoulos, P., Mylopoulos, N. and Loukas, A. (2013) 'Optimal Management of an Overexploited Aquifer under Climate Change: The Lake Karla Case', *Water Resources Management*, 27(6), pp. 1635–1649. doi: 10.1007/s11269-012-0083-4.
- Sillmann, J., Kharin, V. V., Zhang, X., Zwiers, F. W. and Bronaugh, D. (2013) 'Climate extremes indices in the CMIP5 multimodel ensemble: Part 1. Model evaluation in the present climate', *Journal of Geophysical Research Atmospheres*, 118(4), pp. 1716–1733. doi: 10.1002/jgrd.50203.
- Simmons, A. J. and Hollingsworth, A. (2002) 'Some aspects of the improvement in skill of numerical weather prediction', *Quarterly Journal of the Royal Meteorological Society*, 128(580), pp. 647–677. doi: 10.1256/003590002321042135.
- Simpson, J. J. and Paulson, C. A. (1979) 'Mid-ocean observations of atmospheric radiation', *Quarterly Journal of the Royal Meteorological Society*, 105(444), pp. 487–502. doi: 10.1002/qj.49710544412.
- Slivinski, L. C. *et al.* (2019) 'Towards a more reliable historical reanalysis: Improvements for version 3 of the Twentieth Century Reanalysis system', *Quarterly Journal of the Royal Meteorological Society*, 145(724), pp. 2876–2908. doi: 10.1002/qj.3598.
- Smith, B. A., Ruthman, T., Sparling, E., Auld, H., Comer, N., Young, I., Lammerding, A. M. and Fazil, A. (2015) 'A risk modeling framework to evaluate the impacts of climate change and adaptation on food and water safety', *Food Research International*. Elsevier B.V., 68, pp. 78–85. doi: 10.1016/j.foodres.2014.07.006.
- Smith, C. A., Read, J. S. and Vander Zanden, M. J. (2018) 'Evaluating the “Gradual Entrainment Lake Inverter” (GELI) artificial mixing technology for lake and reservoir management', *Lake and Reservoir Management*. Taylor & Francis, 2381, pp. 1–12. doi: 10.1080/10402381.2018.1423586.
- Smith, G. C., Roy, F., Mann, P., Dupont, F., Brasnett, B., Lemieux, J. F., Laroche, S. and Bélair, S. (2014) 'A new atmospheric dataset for forcing ice-ocean models: Evaluation of reforecasts using the Canadian global deterministic prediction system', *Quarterly Journal of the Royal Meteorological Society*, 140(680), pp. 881–894. doi: 10.1002/qj.2194.

- Smith, I. R. (1979) 'Hydraulic conditions in isothermal lakes', *Freshwater Biology*, 9, pp. 119–145.
- Smith, L. A. and Stern, N. (2011) 'Uncertainty in science and its role in climate policy', *Philosophical Transactions of the Royal Society A: Mathematical, Physical and Engineering Sciences*, 369(1956), pp. 4818–4841. doi: 10.1098/rsta.2011.0149.
- Smith, S. J. and Wigley, T. M. L. (2006) 'Multi-Gas Forcing Stabilization with Minicam Published by : International Association for Energy Economics Linked references are available on JSTOR for this article : Multi-Gas Forcing Stabilization with Minicam', *The Energy Journal Special Issue: Multi-Greenhouse Gas Mitigation and Climate Policy*, 27, pp. 373–391.
- Snorheim, C. A., Hanson, P. C., McMahon, K. D., Read, J. S., Carey, C. C. and Dugan, H. A. (2017) 'Meteorological drivers of hypolimnetic anoxia in a eutrophic, north temperate lake', *Ecological Modelling*. Elsevier B.V., 343, pp. 39–53. doi: 10.1016/j.ecolmodel.2016.10.014.
- Sobek, S., Tranvik, L. J., Prairie, Y. T., Kortelainen, P. and Cole, J. J. (2012) 'Patterns and regulations of dissolved organic carbon: an analysis of 7,500 widely distributed lakes', *Limnology and Oceanography*, 52(3), pp. 1208–1219.
- Soetaert, K. and Petzoldt, T. (2010) 'Inverse modelling, sensitivity and monte carlo analysis in R using package FME', *Journal of Statistical Software*, 33(3), pp. 1–28. doi: 10.18637/jss.v033.i03.
- Solman, S. A., Sanchez, E., Samuelsson, P., da Rocha, R. P., Li, L., Marengo, J., Pessacg, N. L., Remedio, A. R. C., Chou, S. C., Berbery, H., Le Treut, H., de Castro, M. and Jacob, D. (2013) 'Evaluation of an ensemble of regional climate model simulations over South America driven by the ERA-Interim reanalysis: Model performance and uncertainties', *Climate Dynamics*, 41(5–6), pp. 1139–1157. doi: 10.1007/s00382-013-1667-2.
- Søndergaard, M., Lauridsen, T. L., Johansson, L. S. and Jeppesen, E. (2017) 'Nitrogen or phosphorus limitation in lakes and its impact on phytoplankton biomass and submerged macrophyte cover', *Hydrobiologia*. Springer International Publishing, 795(1), pp. 35–48. doi: 10.1007/s10750-017-3110-x.

- Sproule-Jones, M. (1999) 'Restoring the great lakes: Institutional analysis and design', *Coastal Management*, 27(4), pp. 291–316. doi: 10.1080/089207599263712.
- Stackhouse Jr., P. W., Gupta, S. K., Cox, S. J., Mikovitz, C., Zhang, T. and Hinkelman, L. M. (2011) 'The NASA/GEWEX surface radiation budget release 3.0: 24.5-year dataset', *GEWEX News*, 21(1), pp. 10–12. Available at: <http://www.gewex.org/resources/gewex-news/>.
- Stadelmann, T. H., Brezonik, P. L. and Kloiber, S. (2001) 'Seasonal patterns of chlorophyll a and secchi disk transparency in lakes of east-Central Minnesota: Implications for design of ground- and satellite-based monitoring programs', *Lake and Reservoir Management*, 17(4), pp. 299–314. doi: 10.1080/07438140109354137.
- Staehr, P. A., Christensen, J. P. A., Batt, R. D. and Read, J. S. (2012) 'Ecosystem metabolism in a stratified lake', *Limnology and Oceanography*, 57(5), pp. 1317–1330. doi: 10.4319/lo.2012.57.5.1317.
- Stainforth, D. A., Allen, M. R., Tredger, E. R. and Smith, L. A. (2007) 'Confidence, uncertainty and decision-support relevance in climate predictions', *Philosophical Transactions of the Royal Society A: Mathematical, Physical and Engineering Sciences*, 365(1857), pp. 2145–2161. doi: 10.1098/rsta.2007.2074.
- Stainsby, E. A., Winter, J. G., Jarjanazi, H., Paterson, A. M., Evans, D. O. and Young, J. D. (2011) 'Changes in the thermal stability of Lake Simcoe from 1980 to 2008', *Journal of Great Lakes Research*. Elsevier B.V., 37, pp. 55–62. doi: 10.1016/j.jglr.2011.04.001.
- Stefan, H. G., Hondzo, M., Fang, X., Eaton, J. G. and McCormick, J. H. (1996) 'Simulated long term temperature and dissolved oxygen characteristics of lakes in the north-central United States and associated fish habitat limits', *Limnology and Oceanography*, 41(5), pp. 1124–1135. doi: 10.4319/lo.1996.41.5.1124.
- Stepanenko, V. M., Goyette, S., Martynov, A., Perroud, M., Fang, X. and Mironov, D. (2010) 'First steps of a Lake Model intercomparison project: LakeMIP', *Boreal Environment Research*, 15(2), pp. 191–202. doi: 10.1017/CBO9781107415324.004.
- Stepanenko, V. M., Jöhnk, K. D., Machulskaya, E., Perroud, M., Subin, Z., Nordbo, A., Mammarella, I. and Mironov, D. (2014) 'Simulation of surface energy fluxes and

stratification of a small boreal lake by a set of one-dimensional models', *Tellus, Series A: Dynamic Meteorology and Oceanography*, 66(1), pp. 1–18. doi: 10.3402/tellusa.v66.21389.

Stepanenko, V. M., Martynov, A., Jöhnk, K. D., Subin, Z. M., Perroud, M., Fang, X., Beyrich, F., Mironov, D. and Goyette, S. (2013) 'A one-dimensional model intercomparison study of thermal regime of a shallow, turbid midlatitude lake', *Geoscientific Model Development*, 6(4), pp. 1337–1352. doi: 10.5194/gmd-6-1337-2013.

Stone, C., Windsor, F. M., Munday, M. and Durance, I. (2019) 'Natural or synthetic – how global trends in textile usage threaten freshwater environments', *Science of the Total Environment*. The Author(s), p. 134689. doi: 10.1016/j.scitotenv.2019.134689.

Storn, R. and Price, K. (1997) 'Differential Evolution – A Simple and Efficient Heuristic for global Optimization over Continuous Spaces', *Journal of Global Optimization*, 11(4), pp. 341–359. doi: 10.1023/A:1008202821328.

Stow, C. A., Carpenter, S. R., Webster, K. E. and Frost, T. M. (1998) 'Long-Term Environmental Monitoring: Some Perspectives from Lakes', *Ecological Applications*, 8(2), p. 269. doi: 10.2307/2641066.

Stroud, J. R., Lesht, B. M., Schwab, D. J., Beletsky, D. and Stein, M. L. (2009) 'Assimilation of satellite images into a sediment transport model of Lake Michigan', *Water Resources Research*, 45(2), pp. 1–16. doi: 10.1029/2007WR006747.

Stroud, J. R., Stein, M. L., Lesht, B. M., Schwab, D. J. and Beletsky, D. (2010) 'An ensemble kalman filter and smoother for satellite data assimilation', *Journal of the American Statistical Association*, 105(491), pp. 978–990. doi: 10.1198/jasa.2010.ap07636.

Stumpf, R. P., Johnson, L. T., Wynne, T. T. and Baker, D. B. (2016) 'Forecasting annual cyanobacterial bloom biomass to inform management decisions in Lake Erie', *Journal of Great Lakes Research*. Elsevier B.V., 42(6), pp. 1174–1183. doi: 10.1016/j.jglr.2016.08.006.

Su, H., Chen, Jun, Wu, Y., Chen, Jianfeng, Guo, X., Yan, Z., Tian, D., Fang, J. and Xie, P. (2019) 'Morphological traits of submerged macrophytes reveal specific positive

feedbacks to water clarity in freshwater ecosystems’, *Science of the Total Environment*. Elsevier B.V., 684, pp. 578–586. doi: 10.1016/j.scitotenv.2019.05.267.

Subin, Z. M., Riley, W. J. and Mironov, D. (2012) ‘An improved lake model for climate simulations: Model structure, evaluation, and sensitivity analyses in CESM1’, *Journal of Advances in Modeling Earth Systems*, 4(2), pp. 1–27. doi: 10.1029/2011MS000072.

Sukenik, A., Zohary, T. and Markel, D. (2014) ‘The Monitoring Program’, in *Lake Kinneret*, pp. 561–575. doi: 10.1007/978-94-017-8944-8.

Swayne, D., Lam, D., MacKay, M., Rouse, W. and Schertzer, W. (2005) ‘Assessment of the interaction between the Canadian Regional Climate Model and lake thermal-hydrodynamic models’, *Environmental Modelling and Software*, 20, pp. 1505–1513. doi: 10.1016/j.envsoft.2004.08.015.

Swinehart, D. F. (1962) ‘The Beer-Lambert law’, *Journal of Chemical Education*, 39(7), pp. 333–335. doi: 10.1021/ed039p333.

Szilagyi, J. (2018) ‘Anthropogenic hydrological cycle disturbance at a regional scale: State-wide evapotranspiration trends (1979–2015) across Nebraska, USA’, *Journal of Hydrology*, 557, pp. 600–612. doi: 10.1016/j.jhydrol.2017.12.062.

Takkouk, S. and Casamitjana, X. (2015) ‘Application of the DYRESM – CAEDYM model to the Sau Reservoir situated in Catalonia , Spain’, *Desalination and Water Treatment*, pp. 1–14. doi: 10.1080/19443994.2015.1053530.

Tan, Z. and Zhuang, Q. (2015) ‘Methane emissions from pan-Arctic lakes during the 21st century: An analysis with process-based models of lake evolution and biogeochemistry’, *Journal of Geophysical Research: Biogeosciences*, 120(12), pp. 2641–2653. doi: 10.1002/2015JG003184.

Tan, Z., Zhuang, Q. and Walter Anthony, K. (2018) ‘Modeling methane emissions from arctic lakes: Model development and site-level study’, *Journal of Advances in Modeling Earth Systems*, 7, pp. 459–483. doi: 10.1002/2017MS001065.

Tanentzap, A. J., Hamilton, D. P. and Yan, N. D. (2007) ‘Calibrating the Dynamic Reservoir Simulation Model (DYRESM) and filling required data gaps for 1-dimensional thermal profile predictions in a boreal lake’, *Limnology and Oceanography: Methods*,

5(December), pp. 484–494. doi: 10.4319/lom.2007.5.484.

Tanentzap, A. J., Yan, N. D., Keller, B., Girard, R., Heneberry, J., Gunn, J. M., Hamilton, D. P. and Taylor, P. A. (2008) ‘Cooling lakes while the world warms: Effects of forest regrowth and increased dissolved organic matter on the thermal regime of a temperate, urban lake’, *Limnology and Oceanography*, 53(1), pp. 404–410. doi: 10.4319/lo.2008.53.1.0404.

Tapiador, F. J., Behrangi, A., Haddad, Z. S., Katsanos, D. and Castro, M. (2016) ‘Disruptions in precipitation cycles: Attribution to anthropogenic forcing’, *Journal of Geophysical Research : Atmospheres*, (121), pp. 2161–2177. doi: 10.1038/175238c0.

Tarek, M., Brissette, F. P. and Arsenault, R. (2019) ‘Evaluation of the ERA5 reanalysis as a potential reference dataset for hydrological modeling over North-America’, *Hydrology and Earth System Sciences Discussions*, (July), pp. 1–35. doi: 10.5194/hess-2019-316.

Tennekes, H. and Lumley, J. L. (1972) *Chapter 1 Introduction, A First Course In Turbulence*. Cambridge, Massachusetts MIT Press.

Thiery, W., Martynov, A., Darchambeau, F., Descy, J. P., Plisnier, P. D., Sushama, L. and Van Lipzig, N. P. M. (2014) ‘Understanding the performance of the FLake model over two African Great Lakes’, *Geoscientific Model Development*, 7(1), pp. 317–337. doi: 10.5194/gmd-7-317-2014.

Thiery, W., Stepanenko, V. M., Fang, X., Jöhnk, K. D., Li, Z., Martynov, A., Perroud, M., Subin, Z. M., Darchambeau, F., Mironov, D. and Van Lipzig, N. P. M. (2014) ‘LakeMIP Kivu: Evaluating the representation of a large, deep tropical lake by a set of one-dimensional lake models’, *Tellus, Series A: Dynamic Meteorology and Oceanography*, 66(1), pp. 1–18. doi: 10.3402/tellusa.v66.21390.

Thorne, P. W. (2008) ‘Arctic tropospheric warming amplification?’, *Nature*, 455(7210), pp. 1–5. doi: 10.1038/nature07256.

Thorne, P. W. and Vose, R. S. (2010) ‘Reanalyses suitable for characterizing long-term trends’, *Bulletin of the American Meteorological Society*, 91(3), pp. 353–361. doi: 10.1175/2009BAMS2858.1.

- Toffolon, M., Piccolroaz, S. and Calamita, E. (2020) 'On the use of averaged indicators to assess lakes' thermal response to changes in climatic conditions', *Environmental Research Letters*. IOP Publishing. doi: 10.1088/1748-9326/ab763e.
- Toffolon, M., Piccolroaz, S., Majone, B., Soja, A., Peeters, F., Schmid, M. and Wu, A. (2014) 'Prediction of surface temperature in lakes with different morphology using air temperature', *Limnology and Oceanography*, 59(6), pp. 2185–2202. doi: 10.4319/lo.2014.59.6.2185.
- Toming, K., Kutser, T., Laas, A., Sepp, M., Paavel, B. and Nõges, T. (2016) 'First experiences in mapping lakewater quality parameters with sentinel-2 MSI imagery', *Remote Sensing*, 8(8), pp. 1–14. doi: 10.3390/rs8080640.
- Torabi Haghghi, A. and Kløve, B. (2017) 'Design of environmental flow regimes to maintain lakes and wetlands in regions with high seasonal irrigation demand', *Ecological Engineering*. Elsevier B.V., 100, pp. 120–129. doi: 10.1016/j.ecoleng.2016.12.015.
- Tranmer, A. W., Weigel, D., Marti, C. L., Vidergar, D., Benjankar, R., Tonina, D., Goodwin, P. and Imberger, J. (2020) 'Coupled reservoir-river systems: Lessons from an integrated aquatic ecosystem assessment', *Journal of Environmental Management*, 260(May 2019). doi: 10.1016/j.jenvman.2020.110107.
- Trebitz, A. S. (2006) 'Characterizing Seiche and Tide-driven Daily Water Level Fluctuations Affecting Coastal Ecosystems of the Great Lakes', *Journal of Great Lakes Research*. Elsevier, 23(2), pp. 102–116. doi: 10.3394/0380-1330(2006)32.
- Trolle, D. *et al.* (2012) 'A community-based framework for aquatic ecosystem models', *Hydrobiologia*, 683(1), pp. 25–34. doi: 10.1007/s10750-011-0957-0.
- Trolle, D., Elliott, J. A., Mooij, W. M., Janse, J. H., Bolding, K., Hamilton, D. P. and Jeppesen, E. (2014) 'Advancing projections of phytoplankton responses to climate change through ensemble modelling', *Environmental Modelling and Software*. Elsevier Ltd, 61, pp. 371–379. doi: 10.1016/j.envsoft.2014.01.032.
- Trolle, D., Nielsen, A., Andersen, H. E., Thodsen, H., Olesen, J. E., Børgesen, C. D., Refsgaard, J. C., Sonnenborg, T. O., Karlsson, I. B., Christensen, J. P., Markager, S. and Jeppesen, E. (2019) 'Effects of changes in land use and climate on aquatic ecosystems:

Coupling of models and decomposition of uncertainties’, *Science of the Total Environment*. The Authors, 657, pp. 627–633. doi: 10.1016/j.scitotenv.2018.12.055.

Tsay, B. T., Member, A., Ruggaber, G. J., Effler, S. W. and Driscoll, C. T. (1992) ‘Thermal Stratification Modeling of Lakes’, *Journal of Hydraulic Engineering*, 118(3), pp. 407–419.

Tsvetova, E. A. (1998) ‘Effect Of The Coriolis Force On Convection In A Deep Lake: Numerical Experiment’, *Journal of Applied Mechanics and Technical Physics*, 39(4), pp. 593–599. doi: 10.1007/BF02471254.

Twiss, M. R., Ulrich, C., Zastepa, A. and Pick, F. R. (2012) ‘On phytoplankton growth and loss rates to microzooplankton in the epilimnion and metalimnion of Lake Ontario in mid-summer’, *Journal of Great Lakes Research*. International Association for Great Lakes Research, 38(SUPPL.4), pp. 146–153. doi: 10.1016/j.jglr.2012.05.002.

Tzabiras, J., Vasiliades, L., Sidiropoulos, P., Loukas, A. and Mylopoulos, N. (2016) ‘Evaluation of Water Resources Management Strategies to Overturn Climate Change Impacts on Lake Karla Watershed’, *Water Resources Management*. Water Resources Management, 30(15), pp. 5819–5844. doi: 10.1007/s11269-016-1536-y.

Umlauf, L., Burchard, H. and Bolding, K. (2005) ‘GOTM - Scientific Documentation Version 3.2’, *Meereswissenschaftliche Berichte - Institut für Ostseeforschung Warnemünde*, 63(63), p. 274. Available at: UmlaufEtAl\_2005.pdf.

UNFCCC (2015) *Adoption of the Paris Agreement, Decision 1/CP.21 of FCCC/CP/2015/10/Add.1*. Available at: <https://unfccc.int/resource/docs/2015/cop21/eng/10a01.pdf>.

United Nations General Assembly (2015) *Transforming our world : the 2030 Agenda for Sustainable Development*. Available at: [https://sustainabledevelopment.un.org/content/documents/21252030 Agenda for Sustainable Development web.pdf](https://sustainabledevelopment.un.org/content/documents/21252030_Agenda_for_Sustainable_Development_web.pdf).

Uusitalo, L., Lehikoinen, A., Helle, I. and Myrberg, K. (2015) ‘An overview of methods to evaluate uncertainty of deterministic models in decision support’, *Environmental Modelling and Software*. Elsevier Ltd, 63, pp. 24–31. doi:

10.1016/j.envsoft.2014.09.017.

UWA (2020) *GitHub - AquaticEcoDynamics/GLM: Code for the General Lake Model*. Available at: <https://github.com/AquaticEcoDynamics/GLM> (Accessed: 7 March 2020).

Vaccari, D. A. (2009) 'Phosphorus: A Looming Crisis', *Scientific American*, 300(6), pp. 54–59.

Valerio, G., Pilotti, M., Barontini, S. and Leoni, B. (2015) 'Sensitivity of the multiannual thermal dynamics of a deep pre-alpine lake to climatic change', *Hydrological Processes*, 29(5), pp. 767–779. doi: 10.1002/hyp.10183.

Valerio, G., Pilotti, M., Marti, C. L. and Imberger, J. (2012) 'The structure of basin-scale internal waves in a stratified lake in response to lake bathymetry and wind spatial and temporal distribution: Lake Iseo, Italy', *Limnol. Oceanogr.*, 57(3), pp. 772–786. doi: 10.4319/lo.2012.57.3.0772.

Vautard, R., Cattiaux, J., Yiou, P., Thépaut, J. N. and Ciais, P. (2010) 'Northern Hemisphere atmospheric stilling partly attributed to an increase in surface roughness', *Nature Geoscience*. Nature Publishing Group, 3(11), pp. 756–761. doi: 10.1038/ngeo979.

Verburg, P. and Antenucci, J. P. (2010) 'Persistent unstable atmospheric boundary layer enhances sensible and latent heat loss in a tropical great lake: Lake Tanganyika', *Journal of Geophysical Research Atmospheres*, 115(11), pp. 1–13. doi: 10.1029/2009JD012839.

Verpoorter, C., Kutser, T., Seekell, D. A. and Tranvik, L. J. (2014) 'A global inventory of lakes based on high-resolution satellite imagery', *Geophysical Research Letters*, 41(18), pp. 6396–6402. doi: 10.1002/2014GL060641.

Versteeg, H. K. and Malalasekera, W. (1995) 'An Introduction to Computational Fluid Dynamics - The Finite Volume Method', *Fluid flow handbook. McGraw-Hill ...*, p. 267. doi: 10.2514/1.22547.

Vincent, W. F. (2009) 'Effects of Climate Change on Lakes', *Université Laval*, pp. 55–60. doi: <http://dx.doi.org/10.1016/B978-012370626-3.00233-7>.

Vitousek, P. M., Aber, J., Howarth, R. W., Likens, G. E., Matson, P. A., Schindler, D.

W., Schlesinger, W. H. and Tilman, G. D. (1997) 'Human Alteration of the Global Nitrogen Cycle: Causes and Consequences Issues in Ecology', *Issues in Ecology*, 1, pp. 1–17. doi: 1092-8987.

Vörösmarty, C. J., Federer, C. A. and Schloss, A. L. (1998) 'Potential evaporation functions compared on US watersheds: Possible implications for global-scale water balance and terrestrial ecosystem modeling', *Journal of Hydrology*, 207(3–4), pp. 147–169. doi: 10.1016/S0022-1694(98)00109-7.

Vrugt, J. A. and Robinson, B. A. (2007) 'Treatment of uncertainty using ensemble methods: Comparison of sequential data assimilation and Bayesian model averaging', *Water Resources Research*, 43(1), pp. 1–15. doi: 10.1029/2005WR004838.

Vu, M. T., Raghavan, S. V. and Liong, S. Y. (2012) 'SWAT use of gridded observations for simulating runoff - A Vietnam river basin study', *Hydrology and Earth System Sciences*, 16(8), pp. 2801–2811. doi: 10.5194/hess-16-2801-2012.

van Vuuren, D. P., Edmonds, J., Kainuma, M., Riahi, K., Thomson, A., Hibbard, K., Hurtt, G. C., Kram, T., Krey, V., Lamarque, J. F., Masui, T., Meinshausen, M., Nakicenovic, N., Smith, S. J. and Rose, S. K. (2011) 'The representative concentration pathways: An overview', *Climatic Change*, 109(1), pp. 5–31. doi: 10.1007/s10584-011-0148-z.

van Vuuren, D. P., Eickhout, B., Lucas, P. L. and den Elzen, M. G. J. (2006) 'Long-Term Multi-Gas Scenarios to Stabilise Radiative Forcing — Exploring Costs and Benefits Within an Integrated Assessment Framework Published by : International Association for Energy Economics Stable URL : <http://www.jstor.org/stable/23297082> Your use', *The Energy Journal*, 27(Multi-Greenhouse Gas Mitigation and Climate Policy), pp. 201–233. doi: 10.2307/23297082.

Wang, B., Ma, Y., Chen, X., Ma, W., Su, Z. and Menenti, M. (2015) 'Observation and simulation of lake-air heat and water transfer processes in a high-altitude shallow lake on the Tibetan Plateau', *Journal of Geophysical Research : Atmospheres*, (120), pp. 327–344. doi: 10.1002/2015JD023863.Received.

Warrach-Sagi, K., Schwitalla, T., Wulfmeyer, V. and Bauer, H. S. (2013) 'Evaluation of a climate simulation in Europe based on the WRF-NOAH model system: Precipitation

in Germany’, *Climate Dynamics*, 41(3–4), pp. 755–774. doi: 10.1007/s00382-013-1727-7.

Warren, D. R., Kraft, C. E., Josephson, D. C. and Driscoll, C. T. (2017) ‘Acid rain recovery may help to mitigate the impacts of climate change on thermally sensitive fish in lakes across eastern North America’, *Global Change Biology*, 23(6), pp. 2149–2153. doi: 10.1111/gcb.13568.

Watanabe, M., Suzuki, T., O’Ishi, R., Komuro, Y., Watanabe, S., Emori, S., Takemura, T., Chikira, M., Ogura, T., Sekiguchi, M., Takata, K., Yamazaki, D., Yokohata, T., Nozawa, T., Hasumi, H., Tatebe, H. and Kimoto, M. (2010) ‘Improved climate simulation by MIROC5: Mean states, variability, and climate sensitivity’, *Journal of Climate*, 23(23), pp. 6312–6335. doi: 10.1175/2010JCLI3679.1.

WateXr (2020) *WateXr | Extreme climate events and water quality*. Available at: <https://watexr.eu/> (Accessed: 8 April 2020).

Watras, C. J., Morrison, K. A., Crawford, J. T., McDonald, C. P., Oliver, S. K. and Hanson, P. C. (2015) ‘Diel cycles in the fluorescence of dissolved organic matter in dystrophic Wisconsin seepage lakes: Implications for carbon turnover: Diel CDOM fluorescence cycles’, *Limnology and Oceanography*, 60(2), pp. 482–496. doi: 10.1002/lno.10026.

Weedon, G. P., Balsamo, G., Bellouin, N., Gomes, S., Best, M. J. and Viterbo, P. (2014) ‘Data methodology applied to ERA-Interim reanalysis data’, *Water Resources Research*, 50, pp. 7505–7514. doi: 10.1002/2014WR015638. Received.

Weinberger, S. and Vetter, M. (2012) ‘Using the hydrodynamic model DYRESM based on results of a regional climate model to estimate water temperature changes at Lake Ammersee’, *Ecological Modelling*, 244, pp. 38–48. doi: 10.1016/j.ecolmodel.2012.06.016.

Wetzel, R. G. (2001) *Limnology - Lake and River Ecosystems*. San Diego: Academic Press. doi: 10.1063/1.3224729.

Weyhenmeyer, G. A., Blenckner, T. and Pettersson, K. (1999) ‘Changes of the plankton spring outburst related to the North Atlantic Oscillation’, *Limnology and Oceanography*,

44(7), pp. 1788–1792. doi: 10.4319/lo.1999.44.7.1788.

White, D. M., Craig Gerlach, S., Loring, P., Tidwell, A. C. and Chambers, M. C. (2007) ‘Food and water security in a changing arctic climate’, *Environmental Research Letters*, 2(4). doi: 10.1088/1748-9326/2/4/045018.

Whitehead, P. G., Wilby, R. L., Battarbee, R. W., Kernan, M. and Wade, A. J. (2009) ‘A review of the potential impacts of climate change on surface water quality’, *Hydrological Sciences Journal*, 54(1), pp. 101–121. doi: 10.1623/hysj.54.1.101.

Wilcke, R. A. I., Mendlik, T. and Gobiet, A. (2013) ‘Multi-variable error correction of regional climate models’, *Climatic Change*, 120(4), pp. 871–887. doi: 10.1007/s10584-013-0845-x.

Wilkinson, G. M., Carpenter, S. R., Cole, J. J., Pace, M. L., Batt, R. D., Buelo, C. D. and Kurtzweil, J. T. (2018) ‘Early warning signals precede cyanobacterial blooms in multiple whole-lake experiments’, *Ecological Monographs*, 88(2), pp. 188–203. doi: 10.1002/ecm.1286.

Williams, G. P. (1963) ‘Heat transfer coefficients for natural water surfaces’, *International Association of Scientific Hydrology. Bulletin*, 62(202), pp. 203–212. Available at: <http://www.nrc-cnrc.gc.ca/obj/irc/doc/pubs/rp/rp202/rp202.pdf>.

Winder, M. and Schindler, D. E. (2004) ‘Climate Change Uncouples Trophic Interactions in an Aquatic Ecosystem’, *Ecology*, 85(8), pp. 2100–2106.

Winslow, L. A., Hansen, G. J. A., Read, J. S. and Notaro, M. (2017) ‘Large-scale modeled contemporary and future water temperature estimates for 10774 Midwestern U.S. Lakes’, *Scientific Data*. The Author(s), 4, pp. 1–11. doi: 10.1038/sdata.2017.53.

Winslow, L. A., Read, J. S., Hansen, G. J. A., Rose, K. C. and Robertson, D. M. (2017) ‘Seasonality of change: Summer warming rates do not fully represent effects of climate change on lake temperatures’, *Limnology and Oceanography*, 62(5), pp. 2168–2178. doi: 10.1002/lno.10557.

Woolway, R. I., Cinque, K., de Eyto, E., Degasperi, C. L., Dokulil, M. T., Korhonen, J., Maberly, S. C., Marszelewski, W., May, L., Merchant, C. J. and Paterson, A. M. (2016) ‘Global climate–lake surface temperatures’, *Bulletin of the American Meteorological*

*Society*, 97(8), pp. S17–S18.

Woolway, R. I., Dokulil, M. T., Marszelewski, W., Schmid, M., Bouffard, D. and Merchant, C. J. (2017) ‘Warming of Central European lakes and their response to the 1980s climate regime shift’, *Climatic Change*. *Climatic Change*, 142(3–4), pp. 505–520. doi: 10.1007/s10584-017-1966-4.

Woolway, R. I., Jennings, E. and Carrea, L. (2020) ‘Impact of the 2018 European heatwave on lake surface water temperature’, *Inland Waters*. Taylor & Francis, 0(0), pp. 1–11. doi: 10.1080/20442041.2020.1712180.

Woolway, R. I., Jones, I. D., Feuchtmayr, H. and Maberly, S. C. (2015) ‘A comparison of the diel variability in epilimnetic temperature for five lakes in the English Lake District’, *Inland Waters*, 5(2), pp. 139–154. doi: 10.5268/IW-5.2.748.

Woolway, R. I., Maberly, S. C., Jones, I. D. and Feuchtmayr, H. (2014) ‘A novel method for estimating the onset of thermal stratification in lakes from surface water measurements’, *Water Resources Research*, 50, pp. 5131–5140. doi: 10.1002/2014WR015716.

Woolway, R. I., Meinson, P., Nöges, P., Jones, I. D. and Laas, A. (2017) ‘Atmospheric stilling leads to prolonged thermal stratification in a large shallow polymictic lake’, *Climatic Change*. *Climatic Change*, 141(4), pp. 759–773. doi: 10.1007/s10584-017-1909-0.

Woolway, R. I. and Merchant, C. J. (2019) ‘Worldwide alteration of lake mixing regimes in response to climate change’, *Nature Geoscience*. Springer US, 12(4), pp. 271–276. doi: 10.1038/s41561-019-0322-x.

Woolway, R. I., Merchant, C. J., Van Den Hoek, J., Azorin-Molina, C., Nöges, P., Laas, A., Mackay, E. B. and Jones, I. D. (2019) ‘Northern Hemisphere Atmospheric Stilling Accelerates Lake Thermal Responses to a Warming World’, *Geophysical Research Letters*, 46(21), pp. 11983–11992. doi: 10.1029/2019GL082752.

Woolway, R. I., Verburg, P., Lenters, J. D., Merchant, C. J., Hamilton, D. P., Brookes, J., de Eyto, E., Kelly, S., Healey, N. C., Hook, S., Laas, A., Pierson, D., Rusak, J. A., Kuha, J., Karjalainen, J., Kallio, K., Lepistö, A. and Jones, I. D. (2018) ‘Geographic and

- temporal variations in turbulent heat loss from lakes: A global analysis across 45 lakes', *Limnology and Oceanography*, 63(6), pp. 2436–2449. doi: 10.1002/lno.10950.
- Wootten, A., Terando, A., Reich, B. J., Boyles, R. P. and Semazzi, F. (2017) 'Characterizing sources of uncertainty from global climate models and downscaling techniques', *Journal of Applied Meteorology and Climatology*, 56(12), pp. 3245–3262. doi: 10.1175/JAMC-D-17-0087.1.
- Wüest, A. and Lorke, A. (2003) 'Small-Scale Hydrodynamics in Lakes', *Annual Review of Fluid Mechanics*, 35(1), pp. 373–412. doi: 10.1146/annurev.fluid.35.101101.161220.
- Wüest, A., Piepke, G. and Senden, D. C. Van (2000) 'Turbulent kinetic energy balance as a tool for estimating vertical diffusivity in wind-forced stratified waters', *Limnology and Oceanography*, 45(6), pp. 1388–1400.
- Wynne, T. T., Stumpf, R. P., Tomlinson, M. C., Fahnenstiel, G. L., Dyble, J., Schwab, D. J. and Joshi, S. J. (2013) 'Evolution of a cyanobacterial bloom forecast system in western Lake Erie: Development and initial evaluation', *Journal of Great Lakes Research*. Elsevier B.V., 39(S1), pp. 90–99. doi: 10.1016/j.jglr.2012.10.003.
- Xia, J., Zhang, L., Liu, C. and Yu, J. (2007) 'Towards better water security in North China', *Water Resources Management*, 21(1), pp. 233–247. doi: 10.1007/s11269-006-9051-1.
- Yacobi, Y. Z. (2006) 'Temporal and vertical variation of chlorophyll a concentration, phytoplankton photosynthetic activity and light attenuation in Lake Kinneret: Possibilities and limitations for simulation by remote sensing', *Journal of Plankton Research*, 28(8), pp. 725–736. doi: 10.1093/plankt/fbl004.
- Yang, Z. and Villarini, G. (2019) 'Examining the capability of reanalyses in capturing the temporal clustering of heavy precipitation across Europe', *Climate Dynamics*. Springer Berlin Heidelberg, 53(3–4), pp. 1845–1857. doi: 10.1007/s00382-019-04742-z.
- Yao, H., Samal, N. R., Jöhnk, K. D., Fang, X., Bruce, L. C., Pierson, D. C., Rusak, J. A. and James, A. (2014) 'Comparing ice and temperature simulations by four dynamic lake models in Harp Lake: Past performance and future predictions', *Hydrological Processes*,

28(16), pp. 4587–4601. doi: 10.1002/hyp.10180.

Yeates, P. S. and Imberger, J. (2003) ‘Pseudo two-dimensional simulations of internal and boundary fluxes in stratified lakes and reservoirs’, *International Journal of River Basin Management*, 1(4), pp. 297–319. doi: 10.1080/15715124.2003.9635214.

Young, C., Liu, W. and Hsieh, W. (2015) ‘Predicting the Water Level Fluctuation in an Alpine Lake Using Physically Based , Artificial Neural Network , and Time Series Forecasting Models’, *Mathematical Problems in Engineering*.

Yu, Z., Yang, J., Amalfitano, S., Yu, X. and Liu, L. (2014) ‘Effects of water stratification and mixing on microbial community structure in a subtropical deep reservoir.’, *Scientific reports*, 4, p. 5821. doi: 10.1038/srep05821.

Zhang, G., Yao, T., Xie, H., Qin, J., Ye, Q., Dai, Y. and Guo, R. (2014) ‘Estimating surface temperature changes of lakes in the Tibetan Plateau using MODIS LST data’, *Journal of Geophysical Research: Atmospheres RESEARCH*, 119, pp. 8552–8567. doi: 10.1002/2014JD021615.

Zhang, Y., Wu, Z., Liu, M., He, J., Shi, K., Zhou, Y., Wang, M. and Liu, X. (2015) ‘Dissolved oxygen stratification and response to thermal structure and long-term climate change in a large and deep subtropical reservoir (Lake Qiandaohu, China)’, *Water Research*. Elsevier Ltd, 75, pp. 249–258. doi: 10.1016/j.watres.2015.02.052.

Zwart, J. A., Hararuk, O., Prairie, Y. T., Jones, S. E. and Solomon, C. T. (2019) ‘Improving estimates and forecasts of lake carbon dynamics using data assimilation’, *Limnology and Oceanography: Methods*, 17(2), pp. 97–111. doi: 10.1002/lom3.10302.

Zwart, J. A., Solomon, C. T. and Jones, S. E. (2015) ‘Phytoplankton traits predict ecosystem function in a global set of lakes’, *Ecology*, 96(8), pp. 2257–2264. doi: 10.1890/14-2102.1.

## **APPENDIX**

The code and data used in each of the chapters of this thesis can be found on the following GitHub repository in the corresponding chapter directory: <https://github.com/tadhgmoore/PhD-thesis>